Characterizing the Telomerase-associated and H/ACA Ribonucleoprotein Dyskerin: Regulation and Function

Deanna MacNeil

Department of Anatomy and Cell Biology, McGill University, Montreal

April 2020

A thesis submitted to McGill University in partial fulfillment of the requirements of the degree of Doctor of Philosophy in Cell Biology

Table of Contents

Abstract (English)

The aim of this thesis is to understand how the function of the H/ACA ribonucleoprotein and telomerase component dyskerin is impacted in premature aging disease, and how dyskerin is regulated at a fundamental level. The H/ACA structural motif is present in many different non-coding RNAs, which assemble with the H/ACA ribonucleoprotein (RNP) complex involving dyskerin, NOP10, NHP2, and GAR1. Assembly with the H/ACA RNP is important for biogenesis of H/ACA RNA, thus dyskerin and the other RNP components play important roles in diverse cellular functions, including regulation of the ribosome, spliceosome, and human telomerase. Dyskerin is a pseudouridine synthase which catalyzes the posttranscriptional modification of ribosomal RNA and small nuclear RNA, guided by H/ACA RNAs. As it pertains to telomerase, the human telomerase RNA (hTR) component bears an H/ACA RNA biogenesis motif, making dyskerin essential for mediating hTR levels and telomerase activity. The importance of dyskerin to telomerase is underlined by mutations in the gene encoding dyskerin, which cause the premature aging disease X-linked dyskeratosis congenita (X-DC). This disease is caused by the accelerated shortening of DNA ends (telomeres). Telomeres are normally maintained by telomerase in stem cells and germ cells, but instead undergo progressive shortening in X-DC patients due to reduced hTR levels, impacting the function of proliferative tissues in patients. However, hTR does not guide pseudouridine synthesis of any target RNA as do other small nucleolar and small Cajal body-specific H/ACA RNA, and the essential nature of dyskerin as a pseudouridine synthase extends beyond telomere maintenance. As such, greater knowledge of dyskerin and how it is regulated contributes to our understanding of both human disease and fundamental cellular processes. Here, we identify the contribution of the poorly characterized dyskerin N-terminus to hTR binding, and a potential telomerase-centric role for this domain in the regulation of hTR biogenesis. This research reveals that the dyskerin-hTR interaction inhibits degradation of precursor hTR species, contributing to maintenance of total hTR levels, and offering an explanation for defective hTR accumulation in patients carrying mutations in the N-terminal hotspot for X-DC. Furthermore, pursuing a foundational study from our lab that identified a regulatory role for the posttranslational modification of dyskerin by SUMOylation in telomerase function, here we demonstrate that SUMOylated dyskerin sites situated in the C-terminal nuclear/nucleolar localization signal regulate dyskerin nuclear and nucleolar localization. We demonstrate that a specific SUMOylated residue in this region, K467,

mediates the interaction between dyskerin and the mature H/ACA complex component GAR1, as well as dyskerin nucleolar localization. We also identify a previously unreported SUMO-interacting motif in GAR1 that is important for an efficient dyskerin-GAR1 interaction. In summary, this thesis contributes a better understanding of dyskerin biology, for both disease-relevant and basic cellular mechanisms of dyskerin regulation and function.

Résumé (French)

Le but de cette thèse est de comprendre comment la fonction de la ribonucléoprotéine H / ACA et la composante de la télomérase dyskérine est impactée dans la maladie du vieillissement prématuré, et comment la dyskérine est régulée à un niveau fondamental. Le motif structurel H/ACA est présent dans de nombreux ARNs non-codants différents, qui s'assemblent avec le complexe de ribonucléoprotéines (RNP) H/ACA composé de la dyskérine, NOP10, NHP2 et GAR1. L'assemblage avec le RNP H/ACA est important pour la biogenèse desARNs H/ACA, ainsi la dyskérine et les autres composants RNP jouent des rôles importants dans diverses fonctions cellulaires, y compris la régulation du ribosome, de la particule d'épissage et de la télomérase humaine. La dyskérine est une pseudouridine synthase qui catalyse la modification post-transcriptionnelle de l'ARN ribosomal et du petit ARN nucléaire, guidée par les ARNs H/ACA. En ce qui concerne la télomérase, le composant ARN de la télomérase humaine (hTR) contient un motif de biogenèse de l'ARN H/ACA, ce qui rend la dyskérine essentielle pour la régulation de la quantité de hTR et de l'activité de la télomérase. L'importance de la dyskérine pour la télomérase est soulignée par des mutations dans le gène codant pour la dyskérine, qui cause la maladie du vieillissement prématuré dyskératose liée à l'X congénitale (X-DC). Cette maladie est causée par le raccourcissement accéléré des extrémités de l'ADN (télomères). Les télomères sont normalement maintenus par la télomérase dans les cellules souches et les cellules germinales, mais subissent un raccourcissement progressif pour les patients X-DC en raison des niveaux de hTR réduits, affectant la fonction des tissus prolifératifs des patients. Cependant, hTR ne guide pas la synthèse de pseudouridine d'aucun ARN cible comme le font d'autres petits ARN H/ACA nucléolaire et spécifiques du corps Cajal, et la nature essentielle de la dyskérine en tant que pseudouridine synthase s'étend au-delà de du maintient des télomères. À ce titre, une meilleure connaissance de la dyskérine et de sa régulation contribue à notre compréhension des maladies humaines et des processus cellulaires fondamentaux. Ici, nous avons exploré la contribution de l'extrémité N-terminale de dyskérine mal caractérisée, à la liaison avec hTR, et un potentiel rôle spécifique de la télomérase dans la régulation de la biogénèse de hTR. Cette recherche révèle que l'interaction dyskérine-hTR inhibe la dégradation des espèces précurseurs de hTR, contribuant au maintien des niveaux totaux de hTR et offrant une explication pour l'accumulation défectueuse de hTR chez les patients porteurs de mutations dans le ‘hotspot’ N-

terminal pour X-DC. De plus, en poursuivant une étude fondamentale de notre laboratoire qui a identifié un rôle régulateur de la modification postraductionelle de dyskérine par la SUMOylation sur la fonction de la télomérase, nous démontrons ici que les sites SUMOylées de dyskérine situés dans le signal de localisation nucléaire/nucléolaire C-terminale régulent la localisation nucléaire et nucléolaire de la dyskérine. Nous démontrons qu'un résidu SUMOylé spécifique dans cette région, K467, contrôle l'interaction entre la dyskérine et le composant du complexe H/ACA mature GAR1, ainsi que la localisation nucléolaire de dyskérine. Nous identifions également un motif d'interaction SUMO non rapporté auparavant dans GAR1 qui est important pour une interaction dyskérine-GAR1 efficace. En résumé, cette thèse contribue à une meilleure compréhension de la biologie de la dyskérine, à la fois pour les mécanismes cellulaires de base et pertinents pour la maladie de la régulation et de la fonction de la dyskérine.

Acknowledgements

I could never have imagined when interviewing with the Autexier lab in October 2013 how joining this group of passionate and kind scientists while embarking on my graduate studies path would change my life, not only scientifically and academically, but on a personal level as well. I am incredibly grateful for my time spent studying in the Autexier lab, as well as for the opportunities to become part of scientific communities in Montreal, Canada, and internationally, in the telomere and DNA integrity fields, and in the RNA field as well. I cannot overstate how much I value getting know everyone in these communities, and how much spending time in these fields has broadened my scientific perspective and my feeling of connectedness with people who love science.

First and foremost I would like to thank my remarkable supervisor Dr. Chantal Autexier. I could not have dreamed for a better mentor, in science and in life. I am so thankful to have studied under your supervision, your kindness and compassion are rare traits in graduate studies supervisors, and have made a sometimes treacherous road through my Ph.D. a smoother one than it may have been. Thank you for sharing with me your foresight, experience, patience, scientific passion, and friendship. I will greatly miss spending time with you in lab and at conferences, and on all of the road trips. Thank you for, metaphorically and quite literally, getting me to my destination safely. It has been an honour and a privilege.

I am also incredibly grateful for the labmates I have shared time with in the Autexier lab over the past five and a half years. We have had laughs, shared work struggles and successes, and consumed an abundance of desserts! My sincerest thanks go to Johanna, Philippe, Hélène, Jeffrey, Florence, Jian, and most recently Adrian, as well as Hannah, Danielle, Erika, and Monique. I would also like to especially thank Josephine (Tsz Wai) Chu and Patrick Lambert-Lanteigne. Josephine: I don't think I could possibly find the words to express how much your mentorship, training, and sisterhood has meant to me, in lab and out. Even after you graduated, I have always been able to count on you in times of joy and strife; I could never have completed this journey without you. Thank you for teaching me the value of scientific rigour, the importance of asking the big questions (and admitting to not having the answers), and the balancing act of life and academia. Patrick: your friendship and wisdom have been indescribably important to me over the course of my studies. It is hard to believe I have only known you since you started in the lab; you have quickly (and easily) become both a mentor and brother to me.

Thank you for sharing so many moments, memories, laughs (and cries), union meal breakfasts, and post-lab scotches with me over the past 5 years. Thank you for contributing your brilliant ideas and benchwork to this thesis, but more importantly thank you for your friendship. I have so appreciated every metal music moment and Star Wars reference, you da real MVP.

The emotional support of my peers has been invaluable to my sanity and passage through Ph.D. studies. My chosen scientific family spans a wide breadth, and I am unbelievably blessed and thankful to be surrounded by such exceptionally kind, smart, funny, and passionate people. If I were to name them all, this thesis would surely reach 300 pages or more. Thank you to the ACB graduate students past and present who have crossed my paths. Specifically, thank you to Kim Gauthier, for being my friend, mentor, and role model all wrapped into one. You have taught me so much about being a strong advocate for graduate students and trainees, and you have shared an incalculable amount of joy and hardship with me along the way. Thank you, and to many more glasses of wine and frozen pizzas. Thank you also to the friends I have made along the way in the telomere/DNA integrity/RNA biology fields. Specifically, I would like to thank members of the Harrington lab: Gus, Maria, Mélanie, Yahya, and Danielle – thank you for sharing wisdom, scientific theories (reasonable and wild), beers and board games, and chalet weekends. It has been a joy to share life and science with you all, thank you for being my peers in academia and in fun. I have been blessed with the community of our research institute as well: thank you to all the trainees at the LDI, in particular those from the pav. F 4th floor. Thank you to Marisa for always sharing a snack and chat, at or away from work. Co-working with you during these thesis times has been fun and motivating, and while I miss the boardroom, pomodoroing from home has been a real treat. Thank you also to Libin for exploring all of the CDN restaurants with me and being my ACB companion at the LDI. You made off-campus feel less distant.

Thank you to the Department of Anatomy and Cell Biology, and especially the many exceptional administrators who have kept me and so many other trainees on track during our studies. Joelle, Anne Marie, Joseph, Penny, Vicki, and Barbara: like raising children, it takes a village for trainees to succeed, and there is no doubt in my mind that we could not without you. Thank you for your time, work, and care. Thank you also to our Departmental Chair Craig Mandato, for always having an open door for trainees, and for championing the voices of graduate students. Additionally, thank you to my committee members Dr. Dieter Reinhardt, Dr.

Ivan Topisirovic, and Dr. Jason Tanny for providing support and feedback throughout my studies, and words of encouragement in between meetings.

Finally, I would like to thank my family. To my mum Ruth, dad Dave, brother Jordan, and sister Justine: thank you for supporting me with every fibre of your beings throughout this process. There have been many tough times, and it has often been hard to be apart. Thank you for your love and encouragement, even if you don't really get it all the time. I love you all so much. Thank you also to my cousins Todd and Christa who have been my safety net, board game gurus, and Montreal indoctrinators. The journey would have been long and lonely without you.

Accepted and Submitted Manuscript Included in this Thesis

MacNeil, D.E., Lambert-Lanteigne, P., & Autexier, C. (2019). N-terminal residues of human dyskerin are required for interactions with telomerase RNA that prevent RNA degradation. *Nucleic Acids Research, 47*(10).

Other Contributions by Candidate

(* indicates co-first authorship)

A manuscript in preparation which accounts for the third chapter of this thesis:

MacNeil, D.E., Lambert-Lanteigne, P., McManus, F., Bonneil, E., Thibault, P., & Autexier, C. SUMOylation- and GAR1-dependent regulation of dyskerin nuclear and subnuclear localization. In preparation for submission (2020).

A review article included in the introduction section of this thesis:

MacNeil, D.E.*, Bensoussan H.J.*, & Autexier, C. (2016). Telomerase regulation from beginning to the end. *Genes, 7*(9).

Author Contributions by Section

Chapter 1: Literature Review

Sections of this literature review are taken directly from a review article written in collaboration with a previous M.Sc. student in the Autexier lab Hélène Bensoussan, and with Dr. Chantal Autexier (MacNeil, Bensoussan et al. 2016). The sections used here were written by Deanna E. MacNeil with editing from Hélène Bensoussan and Dr. Chantal Autexier. The remainder of this section was written by Deanna MacNeil and edited by Dr. Chantal Autexier.

Chapter 2: N-terminal residues of human dyskerin are required for interactions with telomerase RNA that prevent RNA degradation

All experiments were performed by Deanna E. MacNeil, with the exception of experimental replicates of Figure 2.4B which were performed by Patrick Lambert-Lanteigne. The manuscript was written by Deanna E. MacNeil with editing from Dr. Chantal Autexier and Patrick Lambert-Lanteigne. This article is considered original scholarship and is a distinct contribution to knowledge.

Chapter 3: SUMOylation- and GAR1-dependent regulation of dyskerin nuclear and subnuclear localization

Purification of recombinant dyskerin and mass spectrometry experiments were carried out by the laboratory of Dr. Pierre Thibault, by Francis McManus and Eric Bonneil. All other experiments were carried out by Deanna E. MacNeil, or by Patrick Lambert-Lanteigne who assessed interactions between 3xFLAG-GAR1 and endogenous dyskerin, and HA-GAR1 and FLAG-dyskerin. The manuscript was written by Deanna E. MacNeil and edited by Dr. Chantal Autexier and Dr. Pierre Thibault. This manuscript is considered original scholarship and is a distinct contribution to knowledge.

Contributions to Original Knowledge

The results presented in this thesis contribute the following novel observations to the fields of telomere biology and H/ACA RNA biology:

1. The N-terminus of human dyskerin contributes to the interaction between dyskerin and the human telomerase RNA (hTR), and residues in this region that are substituted in

patients with the X-linked premature aging disease dyskeratosis congenita (X-DC) play a potential telomerase-centric role in regulating H/ACA RNA biogenesis.

2. The dyskerin-hTR interaction prevents degradation of both precursor (polyadenylated) and mature hTR species.
3. A shift in the balance between trimming and degradation of hTR precursors caused by disrupting the dyskerin-hTR interaction can contribute to X-DC.
4. Dyskerin nuclear and subnuclear localization is regulated by the posttranslational modification SUMOylation.
5. The SUMO3 site K467 in the C-terminal nuclear/nucleolar localization signal of dyskerin regulates nucleolar localization of dyskerin in a SUMO-dependent and GAR1-dependent manner.
6. The efficient interaction between dyskerin and GAR1 is mediated by the SUMO3 site K467 in dyskerin and a SUMO-interacting motif in GAR1, which is identified and characterized for the first time in this work.

Abbreviations

3D: three dimensional

AAA+ ATPases: ATPases Associated with diverse cellular Activities

ALT: Alternative-Lengthening of Telomeres

APB: ALT-associated PML Body

ATR: Ataxia Telangiectasia and Rad3-related protein

BIR: Break-induced DNA Replication

BLM: Bloom syndrome protein

CAB-box: Cajal body box (ugAG motif)

CB: Cajal Body

CBC: cap-binding complex

CBCA: cap-binding complex A

ChIP: Chromatin Immunoprecipitation

c-Myc: Myc proto-oncogene protein

CR: Conserved region

CRISPR: Clustered regularly-interspaced short palindromic repeats

Cryo-EM: Cryo-electron microscopy

Csm1: Chromosome segregation in meiosis protein 1

CST: Cdc13-Stn1-Ten1 or CTC1-STN1-TEN1

CTC1: Coats plus syndrome protein 1

CTE: C-terminal extension

C-terminal: Carboxy-terminal

DBA: Diamond-Blackfan anemia

DC: Dyskeratosis congenita

DCP2: decapping mRNA 2

DFC: Dense fibrillar component

DGCR8: DiGeorge critical region 8

DKC1: Gene encoding dyskerin (*dkc1*)

DKCLD: dyskeratosis congenita-like domain

DNA: Deoxyribonucleic Acid

D-Loop: Displacement Loop

eGFP: Enhanced green fluorescent protein

FC: Fibrillar component

Fob1: DNA replication fork-blocking protein

FRAP: Fluorescence recovery after photobleaching

FRET: Fluorescence resonance energy transfer

G-rich: Guanine-rich

GAR: Glycine and arginine rich

GC: Granular component

hESC: Human embryonic stem cell

HHS: Hoyeraal-Hreidarsson syndrome

hTERT: Human TERT

hTR: Human TR

hTRAMP: Human TRAMP complex

IDR: Intrinsically disorder regin

IF: Immunofluorescence

IFD: Insertion in Fingers Domain

IP: Immunoprecipitation

IPF: Idiopathic Pulmonary Fibrosis

iPSC: Induced pluripotent stem cell

IRES: Internal ribosome entry site

K: Lysine

kb: Kilobase

kDa: KiloDalton

K-rich: Lysine rich

Las1L: Ribosomal biogenesis protein, LAS1 (lethality in absence of SSD1-v) homologue

LCR: Low complexity region

LLPS: Liquid-liquid phase separation

lncRNA: Long non-coding RNA

MD: Methyltransferase domain

MDN1: Midasin, or Dynein-related AAA-ATPase

MMS21: E3 SUMO-protein ligase Nse2

Mps3: Monopolar spindle protein 3

mRNA: Messenger RNA

MS: Mass spectometry

MTR4: Exosome RNA helicase (TRAMP-like complex helicase)

NAF1: Nuclear assembly factor 1

NB: Nuclear body

ncRNA: Non-coding RNA

NE: Nuclear envelope

Net1: Nucleolar silencing establishing factor and telophase regulator 1

NEXT: Nuclear exosome targeting

NHEJ: Non-Homologous End-Joining

NHP2: Nucleolar protein family A member 2

N/NoLS: Nuclear/nucleolar localization signal

NNS: Nrd1-Nab3-Sen1 complex

NOB: A small stretch of hydrophobic residues N-terminal of the OB fold in TPP1

NOP10: Nucleolar protein 10

Nopp140: 140kDa nucleolar phosphoprotein

NORs: Nucleolar organizer regions

NPC: Nuclear pore complex

NPM1: Nucleophosmin

nt: Nucleotide(s)

NTE: N-terminal extension

N-terminal: Amino-terminal

OB: Oligosaccharide/oligonucleotide binding

Pab2: Poly(A)-binding protein 2

PABPN1: Nuclear poly(A)-binding protein 1

PAGE: Polyacrylamide gel electrophoresis

PAPD5 (Trf4-2): Polyadenylation polymerase-associated domain-containing protein 5 (Terminal nucleotidyltransferase 4B)

PARN: Polyadenosine-specific ribonuclease

PCR: Polymerase chain reaction

PELP1: Proline-, glutamic acid- and leucine-rich protein 1

Pla1: Polyadenylation polymerase 1

PML: Promyelocytic leukemia

PML NBs: PML nuclear bodies

Poly(A): Polyadenylation

POT1: Protection of telomeres 1

pre-rRNA: Precursor rRNA

PUA: Pseudouridine synthase and archaeosine transglycosylase

qPCR: Quantitative RT-PCR

Rad52: DNA repair and recombination 52kDa protein

RAP: Repeat addition processivity

Rap1: Repressor/activator protein 1

rDNA: Ribosomal DNA

RNA: Ribonucleic acid

RNAPI: RNA polymerase I

RNAPII: RNA polymerase II

RNase: Ribonuclease

RNP: Ribonucleoprotein

rRNA: Ribosomal RNA

RRP6: Ribosomal RNA-processing protein 6 (exosome complex exonuclease)

RRP40: Ribosomal RNA-processing protein 40

RS: Revesz Syndrome

RT: Reverse transcriptase

SAE1: SUMO-activating subunit 1

SAE2: SUMO-activating subunit 2

scaRNA: Small Cajal body specific RNA

SDS-PAGE: Sodium dodecyl sulfate polyacrylamide gel electrophoresis

SENP: Sentrin-specific protease/SUMO-specific protease

Siz2: SAP and Miz-finger domain-containing protein 2, E3 SUMO-protein ligase

shRNA: Small hairpin RNA

SHQ1: Small nucleolar RNAs of the box H/ACA family quantitative accumulation protein 1

SIM: SUMO-interacting motif

siRNA: Small interfering RNA

Slx5: Synthetic lethal of unknown function protein 5, E3 ubiquitin-protein ligase complex SLX5-SLX8 subunit

SMC: Structural maintenance of chromosomes

SMN: Survivor of motor neuron

Smt3: Suppressor of Mif Two, Ubiquitin-like protein

snRNA: Small nuclear RNA

snoRNA: Small nucleolar RNA

STUbL: SUMO-targeted ubiquitin ligase

SUMO: Small ubiquitin-like modifier

SUN: Sad1p/UNC-84 protein domain

TCAB1 (WDR79): Telomerase Cajal body protein 1 (WD repeat-containing protein 79)

TEL: TPP1 glutamate (E) and leucine (L)

TEN: Telomerase essential N-terminal

TERT: Telomerase reverse transcriptase

TEX10: Testis-expressed protein 10

TIN2: TRF1-interacting protein 2

t-loop: Telomeric loop

TMG: Trimethylguanosine

TPP1: Tin1/PTOP-PIP1

TRAMP: Trf4/5-Air1/2-Mtr4 complex

TRAP: Telomeric repeat amplification protocol

TRIM: Tripartite Motif

TRF1: Telomeric repeat-binding factor 1

TRF2: Telomeric repeat-binding factor 2

TR: Telomerase RNA

TGS1: Trimethylguanosine synthase 1

Tof2: Topoisomerase 1-associated factor 2

Uba2: Ubiquitin-activating enzyme E1-like subunit 2

UBC9: Ubiquitin carrier protein 9/RING-type E3 SUMO transferase

UBF: Upstream binding factor

Ulp1: Ubiquitin-like-specific protease 1

Ulp2: Ubiquitin-like-specific protease 2

UTR: Untranslated region

VEGF: Vascular endothelial growth factor

WD: Tryptophan-aspartic acid dipeptide

WDR18: WD repeat-containing protein 18

WT: Wildtype

X-DC: X-linked DC

XRN1: 5'-3' Exoribonuclease 1

ZCCHC8: Zinc finger CCHC domain-containing protein 8

Figures List

Supplemental Figure 3.5: Interaction between FLAG-dyskerin and HA-GAR1

Supplemental Figure 3.6: Localization of C-terminal SUMO3-fusions

Introduction

Eukaryotic organisms with linear chromosomes face the molecular dilemma of protecting chromosomal ends from being recognized as DNA breaks, while also preventing loss of genomic information incurred through progressive chromosome shortening caused by the semi-conservative replication of DNA (Levy, Allsopp et al. 1992). The human genome is no exception to this dilemma at DNA ends [known as telomeres]. Telomeric integrity has implications in both cancer and aging, as telomere attrition serves as a key checkpoint in the control of cell proliferation by triggering replicative senescence. There are two broadly defined mechanisms of telomere maintenance in humans: telomerase-mediated maintenance and ALT (alternative lengthening of telomeres). However, the complexity of each of these mechanisms is clear and becomes more evident with every new publication in the field of telomere biology. Approximately 80% of cancers are immortalized by constitutive activation of telomerase to maintain telomeres throughout rapid proliferation (Shay, Reddel et al. 2012). Additionally, defects in telomerase and other telomere maintenance components cause premature aging syndromes like dyskeratosis congenita, due to progressive telomere shortening and subsequent proliferative blocks (Holohan, Wright et al. 2014). As such, greater knowledge of telomerase and its regulation of telomere homeostasis will contribute to our understanding of human disease and natural cellular processes alike.

There are a variety of telomerase components, whether considered part of the active holoenzyme or indirect regulators of telomerase activity. *In vitro* telomerase activity can be reconstituted minimally with the catalytic subunit hTERT (human telomerase reverse transcriptase) in combination with its guide and template RNA component hTR (human telomerase RNA) (Greider and Blackburn 1989, Weinrich, Pruzan et al. 1997, Beattie, Zhou et al. 1998). However, what has been reported as essential for telomerase activity *in vivo* includes functions of RNA processing and biology, proper enzymatic assembly and trafficking, and stimulation of activity at the telomeric substrate itself.

Assessing the regulation and involvement of the telomerase-associated and H/ACA ribonucleo- protein dyskerin in mammalian telomerase biogenesis, assembly, and activity is the unifying focus of this thesis. A conserved H/ACA-box motif at the 3′ terminus of telomerase RNA components (Mitchell, Cheng et al. 1999) has co-opted dyskerin (and other H/ACA ribonucleoprotein factors) into telomerase biology for vertebrates, though the essentiality of

dyskerin as a nucleolar and Cajal body pseudouridine synthase extends beyond telomere maintenance (Wang and Meier 2004). The first chapter of this thesis work characterizes the involvement of human dyskerin in hTR biogenesis and accumulation in a disease context. The second chapter of this thesis fundamentally characterizes how regulation of dyskerin nuclear and subnuclear localization occurs and contributes to function. Taken together, the research carried out for this thesis aims towards a better understanding of dyskerin biology, contributing novel insights into both disease-relevant and basic cellular mechanisms of dyskerin regulation and function.

Chapter 1: Literature Review

1.1 Telomeres and Telomerase

In the late 1930's, Hermann Muller (studying *Drosophila melanogaster*) and Barbara McClintock (studying *Zea mays)* proposed that the ends of chromosomes, coined telomeres were unique structures required to prevent the end-to-end fusions that take place between broken chromosomes (McClintock 1938, McClintock 1939). This hypothesis was made even before the genetic material was known to be DNA, and well before more detailed characterization of telomeric sequences themselves by Elizabeth Blackburn, Jack Szostak, and Carol Greider in the 1980's, who would each go on to be awarded the 2009 Nobel Prize in Physiology or Medicine for their discoveries surrounding the DNA-protective role of telomeres and how telomeres are maintained by the reverse transcriptase enzyme telomerase (Szostak and Blackburn 1982, Greider and Blackburn 1985, Greider and Blackburn 1989). The initial discovery of a repetitive noncoding telomere sequence was made through studying the ciliate model organism *Tetrahymena thermophila*, and this opened the door for discovering telomere sequences and properties in other organisms. In humans, telomeres are comprised of 5-15kb of double stranded DNA repeats encoding 5′-TTAGGG-3′ which end in a single stranded 3′ G-rich overhang of about 50-300 bases [Figure 1.1A] (Moyzis, Buckingham et al. 1988, Makarov, Hirose et al. 1997, Wright, Tesmer et al. 1997).

Telomere maintenance is an essential regulator of cellular lifespan, mediating when a cell reaches the maximum number of divisions it can safely undergo before entering into replicative senescence, known as the Hayflick limit of a cell (Hayflick 1965). Telomere attrition occurs with each replication of DNA during cell division, due to the limitation of the conventional DNA polymerase to synthesize DNA in a 5′ to 3′ direction and a requirement for a temporary RNA primer to initiate this directional DNA synthesis (Lingner, Cooper et al. 1995). Eventually, successive cell divisions lead to shortened telomeres which are unable to sufficiently protect DNA ends from DNA damage signaling typically initiated by double stranded DNA breaks, thus activating DNA damage checkpoints and triggering entry into replicative senescence (d'Adda di Fagagna, Reaper et al. 2003). Most somatic cells lack telomerase, allowing this telomere attrition-mediated signaling to appropriately dictate when a cell enters into senescence (Bodnar, Ouellette et al. 1998) and therefore serving as an important anti-tumorigenic regulatory mechanism that prevents unchecked proliferation. In the germline and somatic stem cells,

telomerase expression extends proliferative life-span and contributes to the importance of these cells in contexts which are highly reliant on cell turnover (Wright, Piatyszek et al. 1996). Contrarily, cells which are able to bypass the replicative senescence checkpoint and activate telomerase expression gain replicative immortality, a hallmark of cancer [Figure 1.1B] (Hanahan and Weinberg 2000, Hanahan and Weinberg 2011).

In addition to DNA maintenance by telomerase, human telomeres are protected by a complex of six proteins known as shelterin [Figure 1.1A]. This complex directly recognizes telomeric DNA through the double-stranded DNA binding components TRF1 and TRF2 (telomere repeat-binding factors 1 and 2), and single-stranded DNA binding protein POT1 (protection of telomeres 1). TIN2 (TRF1-interacting nuclear factor 2) and TPP1 – previously known as TINT1 (TIN2 interacting protein), PTOP (POT1 and TIN2 organizing protein) and PIP1 (POT1 interacting protein) – bridge the double- and single-stranded DNA binding components, while the TRF2-binding protein RAP1 (repressor activator protein 1) functions in regulating telomerase activity based on the number of telomeric DNA repeats present in a given substrate (Baumann and Cech 2001, Ye, Donigian et al. 2004, Palm and de Lange 2008). This protein complex serves several key purposes at the telomere, contributing to DNA protection, telomerase recruitment, and telomerase stimulation.

Figure 1.1 – Telomere Maintenance and Cell Lifespan

A. Telomeres are the tandem repeats of double stranded and single stranded DNA at chromosome ends. In humans, the double stranded telomere ranges from 5-15kb, while the single stranded overhang ranges from 50-300 bases. One telomeric repeat is six bases (TTAGGG). The shelterin components TRF2 and TRF1 each form homodimers which interact with double stranded telomeric repeats, and help regulate dynamic folding and unfolding of telomeric structures like t-loops (invasion of the single stranded overhang into the double stranded telomere DNA, bottom panel). The bridging shelterin component TIN2 interacts with both TRFs, as well as with the shelterin component responsible for telomerase recruitment and stimulation, TPP1. TPP1 regulates recruitment of telomerase through interactions with hTERT, which is shown here bound to substrate single stranded telomeric DNA, and assembled with hTR and the dimeric heterotetramer H/ACA complex components dyskerin, GAR1, NOP10, and NHP2. TPP1 forms a heterodimer with the single strand-binding protein POT1, which functions with TPP1 to stimulate telomerase processivity, but also negatively regulates telomerase activity through recruitment of the CST complex (CTC1/STN1/TEN1 fill-in complex, not shown). RAP1 binds TRF2, but is dispensable for telomere capping in humans.

B. Telomere length and attrition regulate cellular lifespan, and baseline levels of telomerase dictate the amount of telomere shortening a cell undergoes over the course of its lifespan. In normal somatic cells lacking telomerase activity, telomere attrition leads to cellular senescence checkpoint activation (indicated by the red stop sign on the X-axis). If cells bypass this checkpoint (for instance due to defective DNA damage signalling) and continue to grow, the resulting telomere attrition will eventually lead to cell crisis (orange crossed circle) and cell death (☠). Approximately 80% of cancers achieve immortality through aberrant activation of telomerase, allowing them to maintain their telomeres, whereas cells which sustain proliferative compartments of the body, such as germ and stem cells, have higher baseline telomerase activity and thus maintain their telomere length longer through their lifespan.

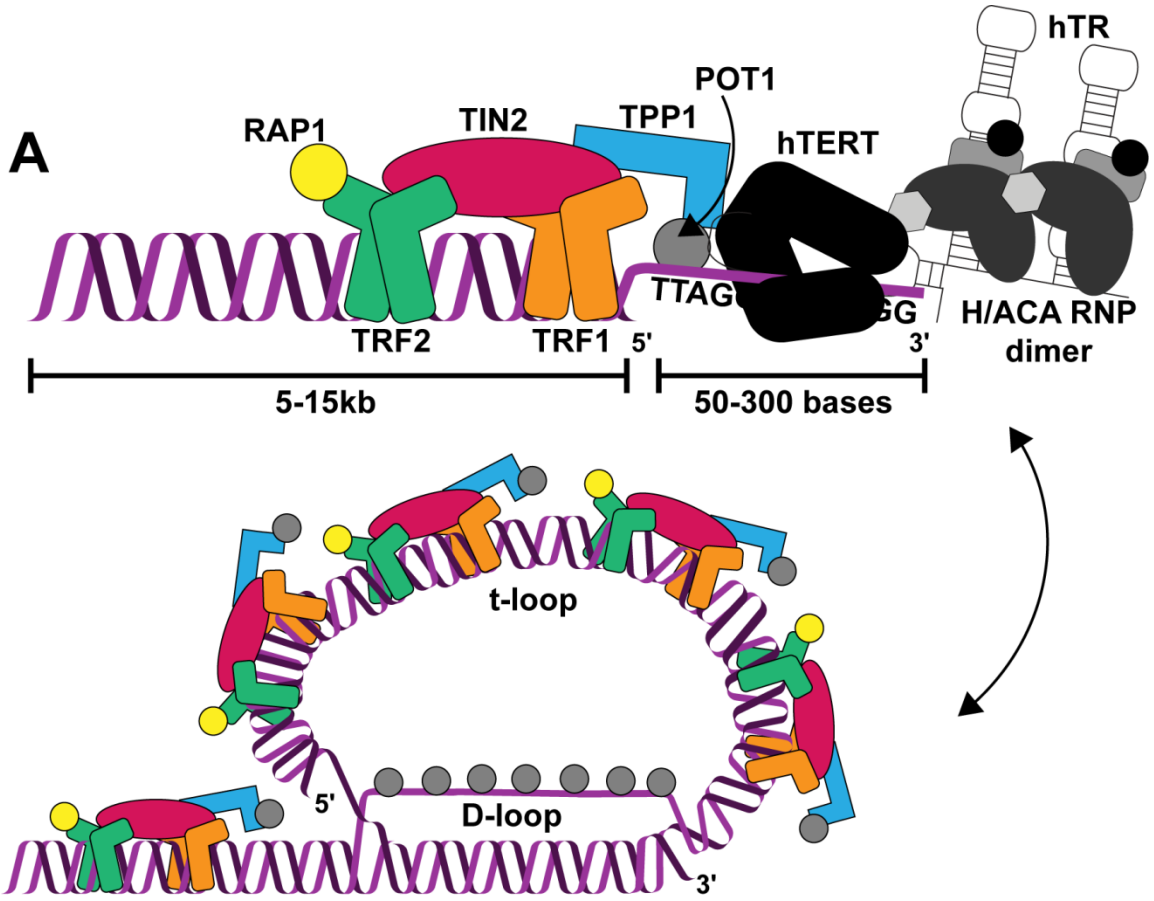
A
hTR
POT1
RAP1
TIN2
TPP1
hTERT
TTAG
GG
H/ACA RNP
dimer
TRF2
TRF1
5'
3'
5-15kb
50-300 bases
t-loop
D-loop
5'
3'

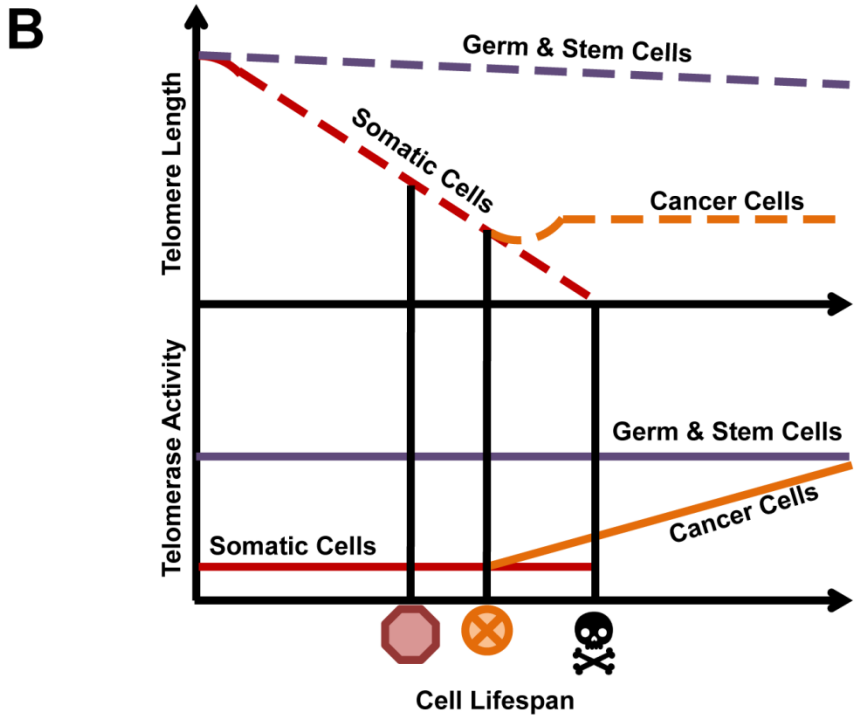
B
Germ & Stem Cells
Somatic Cells
Cancer Cells
Telomere Length
Telomerase Activity
Germ & Stem Cells
Cancer Cells
Somatic Cells
Cell Lifespan

1.1.1 DNA Protection

The repetitive sequence and single-stranded DNA 3′ overhang at telomeres facilitate the formation of complex nucleic acid structures which contribute to telomere protection from the DNA damage response. In particular, telomere loops (t-loops) are formed by invasion of the 3′ overhang into the upstream region of double-stranded telomeric DNA [Figure 1.1A, bottom panel], thus hiding the overhang from recognition as damaged DNA and preventing telomere end-to-end fusions by unwanted non-homologous end joining (NHEJ) (Griffith, Comeau et al. 1999). Formation of a t-loop also necessitates formation of another nucleic acid structure known as a displacement loop (D-loop), which is aptly named as it is produced by the double-stranded telomeric DNA displaced by single-stranded overhang invasion. These structures do not exist as naked nucleic acids, but rather are coated by shelterin complexes. The double-stranded DNA-binding shelterin components TRF1 and TRF2 have been shown to act mostly as negative regulators at the telomere (van Steensel and de Lange 1997). The silencing of these two shelterin proteins leads to telomere elongation, and their overexpression is negatively correlated with telomere length (van Steensel and de Lange 1997, Nandakumar and Cech 2013). These shelterin components affect the available state of the telomeric substrate, as their binding to the double-stranded telomeric DNA drives formation of and stabilizes t-loops (Griffith, Comeau et al. 1999), contributing to the t-loop protective function, and also blocking the telomerase docking site and therefore unregulated telomere elongation.

1.1.2 Telomerase Recruitment

In an endogenous cellular setting, the amounts of telomerase and telomeric substrate are both insufficient for diffusion-mediated encounters to facilitate enzymatic activity. As such, active recruitment of telomerase to its substrate is a necessary regulatory step in telomere maintenance [Figure 1.1A, top panel]. Here too, shelterin plays a role in telomere maintenance, beyond DNA protection. A group of amino acids in the N-terminal OB-fold of TPP1 referred to as the TEL [TPP1 glutamate and leucine-rich] patch directly interacts with the TEN [TERT Essential N-terminal] domain of hTERT (Nandakumar, Bell et al. 2012, Sexton, Youmans et al. 2012, Zhong, Batista et al. 2012, Schmidt, Dalby et al. 2014). Mutating either of these regions and abolishing the interaction prevents telomerase recruitment and telomeric maintenance (Schmidt, Dalby et al. 2014). A study making use of live cell imaging to observe telomerase trafficking in human cells demonstrates the essentiality of this TPP1-hTERT interaction for

recruitment of the enzyme to the telomere (Schmidt, Zaug et al. 2016). Schmidt, Zaug, & Cech observed three distinct populations of hTERT during S phase: one static population of hTERT at subnuclear compartments known as Cajal bodies (CBs); a second static population at the telomere, presumably elongating the end; and a third highly dynamic population diffuse throughout the nucleus and displaying short interactions with chromosome ends, scanning for telomeres in need of elongation. These dynamics are consistent with live cell imaging of the telomerase RNA component in humans, which also demonstrates two telomerase populations at the telomere; one hTR population with shorter telomere residency, and another with slower diffusive properties dependent on TPP1-mediated recruitment, indicating retention of telomerase at the telomere (Laprade, Querido et al. 2020). A separation of function mutation in the TEN domain of hTERT, which renders the enzyme fully active but unable to interact with TPP1, abolishes localization of both static and dynamic hTERT populations to the telomere (Schmidt, Zaug et al. 2016). Furthermore, the small stretch of hydrophobic residues N-terminal of the OB fold (termed NOB) in TPP1 which are unique to humans have also been found to help mediate the TPP1-hTERT interaction, as it pertains to recruitment of telomerase to the telomere, as well as in stimulation of telomerase function once recruited (Grill, Tesmer et al. 2018). Through its TEL patch and NOB region, TPP1 plays a key role in bringing telomerase to the telomeric substrate.

A recruitment function of the shelterin component TIN2 that is separable from its TPP1-interaction has also been identified (Frank, Tran et al. 2015). More specifically, a TIN2 mutant identified in dyskeratosis congenita patients was reported to localize and function at the telomere, with the exception of failed telomerase recruitment. This failed recruitment led to accelerated telomere shortening due to a lack of telomerase-mediated extension (Frank, Tran et al. 2015), consistent with a previous report that this mutant immunoprecipitates less active telomerase than wild-type TIN2 (Yang, He et al. 2011). Importantly, this mutant TIN2 was still able to anchor TPP1 at the telomere. Additionally, though telomerase recruitment was reduced by expression of the mutant TIN2, some telomeres were still extended normally (Frank, Tran et al. 2015). This supports a separation of the TPP1/shelterin-mediated recruitment functions from telomerase stimulatory roles.

Notably, hTERT also contains a region which makes it unique among reverse transcriptase enzymes: the insertion in fingers domain (IFD) located within the reverse

transcriptase motifs (Lue, Lin et al. 2003). The IFD has been characterized to foster recruitment of hTERT to the telomere (D'Souza, Chu et al. 2013) in a TPP1 dependent manner (Chu, D'Souza et al. 2016, Chu, MacNeil et al. 2016). Defects in telomeric association (assessed by fluorescence *in situ* hybridization of hTR/telomere co-localization) and telomere binding (assessed by telomeric chromatin immunoprecipitation) were observed for several IFD variants. These defects could be rescued by TPP1 overexpression for some, but not all IFD variants, indicating that IFD mutants can render hTERT recruitment by TPP1 sub-optimal or entirely impossible (Chu, D'Souza et al. 2016, Chu, MacNeil et al. 2016). It was speculated that these recruitment defects may be mediated through conformational changes to the TEN domain, supported by the proximity of the IFD to the TEN domain in recent cryo-electron microscopy (cryo-EM) mapping of the *Tetrahymena thermophila* TERT (Jiang, Chan et al. 2015), and an even more recent cryo-EM structure of *Tetrahymena* telomerase with a telomeric substrate, which demonstrated the proximity of the IFD to both the *Tetrahymena* TPP1 orthologue and the TEN domain of TERT (Jiang, Wang et al. 2018). More recently still, it was biochemically demonstrated that both the TEN domain and a region of the IFD termed IFD-TRAP can mediate the interaction between hTERT and human TPP1, as swapping these regions into the mouse TERT homologue allows the mouse TERT homologue to uniquely and specifically interact with human TPP1 (Tesmer, Smith et al. 2019).

1.1.3 Telomerase Activity and Stimulation

Telomere synthesis by hTERT is guided and templated by hTR. The template region of hTR is complementary to approximately two telomeric repeats, and is reverse transcribed into DNA by hTERT, forming the short tandem telomeric repeats present at human chromosome ends (Feng, Funk et al. 1995). A newly synthesized strand of telomeric DNA is translocated in a 5′ direction, allowing for processive synthesis of repeats on the same telomere by telomerase. This repetitive addition processivity (RAP) is a unique characteristic of the telomerase enzyme, and is the ability of hTERT to add multiple telomeric sequences at the same telomeric substrate without completely dissociating from the substrate (Greider 1991). RAP of telomerase is distinct from telomerase activity, which is the capacity of the enzyme to elongate the telomere at the G-rich single-stranded overhang. Recently, a high resolution single molecule analysis of telomerase using optical tweezers demonstrated the kinetics of telomerase RAP (Patrick, Slivka et al. 2020). This study by Patrick

et al. confirmed that telomerase associates with the telomeric DNA substrate through both hTR base pairing with the telomere and through an hTERT anchor site, allowing for multiple cycles of telomeric repeat synthesis, telomerase translocation, and hTR-telomere DNA substrate re-annealing to occur without product release from the telomerase anchor site (Patrick, Slivka et al. 2020).

The TEN domain of hTERT is responsible for anchoring telomerase to the single stranded DNA next to the primer-template site where hTR hybridizes with its substrate (Lue 2004, Moriarty, Ward et al. 2005). As such, the TEN domain helps regulate telomerase RAP through mediating stability of the RNA/DNA hybrid at the telomere. Mutations in the TEN domain can reduce this stability and cause failed telomeric primer elongation (Akiyama, Parks et al. 2015). Moreover, certain residues in the IFD are also critical for regulating telomerase activity and RAP. Some IFD variants (such as V763S) have reduced telomerase activity but unaffected RAP, while others (such as V791Y and L805A) are defective in both activity and RAP (D'Souza, Chu et al. 2013, Chu, D'Souza et al. 2016). As discussed above regarding telomerase recruitment, the IFD interfaces with both the TEN domain as well as the shelterin component TPP1. As such, it is likely that IFD regulation of telomerase activity and processivity is due to defective interactions between hTERT and the TPP1/POT1 complex. In addition to its aforementioned role in recruitment, TPP1 has been demonstrated to regulate telomerase processivity (Wang, Podell et al. 2007). Specifically, the TPP1/POT1 heterodimer stimulates telomerase processivity in a TPP1 OB domain-dependent manner (Nandakumar, Bell et al. 2012, Sexton, Youmans et al. 2012, Kocak, Ballew et al. 2014, Schmidt, Dalby et al. 2014, Sexton, Regalado et al. 2014) . The aforementioned RAP and activity defects of IFD variants were observed *in vitro* using a direct primer extension assay, and as such can be separated from telomerase recruitment *per se*.

It is important to note that POT1 has also been observed to act as an inhibitor of telomere elongation, and was postulated to dually regulate telomerase activity and RAP by promoting telomerase translocation when complexed with TPP1, as well as independently functioning as a stop sign at the end of the overhang when telomerase is not needed (Baumann and Price 2010, Gomez, Armando et al. 2012). However, the inhibitory role of POT1 may be an indirect recruitment-related regulation. Interestingly, though the TPP1/POT1 heterodimer stimulates telomerase activity and processivity *in vitro* (Schmidt, Dalby et al. 2014), it was also recently

speculated that the known POT1-mediated negative regulation of telomerase *in vivo* may function through telomeric recruitment of the CST (CTC1/STN1/TEN1) fill-in complex, which can occlude telomerase recruitment and activity (Takai, Jenkinson et al. 2016). A mutated POT1 protein identified in two patients with the autosomal recessive disorder Coats plus (CP) was reported to function canonically with respect to telomeric localization, TPP1 interaction, and protection against inappropriate ATR kinase-mediated DNA damage response at the telomere. However, CP POT1 was unable to negatively regulate telomerase, causing defects in telomere processing and leading to unstable extended 3′ overhangs (Takai, Jenkinson et al. 2016). This is similar to what is observed in cells from CP patients with mutant CST complex component CTC1. These patients display a failure to fill-in the 5′ telomeric C-strand, thus suggesting a cooperative role between POT1 and CST in the negative regulation of telomerase recruitment to the telomeres (Wu, Takai et al. 2012, Takai, Jenkinson et al. 2016).

1.2 hTR Biogenesis and Processing

Protection and maintenance of the telomere is mediated by an intricate interplay of telomeric DNA, shelterin, and telomerase. Beyond the telomerase catalytic component hTERT, telomerase function and consequently telomere maintenance relies on a key RNA component – hTR. The mature RNA guide and template component of telomerase is a highly divergent transcript, varying across species with respect to sequence, length, structure, and synthesis (Greider and Blackburn 1987, Feng, Funk et al. 1995, Podlevsky, Bley et al. 2008). In humans, mature hTR is a non-polyadenylated 451nt product of RNA polymerase II (RNAPII) transcription (Feng, Funk et al. 1995). In contrast to fungal TRs (telomerase RNAs) which structurally resemble snRNAs (small nuclear RNAs) (Seto, Zaug et al. 1999, Leonardi, Box et al. 2008, Webb and Zakian 2008), hTR contains a conserved H/ACA-box motif at its 3′ terminus similar to that of the so-named H/ACA small nucleolar (sno-) and small Cajal body specific (sca) RNAs (Mitchell, Cheng et al. 1999, Chen, Blasco et al. 2000, Jady, Bertrand et al. 2004). This hairpin-hinge-hairpin-tail structural motif fosters interactions with a wide variety of processing and ribonucleoprotein (RNP) assembly factors, including co-transcriptional association with the H/ACA pre-RNP complex components dyskerin, NOP10 (nucleolar protein 10), NHP2 (nucleolar protein family A member 2), and NAF1 (nuclear assembly factor 1) [Figure 1.2A] (Egan and Collins 2012). More specifically, hTR is considered a scaRNA due to the presence of a CAB-box motif in its conserved region (CR) 7 (Jady, Bertrand et al. 2004, Cristofari, Adolf et

al. 2007). While not needed for telomerase activity *in vitro*, the H/ACA domain of hTR is required for its *in vivo* accumulation and telomerase biogenesis (Mitchell, Cheng et al. 1999, Bachand and Autexier 2001). Unlike most human sno/scaRNAs which are exonucleolytically processed from spliced pre-mRNA introns (Kiss, Fayet et al. 2006), hTR synthesis is more similar to that of yeast snoRNAs in that it is an independent transcriptional unit of RNAPII (Feng, Funk et al. 1995, Fu and Collins 2003, Dieci, Preti et al. 2009). Furthermore, as is the case for many RNAPII transcripts (Richard and Manley 2009), hTR species are initially polyadenylated and possess genomically encoded 3′ extensions due to RNAPII read-through, and these species then undergo processing posttranscriptionally into a mature form (Theimer, Jady et al. 2007, Goldfarb and Cech 2013, Tseng, Wang et al. 2018, Roake, Chen et al. 2019). Recent advances have been made towards elucidating the mechanisms behind this processing and quality control of hTR maturation and accumulation [Figure 1.2]. As such, it is becoming increasingly clear that these mechanisms are yet more examples of TR divergence.

Figure 1.2 – Biogenesis of hTR (figure adapted from (MacNeil, Bensoussan et al. 2016))

A. The H/ACA pre-RNP (ribonucleoprotein) complex involving dyskerin, NOP10, NHP2, and NAF1 co-transcriptionally assembles on the 3′ hairpin-hinge-hairpin-tail structure of hTR, possibly mediating RNAPII transcription termination. RNAPII read-through can generate 3′ extended hTR products, which need to be processed into mature hTR or degraded. The generation of shorter extended products versus longer extended products due to RNAPII read-through may be regulated by assembly of the H/ACA pre-RNP. The specific definition of what constitutes a short versus long extension varies among and is sometimes absent from reports in the literature. Trimethylation of the 5′ guanosine (TMG) cap by TGS1 regulates CBCA complex occupancy, and prevents over-accumulation and cytosolic mislocalization of hTR.

B. Defects in dyskerin-hTR interactions and H/ACA RNP assembly lead to the generation of long extended hTR species, which can be exported to the cytosol for DCP2/XRN1 mediated degradation. It is possible that this export occurs in the absence of NEXT recruitment (of which ZCCHC8 is a component) through CBCA, as NEXT is involved in the recruitment of the nucleolar Rrp6 exosome. It is possible that hTR would still undergo hypermethylation by TGS1 in this context of deficient H/ACA complex formation, and as such aberrant shuttling out of the nucleus leads to DCP2-mediated decapping due to the TMG, and subsequently is degraded by downstream XRN1. The Rrp6-mediated human exosome may be involved in both maturation and degradation pathways for extended products, in conjunction with the micro-RNA processing component DGCR8. Long extended precursors lacking an H/ACA complex undergo rapid degradation.

C. Long extended precursors of hTR that are protected by dyskerin and the H/ACA complex (and therefore do not form tertiary structures that promote degradation) may undergo initial trimming by the Rrp6 exosome in an hTRAMP-mediated polyadenylation-dependent manner. hTRAMP is conventionally responsible for adding shorter poly(A) tails than the canonical polyadenylation machinery, and can be recruited to RNA substrates by CBCA. Short extended polyadenylated hTR species undergo trimming by PARN to become mature 451nt hTR, or are degraded by the Rrp6 exosome in the absence of PARN.

D. Short extended species of hTR are targeted for processing by hTRAMP/PAPD5-mediated polyadenylation and/or through the canonical polyadenylation machinery involving PAPα/γ, in a PABPN1 and PARN dependent manner. Poly(A) tails added by the hTRAMP complex may be extended by PAPα/γ to generate PABPN1/PARN processing targets. Given that CBCA is known to recruit hTRAMP and repress PARN, the presence of CBCA at the pre-hTR species 5′ end may be relevant in mediating these pathways, and under normal conditions the removal of CBCA due to TMG capping by TGS1 should take place upstream of trimming of hTR precursors. However, the absence of the TMG cap due to TGS1 depletion (and thus persistent CBCA assembly with hTR) does not disrupt processing or polyadenylation, but rather leads to accumulation of hTR species overall. Importantly, while polyadenylation/deadenylation has been shown to regulate maturation rates of short extended hTR species rather than mediating degradation/quality control, in the absence of the H/ACA complex, PARN is capable of degrading hTR beyond the mature end. This adapted figure is reprinted from (MacNeil, Bensoussan et al. 2016) in accordance with the MDPI Open Access Information and Policy.

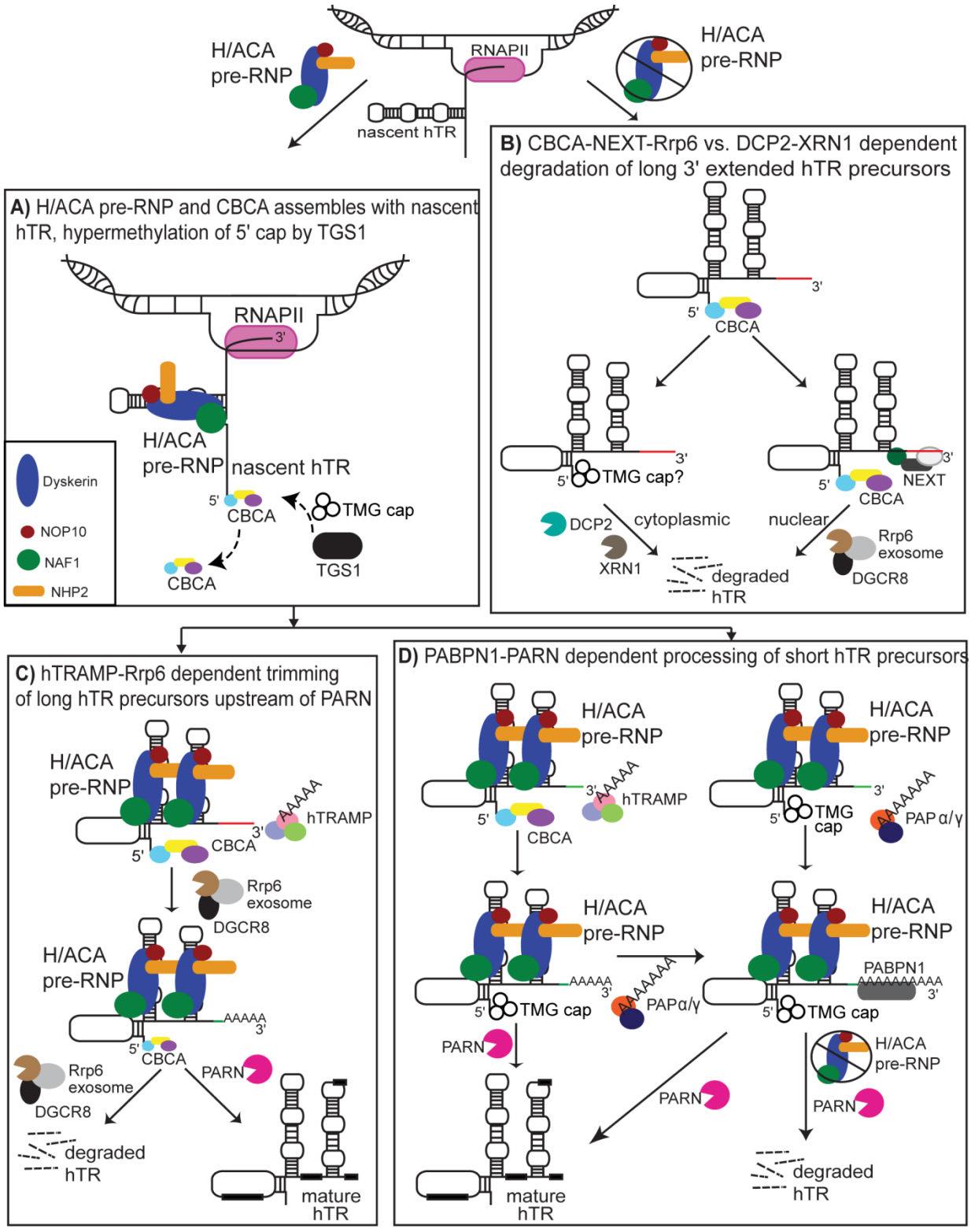
H/ACA
pre-RNP
RNAPII
nascent hTR
H/ACA
pre-RNP
A) H/ACA pre-RNP and CBCA assembles with nascent hTR, hypermethylation of 5' cap by TGS1
RNAPII
3'
H/ACA
pre-RNP
nascent hTR
5'
CBCA
TMG cap
TGS1
CBCA
Dyskerin
NOP10
NAF1
NHP2
B) CBCA-NEXT-Rrp6 vs. DCP2-XRN1 dependent degradation of long 3' extended hTR precursors
3'
5'
CBCA
TMG cap?
NEXT
DCP2
cytoplasmic
nuclear
XRN1
degraded
hTR
Rrp6
exosome
DGCR8
C) hTRAMP-Rrp6 dependent trimming of long hTR precursors upstream of PARN
H/ACA
pre-RNP
AAAAA
hTRAMP
CBCA
Rrp6
exosome
DGCR8
PARN
degraded
hTR
mature
hTR
D) PABPN1-PARN dependent processing of short hTR precursors
TMG
cap
PAP α/γ
PABPN1
PAPα/γ

1.2.1 hTR and the Spliceosome

Two main mechanisms of TR processing have been reported in yeast. One seemingly common pathway of 3′ TR maturation among fungi including fission yeast (*Schizosaccharomyces pombe*) resembles a removal mechanism for improper splicing products (Box, Bunch et al. 2008, Gunisova, Elboher et al. 2009). However, Tseng *et al.* provided evidence against the involvement of the spliceosome in hTR 3′ processing, demonstrating that while the spliceosomal inhibitor isoginkgetin contributed to accumulation of 3′ extended hTR, another spliceosome inhibitor spliceostatin A had no effect. Furthermore, modification of potential 5′ splice sites downstream of the mature hTR 3′ terminus did not affect the number of accumulated long products. Rather, they found the hTR processing effects of isoginkgetin resembled those of exosome inhibition (Tseng, Wang et al. 2015).

1.2.2 hTR and the Exosome

Interestingly, the other previously reported mechanism of TR processing in yeast (more specifically, in the budding yeast *Saccharomyces cerevisiae*) relies on the nuclear exosome for trimming or degradation of precursors and extended products (Jamonnak, Creamer et al. 2011, Kuehner, Pearson et al. 2011, Noel, Larose et al. 2012). This pathway reported in *S. cerevisiae* relies on transcriptional termination mediated by the NNS (Nrd1-Nab3-Sen1) complex, which recruits the non-canonical nuclear polyadenylation TRAMP (Trf4/5-Air1/2-Mtr4) complex. Another polyadenylation-dependent processing pathway resembling mRNA 3′ maturation has been reported for snoRNAs in *Schizosaccharomyces pombe*, involving the canonical polyadenylation polymerase Pla1 and the poly(A)-binding protein Pab2 (Grzechnik and Kufel 2008, Lemay, D'Amours et al. 2010). Ultimately, both of these pathways recruit the nuclear exosome involving Rrp6 as the exonuclease subunit for processing or degradation (Mitchell 2014). Excluding the NNS complex which does not appear to be conserved in mammals (Porrua and Libri 2015), human analogues of the key components in these pathways are beginning to be examined for hTR maturation. A role for the nucleolar human Rrp6-exosome in quality control of hTR-extended products has been proposed by several groups (Macias, Cordiner et al. 2015, Nguyen, Grenier St-Sauveur et al. 2015, Tseng, Wang et al. 2015, Shukla, Schmidt et al. 2016), and this involvement is at least in part dependent upon a non-canonical role of the micro-RNA processing component DGCR8 (DiGeorge critical region 8) (Macias, Cordiner et al. 2015). Tseng *et al.* reported that inhibition and knockdown of the exosome leads to accumulation of

long hTR precursors/3′ extended hTR transcripts, and that exosomal degradation of these products is dependent upon the 5′ CBCA (cap-binding complex A) along with its recruitment of the NEXT (nuclear exosome targeting) complex [Figure 1.2B] (Macias, Cordiner et al. 2015). The accumulation of 3′ extended hTR species upon depletion of any of these three complexes suggests a functional conservation between NEXT and the NNS transcription termination complex, as the CBC in *S. cerevisiae* is necessary for co-transcriptional recruitment of the NNS to promote proper termination and 3′ end processing of RNAPII transcripts (Vasiljeva and Buratowski 2006, Tseng, Wang et al. 2015). The essentiality of the NEXT complex in mediating hTR levels is emphasized by the recent identification of a heterozygous loss of function mutant of the NEXT complex component ZCCHC8 in a patient with an autosomal dominant form of the telomere syndrome familial idiopathic pulmonary fibrosis (Gable, Gaysinskaya et al. 2019). This mutation leads to reduced hTR levels overall, and an increased amount of 3′ extended hTR species due to haploinsufficiency of ZCCHC8. It has also been further elucidated that longer 3′ extended hTR species are favoured for degradation by the Rrp6-exosome due to unique tertiary RNA interactions which form 3′ of the mature hTR terminus. These tertiary RNA interactions are prevented *in vitro* by dyskerin and the H/ACA complex, allowing extended hTR species to undergo processing rather than degradation (Tseng, Wang et al. 2018). Interestingly, under normal conditions, the Rrp6-exosome is capable of acting in an initial trimming step of longer 3′ extended species, which are then further processed into mature hTR by the polyadenosine-specific ribonuclease (PARN) [Figure 1.2C] (Tseng, Wang et al. 2018). A model of TRAMP-mediated exosomal degradation of extended hTR products was also proposed by Nguyen *et al.*, in which decay and processing were found to be separate pathways in competition (Nguyen, Grenier St-Sauveur et al. 2015). It was speculated that long 3′ extended products are non-functional hTR species which result from improper transcription termination and RNAPII read-through, though the mechanism of hTR transcription termination has yet to be reported (Nguyen, Grenier St-Sauveur et al. 2015). It has also been demonstrated that shorter hTR precursors are processed by PARN into mature hTR following polyadenylation by the human TRAMP complex, which can also be recruited by the CBCA [Figure 1.2C,D] (Mitchell 2014, Tseng, Wang et al. 2015, Tseng, Wang et al. 2018, Roake, Chen et al. 2019).

It is possible that the involvement of NEXT versus TRAMP depends upon co-transcriptional assembly of the precursor hTR with H/ACA pre-RNP components. In particular,

precursors which do not efficiently assemble with the pre-RNP may be more likely to assemble with the NEXT complex [Figure 1.2B] (Tseng, Wang et al. 2015), given that they may be subject to excessive RNAPII read-through. It has been reported that the dyskerin homologue in *S. cerevisiae* (Cbf5p) is required at snoRNA genes during transcription to prevent RNAPII read-through and promote efficient transcription termination (Ballarino, Morlando et al. 2005). Indeed, Tseng *et al.* suggested that coupling co-transcriptional pre-RNP assembly to processing of hTR would act as an efficient quality control mechanism, similar to that observed for snRNAs (Shukla and Parker 2014, Tseng, Wang et al. 2015). It has since been confirmed *in vitro* that the H/ACA complex is responsible for protecting the 3′ terminus of mature hTR from misregulated PARN-mediated degradation [Figure 1.2D], as well as stimulating efficient processing through preventing formation of the aforementioned tertiary RNA interactions which favour degradation of long hTR extended species (Tseng, Wang et al. 2018). Additionally, the negative effects of deficiencies in dyskerin or hTR's inability to assemble with the RNP have been attributed to exosome-dependent quality control of hTR (Shukla, Schmidt et al. 2016). Specifically, reduction of hTR levels and telomerase activity caused by dyskerin depletion or hTR mutations which disrupt RNP biogenesis can be rescued by knockdown of Rrp6. It was reported that Rrp6-mediated decay of hTR is enhanced by polyadenylation by the human TRAMP complex poly(A) polymerase (human PAPD5, also known as Trf4-2, homologue of Trf4) (Shukla, Schmidt et al. 2016). Interestingly, in human embryonic stem cells (hESCs) derived from patients with X-linked dyskeratosis congenita (X-DC), depletion of PAPD5 or the core exosome component Rrp40 leads to increased levels of hTR, telomerase activity, and telomere length, and reduces the amount of active DNA damage signaling. However, X-DC derived hESCs show defects in definitive hematopoiesis which can only be rescued by depletion of PAPD5, not by depletion of Rrp40 (Fok, Shukla et al. 2019).

There is also evidence of a cytoplasmic 5′-3′ decay mechanism for dysfunctional hTR precursors, involving DCP2 (decapping mRNA 2) which canonically removes the [mono-methyl guanosine cap and] CBCA from faulty mRNA transcripts exported to the cytoplasm for targeted degradation by XRN1 (5'-3' Exoribonuclease 1). This mechanism was reported to function independently of exosome-mediated decay [Figure 1.2B] (Shukla, Schmidt et al. 2016). It will be interesting to examine the nature of the 3′ extensions for these cytoplasmically exported hTR species, which seem to result from a lack of dyskerin assembly. Strikingly, an increase in the

amount of nuclear CBC-bound hTR caused by depletion of the enzyme responsible for hypermethylation of the hTR 5′ mono-methylguanosine cap leads to accumulation of total hTR species including 3′ extensions, rather than hTR decay (Chen, Roake et al. 2020). Trimethylguanosine synthase 1 (TGS1) is responsible for formation of the 5′ trimethylguanosine (TMG) cap on hTR [Figure 1.2A]. Depletion of TGS1 leads to reduced TMG-hTR, increased hTR interactions with CBC and Sm chaperone proteins, increased hTR levels in both the nucleus and cytoplasm, and an increased assembly of hTR with hTERT. This increased telomerase assembly ultimately causes increased telomerase activity and telomere elongation in TGS1 mutant cells (Chen, Roake et al. 2020). Thus, though the cytoplasmic 5′-3′ decay machinery is able to regulate hTR decay independently of the exosome [Figure 1.2B], in the absence of 5′ cap hypermethylation hTR remains persistently assembled with CBC in the nucleus and accumulates in all cellular compartments including the cytoplasm. This implies that when hTR is hypomethylated, cytoplasmic shuttling of hTR driven by CBC occupancy does not necessitate decay of hTR, but rather leads to protection of hTR from decay such that an increased abundance of hTR in TGS1 mutant cells can result in re-import of cytoplasmic hTR to the nucleus for functional telomerase assembly and telomere elongation. This protection could be due to abnormally increased assembly of hTR with Sm proteins, as speculated by Chen, *et al.* to lend resistance to exosome-mediated decay (Chen, Roake et al. 2020). Importantly, DCP2 has been reported to remove the mono-methyl guanine cap structure from mRNA, but orthologues of DCP2 in other organisms are capable of decapping the TMG of snoRNA (van Dijk, Cougot et al. 2002, Piccirillo, Khanna et al. 2003, Ghosh, Peterson et al. 2004, Cohen, Mikhli et al. 2005, Song, Li et al. 2010). It is also worth noting that it has previously been reported that human snoRNA/scaRNA, including hTR, do not conventionally undergo cytoplasmic export during biogenesis (Pradet-Balade, Girard et al. 2011). As such, perhaps under certain abnormal conditions of hTR nuclear export (for example, when dyskerin is depleted (Shukla, Schmidt et al. 2016)), DCP2 is capable of removing the TMG cap which leads to XRN1-mediated degradation, while in a different abnormal context of persistent hTR mono-methylation (for example, when TGS1 is depleted (Chen, Roake et al. 2020)), cytoplasmic export does not lead to decapping and degradation specifically because of this difference in methylation status. In budding yeast the telomerase RNA component contains an Sm-like biogenesis domain and undergoes nucleocytoplasmic shutting in the canonical biogenesis pathway (Seto, Zaug et al. 1999,

Gallardo, Olivier et al. 2008). Thus, cytoplasmic protection of human telomerase RNA by Sm proteins in the context of TGS1 depletion may also be an important step differentiating DPC2/XRN1 cytoplasmic degradation from hypomethylation and nuclear re-import of hTR. However, this is speculation in an attempt to reconcile differences of observations reported regarding cytoplasmic hTR. The presence and regulation of cytoplasmic hTR species is in need of further experimental investigation.

A balance between trimming and degradation of hTR 3′ extended species must be maintained for sufficient mature hTR accumulation and telomerase function, and the nucleolar exosome and cytoplasmic decay machinery are key components in this process. Importantly, the upstream role of polyadenylation/deadenylation in hTR processing and quality control must also be factored into our understanding of hTR biogenesis.

1.2.3 A Processing Role for PARN

As previously stated, involvement of the canonical mRNA 3′ maturation pathway in *S. pombe* snoRNA processing has been reported to involve the exosome. This mechanism is dependent upon the polyadenylation polymerase Pla1 and the nuclear poly(A)-binding protein Pab2 (Grzechnik and Kufel 2008, Lemay, D'Amours et al. 2010). Notably, the human homologue of Pab2, PABPN1 was recently implicated in hTR 3′ maturation through a polyadenylation dependent pathway [Figure 1.2D] (Nguyen, Grenier St-Sauveur et al. 2015). In contrast to the exosome-driven snoRNA maturation mechanism in fission yeast, it seems that PARN is the key nuclease for trimming of polyadenylated precursor hTR (Moon, Segal et al. 2015, Nguyen, Grenier St-Sauveur et al. 2015). In fact, a competing or antagonistic role has been indicated for exosomal decay versus PARN-mediated processing of hTR precursors [Figure 1.2C,D] (Nguyen, Grenier St-Sauveur et al. 2015, Tseng, Wang et al. 2015, Shukla, Schmidt et al. 2016, Roake, Chen et al. 2019). Nguyen *et al.* reported that depletion of either PABPN1 or PARN contributes to increased cellular amounts of polyadenylated and 3′ extended hTR species, and a reduction of mature hTR. In addition, depletion of the canonical polyadenylation Pla1 human homologues PAPα/γ led to a reduction of hTR, and approximately half of PABPN1-associated poly(A) hTR species were reported to have long (>15nt) poly(A) tails typical of canonical polyadenylation polymerases. Meanwhile, depletion of components from the TRAMP complex led to an increased accumulation of mature hTR, presumably due to a lack of exosome-mediated decay, thus demonstrating the possible competition between exosome-mediated

degradation and PARN-mediated trimming (Nguyen, Grenier St-Sauveur et al. 2015). Furthermore, Shukla *et al.* have also suggested competition between PARN and the exosome for poly(A) hTR processing. However, it was reported that the poly(A) substrates of these nucleases are products of TRAMP polyadenylation (Shukla, Schmidt et al. 2016). While this is in disagreement with the proposal of canonical polyadenylation by PAPα/γ for proper hTR maturation (Nguyen, Grenier St-Sauveur et al. 2015), the ability of PARN to remove TRAMP polyadenylation products from hTR was also reported by Tseng *et al.* who proposed that PARN activity would be favoured when the 5′ terminus of hTR is mono-methyl guanosine capped and negatively regulated by the presence of CBCA bound to hTR (Tseng, Wang et al. 2015). It was suggested that, though TRAMP-synthesized poly(A) tails are traditionally short (4-5nt), it is possible for canonical polyadenylation polymerases to extend TRAMP products in order to foster PABPN1 interaction and PARN recruitment [Figure 1.2D] (Tseng, Wang et al. 2015). As previously discussed, it has since been demonstrated that TGS1 depletion, and thus an increase in the 5′ mono-methylguanosine capped state of hTR leads to an increased CBC-hTR interaction and hTR accumulation. However, no changes in 3′ end processing or polyadenylated hTR levels are caused by TGS1 depletion (Chen, Roake et al. 2020). Thus the speculation that PARN-mediated deadenylation of hTR may be negatively regulated by CBC or promoted by the 5′ mono-methylguanosine cap is in need of reconsideration.

Regardless, it is evident that polyadenylation and PARN-mediated deadenylation are essential for accumulation of mature hTR and effective telomere maintenance. Indeed, it has been further demonstrated that oligoadenylation and deadenylation of extended hTR species by PAPD5 and PARN, respectively, is responsible for controlling hTR maturation rates (Roake, Chen et al. 2019). Using a novel technique termed nascent RNAend-Seq, Roake, *et al.* were able to demonstrate that short 3′ extended hTR precursors can be derived into mature hTR species following oligoadenylation by PAPD5 and subsequent deadenylation by PARN. Interestingly, their findings also suggest that hTR maturation can take place in the absence of the regulatory PAPD5/PARN loop, as depleting both components rescues altered hTR maturation rates (Roake, Chen et al. 2019). It is possible that other enzymes may function redundantly with this polyadenylation/deadenylation loop as well, such as the enzyme TOE1 which has been reported to deanylate hTR *in vitro* and affects the levels of 3′ extended hTR species (Deng, Huang et al. 2019). Finally, in their study of the PAPD5/PARN regulatory loop, Roake, *et al.* suggest that the

H/ACA box of hTR is a crucial element for mediating choice of RNA processing pathway [Figure 1.2D], consistent with the role of the H/ACA complex governing trimming and degradation of hTR extended species *in vitro* (Tseng, Wang et al. 2018).

1.3 Dyskerin, H/ACA RNAs and the H/ACA Complex

As has been previously mentioned, vertebrate telomerase RNAs like hTR possess a structural element responsible for proper biogenesis and processing, which is also found in a family of non-coding (nc)RNAs classified as H/ACA RNA. This hairpin-hinge-hairpin-tail motif containing an H-box (5′-ANANNA-3′ where N is any nucleotide) in its hinge region and terminating in an ACA tail is present in the 3′ biogenesis domain of hTR, and hundreds of other ncRNAs which carry out a wide variety of functions. These other ncRNAs include H/ACA snoRNA and scaRNA that guide posttranscriptional modifications of pre-ribosomal RNA (pre-rRNA) and snRNA, respectively (Balakin, Smith et al. 1996, Ganot, Bortolin et al. 1997, Ganot, Caizergues-Ferrer et al. 1997, Ni, Tien et al. 1997, Darzacq, Jady et al. 2002). Like hTR, these H/ACA RNAs depend on assembly with dyskerin and other components of the H/ACA RNP complex for biogenesis, stability, and function [Figure 1.3] (Lafontaine, Bousquet-Antonelli et al. 1998, Zebarjadian, King et al. 1999). H/ACA RNPs are highly evolutionarily conserved complexes, present in archaea, plants, and eukaryotes, as well as having evolutionary ties to bacteria through the catalytic TruB domain of dyskerin (Lafontaine and Tollervey 1998). Structural and functional studies of the components of the H/ACA RNP and its assembly factors, individually and in complex, have provided insight into the essentiality of H/ACA RNP biology and its useful moonlighting responsibilities in TR biogenesis and function.

Figure 1.3 – Stepwise H/ACA complex assembly (figure adapted from (MacNeil, Bensoussan et al. 2016))

A. The RNA-mimic and chaperone SHQ1 plays a very early role in human H/ACA RNP biogenesis, upstream of NAF1 and pre-H/ACA complex interaction with H/ACA RNAs. It is likely to interact with dyskerin in the cytoplasm as human SHQ1 has been observed predominantly localized in the cytoplasm. Structural studies have revealed that SHQ1 blocks a large portion of the RNA-binding interface of dyskerin, and therefore should dissociate from dyskerin upstream of H/ACA RNP assembly with an RNA component.

B. The AAA+ ATPases pontin and reptin form a heterohexameric ring-like structure. Both pontin and reptin have been reported to interact with dyskerin.

C. These AAA+ ATPases stimulate the dissociation of SHQ1 from dyskerin in an ATP-dependent manner. Pontin and reptin can be purified with active telomerase, and as such it is unclear at which step during H/ACA RNP biogenesis they disassemble from dyskerin, if at all. Thus, for the purpose of this schematic, they remain assembled with the H/ACA RNP.

D. The pre-H/ACA complex consists of the core trimer (dyskerin-NHP2-NOP10) and NAF1. These four components are found at transcription start sites of H/ACA RNAs, and the pre-H/ACA complex is presumed to assemble with nascent H/ACA RNAs during transcription by RNAPII. It was proposed that NAF1 may mediate nuclear/subnuclear H/ACA RNP biogenesis as a chaperone present with dyskerin upstream of the mature complex due to its own nucleocytoplasmic shuttling and its absence from sites of mature H/ACA complexes. The preference of human SHQ1 to interact with uncomplexed dyskerin suggests that the downstream H/ACA RNP biogenesis role for NAF1 begins at the subnuclear level.

E. GAR1 does not co-localize with H/ACA RNA transcription sites, and is not required for stability of H/ACA RNAs, but provides H/ACA RNP complex-to-H/ACA RNA affinity, as well as proper H/ACA RNA positioning accuracy on target RNAs. There is a direct competition between NAF1 and GAR1 for interactions with the core trimer, and more specifically these proteins compete for the same interaction interface on dyskerin. An exchange of GAR1 for NAF1 takes place during H/ACA RNP biogenesis to form the mature H/ACA complex. Importantly, two heterotetramers comprised of the mature H/ACA RNP components assemble with a single H/ACA RNA in humans, with one set of proteins (GAR1-dyskerin-NOP10-NHP2) per H/ACA domain hairpin.

F. Mature H/ACA complexes assembled with snoRNA localize to the nucleolus, where they function in pseudouridine synthesis of rRNA.

G. Mature H/ACA complexes assembled with scaRNA localize to the Cajal bodies, via interaction with the scaffolding protein TCAB1 (Telomerase Cajal body protein 1, also known as WDR79 - WD repeat-containing protein 79) through a CAB-box motif (absent from snoRNA). scaRNA guide pseudouridine synthesis of snRNA by H/ACA RNPs in Cajal bodies.

H. In humans, telomerase assembly takes place at Cajal bodies, with hTR containing a CAB-box motif and interacting with TCAB1. hTR has a longer residency at Cajal bodies than the telomerase reverse transcriptase hTERT, though both localizes to these membrane-free subnuclear compartments. There is no evidence that hTR guides pseudouridine synthesis. This adapted figure is reprinted from (MacNeil, Bensoussan et al. 2016) in accordance with the MDPI Open Access Information and Policy.

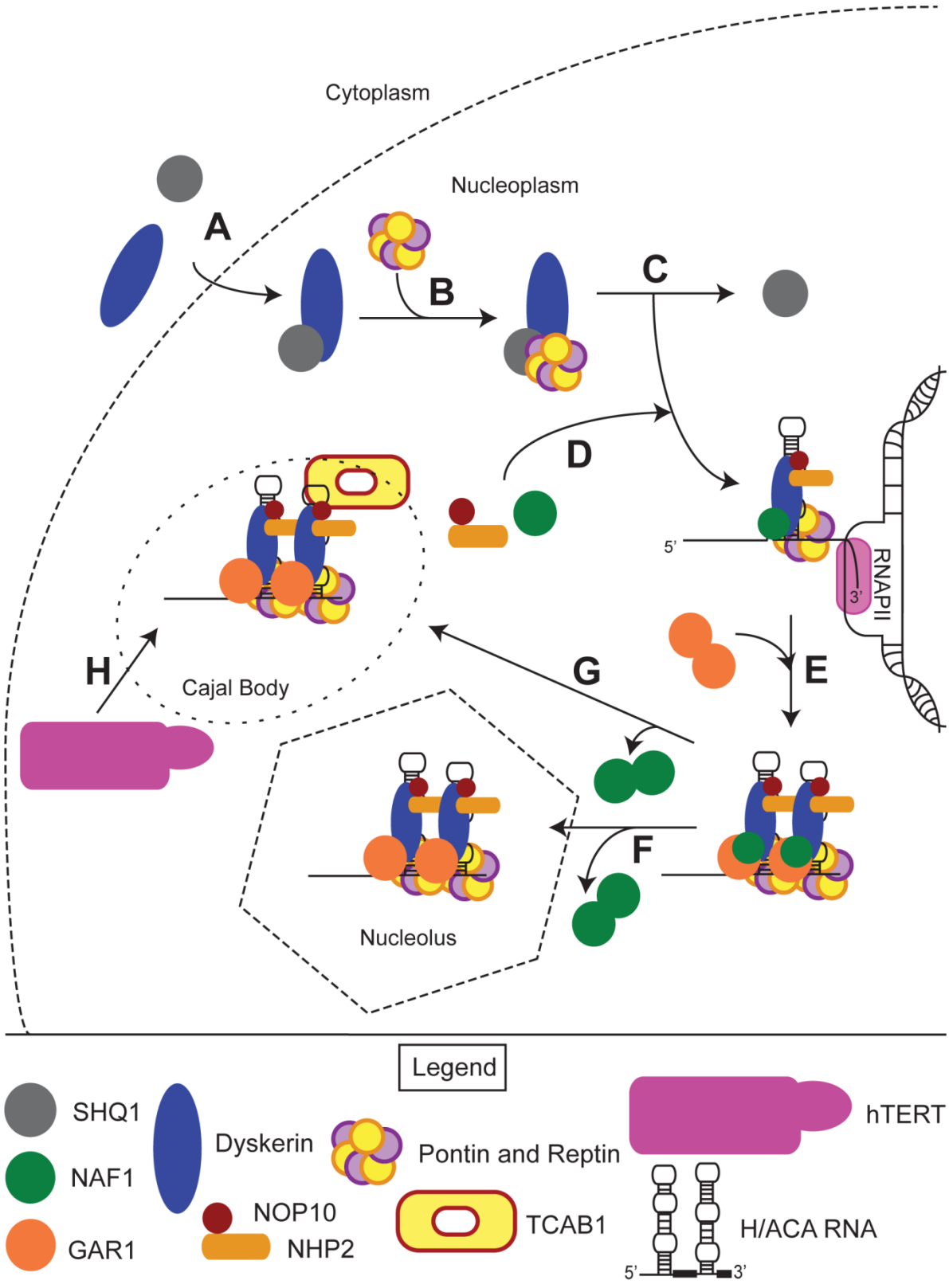
Cytoplasm
Nucleoplasm
A
B
C
D
E
F
G
H
Cajal Body
Nucleolus
5'
3'
RNAPII
Legend
SHQ1
NAF1
GAR1
Dyskerin
NOP10
NHP2
Pontin and Reptin
TCAB1
hTERT
H/ACA RNA
5'
3'

1.3.1 The H/ACA RNPs

There are four proteins assembled with a guide RNA and a target RNA in a functional H/ACA complex: dyskerin (Jiang, Middleton et al. 1993, Meier and Blobel 1994, Heiss, Knight et al. 1998, Lafontaine, Bousquet-Antonelli et al. 1998, Giordano, Peluso et al. 1999), GAR1 (Girard, Lehtonen et al. 1992, Balakin, Smith et al. 1996), NOP10, and NHP2 (Henras, Henry et al. 1998). Dyskerin, whose other nomenclature includes minifly/Nop60B (in flies), Cbf5 (in archaea), CBF5p (in yeast), and NAP57 (in rat), is the pseudouridine synthase of the H/ACA complex and is responsible for catalyzing the isomerization of uridine into pseudouridine at specific bases of target RNA, guided by the H/ACA RNA with which it is assembled. Together with NHP2 and NOP10, dyskerin is able to assemble with H/ACA RNAs at the ncRNA transcription sites (Darzacq, Kittur et al. 2006), and all three proteins are required for H/ACA RNA stability, as well as complex function. Interestingly, GAR1 does not co-localize with H/ACA RNA transcription sites, and is not required for snoRNA stability, though this glycine and arginine-rich protein is necessary for H/ACA complex function (Girard, Lehtonen et al. 1992, Bousquet-Antonelli, Henry et al. 1997, Darzacq, Kittur et al. 2006). GAR1 was one of the first H/ACA RNPs reported, and was postulated to play a role in snoRNAs posttranscriptional functions (Balakin, Smith et al. 1996). Indeed, studies since have suggested that the role of GAR1 in the complex occurs later during snoRNA biogenesis and function, ensuring accurate H/ACA complex placement on target RNAs in archaea (Wang, Yang et al. 2015), and providing high complex-to-guide RNA affinity and guide positioning accuracy in eukaryotes (Caton, Kelly et al. 2018). A heterotetrameric complex involving dyskerin, NHP2, NOP10, and GAR1 binds each hairpin of the H/ACA RNA (i.e. two protein complexes per H/ACA RNA) [Figure 1.3F,G] (Egan and Collins 2010, Nguyen, Tam et al. 2018), and each complex positions pseudouridine synthesis of a target RNA in the catalytic pocket created by H/ACA RNA-target RNA base pairing, which likely creates a common structural element recognized by dyskerin for site-specific pseudouridine synthesis (Ni, Tien et al. 1997, Wang and Meier 2004, Baker, Youssef et al. 2005, Xiao, Yang et al. 2009). As previously discussed, all four components of the mature H/ACA complex are also part of the active human telomerase holoenzyme, and contribute to hTR levels and telomerase assembly (Mitchell, Cheng et al. 1999, Fu and Collins 2007, Kiss, Fayet-Lebaron et al. 2010, Nguyen, Tam et al. 2018). Assembly of this mature H/ACA complex with various H/ACA RNAs is essential for its functions in pseudouridine synthesis and

telomerase biogenesis alike [Figure 1.3F-H], though its involvement in telomerase is less evolutionarily conserved than its role in pseudouridine synthesis, arising as a biogenesis factor for telomerase only in complex metazoans (Podlevsky and Chen 2016, Logeswaran, Li et al. 2020). Nonetheless, much of what is known about H/ACA complex formation is true across H/ACA RNPs, including telomerase.

1.3.2 H/ACA RNP Assembly

Upstream of the mature H/ACA complex formation, many chaperones and protein placeholders take part in biogenesis of these RNPs [Figure 1.3]. The pre-H/ACA complex [Figure 1.3D], which consists of the core trimer (dyskerin-NHP2-NOP10) plus NAF1 in the place of GAR1, is found at transcription start sites of H/ACA RNAs (Ballarino, Morlando et al. 2005, Yang, Hoareau et al. 2005, Darzacq, Kittur et al. 2006). While this has not been specifically demonstrated for hTR, the assembly of NAF1 with hTR has similar requirements as other H/ACA RNA both *in vitro* and in cells, including the need for the core trimer in order to efficiently interact with H/ACA RNA, and a NAF1-RNA interaction which is likely mediated by dyskerin (Wang and Meier 2004, Darzacq, Kittur et al. 2006, Trahan and Dragon 2009, Trahan, Martel et al. 2010). It was initially proposed that NAF1 may mediate nuclear/subnuclear H/ACA RNP biogenesis as a chaperone present with dyskerin upstream of the mature complex based on: its own nucleocytoplasmic shuttling; exclusion of NAF1 from subnuclear compartments where mature H/ACA RNPs co-localize with GAR1 (nucleoli and Cajal bodies) [Figure 1.3F,G], and exclusion of GAR1 from H/ACA RNA transcription start sites; as well as a direct competition between GAR1 and NAF1 for core trimer complex interaction [Figure 1.3E] (Darzacq, Kittur et al. 2006). Indeed, based on structural homology between NAF1 and GAR1, and interaction studies involving archaeal and yeast homologues of these proteins, NAF1 and GAR1 have been demonstrated to compete for the same interaction interface on dyskerin (Rashid, Liang et al. 2006, Leulliot, Godin et al. 2007). Based on these structural analyses, it has also been speculated that NAF1 stabilizes the β7- β10 active site loop of dyskerin in a conformation such that it cannot function as a pseudouridine synthase prior to exchange of NAF1 for GAR1, lending the complex fidelity for target RNA modifications (Leulliot, Godin et al. 2007).

NAF1 was one of the first upstream assembly factors identified for maintaining H/ACA RNP stability, and was initially characterized along with another chaperone SHQ1 in *S. cerevisiae* (Yang, Rotondo et al. 2002). Both were reported as essential nuclear factors in

ribosome biogenesis through a role in regulating snoRNA levels, and interestingly were found to interact not only with core components (dyskerin and NHP2 homologues), but also with each other, independent of GAR1. However, the human homologue of SHQ1 shows a preference for interacting with dyskerin alone *in vitro*, which is an interaction that cannot compete with excess NAF1 but can be maintained *in vitro* in the presence of the core trimer [Figure 1.3A] (Grozdanov, Roy et al. 2009). Strikingly, in the same study using human cells expressing a LacO-tethered SHQ1, dyskerin is the only H/ACA RNP component which can be recruited to the SHQ1 focus in the nucleus, including cellular H/ACA RNAs which remain excluded from co-localization with LacO-SHQ1. In contrast to the yeast homologue, human SHQ1 was observed to be prominently cytoplasmic, and though it shuttles in and out of the nucleus, is excluded from nucleoli, CB's, and H/ACA RNA transcription start sites. However, consistent with what was observed in yeast, depletion of human SHQ1 does lead to reduced H/ACA RNA levels, and in human cells this reduction of H/ACA RNA also applies to hTR. Furthermore, excess human SHQ1 protein which is competent for interaction with dyskerin disrupts purified H/ACA complex pseudouridine synthesis *in vitro* when added to the complex before the H/ACA RNA, but not concomitantly (Grozdanov, Roy et al. 2009). Taken together, these data suggest a hypothesis in which H/ACA complex assembly in lower eukaryotes differs from that in humans, as well as a potential role for human SHQ1 in very early RNP biogenesis upstream of NAF1 and complex interaction with H/ACA RNAs, likely in the cytoplasm. Structural studies have indeed confirmed that SHQ1 is not only capable of interacting with dyskerin, but that SHQ1 functions as an RNA mimic blocking a large portion of the RNA-binding interface of dyskerin both in yeast and humans (Li, Duan et al. 2011, Walbott, Machado-Pinilla et al. 2011, Singh, Wang et al. 2015). Importantly, Li *et al.* demonstrated using biochemical analyses and crystal structures of yeast homologues that *in vitro*, SHQ1 is able to interact with the entirety of the pre- and mature H/ACA complex proteins, and as such the SHQ1-dyskerin interface in yeast does not likely coincide with the dyskerin-protein interface for any other H/ACA protein components (Li, Duan et al. 2011).

While NAF1 and SHQ1 are the two main assembly factors extensively characterized for their role in H/ACA RNP biogenesis, understanding this complex assembly pathway remains a challenge predominantly due to inconsistencies between data from studies of archaeal, yeast, and human homologues, as previously mentioned. It is not unlikely that differences in these

pathways have arisen evolutionarily, as organisms progressed from nucleus-free to ever more complex nuclear and subnuclear compartmentalization, and their needs for organizing these complexes and their targets changed. How human dyskerin is seemingly handed off between chaperones and complex components still remains incompletely understood, though it is clear that this process is regulated by other factors such as the AAA+ ATPases (ATPases Associated with diverse cellular Activities) pontin and reptin [Figure 1.3B]. Both of these AAA+ ATPases have been reported to interact with dyskerin *in vitro* (Machado-Pinilla, Liger et al. 2012) and in cells (Venteicher, Meng et al. 2008). Pontin and reptin were reported to stimulate release of SHQ1 from dyskerin *in vitro* [Figure 1.3C], and depletion of either by siRNA knockdown leads to reduced H/ACA RNA levels in cells, including reduced hTR (Machado-Pinilla, Liger et al. 2012). Additionally, Venteicher *et al.* reported that hTR levels in cells are maintained by pontin in an ATPase domain-dependent manner, as well as pontin/reptin involvement in telomerase biogenesis being cell cycle regulated, with a peak of the AAA+ ATPases' recruitment to the telomerase RNP in S phase (Venteicher, Meng et al. 2008). Using HeLa cell cytosolic extract (S100), Machado-Pinilla *et al.* demonstrated that the *in vitro* interaction between SHQ1 and dyskerin could be disrupted in an ATP-independent manner by components in S100. Anti-pontin or anti-reptin sera were able to block the S100-mediated disrupted interaction, and in turn these antibody-stabilized SHQ1-dyskerin interactions were disrupted by excess recombinant pontin or reptin, specific to the antibody target. Furthermore, dyskerin lacking the C-terminal extension (truncated at aa422) does not dissociate from SHQ1 in an S100-dependent manner. Crystal structures of pontin and reptin in complex revealed that these proteins assemble with one another as a hexameric ring (Torreira, Jha et al. 2008), leading to the speculation that the pontin-reptin hexamer catches the highly charged and unstructured dyskerin C-terminal tail and stabilizes it in order to facilitate removal of SHQ1 during RNP biogenesis through inducing conformational changes to dyskerin. Depletion of pontin or reptin through siRNA or shRNA treatment also leads to a reduction in cellular dyskerin protein levels, which may explain the effect of these co-factors on H/ACA RNA level maintenance (Venteicher, Meng et al. 2008, Machado-Pinilla, Liger et al. 2012). Taken together, these data also suggest that dyskerin stability is impeded by a persistent interaction with SHQ1, supporting the notion that SHQ1 is an early assembly factor that must be removed in order for H/ACA complex maturation, and for dyskerin to carry out its role both in telomerase and in pseudouridine synthesis.

1.3.3 The H/ACA RNP and Pseudouridine Synthesis

Posttranscriptional modification of pre-rRNA occurs in all living organisms, and base rotation of uridine into pseudouridine (ψ) is a common modification present at the active interfaces of ribosomes in bacteria and eukaryotes alike. Interestingly, for rRNA this posttranscriptional modification is much more prevalent in higher eukaryotes than in early organisms (Taoka, Nobe et al. 2018), and seems to have evolved a more complex mechanism of synthesis from one requiring protein-only **p**seudo**u**ridine **s**ynthases (PUSs) which modify many different target RNA sites, to the involvement of a variety of guide ncRNAs directing site-specific modifications by a single protein complex (H/ACA RNPs) (Lafontaine and Tollervey 1998, O'Connor, Leppik et al. 2018, Penzo and Montanaro 2018). Chemically, this base modification provides structural stability through generating greater rigidity for the RNA phosphodiester backbone, improved base stacking compared with uridine, and increased RNA thermostability (Davis 1995, Charette and Gray 2000, Penzo, Guerrieri et al. 2017, Penzo and Montanaro 2018); yet the functional importance of pseudouridine in the human ribosome remains somewhat a mystery.

In yeast, deletion of single snoRNAs (and thus single pseudouridines in the rRNA) typically does not disrupt fitness. However, combinatorial deletions of snoRNAs, targeting bases in the A-site, P-site, and intersubunit interface of mature ribosomes, lead to slower cell growth, impaired amino acid incorporation during peptide synthesis, and deficiency of free small ribosome subunits (King, Liu et al. 2003, Liang, Liu et al. 2007, Liang, Liu et al. 2009, Lemay, D'Amours et al. 2010). Positioning of pseudouridine at functionally important sites of the mature ribosome in early organisms and higher eukaryotes alike implies the importance of this modification for function (Decatur and Fournier 2002), but in humans a direct connection between pseudouridine and ribosome function is still lacking. Analyses of X-DC causative mutations or depletion of dyskerin have been used as readout for the importance of pseudouridine in ribosomal function regulation. Importantly, studies of X-DC mutations and dyskerin depletion in mice account for a majority of data supporting the notion of pseudouridine regulating ribosome function, though several studies in human cancer cells and induced pluripotent cells (iPSCs) have also connected dyskerin function (and thus pseudouridylation) to ribosome function. Impaired translation of a subset of mRNAs carrying internal ribosome entry sites (IRESs) in mouse cells harboring X-DC mutations has been reported as a consequence of

reduced pseudouridine levels (Ruggero, Grisendi et al. 2003, Yoon, Peng et al. 2006). IRES elements allow for translation of mRNA containing these structural elements to occur in the absence of conventional cap-mediated translation regulation (Komar and Hatzoglou 2005), and as such it has been proposed that pseudouridine may provide specialized ribosome regulation in the case of IRES-containing mRNA. This has been further supported by observed impairment of IRES-mediated translation in X-DC patient fibroblasts and lymphoblasts for tumor suppressors p27 and p53 (Yoon, Peng et al. 2006, Bellodi, Kopmar et al. 2010), as well as differences in IRES translation in mice and cancer cells with reduced dyskerin levels (Bellodi, Krasnykh et al. 2010). In contrast, IRES-mediated translation of vascular endothelial growth factor (VEGF) was reported to increase in the context of dyskerin depletion for both transformed and primary human cells (Rocchi, Pacilli et al. 2013). However, several X-DC patient cells lines have been reported to have no changes in IRES or protein synthesis whatsoever, and many studies in X-DC patient cells have revealed no changes in ribosome biogenesis (indicated by 18S/28S rRNA ratios), nor polysome fractionation profiles (Wong, Kyasa et al. 2004, Wong and Collins 2006, Zeng, Thumati et al. 2012, Thumati, Zeng et al. 2013). Importantly, many studies performed in X-DC patient cells have revealed no reductions in pseudouridine levels (Mitchell, Wood et al. 1999, Wong and Collins 2006, Gu, Apicella et al. 2015, Xu, Khincha et al. 2016), and as such X-DC mutations may not be an ideal model for analyzing the functional relevance of pseudouridine in the ribosome. Regardless, the prevalence and positional evolutionary conservation of pseudouridine in rRNA indicate the importance of better understanding its biological role and thus the importance of the H/ACA complex.

H/ACA RNPs also guide the posttranscriptional modification of snRNAs, though as for rRNA, the functional consequences of pseudouridylation of snRNA are not well understood. It has been proposed to regulate function and biogenesis of snRNA/snRNPs. Using *in vitro* reconstitution of snRNPs from HeLa cell extracts, it was demonstrated that 3 pseudouridines in the U2 snRNA have a cumulative role in the ability of the snRNP to splice pre-mRNA, and in early formation of the spliceosome with a pre-mRNA target (Donmez, Hartmuth et al. 2004). However there is also evidence of pseudouridine being dispensable for spliceosome function, including the observation that *in vitro* transcribed U1 snRNA lacking modification can reconstitute the U1 snRNP from mammalian cell extracts depleted of U1 snRNA (Will, Rumpler et al. 1996). Similar to rRNA, the prevalence and positioning of pseudouridine in snRNA is

evolutionarily conserved (Adachi and Yu 2014), lending support to the notion that it plays an important regulatory role for snRNPs, though greater direct evidence of exactly what function it is regulating for snRNPs is still needed.

1.3.4 The H/ACA RNP and Telomerase

All telomerase RNA components contain a biogenesis motif, which are highly divergent across phyla. Each motif incorporates various evolutionarily discrete RNA metabolism pathways into processing of TR 3′ termini, as well as mediating TR stability and nuclear compartmentalization (Podlevsky and Chen 2016). Biogenesis motifs foster interactions with accessory proteins respective to the TR maturation domain for which they are responsible, and these domains are typically variations on structural elements present in other ncRNA families. This includes, for instance, snRNA-like domains in the 3′ termini of fungal TRs as previously mentioned, some of which make use of Sm proteins and/or spliceosome-mediated end processing (Seto, Zaug et al. 1999, Leonardi, Box et al. 2008, Tang, Kannan et al. 2012). The H/ACA structural domain is the biogenesis motif present in vertebrate and echinoderm TRs, employing the H/ACA RNP assembly factors and complex components previously discussed towards maintaining TR processing and stability. Intriguingly, though ciliate TRs like that of *Tetrahymena thermophila* use a small RNA/U-rich termination element for biogenesis (McCormick-Graham and Romero 1995), evolutionarily closely related flagellates like *Trypanosoma brucei* have adopted a biogenesis motif related to sno/scaRNA biogenesis - a sister of H/ACA RNPs known as C/D RNPs (Gupta, Kolet et al. 2013, Vasconcelos, Nunes et al. 2014), which typically guide the posttranscriptional modification 2′-O-methylation in rRNA and snRNA (Cavaille, Nicoloso et al. 1996, Kiss-Laszlo, Henry et al. 1996, Tycowski, You et al. 1998, Ganot, Jady et al. 1999, Jady and Kiss 2001). This represents an interesting molecular example of convergent evolution in TR biogenesis, whereby nucleolar/CB RNP components function in two dramatically evolutionarily distinct organisms towards a similar goal – telomerase biogenesis.

In humans, the H/ACA domain contributes stability to hTR just as the H/ACA RNP components stabilize all H/ACA sno/scaRNAs. Importantly, hTR differs from conventional H/ACA RNAs in several ways, largely in relation to its status as a long non-coding RNA (lncRNA). Though typical sno/scaRNA length is under 200nt, mature hTR is 451nt long and contains unique 5′ structural elements [Figure 1.4A,B] including two hTERT-interacting

elements required for catalytic activity: the template-adjacent pseudoknot (Chen, Blasco et al. 2000, Mitchell and Collins 2000, Ly, Blackburn et al. 2003, Chen and Greider 2005) and the functionally conserved CR4/5 distal stem-loop (Chen, Opperman et al. 2002). This second element is a direct extension of the 5′ H/ACA stem-loop, generating a longer more flexible hairpin than those of conventional H/ACA RNAs, which is essential for telomerase assembly and activity (Mitchell and Collins 2000, Ketele, Kiss et al. 2016, Nguyen, Tam et al. 2018). Additionally, the internal stem-loop structure within CR4/5 of hTR (P6.1) provides another unique structural feature of this domain that has been demonstrated to mediate telomerase assembly and activity, as characterized by mutational analyses and structural studies (Mitchell and Collins 2000, Chen, Opperman et al. 2002, Leeper, Leulliot et al. 2003, Moriarty, Marie-Egyptienne et al. 2004, Nguyen, Tam et al. 2018). Finally, hTR is considered a scaRNA due to the presence of a CAB-box motif in CR7 (Jady, Bertrand et al. 2004, Cristofari, Adolf et al. 2007), which is a conserved motif responsible for localizing scaRNA to CBs, initially characterized as the sequence ugAG, with frequent variations of the first and second positions (Richard, Darzacq et al. 2003).

Figure 1.4 – hTR, H/ACA RNAs, and Subnuclear Compartmentalization (part A of figure adapted from (MacNeil, Bensoussan et al. 2016))

A. Mature hTR is 451nt and contains complex 5′ structural elements in addition to the H/ACA-biogenesis domain. The structural domains of mature hTR are denoted in coloured boxes: the pseudoknot region in pink containing the template; the CR4/5 domain in yellow containing the P6.1 stem-loop; and the CR7 domain in blue, containing both the H/ACA and CAB boxes. This adapted figure is reprinted from (MacNeil, Bensoussan et al. 2016) in accordance with the MDPI Open Access Information and Policy.

B. Conventional H/ACA RNAs are typically smaller than hTR in length, approximating 200nt on average and lacking 5′ structural elements. H/ACA RNA guide pseudouridine (ψ) synthesis by dyskerin and the H/ACA complex, and the target of each H/ACA RNA is site specific as a result of base pairing between the target RNA and guide RNA, as well as on localization. For pseudouridine synthesis of rRNA, snoRNA (left) localize with the mature H/ACA complex in the nucleolus. For pseudouridine synthesis of snRNA, scaRNA (right) localize with the mature H/ACA complex in the Cajal bodies, via an interaction between the scaffolding protein TCAB1 and the CAB-box motif (ugAG) which is specific to scaRNAs.

C. Membrane-based compartmentalization like that of the nucleus as a whole (a schematic of which is depicted here) allows for organization of cellular processes, with selectivity of compartmentalization provided by the nuclear envelope and nuclear pores. Subnuclear compartmentalization in the absence of membranes allows for dynamic organization of complex processes, like the specifically regulated posttranscriptional modification by H/ACA RNPs, with selectivity of compartmentalization provided by phase-transitions. The nucleolus is a well-studied example of phase-separated compartmentalization, demonstrating four phases: 1) the nucleoplasm, 2) the granular component (GC) where pre-rRNA processing and ribosome subunit assembly takes place, 3) the dense fibrillar component (DFC) where pre-rRNA posttranscriptional modification by H/ACA and C/D RNPs takes place, and 4) the fibrillar component (FC) surrounding nucleolar organizer regions built on rDNA repeats. Transcription of rDNA takes place at the interface of the FC and DFC, with phase-mediated compartmentalization allowing for coordinated radially sorting of pre-rRNA out of the nucleolus as it is transcribed, modified, and processed. Cajal bodies are one of many other

smaller membrane-free compartments in the nucleus, serving as dynamic organizers of distinct subnuclear functions.

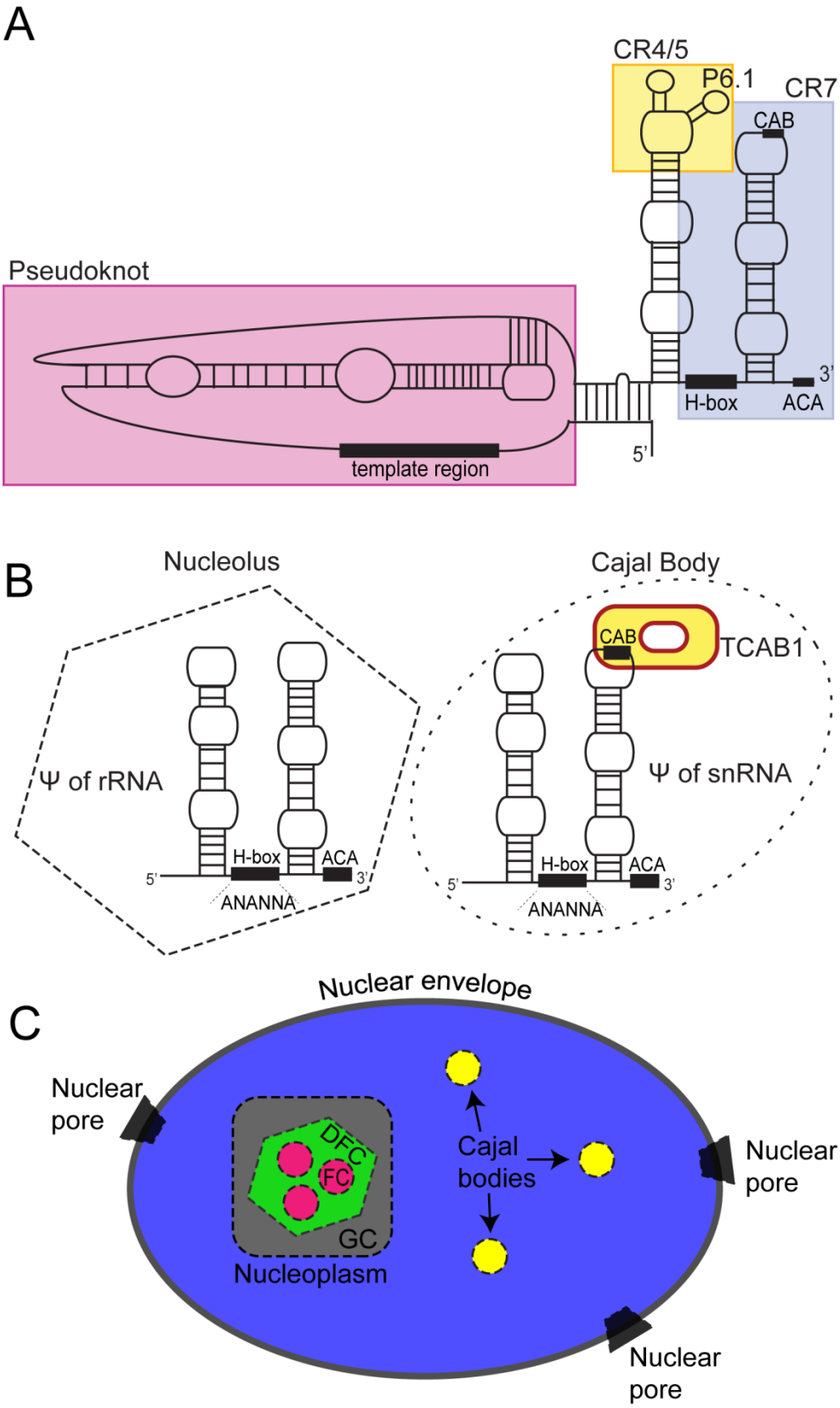
A
CR4/5
P6.1
CR7
CAB
Pseudoknot
template region
H-box
ACA
3'
5'
B
Nucleolus
Cajal Body
CAB
TCAB1
Ψ of rRNA
Ψ of snRNA
H-box
ACA
5'
3'
ANANNA
C
Nuclear envelope
Nuclear pore
DFC
FC
GC
Nucleoplasm
Cajal bodies
Nuclear pore
Nuclear pore

A recent structural analysis of the active human telomerase holoenzyme, solved by cryo-EM, provides important insight not only into telomerase function but also serves as the only current structure of an entire eukaryotic H/ACA RNP [Figure 1.5] (Nguyen, Tam et al. 2018). Indeed, in contrast to the human telomerase stoichiometry originally proposed based on purification and mass spectrometric analysis (two TERT, two hTR, and two dyskerin) (Cohen, Graham et al. 2007), this cryo-EM structure confirms the occupancy of the entire mature H/ACA complex on the 3′ terminus of hTR of functional telomerase as a dimeric heterotetramer; two sets of H/ACA RNP components were fitted into the observed cryo-EM density based on the archaeal H/ACA RNA-bound RNP crystal structure (Li and Ye 2006). This is consistent with previously reported low resolution structures of purified yeast H/ACA RNPs which revealed a bipartite or two domain structure (Lubben, Fabrizio et al. 1995, Watkins, Gottschalk et al. 1998), as well as biochemical analysis which revealed stoichiometry of the human telomerase H/ACA domain (Egan and Collins 2010). This structure also demonstrated that the set of H/ACA proteins in contact with the 5′ hairpin stem of hTR is mediated exclusively through dyskerin-RNA interaction, whereas all four H/ACA protein components form more extensive interactions with the 3′ hairpin stem and stem-loop. The ability of dyskerin to act as an anchor for the entire protein complex at the base of the 5′ hairpin is consistent with a previous report of the tolerance of this hairpin to changes in both stem and pocket structure with respect to hTR stability and biogenesis, as well as the evolutionary divergence for the 5′ H/ACA hairpin in vertebrate TRs which are hypervariable in this region (Chen, Blasco et al. 2000, Egan and Collins 2012). Previous biochemical analysis also demonstrated that H/ACA proteins display increased hTR-specific binding to the 3′ hairpin (Egan and Collins 2010), and the telomerase cryo-EM structure suggests that this may compensate for the lack of 5′ hairpin-H/ACA protein contacts with hTR, aside from the interaction with dyskerin. Furthermore, the positions and critical RNA interactions of the two dyskerin densities in the cryo-EM structure provide an explanation for why GAR1, NOP10 and NHP2 have been reported to be capable of exchange on the H/ACA domain in cell extracts, while dyskerin is unable (Kittur, Darzacq et al. 2006). The extended 5′ H/ACA hairpin of hTR which fosters the interaction between the CR4/5 domain and hTERT confirms the structural uniqueness of hTR with respect to other H/ACA RNAs, contributing to the flexibility of the active bi-lobed telomerase holoenzyme, and also demonstrating evident structural variability in H/ACA domains and RNP assembly interfaces (Nguyen, Tam et al.

2018). Importantly, this cryo-EM structure further confirms the essentiality of dyskerin to all H/ACA RNA functions, whether as a component of telomerase assembled with hTR or pseudouridine synthase assembled with sno/scaRNAs.

Figure 1.5 – Human telomerase cryo-EM structure (figure adapted from (Nguyen, Tam et al. 2018))

The human telomerase enzyme structure was solved by cryo-EM analysis, providing not only the first high resolution structure of human telomerase but also the first structure of a complete human H/ACA RNP. This structure reveals the flexibility of the human telomerase RNA, the bi-lobed nature of human telomerase, and differences in H/ACA complex contacts with the 5′ and 3′ stemloops of the H/ACA biogenesis domain in hTR. The interface between the two dyskerin subunits of the heterotetrameric H/ACA RNP dimer near the RNA-binding interface (boxed in green) has been proposed to mediate the security of the 5′ stemloop-bound RNP for hTR, and this region was also mapped as the location of a cluster of disease-causing mutations in patients with the premature aging disease X-linked dyskeratosis congenita. This adapted figure is reprinted from (Nguyen, Tam et al. 2018) in accordance with the Springer Nature and Copyright Clearance Center.

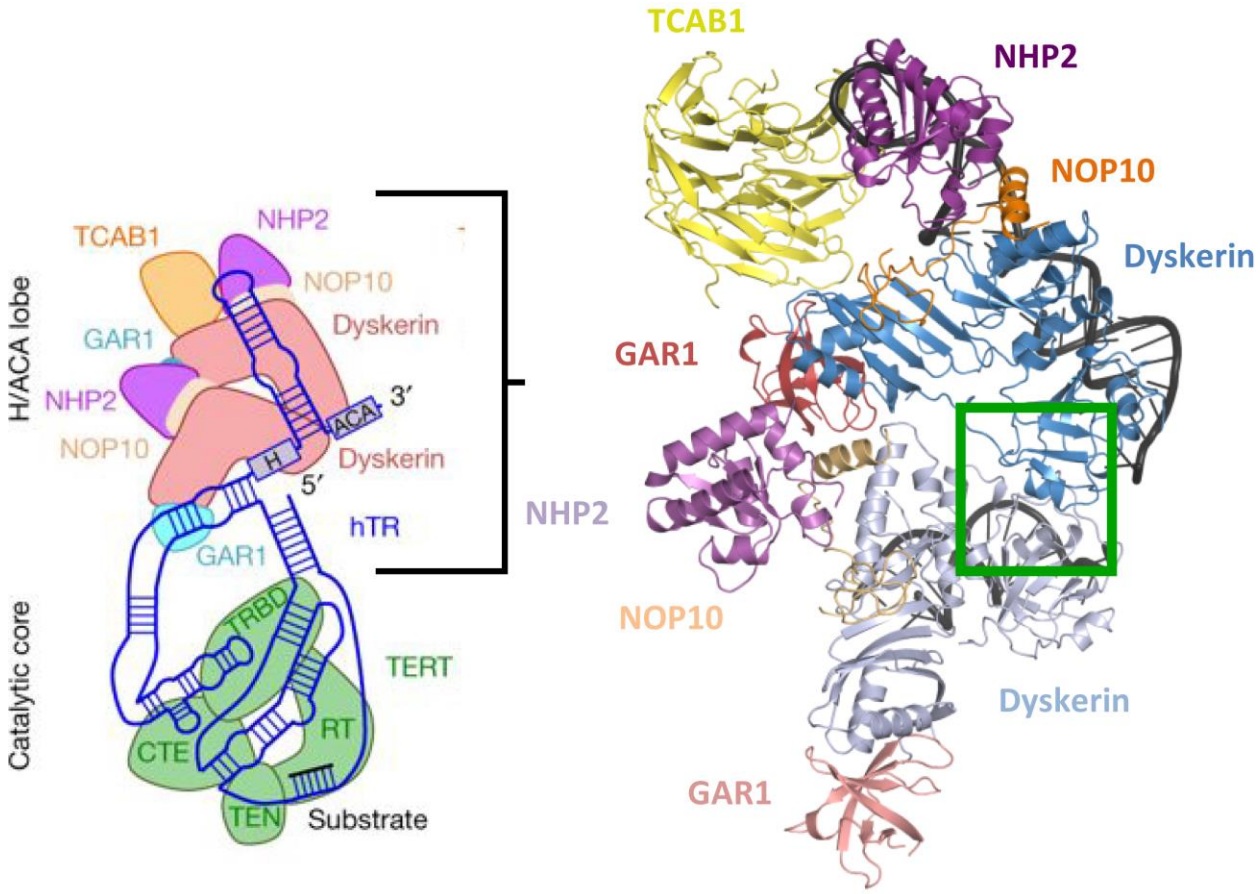
TCAB1
NHP2
NOP10
Dyskerin
GAR1
NHP2
NOP10
Dyskerin
H/ACA lobe
ACA
H
3′
5′
hTR
GAR1
TRBD
TERT
RT
CTE
TEN
Substrate
Catalytic core
NHP2
TCAB1
NHP2
NOP10
Dyskerin
GAR1
NOP10
Dyskerin
GAR1

1.4 Dyskerin Function and Localization

Just as essential as H/ACA RNP assembly, the properly regulated localization of dyskerin to subnuclear compartments is critical for it to carry out its duties in telomere maintenance and rRNA/snRNA posttranscriptional modification [Figure 1.4]. A great deal remains unknown about what is governing the correct localization of dyskerin (and consequently mature H/ACA RNPs), though its localization in the nucleoplasm, nucleolus, CBs, and at telomeres has been reported through live cell imaging and telomeric chromatin immunoprecipitation (ChIP) experiments (Heiss, Girod et al. 1999, Stern, Zyner et al. 2012). Understanding the localization, and therefore function of dyskerin necessitates an understanding of the subnuclear membrane-free compartments where H/ACA RNPs reside and how these compartments themselves are managed by dynamic protein-protein and protein-RNA interactions.

1.4.1 Membrane-free Subnuclear Compartmentalization: Nucleoli and Cajal Bodies

The nucleus itself is a conventional example of cellular compartmentalization, in that it relies on lipid bilayers (the nuclear envelope or NE) to impart a boundary between cytoplasmic and nuclear cellular constituents [Figure 1.4C]. There is an ever-growing amount of evidence that subnuclear membrane-free compartmentalization such as that of the nucleolus and the CBs is governed by phase transition dynamics, in particular by liquid-liquid phase separation (LLPS) [Figure 1.6B] (Banani, Lee et al. 2017, Strom and Brangwynne 2019). A helpful analogy for understanding LLPS that is typically used to describe the concept of this compartmentalization is one of water-oil immiscibility – that is, these two liquids do not easily form a homogeneous mixture when combined, but rather produce a two-phase liquid with an aqueous phase surrounding hydrophobic liquid droplets or condensates, or vice versa. The size and shape of the condensates is relative to the amount of each component in the system, and as these variables change so too does the separation of the condensates in the system. For instance, if the majority of the mixture is oil, then the droplets will consist of water molecules. As more water is added to the mixture, this system will eventually change to one in which the observed droplets or condensates are composed of oil molecules. While this is a simplistic view of a two-phase liquid-liquid phase separation, it is nonetheless an accurate physical description of what takes place in biological systems with ever-changing variables and dynamic phase exchanges. In the case of cellular compartmentalization, this phase separation is driven by protein and nucleic acid interactions which can foster either separation or dissolution of membrane-free condensates that

dynamically change in shape, size, and composition. In particular, the ideal recipe for phase separated bodies in biological systems has been suggested to involve: proteins with intrinsically disordered or low complexity regions (IDRs or LCRs); many weak multivalent interactions between components; and interactions with polymeric scaffolds like RNA molecules (Brangwynne, Eckmann et al. 2009, Kato, Han et al. 2012, Li, Banjade et al. 2012, Zhang, Elbaum-Garfinkle et al. 2015, Saha, Weber et al. 2016). However, there is evidence that not all these conditions need to be met for phase separation to occur in biological systems (for instance, RNA molecules that induce phase separation alone (Jain and Vale 2017)), and the ability of a biomolecule to phase separate is not necessarily an indicator of LLPS. It is important to bear in mind that aggregation is not equivalent to complex coacervation (Overbeek and Voorn 1957), and though they both rely on similar principles of immiscibility, not all membrane-free compartmentalization is created equal. Indeed, proteins with IDRs have been known to form aggregates in many different pathological neurodegenerative states (such as tau and amyloid β in Alzheimer's disease), creating insoluble compartments that do not undergo regulated condensation and dissolution (Elbaum-Garfinkle 2019). This is in contrast to membrane-free compartments like the nucleolus which dissolves during mitosis and is reformed in a regulated manner every cell cycle through nucleation and growth at active rRNA transcriptional sites, namely nucleolar organizer regions (NORs) (Shevtsov and Dundr 2011).

The nucleolus is perhaps one of the most useful examples of membrane-free LLPS in living systems due to the extensive amount of research focused on its components and functions, and made easier to study due to the large size of the nucleolus in comparison to other membrane-free compartments. Nucleolar compartmentalization has been demonstrated to represent a four-phase system [Figure 1.4C] entailing: separation of the nucleolus as a whole from the nucleoplasm (phase 1) (Brangwynne, Mitchison et al. 2011, Weber and Brangwynne 2015); and separation of each of the three overlapping but functionally and compositionally distinct nucleolar components – the outer granular component or GC (phase 2), the middle dense fibrillar component or DFC (phase 3), and the inner fibrillar component or FC (phase 4) (Scheer and Weisenberger 1994, Boisvert, van Koningsbruggen et al. 2007, Feric, Vaidya et al. 2016). Nucleolar separation into these three components is important for the sequential transcription, sorting, and processing of pre-rRNA, and assembly of the ribosome – though mechanistically understanding the separation of these components and their functions is just beginning to be

revealed by analyses of LLPS (Feric, Vaidya et al. 2016, Yao, Xu et al. 2019). The DFC is thought to be the site of posttranscriptional modification for pre-rRNA, as this middle nucleolar component is where mature C/D and H/ACA RNPs localize (Ochs, Lischwe et al. 1985, Yao, Xu et al. 2019). Much of what is known regarding the phase dynamics of the DFC has come from studying fibrillarin and its ability to form viscoelastic semiliquid-like droplets both *in vitro* and in cells (Brangwynne, Mitchison et al. 2011, Feric, Vaidya et al. 2016, Yao, Xu et al. 2019).

Fibrillarin is the catalytic component of C/D RNPs, analogous to the role of dyskerin in H/ACA RNPs as a pseudouridine synthase; fibrillarin is a methyltransferase responsible for 2′-O-methylation of rRNA and snRNA. It has two characterized domains, an N-terminal glycine and arginine rich (GAR) domain, and a C-terminal methyltransferase domain (MD). While the MD is required for catalytic activity and interaction of fibrillarin with RNA, the GAR domain is a low complexity domain with high intrinsic disorder, and considering these properties in the context of fibrillarin localization to the pre-rRNA-rich DFC it is a logical hypothesis that fibrillarin is a textbook candidate for partitioning via LLPS-mediated compartmentalization. Indeed, fibrillarin can form concentrated liquid-phase droplets *in vitro* at near-physiological protein and salt concentrations, and does so optimally in the presence of an RNA scaffold or heparin, acting as a polyanionic electrostatic interaction-mediator (Feric, Vaidya et al. 2016, Yao, Xu et al. 2019). Determining association kinetics of full length fibrillarin in the nucleolus of cells or in liquid droplets *in vitro* by fluorescence recovery after photobleaching (FRAP) revealed that this protein only partially recovers in a photobleached area within a given timescale, which is a property of viscoelasticity rather than a fully fluid-like behavior of complete recovery (Feric, Vaidya et al. 2016). Strikingly, *in vitro* droplets formed by full length fibrillarin display further reductions in FRAP as droplets age, and these droplets acquire gel-like properties over time. In contrast, liquid-droplets of the GAR domain of fibrillarin alone display complete FRAP *in vitro* and do not take on gel-like properties as they age, leading to the interpretation by Feric *et al.* that this LCR of fibrillarin confers fluid-like properties to the full length protein *in vitro*. While the MD alone cannot form liquid-droplets *in vitro*, FRAP experiments within the nucleolus of cells revealed that the MD also possesses greater recovery and therefore lower association kinetics/more fluid-like behavior than the full length protein, complicating the notion that one domain or another confers fluid-like phase separation properties representative of the behavior of a full length protein in membrane-free compartments (Yao, Xu et al. 2019). Indeed, these two

studies draw different conclusions regarding each domain's role in fibrillarin LLPS, as Yao *et al.* speculated conversely that the GAR domain may confer the solid-like dynamics of fibrillarin in the DFC. These differences in interpretation are likely due to experimental differences, largely dependent on the presence or absence of RNA and/or full length fibrillarin in the phase systems being assessed. In cells where full length fibrillarin is also present, the individual domains of fibrillarin partition differently when exogenously expressed: the GAR domain localizes to both the GC and the DFC, whereas the MD strongly partitions to the DFC and displays no miscibility with the GC (Feric, Vaidya et al. 2016). High resolution imaging with structured illumination microscopy revealed that in fact, the MD localizes in a small cluster at the border of the FC and DFC interior to full length fibrillarin, and is able to constrain pre-rRNA at this border but unable to effect efficient pre-rRNA processing in cells depleted of endogenous fibrillarin. Though the MD is required for RNA-binding by fibrillarin and the GAR domain alone cannot interact with RNA, real-time fluorescence imaging demonstrated that RNA is less efficiently sorted into *in vitro* liquid-droplets of fibrillarin possessing a shorter GAR domain than droplets comprised of full length fibrillarin. Extensive analyses by fluorescence resonance energy transfer (FRET) between N-terminal and C-terminal acceptor/donor tagged fibrillarin, and oligomerization state assessment through native polyacrylamide gel electrophoresis (PAGE) revealed that the GAR domain is responsible for self-assembly of fibrillarin and that the efficiency of this self-assembly is proportional to the length of GAR domain irrespective to orientation or position of glycine/arginine-rich clusters. Replacing the GAR domain of fibrillarin with a GAR domain from another protein, such as that of the H/ACA component GAR1, also conferred the ability to self-assemble and mediate efficient rRNA sorting/processing to fibrillarin chimera proteins. Importantly, catalytic dead mutants of fibrillarin show no defects in localization or rRNA sorting/processing in cells depleted of endogenous fibrillarin, and as such the methyltransferase function is not involved in the compartmentalization of fibrillarin *per se* (Yao, Xu et al. 2019).

Fibrillarin is just one protein component of the DFC, but understanding its physical properties and its partitioning provides insight to what is governing regulation of miscibility and thus localization of other components of the DFC. Indeed, the high resolution imaging applied for visualizing fibrillarin localization by Yao *et al.* also revealed that the particular ring-shaped clustering pattern of fibrillarin in the DFC is observed for other snoRNPs including dyskerin, NOP10, NHP2, and GAR1 (Yao, Xu et al. 2019). Beyond nucleation of the nucleoli themselves

by rRNA transcription, there is a critical gap in our knowledge of what regulates H/ACA RNP maturation and localization to its functional subnuclear compartments like the nucleolus, and understanding LLPS dynamics of fibrillarin will lead to better comprehension of this process for all subnuclear compartment components.

Protein components of C/D and H/ACA RNPs are also found in the spherical subnuclear coiled-body compartments CBs (Machyna, Heyn et al. 2013). While experimental evidence of CBs forming as a result of LLPS is lacking, the components of CBs undergo constant exchange with the nucleoplasm and are characteristic candidates for LLPS-mediated compartmentalization based on the conditions specified previously in this section. Indeed, the equilibrium of CB composition is largely mediated by protein-protein and protein-RNA interactions within these compartments themselves (Handwerger, Murphy et al. 2003, Dundr, Hebert et al. 2004, Handwerger, Cordero et al. 2005), and similar to the nucleolus forming at NORs, nucleation of CBs appears to take place at sites of snRNA transcription (Frey, Bailey et al. 1999), though their number and size varies between cell type and across the cell cycle with complete disassembly occurring during mitosis (Andrade, Tan et al. 1993). In addition to being sites of snRNA modification, these compartments are important for telomerase biogenesis and regulation. Biogenesis and maturation of hTR relies on compartmentalization in the CBs, and while there have been some confounding reports about the exact role of these compartments in telomere maintenance, live imaging studies have revealed that CBs are likely where telomerase assembly occurs (Schmidt and Cech 2015, Schmidt, Zaug et al. 2016, Laprade, Querido et al. 2020). Both hTERT and hTR dynamically localize to CBs, with hTR having a longer residency time in these compartments than hTERT. These live imaging studies demonstrate that telomere elongation takes place outside of CBs, in contrast to a hypothesis based on an earlier study revealing co-localization of telomeres with CBs during S-phase in fixed cells (Jady, Bertrand et al. 2004). Furthermore, two key protein components which help to differentiate the localization of H/ACA RNPs assembled with scaRNAs, including human telomerase from the localization of H/ACA RNPs assembled with snoRNAs have been elucidated. This difference in localization is related to the presence of the CAB-box, which is found in all scaRNAs and absent from snoRNAs. The CAB-box binding scaffolding protein TCAB1 (Telomerase Cajal body protein 1, also known as WDR79 - WD repeat-containing protein 79) and the intrinsically disordered C/D and H/ACA RNP-binding phosphoprotein Nopp140 both play roles in localizing and anchoring scaRNPs to

CBs (Yang, Isaac et al. 2000, Tycowski, Shu et al. 2009, Venteicher, Abreu et al. 2009, Bizarro, Bhardwaj et al. 2019). CAB-box mutations or mutations in TCAB1 displace scaRNPs from the CBs, and in the case of telomerase disrupt telomerase activity and lead to telomere shortening (Jady, Bertrand et al. 2004, Cristofari, Adolf et al. 2007, Venteicher, Abreu et al. 2009, Chen, Roake et al. 2018). However, while depletion of Nopp140 also displaces scaRNPs specifically from CBs, telomere extension by telomerase gradually increases in the absence of Nopp140. This may be due to differential roles in telomerase regulation, as TCAB1 regulates scaRNA accumulation and mediates hTR folding for telomerase activity, whereas Nopp140 does not regulate accumulation of scaRNAs or the assembly of scaRNPs (Chen, Roake et al. 2018, Bizarro, Bhardwaj et al. 2019). Interestingly, as with H/ACA RNP components, Nopp140 is found in both the nucleolus and CBs at steady state, whereas TCAB1 exclusively localizes to the CBs (Yang, Isaac et al. 2000, Tycowski, Shu et al. 2009, Venteicher, Abreu et al. 2009). It has been proposed that while TCAB1 helps to localize scaRNPs to the CBs, Nopp140 regulates the residency or anchoring of scaRNPs in the CBs (Bizarro, Bhardwaj et al. 2019), though exactly how this dynamic process is governed such that distinct partitioning of CBs from the nucleoplasm occurs is in need of further elucidation. Strikingly, a core protein component of CBs, coilin contains a GAR motif with intrinsic disorder which governs self-oligomerization, similar to that of fibrillarin (Hebert, Szymczyk et al. 2001), suggesting the possibility that GAR domain-mediated phase separation may mediate compartmentalization of the DFC and CBs alike.

1.4.2 Posttranslational Modifications and LLPS

As for oil-water immiscibility, changing concentration of a component in a system is one way to affect condensation or dissolution of a phase separated compartment. However, in situations of fixed concentration, phase separation can instead be affected by changing interaction strengths of components in the system [Figure 1.6B] (Strom and Brangwynne 2019). The aforementioned assistance of polyanionic electrostatic scaffolds like RNA or heparin in LLPS is one way to do this, but in the case of protein-protein interactions this can also be regulated by reversible posttranslational modifications [Figure 1.6]. Indeed, a family of kinases referred to as DYRK kinases have been demonstrated to govern the compartmentalization of many different membrane-free condensates through regulated phosphorylation events, particularly in cell cycle regulated dissolution of cytoplasmic and splicing bodies (Saunders, Pan

et al. 2012, Wippich, Bodenmiller et al. 2013, Rincon, Bhatia et al. 2014, Wang, Smith et al. 2014, Rai, Chen et al. 2018). In the case of subnuclear compartments, the small ubiquitin-like modifier (SUMO) has been implicated in the localization and phase transition of several factors, with a great deal of focus on promyelocytic leukemia (PML) nuclear bodies (NBs), though nucleolar and CB localization regulation by SUMOylation has also been demonstrated for certain proteins.

SUMOylation is a posttranslational modification that involves the reversible conjugation of the small modifier protein SUMO to a lysine residue of a target protein. This conjugation involves an enzymatic cascade that: matures SUMO proteins through SUMO-specific protease-mediated cleavage to reveal a C-terminal diglycine repeat; activation of SUMO by an E1 enzyme in an ATP-dependent manner; and conjugation by an E2 enzyme UBC9 (Desterro, Rodriguez et al. 1999, Gong and Yeh 1999, Okuma, Honda et al. 1999), which is sometimes assisted in efficiency and target specificity by E3 SUMO ligases [Figure 1.6A] ((Pichler, Gast et al. 2002), and reviewed in (Melchior, Schergaut et al. 2003, Varejao, Lascorz et al. 2019)). The same SUMO-specific proteases involved in maturation of SUMO proteins are also involved in removing SUMO from target proteins and trimming SUMO chains (Li and Hochstrasser 1999, Gong, Millas et al. 2000, Li and Hochstrasser 2000, Takahashi, Mizoi et al. 2000), which form through conjugation of SUMO to SUMO 2/3 isoforms that are already conjugated to a target protein. Importantly, SUMO2/3 isoforms are nearly identical and contain a target lysine residue themselves, whereas the SUMO1 isoform is only about 50% identical in sequence to SUMO2/3 and does not contain a target lysine, and therefore can only cap SUMO chains or be directly conjugated to a target lysine (Saitoh and Hinchey 2000, Tatham, Jaffray et al. 2001, Hay 2005). Importantly, SUMOylation has been reported to have a wide variety of regulatory roles, depending on the target to which it is conjugated. This posttranslational modification is particularly useful for mediating protein-protein interactions between target proteins and proteins that contain SUMO-interacting motifs (SIMs), which are typically short hydrophobic stretches of residues that form an extended β-strand backbone which non-covalently interacts with SUMO moieties (Song, Durrin et al. 2004, Song, Zhang et al. 2005, Hecker, Rabiller et al. 2006, Varejao, Lascorz et al. 2019). Indeed, one such well-studied example is SUMOylation of PML, which has been demonstrated to regulate interactions between the PML protein and SIM-

containing proteins including PML itself, mediating formation of PML NBs through SUMO-SIM interactions (Shen, Lin et al. 2006).

Figure 1.6 – SUMOylation and Modulating Interaction Strength to Govern Membrane-free Compartmentalization

A. SUMOylation is a posttranslational modification that is analogous to ubiquitination, in that it involves an enzymatic cascade of E1, E2, and E3 enzymes responsible for conjugation of a small modified protein (SUMO) to a lysine (K) residue of a target protein. Before entering into this enzymatic cascade, SUMO proteins undergo cleavage by SUMO-specific proteases (in humans, SENPs), which cleave just after a C-terminal diglycine (GG), which is then activated in an ATP-dependent manner by formation of a thioester bond with the active site cysteine residue in the E1 enzyme. In humans, the E1 enzyme involved in this process is a heterodimer made of SAE2 and SAE1. Activated SUMO is transferred to the E2 conjugating enzyme, known as UBC9 via another thioester bond between the SUMO glycine and an active site cysteine on UBC9. UBC9 is capable of catalyzing SUMO conjugation on its own, though is thought to be aided in efficiency and target protein specificity by E3 SUMO ligases, of which there are many in humans. Importantly, UBC9 is also able to catalyze the formation of SUMO chains, with SUMO2/3 isoforms containing target lysine residues themselves. SUMOylation is a reversible posttranslational modification, with SUMO-specific proteases also being responsible for removal of SUMO through cleavage of the isopeptide bond between the SUMO GG tail and the target lysine.

B. Liquid-liquid phase separation (LLPS) is a means through which the components of membrane-free compartments in biological systems are organized and regulated. One way to consider LLPS is in the context of components with defined and unchanging interaction strengths. The phase diagram schematic on the left of this figure indicates that mixing of components is governed by energy of the system, energy of the interactions between components, and the concentration of components. In an environment with a constant temperature, mixing of two components with constant interaction energies is governed by concentration of each component. At a relatively high temperature for example, it may be energetically favourable for two components to mix into a single phase regardless of component concentrations. However, when single phase mixing is not energetically favourable for these two same components due to the energy of the system, for example at a relatively low temperature, mixing involves formation of multiple separated phases (in this case, two), the compositions of which vary based on component concentrations in the system.

These three determinants of mixing (energy of the system, energy of the interaction, and concentration) can be manipulated to change the phase behaviour of a system (right panel). Changing the concentration of components with constant interaction energies in a system may drive the system in or out of a single phased mix at a particular energy state of the system. Likewise, changing the interaction strength of two components in a constant system may drive the system in or out of a single phased mix at a particular concentration of components. In a biological system, we can think of changing concentration as changing the amount of a component in the system (i.e. changing translation or degradation of a protein) or changing the amount of a component in a particular compartment, for example through changes in protein trafficking or multivalent protein-protein/protein-RNA interactions. We can also think of changing interaction strength through transient modifications that foster or impede interactions. For example, SUMOylation of a target protein may strengthen the interaction of the target with a protein containing a SUMO-interacting motif (SIM), and due to the reversibility of SUMOylation, this posttranslational modification provides a means to dynamically control interaction strength of components, and thus phase separation/mixing. The information for building these schematics was found in the review article (Strom and Brangwynne 2019).

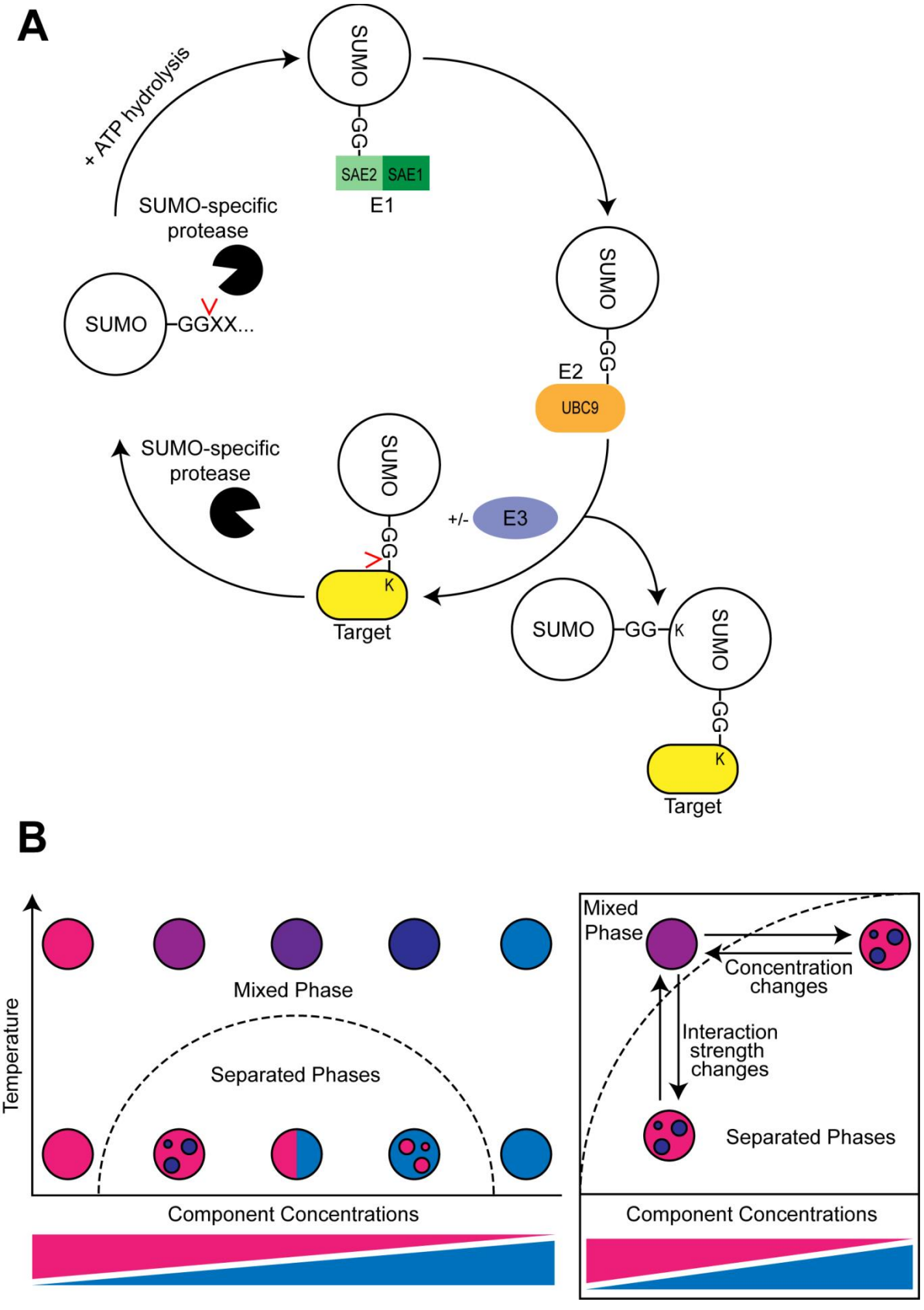
A
+ ATP hydrolysis
SUMO
GG
SAE2
SAE1
E1
SUMO-specific protease
SUMO
GGXX...
SUMO
GG
E2
UBC9
SUMO-specific protease
SUMO
GG
K
Target
+/-
E3
SUMO
GG
K
SUMO
GG
K
Target
B
Temperature
Mixed Phase
Separated Phases
Component Concentrations
Mixed Phase
Concentration changes
Interaction strength changes
Separated Phases
Component Concentrations

PML NBs are subnuclear structures that have been reported to carry out a number of functions, co-localizing with protein components involved in genome integrity maintenance, apoptosis, transcriptional regulation, and the proteasome (Zhong, Salomoni et al. 2000, Zhong, Salomoni et al. 2000, Jensen, Shiels et al. 2001, Hofmann and Will 2003, Lamoliatte, McManus et al. 2017). PML protein is the core component required for PML NB compartmentalization, as depletion of PML, preventing SUMOylation of PML, or mutating the SIM in PML disrupts compartmentalization (Ishov, Sotnikov et al. 1999, Zhong, Muller et al. 2000, Lallemand-Breitenbach, Zhu et al. 2001, Shen, Lin et al. 2006, Nisole, Maroui et al. 2013). PML NB nucleation can still occur with PML that has impaired SUMOylation or with PML protein lacking a SIM, though fewer PML NBs form and there is impaired recruitment of other PML NB SUMOylated components such as DAXX and SP100 in cells depleted of SUMO by siRNA (Sahin, Ferhi et al. 2014). PML can also self-assemble through a TRIM (Tripartite Motif) (Antolini, Lo Bello et al. 2003, Huang, Naik et al. 2014), though it is evident that interactions between SUMO and the PML SIM domain strongly contribute to PML NB compartmentalization and architecture. As with other subnuclear bodies, PML NB components are able to readily exchange in and out of the nucleoplasm due to a spherical shell-like 3D conformation of PML and components with which it interacts, including SUMO (Lang, Jegou et al. 2010). SUMO/SIM mediated LLPS of cellular bodies has also been modeled with artificial SUMO-chains and SIM domains *in vitro* and in cells, and the natural partitioning of PML NBs was observed to display similar recruitment stoichiometry as the SUMO/SIM model of LLPS (Banani, Rice et al. 2016). This model of SUMO/SIM mediated phase transition also sets an intriguing precedent for other SUMOylation targets localized to membrane-free compartments like the nucleolus and CBs. Indeed, the core structural component in CBs, SMN (survival motor neuron) protein, has been reported to be both a SUMOylation target and a SIM-containing protein, both of which are key for CB formation and recruitment of CB components such as SmD1 and coilin (Tapia, Lafarga et al. 2014). Importantly, many of the proteins that have been demonstrated to have SUMO-regulated nucleolar miscibility or exclusion do so in response to stress, such as topoisomerase I and p21 (Rallabhandi, Hashimoto et al. 2002, Latonen 2011, Latonen, Moore et al. 2011, Brun, Abella et al. 2017, Latonen 2019) which are not resident nucleolar proteins, suggesting that the nucleolar aggresome rather than LLPS-mediated compartmentalization has been the regulatory target of focus for SUMOylation and the nucleolus to date. However, SUMOylation machinery

including the SUMO-specific proteases SENP3 and SENP5 have been observed in the nucleolus, and targets of this machinery including nucleophosmin (NPM1) and the C/D RNP component Nop58 have been demonstrated to require SUMO regulation to carry out functions in rRNA processing and snoRNP biogenesis (Gong and Yeh 2006, Haindl, Harasim et al. 2008, Westman, Verheggen et al. 2010). Regardless of whether SUMO is regulating aggregation or LLPS, determining the importance of SUMOylation and other posttranslational modifications for efficient membrane-free compartmentalization will allow for a better understanding of how the dynamic exchange of subnuclear components like dyskerin and the H/ACA complex takes place. Importantly, dyskerin and another H/ACA complex component NHP2 have been demonstrated to be SUMOylation targets (Westman, Verheggen et al. 2010, Brault, Lauzon et al. 2013), and though the functional relevance of NHP2 SUMOylation remains unknown, dyskerin SUMOylation was shown to regulate dyskerin protein stability and hTR levels, and as such can mediate telomerase activity and telomere maintenance. In particular, substituting either of two DC-implicated dyskerin SUMOylation sites (K39 and K43) to arginine, and thus reducing the amount of SUMOylated dyskerin, leads to reductions in hTR, less telomerase activity, and accelerated telomere shortening (Brault, Lauzon et al. 2013). Many proteome-wide studies of SUMOylation targets have also identified dyskerin SUMOylation sites, some of which are located in the nuclear/nucleolar localization regions, but remain functionally uncharacterized (Becker, Barysch et al. 2013, Hendriks, D'Souza et al. 2014, Impens, Radoshevich et al. 2014, Hendriks, Treffers et al. 2015, Xiao, Chang et al. 2015, Hendriks, Lyon et al. 2017, Lamoliatte, McManus et al. 2017, Hendriks, Lyon et al. 2018, El-Asmi, McManus et al. 2020). As such, it will be important to investigate the role SUMOylation plays in regulating dyskerin and H/ACA complex compartmentalization, and the downstream functional consequences of this compartmentalization regulation.

1.5 SUMOylation Orchestrating Ribosomes and Telomere Maintenance

There is precedent for SUMOylation regulating pathways that coincide with dyskerin function, including ample evidence of the involvement of SUMO in telomere maintenance and ribosome biogenesis (Jentsch and Psakhye 2013, Zhao 2018). While dyskerin SUMOylation has been shown to regulate telomerase and telomere maintenance (Brault, Lauzon et al. 2013), to date there has been no direct link between dyskerin SUMOylation specifically and the ribosome. Rather, the importance of SUMOylation in ribosome biogenesis has been demonstrated for

several other factors in this complex multiplayer process, emphasizing a broader role for SUMOylation in ribosome biology. Indeed, there are many SUMOylation targets involved in both functional pathways of dyskerin, as reported telomere regulatory roles for SUMOylation also extend beyond dyskerin.

1.5.1 Ribosome Biogenesis and SUMOylation

The coordination of production, processing, and assembly of ribosomes is a core essential pathway that requires tight regulation. Fundamentally, ribosomes are the molecular factories governing protein synthesis, and as for telomere maintenance, misregulation of ribosome biology can be disastrous for human health; inefficient ribosome biogenesis leads to diseases known as ribosomopathies, while overproduction of ribosomes is a common aberrancy in many cancers due to oncogenic dysregulated translational control and higher metabolic needs in cancer cells (Mills and Green 2017, Sulima, Hofman et al. 2017). Ribosomes are intricate ribonucleoprotein complexes, with subunit synthesis and assembly centered on the nucleolus as the location of rRNA transcription, modification, and processing (Cheutin, O'Donohue et al. 2002, Boisvert, van Koningsbruggen et al. 2007). Nucleolar resident proteins carry out various roles in ribosome biogenesis, and as has been previously discussed briefly in section 4.1, compartmentalization of the nucleolus and its components contributes to the coordination of stepwise rDNA transcription by RNA Polymerase I (RNAPI) at the interface of the FC and DFC, pre-rRNA modification in the DFC, and processing of pre-rRNA as well as ribosome subunit assembly in the GC (Scheer and Weisenberger 1994, Cheutin, O'Donohue et al. 2002, Boisvert, van Koningsbruggen et al. 2007, Feric, Vaidya et al. 2016, Yao, Xu et al. 2019). Regulation of this process by SUMOylation has been reported for rDNA transcription regulation and for pre-rRNA processing/subunit assembly.

In *Saccharomyces cerevisiae*, SUMOylation of several nucleolar rDNA-binding factors has been shown to mediate silencing of transcription of rRNA in a SUMO-targeted ubiquitin ligase (STUbL) dependent manner (Gillies, Hickey et al. 2016, Liang, Singh et al. 2017). More specifically, nucleolar targets of the SUMO-specific protease Ulp2 (Tof2, Net1, and Fob1) were observed to lose rDNA binding in yeast with mutant Ulp2 as a result of increased SUMOylation and subsequent ubiquitylation, which could be rescued by combining the Ulp2 mutation with a mutation in the ubiquitin ligase Slx5 (Gillies, Hickey et al. 2016). Liang *et al.* demonstrated that Ulp2 deSUMOylation of nucleolar proteins is mediated by an interaction between Ulp2 and the

rDNA-binding protein Csm1, and disruption of this interaction leads to degradation of Tof2 in an Slx5-dependent manner, leading to reduced rDNA silencing by Tof2. SUMOylation-mediated regulation of later steps in the ribosome biogenesis pathway has also been demonstrated in *S. cerevisiae*. A thermosensitive yeast mutant with pre-60S ribosomal subunit export defects causing nucleolar accumulation of pre-ribosomes can be rescued by exogenous expression of the E1 SUMOylation enzyme Uba2, or phenocopied by mutations in various SUMO pathway components (Ubc9, the SUMO1 orthologue Smt3, and the SUMO-specific protease Ulp1) (Panse, Kressler et al. 2006). SUMO pathway mutants were demonstrated by Panse *et al.* to have defects in pre-rRNA processing, and this study also genetically showed that compromising the SUMO pathway exacerbates lethality in 60S biogenesis mutants. Indeed, many nuclear *trans*-acting and assembly factors of both 40S and 60S pre-ribosomes were demonstrated to be SUMOylation targets themselves, and deSUMOylation of the 60S pre-ribosomal subunit at the nuclear pore complex (NPC) where Ulp1 localizes was speculated to be required for nuclear export of pre-ribosomes based on the genetic interaction of Ulp1 with the pre-60S export factor Mtr2 (Panse, Kressler et al. 2006).

Similarly, SUMO-mediated regulation of ribosome biogenesis has also been demonstrated in human cells, and has also largely focused on SUMO-specific proteases and their targets. In contrast to the two known SUMO-specific proteases in *S. cerevisiae*, Ulp1 at the NPC and Ulp2 in the nucleolus, there are many SUMO-specific proteases in humans (Gong, Millas et al. 2000, Jentsch and Psakhye 2013). Two nucleolar SUMO-specific proteases have been reported in humans, which both have been implicated in ribosome biogenesis: SENP3 and SENP5 (Di Bacco, Ouyang et al. 2006, Haindl, Harasim et al. 2008, Yun, Wang et al. 2008). Both SENP3 and SENP5 are found in the GC, and interact with the GC component NPM1 (Haindl, Harasim et al. 2008, Yun, Wang et al. 2008). Yun *et al.* reported that depletion of either of these SUMO-specific proteases affects ribosome biogenesis by leading to pre-rRNA processing defects, with increased precursor levels (32S in the case of SENP3 depletion and 47S in the case of SENP5 depletion) at the expense of mature rRNA levels. Haindl *et al.* also demonstrated that rRNA processing is affected by SENP3 depletion, with increased 32S and decreased 28S levels that resemble pre-rRNA processing defects in cells depleted of NPM1. Intriguingly, while NPM1 itself is a SUMOylation target and can be deSUMOylated by SENP3, mimicking constitutive SUMOylation of NPM1 through fusion to SUMO2 does not rescue pre-

rRNA processing defects in cells depleted of endogenous NPM1 (Tago, Chiocca et al. 2005, Haindl, Harasim et al. 2008). However, it has been confirmed that SENP3 localizes to the nucleolus in a NPM1 interaction-dependent manner (Raman, Nayak et al. 2014). Furthermore, SENP3 has been reported to be a key component of a human 60S ribosomal maturation complex comprised of PELP1, TEX10, and WDR18, which is responsible for nucleolar release of the 60S subunit, and which is associated with the ribosomal maturation/export components MDN1 and Las1L (Castle, Cassimere et al. 2010, Finkbeiner, Haindl et al. 2011, Castle, Cassimere et al. 2012). Finkbeiner *et al.* observed that SENP3 is able to deSUMOylate both PELP1 and Las1L *in vitro* and in cells, and that by increasing SUMOylation of PELP1 by overexpressing SUMO2 or depleting SENP3, PELP1 is excluded from the nucleolar compartment. As such, it was speculated that SENP3-mediated deSUMOylation of PELP1 is required for nucleolar localization of this complex and subsequent 60S subunit maturation, with SUMOylation serving as a quality control mechanism for ribosomal maturation in this context (Finkbeiner, Haindl et al. 2011, Finkbeiner, Haindl et al. 2011). Regulation of ribosome biogenesis steps in the DFC where the H/ACA complex is found have not yet been reported for humans, though indirect SUMO-mediated repression of RNAPI rDNA transcription has been shown through regulation of expression levels of the transcription initiator UBF (upstream binding factor) and the transcription factor c-Myc. In contrast to increased SUMOylation causing less rDNA silencing in yeast, this study demonstrated that reductions in SUMOylation due to depletion of Ubc9 or E3 SUMO ligases in HEK293 and HeLa cells increased pre-rRNA levels and transcription in the nucleolus, and that SUMO-mediated rDNA repression correlates with expression levels of UBF and c-Myc (Peng, Wang et al. 2019). This suggests that regulation of rDNA silencing/transcription by SUMOylation takes place in yeast and humans alike, but acts through functionally different pathways.

1.5.2 Telomere Maintenance and SUMOylation

As for the many reported SUMOylation targets implicated in ribosome biogenesis, a variety of telomere maintenance factors are SUMOylated, and there are several contexts in which SUMOylation governs regulation of telomeres. However, a key aspect of telomere biology that revolves around SUMOylation is independent from telomerase and dyskerin altogether; the alternative lengthening of telomeres (ALT) pathway is a DNA recombination-based mechanism of telomere maintenance that does not rely on telomerase and accounts for telomere maintenance

in a subset of cancers that are telomerase-negative (Bryan, Englezou et al. 1995, Muntoni and Reddel 2005). A key feature of ALT is the presence of large PML NBs which coincide with telomere clusters, known as APBs (ALT-associated PML bodies), which are enriched in the nucleus in G2 phase (Yeager, Neumann et al. 1999, Grobelny, Godwin et al. 2000). As was described in section 4.2, interactions between SUMO and SIM-containing proteins are important for formation of subnuclear compartments (including PML NBs in non-ALT contexts), and indeed there are known roles for SUMO in mediating APB formation as well as telomere maintenance within APBs (Potts and Yu 2007, Chung, Leonhardt et al. 2011, Min, Wright et al. 2019). The E3 SUMO ligase of the SMC5/6 complex (Mms21) in particular has been reported to regulate SUMOylation of shelterin components, which in turn leads to clustering of telomeres in APBs along with factors involved in recombination-based repair pathways, where DNA ends then undergo telomeric DNA synthesis (Potts and Yu 2007, Chung, Leonhardt et al. 2011, Min, Wright et al. 2017, Barroso-Gonzalez, Garcia-Exposito et al. 2019, Min, Wright et al. 2019, Zhang, Yadav et al. 2019). As such, the role of SUMOylation in this process is consistent with what is known about PML NBs, which mainly serve as condensates built around SUMOylated PML, responsible for clustering a number of factors together to carry out a variety of different functions. In the case of APBs, SUMOylation of TRF2 and TRF1 in particular has been shown to drive APB formation (Potts and Yu 2007), likely through accumulation of PML at the telomere which possibly acts as a nucleating event for APB formation and allowing for further clustering of proteins involved in recombination-based DNA synthesis such as factors involved in break-induced DNA replication (BIR) (Brouwer, Schimmel et al. 2009, Zhang, Yadav et al. 2019). Indeed, the phase-separated nature of APBs and their components has recently been established, and SUMO-SIM interactions are critical to this process, driving not only the function of BIR factors like BLM and Rad52 at telomeres, but also the appearance of other ALT features including mitotic DNA synthesis, extrachromosomal DNA C-circle formation, and heterogeneous telomere length typical of ALT telomeres (Min, Wright et al. 2019). In yeast, SUMOylation by Mms21 or the SUMO E3 ligase Siz2 contributes to the localization of DNA damage foci to the nuclear periphery either through interactions with nuclear pore proteins or the SUN domain protein Mps3 (Horigome, Bustard et al. 2016). Importantly, these distinct periphery sites seem to mediate different mechanisms of DNA repair, likely due to the differences in components found at nuclear pores compared to Mps3 sites, with a BIR-like mechanism taking

place at nuclear pores (Horigome, Bustard et al. 2016). The localization of eroded telomeres to nuclear pores in the context of telomerase-negative type II survivor yeast (i.e. yeast immortalized by an ALT-like mechanism) also drives telomere maintenance through a SUMO-dependent and BIR-like mechanism (Churikov, Charifi et al. 2016). As for APBs, there is evidence that nuclear pores behave as phase-separated bodies, contributing to the selective partitioning of the nucleus and the cytoplasm (Celetti, Paci et al. 2020). Thus, similar to functionally conserved orchestration of ribosome biogenesis, the role of SUMOylation in mediating telomere clustering along with BIR pathway components seems to be a functionally conserved mechanism of telomere maintenance in the absence of telomerase for both yeast and humans. The focus on the crucial role of SUMOylation in regulating telomere homeostasis has concentrated on telomerase-negative contexts, and as such, further investigation of how SUMO may regulate telomerase-mediated maintenance is needed, for example through regulation of the H/ACA complex. Indeed, as has already been discussed, the H/ACA complex is an important associate of telomerase in humans, emphasized by its implication in human health, which will be the final focus of this literature review.

1.6 Telomerase RNP and Premature Aging Disease

Mutations in genes encoding many different telomere maintenance components, including H/ACA complex components and assembly factors, have been identified to cause the premature aging disease dyskeratosis congenita (DC) (Podlevsky, Bley et al. 2008). Mutations in the *dkc1* gene which encodes dyskerin lead to an X-linked form of this disease (X-DC) (Heiss, Knight et al. 1998, Mitchell, Wood et al. 1999) characterized by pathology targeting proliferative tissues of patients including reticulate skin pigmentation, nail dystrophy, oral leukoplakia, and bone marrow failure (Connor, Gatherer et al. 1986, Drachtman and Alter 1992, Arngrimsson, Dokal et al. 1993, Dokal 1996). X-DC hotspots for mutations coincide with regions encoding the PUA (pseudouridine synthase and archaeosine transglycosylase) RNA binding domain/C-terminal extension, and in an N-terminal extension/dyskeratosis congenita-like domain (DKCLD) (Podlevsky, Bley et al. 2008). Patients with X-DC have reduced hTR levels which leads to telomerase defects and accelerated telomere shortening (Mitchell, Wood et al. 1999). X-DC is not the only mode of inheritance for DC that is characterized by reductions in hTR, and indeed many patients with DC and the related premature aging diseases IPF (idiopathic pulmonary fibrosis), RS (Revesz Syndrome), and HHS (Hoyeraal Hreidarsson syndrome), have been

reported to have impaired hTR accumulation (Stanley, Gable et al. 2016, Gable, Gaysinskaya et al. 2019). Among the factors implicated in these forms of premature aging disease that have characteristically low hTR accumulation are NOP10, NHP2, NAF1, PARN, SHQ1, ZCCHC8, TCAB1, and hTR itself (Podlevsky, Bley et al. 2008). Excluding telomere proteins and hTERT itself which are also implicated in DC pathology, mutations that disrupt hTR biogenesis account for a large proportion of patients with telomere syndromes, and though these diseases are rare, the importance of understanding defective hTR biogenesis in these patients cannot be understated. Each of these disease-implicated factors has been discussed in some detail throughout this literature review, and in this concluding section, how disease-causative mutations in these components relate to function will be briefly discussed.

1.6.1 H/ACA complex and assembly factors in premature aging disease

Mutations in *nola3* and *nola2* (encoding NOP10 and NHP2, respectively) cause autosomal recessive forms of DC, with the reported R34W substitution in NOP10 affecting a conserved residue thought to be involved in RNA interactions (Walne 2007), and several reported mutations disrupting the last exon of NHP2 with no demonstrated functional defect beyond reduced hTR levels (Vulliamy, Beswick et al. 2008). Most recently, disease variants were identified in and near the core L7Ae-homology region of NHP2 – one of which (R41H) dramatically disrupts hTR accumulation and levels of other H/ACA sno/scaRNAs through reductions in NHP2 protein, leading to defective rRNA biogenesis and accelerated telomere shortening, causing the severe premature aging disease HHS (Benyelles, O'Donohue et al. 2020). Interestingly, there have been no reported mutations in the gene encoding GAR1 in patients with premature aging disease (Sarek, Marzec et al. 2015), however the assembly factors upstream of GAR1 assembly with the H/ACA complex, NAF1 and SHQ1 have both been linked to telomere syndromes. In particular, NAF1 variants are implicated in IPF, with mutations causing decreased telomerase RNA accumulation and telomere shortening, as well as affecting levels of other H/ACA RNAs, though no rRNA pseudouridylation defects or ribosomal pathology was observed in first generation mice carrying these mutations (Stanley, Gable et al. 2016). A patient with autosomal recessive inherited HHS was recently identified carrying mutations in the gene encoding SHQ1, and these mutations ultimately disrupt the protein-protein interaction between SHQ1 and dyskerin (Bizarro and Meier 2017). This is consistent with SHQ1-binding domain

variants of dyskerin that cause X-DC, which result in lower levels of dyskerin and hTR (Grozdanov, Fernandez-Fuentes et al. 2009).

Autosomal dominant cases of DC caused by mutations in hTR itself also affect the H/ACA domain, with patient mutations or deletions reported in the H-box, ACA tail, and both hairpins (Podlevsky, Bley et al. 2008). One mutation in the H-Box (A377G) has been reported to lead to reductions in telomerase activity and accelerated telomere shortening due to reduced hTR accumulation, and a mutation at a conserved base adjacent to the CAB-box motif (C408G) disrupts the dyskerin-hTR interaction leading to reduced hTR levels and defects in telomerase activity (Theimer, Jady et al. 2007, Trahan and Dragon 2009, Ueda, Calado et al. 2014, Shukla, Schmidt et al. 2016). Concordantly with this CAB-box adjacent motif disrupting hTR biogenesis, mutations disrupting TCAB1 have been identified in patients with autosomal recessive inheritance of DC, which ultimately disrupt telomerase RNA trafficking out of the CBs and into the nucleolus, and prevent telomerase from elongating telomeres(Zhong, Savage et al. 2011).

1.6.2 RNA surveillance machinery in premature aging disease

PARN was the first RNA processing component implicated in the disease pathology of the premature aging disease dyskeratosis congenita (Dhanraj, Gunja et al. 2015, Stuart, Choi et al. 2015, Tummala, Walne et al. 2015). While it was originally suggested that PARN dysfunction may affect any number of genes implicated in DC, depletion of the PARN-recruiting component PABPN1 does not affect the mRNA levels of many telomere maintenance gene products, nor does it affect the normal expression of approximately 96% of polyadenylated mRNAs (Beaulieu, Kleinman et al. 2012). Further study of PARN depletion or overexpression also revealed no gross changes in protein levels for other telomere maintenance factors (Tseng, Wang et al. 2015), strengthening the conclusion that the observed telomeric effects of PARN mutations are truly due to disrupted hTR processing and end maturation (Moon, Segal et al. 2015). Taking into consideration these patients carrying *PARN* mutations with the very recent identification of mutations disrupting ZCCHC8 and thus hTR processing/accumulation in patients with IPF (Gable, Gaysinskaya et al. 2019), there is an evident importance of screening for mutations in other factors implicated in hTR processing and biogenesis when performing genetic diagnoses on patients presenting with telomere syndromes but unknown genetic etiology. Indeed, many premature aging patients have no identified genetic cause (Stanley, Gable et al. 2016, Gable,

Gaysinskaya et al. 2019), and thus a more comprehensive understanding of factors contributing to telomere maintenance can only improve diagnosis and treatment of telomere syndromes.

Chapter 2 – N-terminal residues of human dyskerin are required for interactions with telomerase RNA that prevent RNA degradation

2.1 Preface

The work presented in Chapter 2 investigates the impact of the N-terminal domain of dyskerin in mediating the interaction between dyskerin and hTR. Previous structural studies in yeast suggested that this region may act as an extension of the conventional RNA binding region of dyskerin, the PUA. This work is the first confirmation that in human dyskerin, residues in the N-terminus can mediate the hTR-dyskerin interaction, and demonstrates the importance of this X-DC hotspot in hTR biogenesis, accumulation, and subsequent telomerase activity.

N-terminal residues of human dyskerin are required for interactions with telomerase RNA that prevent RNA degradation

2.2

Deanna E. MacNeil[1,2], Patrick Lambert-Lanteigne[1] and Chantal Autexier[1,2,*]

[1]Jewish General Hospital of McGill University, Lady Davis Institute, Montreal, Quebec H3T 1E2, Canada and; [2]Department of Anatomy and Cell Biology, McGill University, Montreal, Quebec H3A 0C7, Canada

*Address correspondence to Chantal Autexier, chantal.autexier@mcgill.ca

2.3 Abstract

The telomerase holoenzyme responsible for maintaining telomeres in vertebrates requires many components *in vivo*, including dyskerin. Dyskerin binds and regulates the accumulation of the human telomerase RNA, hTR, as well as other non-coding RNAs that share the conserved H/ACA box motif. The precise mechanism by which dyskerin controls hTR levels is unknown, but is evidenced by defective hTR accumulation caused by substitutions in dyskerin, that are observed in the X-linked telomere biology disorder dyskeratosis congenita (X-DC). To understand the role of dyskerin in hTR accumulation, we analyzed X-DC substitutions K39E and K43E in the poorly characterized dyskerin N-terminus, and A353V within the canonical RNA binding domain (the PUA). These variants exhibited impaired binding to hTR and polyadenylated hTR species, while interactions with other H/ACA RNAs appear largely unperturbed by the N-terminal substitutions. hTR accumulation and telomerase activity defects of dyskerin-deficient cells were rescued by wildtype dyskerin but not the variants. hTR 3' extended or polyadenylated species did not accumulate, suggesting hTR precursor degradation occurs upstream of mature complex assembly in the absence of dyskerin binding. Our findings demonstrate that the dyskerin-hTR interaction mediated by PUA and N-terminal residues of dyskerin is crucial to prevent unchecked hTR degradation.

2.4 Introduction

The ends of linear chromosomes, known as telomeres are incompletely replicated due to the conventional DNA polymerase requiring a 3' hydroxyl to initiate DNA synthesis and the semi-conservative nature of DNA replication. This generates a problem for replicated DNA ends: the potential loss of genomic information. Eukaryotic organisms have evolved mechanisms to maintain telomeres, providing a solution to the end replication problem, and serving as protection against the inappropriate recognition of DNA ends as breaks. Telomeric integrity has implications in cellular aging, as the natural occurrence of telomere attrition serves as a key checkpoint in the control of cell proliferation by triggering replicative senescence (Lopez-Otin, Blasco *et al.* 2013). However, defects in the telomere-synthesizing enzyme telomerase and other telomere maintenance components cause premature aging syndromes like dyskeratosis congenita (DC) due to progressive telomere shortening in dividing cells and subsequent proliferative-block (Bertuch 2016, Wegman-Ostrosky and Savage 2017).

The rare premature aging disease and telomere biology disorder DC is characterized by pathologic presentation in the proliferative tissues of patients, including the classical triad of diagnostic symptoms: oral leukoplakia, hyperpigmentation of the skin, and nail dystrophy. These patients have higher rates of age-related predispositions, including pulmonary disease and malignancies (Alter, Giri *et al.* 2018). The most common cause of mortality in DC patients is bone marrow failure caused by the depletion of the hematopoietic stem cell compartment. Ultimately, DC-causative mutations leads to impaired maintenance of telomeres and, in turn, cells in regenerative tissues are unable to maintain their highly proliferative capacity, causing the observed pathology in patients (Bertuch 2016, Wegman-Ostrosky and Savage 2017).

X-linked DC (X-DC), caused by mutations in the *dkc1* gene encoding dyskerin, is the most common inherited form of DC (Knight, Heiss *et al.* 1999, Mitchell, Cheng *et al.* 1999). As with all factors implicated in DC to date, dyskerin is important for proper telomere maintenance. The telomerase enzyme is minimally composed of a reverse transcriptase (hTERT in humans) and an RNA template (hTR in humans) that are able to synthesize telomeric DNA *in vitro* (Feng, Funk *et al.* 1995, Meyerson, Counter *et al.* 1997, Nakamura, Morin *et al.* 1997). However, this holoenzyme requires many other components *in vivo*, including dyskerin and the other H/ACA ribonucleoprotein (RNP) complex components NHP2, NOP10, and GAR1. Dyskerin binds hTR, as well as other small non-coding RNAs that share a conserved structural motif known as the H/ACA box (Lafontaine, Bousquet-Antonelli *et al.* 1998). Dyskerin is integral for accumulation of hTR, biogenesis of the mature telomerase complex and telomerase activity. X-DC patients suffer from hTR accumulation defects and consequent telomere shortening (Mitchell, Cheng *et al.* 1999). Several recent studies have identified key factors and pathways implicated in the trimming of hTR 3' extended and/or polyadenylated species, as well as components involved in hTR degradation (Nguyen, Grenier St-Sauveur *et al.* 2015, Tseng, Wang *et al.* 2015, Shukla, Schmidt *et al.* 2016, Deng, Huang *et al.* 2019, Son, Park *et al.* 2018). The involvement of various pathways, including the nuclear RRP6-exosome, PABPN1 and PARN, human TRAMP and NEXT complexes, CBCA complex, XRN1/DCP2, and most recently TOE1, demonstrates the complexity of hTR processing. It has been posited as well as demonstrated that dyskerin interacts with components in these pathways (Nguyen, Grenier St-Sauveur *et al.* 2015, Tseng, Wang *et al.* 2015, Shukla, Schmidt *et al.* 2016), and in the absence of dyskerin, accelerated hTR decay in HeLa cells can be partially rescued by co-depleting RRP6 (Shukla, Schmidt *et al.* 2016).

However, the role and regulatory mechanisms of dyskerin in hTR processing, telomerase biogenesis and telomere maintenance remain to be fully elucidated.

There are two hotspots within the dyskerin gene for X-DC causative mutations: one hotspot coincides with the poorly characterized eukaryotic N-terminal extension (amino acids 18-47) and dyskeratosis congenita-like domain (DKCLD) (amino acids 48-106) (Cerrudo, Ghiringhelli *et al.* 2014), while the other spans a more C-terminal region encompassing the pseudouridine synthase and archaeosine transglycosylase (PUA) domain (amino acids 297-370) and an uncharacterized domain between the PUA and C-terminal nuclear localization signal (Podlevsky, Bley *et al.* 2008, Zeng, Thumati *et al.* 2012) (Figure 2.1A). Among the affected residues in the N-terminal hotspot are two lysine residues that have been reported to be substituted to glutamate [K39E (Heiss, Megarbane *et al.* 2001) and K43E (Knight, Heiss *et al.* 1999)] in two unrelated X-DC families. We previously demonstrated that in HEK293 cells depleted of endogenous dyskerin, the expression of FLAG-tagged dyskerin variants harboring arginine substitutions at either K39 or K43 results in reduced telomerase RNA levels, decreased telomerase activity, and subsequent telomere shortening (Brault, Lauzon *et al.* 2013). Additionally, the most commonly reported substitution in X-DC [A353V (Knight, Heiss *et al.* 1999)], lies near the second X-DC hotspot within the PUA, which is the putative RNA binding domain of dyskerin based on homology with other pseudouridine synthases, including the archaeal dyskerin homologue Cbf5 (Li and Ye 2006, Duan, Li *et al.* 2009). X-DC patient-derived cells harboring various mutations, including the recurring A353V variant, exhibit reduced telomerase activity driven by impaired hTR accumulation (Mitchell, Cheng *et al.* 1999, Wong, Kyasa *et al.* 2004, Wong and Collins 2006, Zeng, Thumati *et al.* 2012).

Beyond our previous study (Brault, Lauzon *et al.* 2013) and the reported hTR accumulation defects in patient cells harboring certain N-terminal hotspot mutations (Mitchell, Cheng *et al.* 1999, Wong, Kyasa *et al.* 2004, Wong and Collins 2006, Batista, Pech *et al.* 2011, Parry, Alder *et al.* 2011, Machado-Pinilla, Carrillo *et al.* 2012, Zeng, Thumati *et al.* 2012, Alder, Parry *et al.* 2013, Bellodi, McMahon *et al.* 2013, Moon, Segal *et al.* 2015), substitutions in the N-terminal extension of dyskerin including K39E and K43E have not been thoroughly characterized. In addition, the precise mechanism by which dyskerin regulates hTR accumulation is unknown. We aimed to better understand the role of the N-terminal K39 and K43 residues in regulating hTR accumulation through examining the effects of X-DC substitutions at these

positions. Thus, in the current study, we characterized the K39E and K43E variants alongside the A353V variant previously reported to exhibit reduced hTR levels. We observed that all three dyskerin variants are defective at binding polyadenylated species and mature hTR. Interactions with other H/ACA RNAs appear largely unperturbed by the K39E or K43E substitutions, consistent with distinct biogenesis pathways for hTR and other H/ACA class RNAs demonstrated by Fu and Collins in 2003, which implies the sensitivity of hTR in particular to X-DC mutations (Fu and Collins 2003). However, the A353V variant displays more substantial H/ACA RNA interaction defects, indicating that the PUA domain might play a more global role in H/ACA RNA interaction and suggesting a potential telomerase-centric role for the eukaryotic N-terminal extension of human dyskerin. Depletion of dyskerin leads to reduced levels of some H/ACA RNAs, which can be rescued by wildtype dyskerin and variants alike. However, reduced hTR levels in dyskerin-depleted cells can only be rescued by wildtype dyskerin expression. Our observation that other H/ACA RNA levels are comparable between dyskerin-depleted cells expressing wildtype dyskerin or dyskerin variants is consistent with our findings that H/ACA RNP assembly and dyskerin subnuclear localization are unaffected for these variants. The interaction between dyskerin and hTR is probably necessary to mediate the accumulation of hTR to levels required for active telomerase, as total hTR levels in dyskerin-depleted cells with or without expression of dyskerin variants cannot sustain telomerase activity comparable to cells expressing wildtype dyskerin. This is likely because disruption of the dyskerin-hTR interaction favours the degradation of hTR precursors upstream of the assembly of the mature telomerase complex, suggesting an early involvement of dyskerin in hTR biogenesis. This role differs from other recently reported processing factors, in that dyskerin depletion reduces the amount of hTR polyadenylated species rather than causing accumulation of these non-functional RNA species. hTR accumulation defects caused by the inability of dyskerin variants to interact with hTR cannot be rescued by depletion of individual processing pathway components PARN or the core exosome component RRP40, designating a requirement for dyskerin in preventing excessive hTR degradation. Our findings demonstrate that the dyskerin-hTR interaction mediated by PUA and N-terminal residues of dyskerin is crucial to prevent unchecked hTR degradation, and highlights mechanistic links between the regulation of hTR trimming and degradation processes, and the telomere biology disorder X-DC.

2.5 Materials and Methods

Plasmids and Site Directed Mutagenesis

The plasmid pcDNA3.1-FLAG-dyskerinWT from the lab of Dr. François Dragon was used to generate point mutations or the ΔCterm deletion via site directed mutagenesis, as previously described (Brault, Lauzon *et al.* 2013). Specifically, primers (Supplemental Table 2.1) were designed to generate K39E (c. 115A>G), K43E (c. 127A>G), A353V (c. 1058C>T), and K446X (c. 1336A>T). Expression of FLAG-tagged dyskerin was controlled by the CMV promoter. For expression of HA-SHQ1 in human cells, the coding sequence of HA-SHQ1 was cloned into a pcDNA3 backbone using KpnI and EcoRI cut sites and the plasmid pSR38 obtained from Dr. Tom Meier (Grozdanov, Roy *et al.* 2009). The plasmid pcDNA6/myc-HisC-hTERT from the lab of Dr. Joachim Lingner (Cristofari and Lingner 2006) was used for expression of wildtype human TERT in cells.

Cell Culture and Transfection

Human embryonic kidney (HEK293) cells were maintained in Dulbecco's Modification Eagle's Medium DMEM (Wisent) supplemented with 10% fetal bovine serum FBS (Wisent), and Antibiotic-Antimycotic (Gibco), at 37˚C 5% CO2. Polyclonal FLAG-dyskerin stable cells were maintained under selective pressure in G418 (750 µg/ml). Transfection of pcDNA3.1 (empty vector), pcDNA3.1-FLAG-dyskerin constructs, pcDNA3-HA-SHQ1, and/or pcDNA6/myc-HisC-hTERT was performed using Lipofectamine 2000 Transfection Reagent (Invitrogen) according to the reagent protocol. Prior to transfection, media was changed to DMEM with 10% FBS and lacking Antibiotic-Antimycotic, and 6 hours after transfection the media was replaced with DMEM containing both FBS and Antibiotic-Antimycotic.

Immunofluorescence

In order to assess localization of FLAG-dyskerin to the Cajal Bodies, immunofluorescence experiments were performed on HEK293 cells overexpressing FLAG-dyskerinWT, X-DC variants, or ΔCterm following a previously described protocol (Chu, D'Souza *et al.* 2016). Specifically, to probe for FLAG-dyskerin constructs rabbit anti-FLAG (Sigma-Aldrich F7425, 1:500) was used in PBG (1% cold fish water gelatin, 0.5% bovine serum albumin (BSA), in PBS), followed by mouse anti-coilin (from Dr. Michael Terns (Tomlinson, Ziegler *et al.* 2006), 1:10,000) in PBG. Nuclei showing FLAG-dyskerin localization to at least

one Cajal body were scored out of the number of nuclei with both FLAG and coilin signal detected, and ≥180 nuclei were counted for scoring of localization of each nuclear FLAG-tagged dyskerin construct.

To assess localization of FLAG-dyskerin to the nucleolus, HEK293 cells overexpressing FLAG-dyskerin constructs were fixed with 4% formaldehyde-PBS for 10 minutes at room temperature. The fixing solution was removed and coverslips were briefly rinsed with PBS, followed by permeabilization of cells with 0.1% Triton X-100-PBS for 5 minutes at 4˚C. Permeabilized cells were incubated with 2XSSC-50% Formamide for 5 minutes at room temperature, and then washed with PBS before blocking in 3% BSA-PBS-T for 1 hour at room temperature. Cells were probed for FLAG-dyskerin constructs with rabbit anti-FLAG (Sigma-Aldrich F7425, 1:500) in PBG, followed by mouse anti-fibrillarin (monoclonal antibody 72B9 obtained from Dr. Kenneth Michael Pollard (Pogacic, Dragon *et al.* 2000), 1:30) as a nucleolar marker in 3% BSA-PBS-T. Coverslips were washed with PBS and immunostained in PBG with secondary antibodies conjugated to fluorescein isothiocyanate (FITC) (donkey anti-mouse IgG; Jackson ImmunoResearch Lab, Inc., 1:125) or Cy3 (donkey anti-rabbit; Jackson ImmunoResearch Lab, Inc., 1:125). Coverslips were washed with PBS and mounted in Vectashield with DAPI (Vector Laboratories). Nuclei showing FLAG-dyskerin localization to the nucleolus were scored out of the number of nuclei with both FLAG and fibrillarin signal detected, and ≥180 nuclei were counted for scoring of localization of each FLAG-tagged dyskerin construct. Images were captured using an Axio Imager M1 (63X; Carl Zeiss, Jena, Germany).

Co-immunoprecipitation for Protein-Protein Interactions and FLAG-Dyskerin-H/ACA RNA Interactions

With the exception of co-overexpression of HA-SHQ1 or hTERT with FLAG-dyskerin, all protein-protein interactions were assessed by immunoprecipitating FLAG-dyskerin wildtype or X-DC variants from HEK293 cells and immunoblotting for endogenous dyskerin-interacting proteins. Monoclonal M2 mouse anti-FLAG antibody (Sigma-Aldrich F3165) and Protein G Sepharose (GE Healthcare) were used to immunoprecipitate (IP) FLAG-dyskerin wildtype or X-DC variants. The protocols from the laboratory of Dr. Steven Artandi for assessing the interaction between FLAG-dyskerin and hTERT (with and without RNase A treatment), TCAB1, or Reptin have all been described in detail (Venteicher, Meng *et al.* 2008, Venteicher, Abreu *et*

al. 2009), and was also used to asses co-IP of the negative control TIP60. The protocol used to assess the interaction of FLAG-dyskerin with HA-SHQ1, the pre-H/ACA RNP components NAF1, NHP2, and NOP10, or mature H/ACA RNP complex component GAR1 was the same used to analyze the interaction between FLAG-dyskerin and H/ACA box RNAs including hTR, and has been described for another hTR-interacting protein (Booy, Meier *et al.* 2012). For protein-protein interactions, elution from Protein G Sepharose was performed with Laemmli buffer and boiling. For protein-RNA interactions, elution was performed with TRIzol reagent (Invitrogen), followed by chloroform extraction and reverse transcription. Inputs (10% of lysate volume used for IP) were collected prior to IP, and treated with either Laemmli buffer and boiled, or with TRIzol reagent.

Immunoblotting and Antibodies

Analysis of protein expression and IP experiments was performed by resolving proteins by SDS-PAGE, transfer to PVDF and immunoblotting. Primary antibodies used for immunoblotting were: anti-FLAG (Proteintech, 20543-1-AP, 1:4000), anti-HA (Cell Signaling, 2367, 6E2, 1:1125), anti-NAF1 (Abcam, ab157106, 1:1000), anti-NHP2 (Proteintech, 15128-1-AP, 1:5000), anti-NOP10 (Abcam, ab134902, 1:500) anti-TCAB1 (Novus, NB100-68252, 1:2000), anti-reptin (Abcam, ab51500, 1:5000), anti-hTERT (Santa Cruz, sc7215, C-20, 1:500), anti-dyskerin (Santa Cruz, sc-373956, H-3, 1:1500), anti-PARN (Abcam, ab154214, 1:500), anti-RRP40 (Bethyl, A303-909A-T, 1:1500), anti-TIP60 (Santa Cruz, sc5725, N-17, 1:1000), anti-hGAR1 (from Dr. Witold Filipowicz (Dragon, Pogacic *et al.* 2000), 1:2000), and anti-actin (Chemicon MAB1501, 1:5000).

RNA Extraction and RT-qPCR

RNA was extracted using TRIzol reagent (Invitrogen), according to the reagent protocol. Reverse transcription was performed with SuperScript II Reverse Transcriptase (Invitrogen) according to the user protocol, either with hexameric random primers for total RNA or oligo-d(T) primer for polyadenylated RNA. PerfeCTa SYBR Green FastMix with Low ROX (Quanta) was used for all qPCR analyses, in a 7500FAST real-time PCR system (ABI) as previously described (Brault, Lauzon *et al.* 2013). The comparative $\Delta\Delta C_T$ method was used to compare RNA enrichment between samples. For analysis of protein-RNA interactions, 5 µl of RNA from input and 5 µl of RNA from IP fractions were reverse transcribed into cDNA and subjected to

qPCR using specific primers for target RNAs (Supplemental Table 2.1). The $\Delta\Delta C_T$ was calculated between the mean C_T of the IP and the mean C_T of the input for each sample. For analysis of RNA levels, 1 µg of RNA per condition was reverse transcribed into cDNA and subjected to qPCR using specific primers for target RNAs (Supplemental Table 2.1). The $\Delta\Delta C_T$ was calculated between the mean C_T of the target and the mean C_T of GAPDH for each sample.

siRNA

Transfection of siRNA was performed with Lipofectamine RNAiMAX Transfection Reagent (Invitrogen) according to the user protocol. For dyskerin depletion, two siRNAs targeting the 3' UTR (24 nM, 72h treatment, sidkc1.A or sidkc1.B) were tested for depletion of endogenous dyskerin (Supplemental Table 2.1). The siRNA sequences targeting the 3' UTR were previously described (Lin, Mobasher *et al.* 2014). A mock transfection (no siRNA) and transfection of a scramble siRNA were used as negative controls in each experiment. For double depletion experiments, siRNA targeting PARN, or human RRP40 (20 nM, two 48h treatments) was combined with sidkc1.B (24 nM, 48h treatment followed by 12 nM, 48h treatment). The siRNA sequences targeting PARN, or RRP40 (Supplemental Table 2.1) were previously described (Tseng, Wang *et al.* 2015). The siRNA targeting MTR4 was kindly provided by the laboratory of François Bachand (Nguyen, Grenier St-Sauveur *et al.* 2015). All other siRNAs were ordered through ThermoFisher Scientific.

RT-PCR Analysis of hTR 3' Extended Species

Analysis of 3' extended hTR species was performed as previously described (Nguyen, Grenier St-Sauveur *et al.* 2015). Primers were as follows: F1 forward primer annealing 325 nt upstream of hTR transcription start site (TSS), F2 forward primer annealing 323 nt after hTR TSS, R1 reverse primer annealing 610 nt after the hTR TSS (159 nt after mature hTR end), and GAPDH Forward and Reverse (Supplemental Table 2.1). The PCR conditions were as follows: 95˚C for 3 min; 30 cycles of 95˚C for 30 sec, 55˚C for 40 sec, 72˚C for 1 min; final extension at 72˚C for 8 min. PCR products were analyzed by electrophoresis on 1.5% agarose-TAE gels stained with Ethidium Bromide.

Q-TRAP

Quantitative analysis of telomerase activity was done using the Q-TRAP protocol previously described (Herbert, Hochreiter *et al.* 2006). Briefly, HEK293 cells with or without

expression of FLAG-dyskerin constructs were treated with scramble siRNA or siRNA to deplete endogenous dyskerin for 72h prior to harvesting by scraping and lysis in NP-40 lysis buffer. A standard curve was generated with a serial dilution of mock lysate (HEK293 cells untreated with siRNA and not expressing FLAG-dyskerin) for each experimental replicate (n=3), with 1 µg, 0.2 µg, 0.04 µg, 0.008 µg, and 0.0016 µg of total protein. For comparison of telomerase activity between conditions, 0.2 µg of total protein was used for each sample.

Statistical Analyses

All statistical analyses were performed using GraphPad Prism 7. Unpaired t-tests ($p < 0.01$) were used to compare RNA enrichment/levels in qPCR experiments, and for comparison of relative telomerase activity (RTA) in Q-TRAP experiments. For analysis of RNA interaction and levels, the enrichment of each RNA target was separately compared to the enrichment of the target in the FLAG-dyskerin wildtype condition. For analysis of telomerase activity, the RTA percentage of each condition was separately compared to the scramble siRNA RTA percentage. Each experiment was performed in triplicate, and error bars represent the standard error of the mean between experimental replicates.

2.6 Results

N-terminal or PUA domain variants of dyskerin localize to Cajal bodies and the nucleolus, and do not disrupt pre-H/ACA RNP assembly, or telomerase associated protein-protein interactions

Correct dyskerin localization is essential for its functions both in telomerase and H/ACA RNP biology. Conventionally, dyskerin localizes to both the nucleolus and Cajal bodies, important sites of telomerase trafficking, assembly, and activity (MacNeil, Bensoussan *et al.* 2016). Additionally, H/ACA RNP complex-guided pseudouridylation for rRNA and snRNA by dyskerin takes place within these subnuclear organelles (Yu and Meier 2014). In order to examine the effect of the K39E, K43E, and A353V substitutions on dyskerin localization, immunofluorescence experiments were performed in HEK293 cells transiently expressing FLAG-tagged dyskerin (wildtype and dyskerin variants). The expected localization of dyskerin to Cajal bodies (Figure 2.1B) and the nucleolus (Figure 2.1C) was observed for wildtype and disease variants, as indicated by co-localization of FLAG-dyskerin/coilin and FLAG-dyskerin/fibrillarin foci, respectively. A variant of dyskerin lacking a complete C-terminal

N/NoLS that has been previously reported to display reduced nuclear import was used as a positive control for mislocalization (Heiss, Girod *et al.* 1999). Indeed, this C-terminal deletion variant accumulated outside of the nucleus as expected (Figure 2.1B, bottom row). We conclude that the K39E, K43E, and A353V variants of dyskerin localize to the nuclear sites of maturity which are essential for both H/ACA complex and telomerase assembly.

Although these dyskerin variants are able to localize to Cajal bodies and the nucleolus, this does not exclude the possibility that dyskerin is dysfunctional at these sites. For instance, the assembly of dyskerin with its known interacting partners could be disrupted. To test this hypothesis, we immunoprecipitated FLAG-tagged dyskerin (wildtype or variants) and assessed interactions of endogenous H/ACA RNP components with FLAG-tagged dyskerin by immunoblotting. We analyzed NAF1, found only in the pre-RNP; and NOP10 and NHP2, found in both the pre- and mature RNP. We observed that dyskerin variants efficiently associated with H/ACA pre-RNP and RNP components as compared to wildtype (Figure 2.2A). The observation that the A353V variant is able to interact with these components is consistent with what has been reported for the H/ACA pre-RNP and RNP complex components *in vitro* (Trahan, Martel *et al.* 2010). Additionally, these variants do not display disruptions in the interactions between dyskerin and other associated proteins important for both H/ACA RNP and telomerase assembly such as SHQ1 (using exogenously expressed HA-SHQ1)(Figure 2.2B), TCAB1 (Figure 2.2C), and reptin (Figure 2.2D). The mature H/ACA complex factor GAR1 was also observed to interact with FLAG-dyskerin variants, as well as wildtype (Figure 2.2E). Finally, none of the three variants display a defect in interaction with the telomerase reverse transcriptase hTERT when it is exogenously over-expressed in this assay (Figure 2.2F). This interaction is reduced for all FLAG-tagged dyskerin variants by RNase A treatment during immunoprecipitation (IP), consistent with the interaction between dyskerin and hTERT being dependent on hTR (Venteicher, Abreu *et al.* 2009) (Supplemental Figure 2.1A). However, the telomerase activity levels are reduced upon dyskerin depletion with siRNA, and can only be recovered by stable expression of wildtype dyskerin, not X-DC variants (Figure 2.2G, Supplemental Figure 2.1B). To further confirm the specificity of the co-IP assay, we assessed whether or not the nuclear chromatin-associated histone acetyltransferase TIP60 could be observed in the FLAG-dyskerin IP fraction. TIP60 assembles with reptin and its AAA+ ATPase partner pontin in a complex independent of dyskerin (Ikura, Ogryzko *et al.* 2000), and as such should not be found to interact

with dyskerin. Indeed, we did not observe TIP60 in the FLAG-dyskerin IP fractions (Figure 2.2H). We conclude that neither the substitutions in the N-terminal extension nor the PUA of dyskerin hinder the assembly of dyskerin into the pre- or mature H/ACA RNP complex, but impede endogenous telomerase complex function.

Figure 2.1: N-terminal and PUA domain dyskerin variants localize to Cajal bodies and the nucleolus. a. A linear schematic of dyskerin domains. The amino acid (aa) ranges corresponding to the N-terminal extension (18-47) and the pseudouridine synthase and archaesoine transglycosylase domain (PUA – 297-370) are denoted below the schematic. Above the schematic, pink arrows indicate K39 and K43, while the purple arrow indicates A353. All reported X-DC substitutions are indicated by vertical black lines along the top of the schematic. Representative images of the co-localization of FLAG-dyskerin (wildtype WT and dyskerin variants K39E, K43E, and A353V – Cy3 shown in red) with b. Cajal body marker coilin (FITC shown in green) and c. nucleolar marker fibrillarin (FITC shown in green), as observed by indirect immunofluorescence. No deviation in localization was observed, as all cells expressing nuclear FLAG-tagged dyskerin (wildtype or X-DC variants) displayed expected co-localization with the nucleolar marker fibrillarin or the Cajal body marker coilin (the number of nuclei with expected co-localization and the number of nuclei counted is indicated for each condition in the merged column). FITC signal is not detected by the Cy3 channel using mock HEK293 cells lacking expression of FLAG-tagged dyskerin, nor is nucleolar FLAG-dyskerin detected by the FITC channel when examining co-localization with coilin. In the bottom panel of b. the ΔCterm dyskerin variant (Cy3 shown in red) was used as a control for mislocalization. This truncation lacking most of the C-terminal nuclear/nucleolar localization sequence has been previously reported to cause cytosolic accumulation of dyskerin. In b. the co-localization foci for Cajal bodies are indicated by white arrows in the Cy3 and merged columns. The nucleus is indicated by DAPI staining of nuclear DNA (in blue).

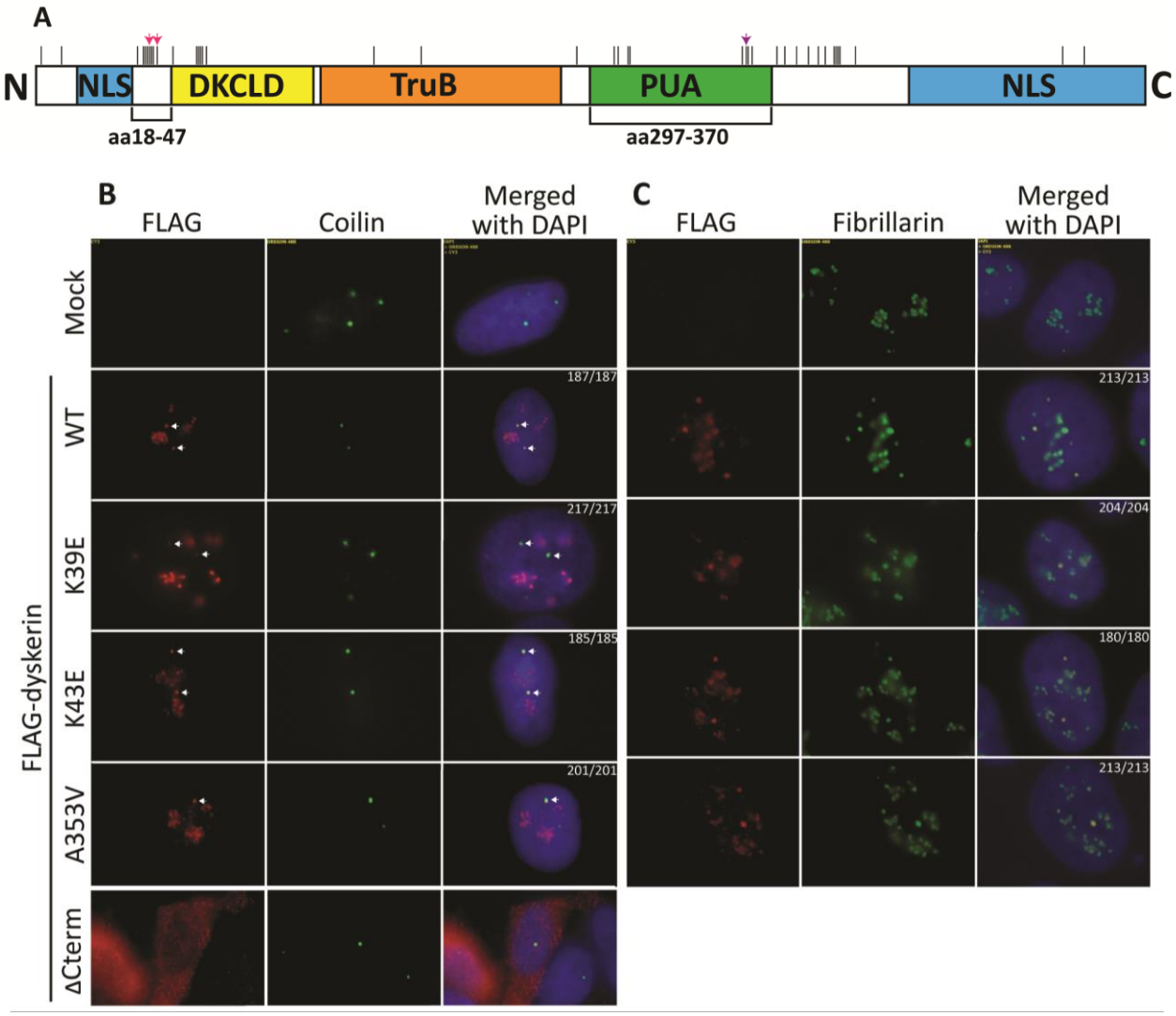
A
N
NLS
DKCLD
TruB
PUA
NLS
C
aa18-47
aa297-370
B
FLAG
Coilin
Merged with DAPI
C
FLAG
Fibrillarin
Merged with DAPI
FLAG-dyskerin
Mock
WT
K39E
K43E
A353V
ΔCterm
187/187
217/217
185/185
201/201
213/213
204/204
180/180
213/213

Figure 2.2: Dyskerin variants co-immunoprecipitate (co-IP) H/ACA RNP assembly factors comparable to wildtype dyskerin, but result in reduced telomerase activity in cells depleted of endogenous dyskerin. Interactions of FLAG-dyskerin WT and variants with factors needed for assembly of the H/ACA ribonucleoprotein complex and telomerase were assessed by co-immunoprecipitation from HEK293 cell lysates. Assembly of the a. H/ACA pre-RNP complex involving NAF1 (input protein not detectable), NHP2, and NOP10 was investigated by immunoblotting for the endogenous H/ACA pre-RNP components and FLAG-dyskerin proteins. Interaction with the cytosolic chaperone and RNA mimic b. SHQ1 was assessed by co-expressing HA-tagged SHQ1 and FLAG-tagged dyskerin, and immunoblotting for HA and FLAG. Similar to the H/ACA pre-RNP complex, the interaction between dyskerin and nuclear RNP assembly factors c. TCAB1 and d. reptin, and mature H/ACA complex component e. GAR1 was examined by immunoblotting for endogenous assembly factors and FLAG-dyskerin. f. The interaction between dyskerin and the telomerase reverse transcriptase hTERT was assessed by co-expressing hTERT and FLAG-tagged dyskerin, and immunoblotting for hTERT and FLAG. g. Q-TRAP was repeated in experimental replicate n=3, and quality of telomeric repeat amplification products were visually assessed on 10% non-denaturing acrylamide gel (see Supplemental Figure 2.1B for representative image). Statistically significant reductions in relative telomerase activity are indicated by * (P value < 0.01). Error bars represent SEM. h. The nuclear chromatin-associated histone acetyltransferase TIP60 could not be observed in the FLAG-dyskerin IP fraction, though the expected 55 kDa protein band was observed in the input fractions (note that the upper band in the input panel represents a non-specific band that is expected based on the antibody datasheet). Immunoblotting targets are indicated to the right of each panel as WB: α target, and a list of antibodies can be found in the materials and methods section. In the IP panel of e. the GAR1-specific band is indicated by an arrow, while immunoglobulin light chain is the strong band present in all IP fractions indicated by the asterisk. Each co-IP and immunoblotting was performed in experimental replicate a minimum of n=2, representative blots are shown.

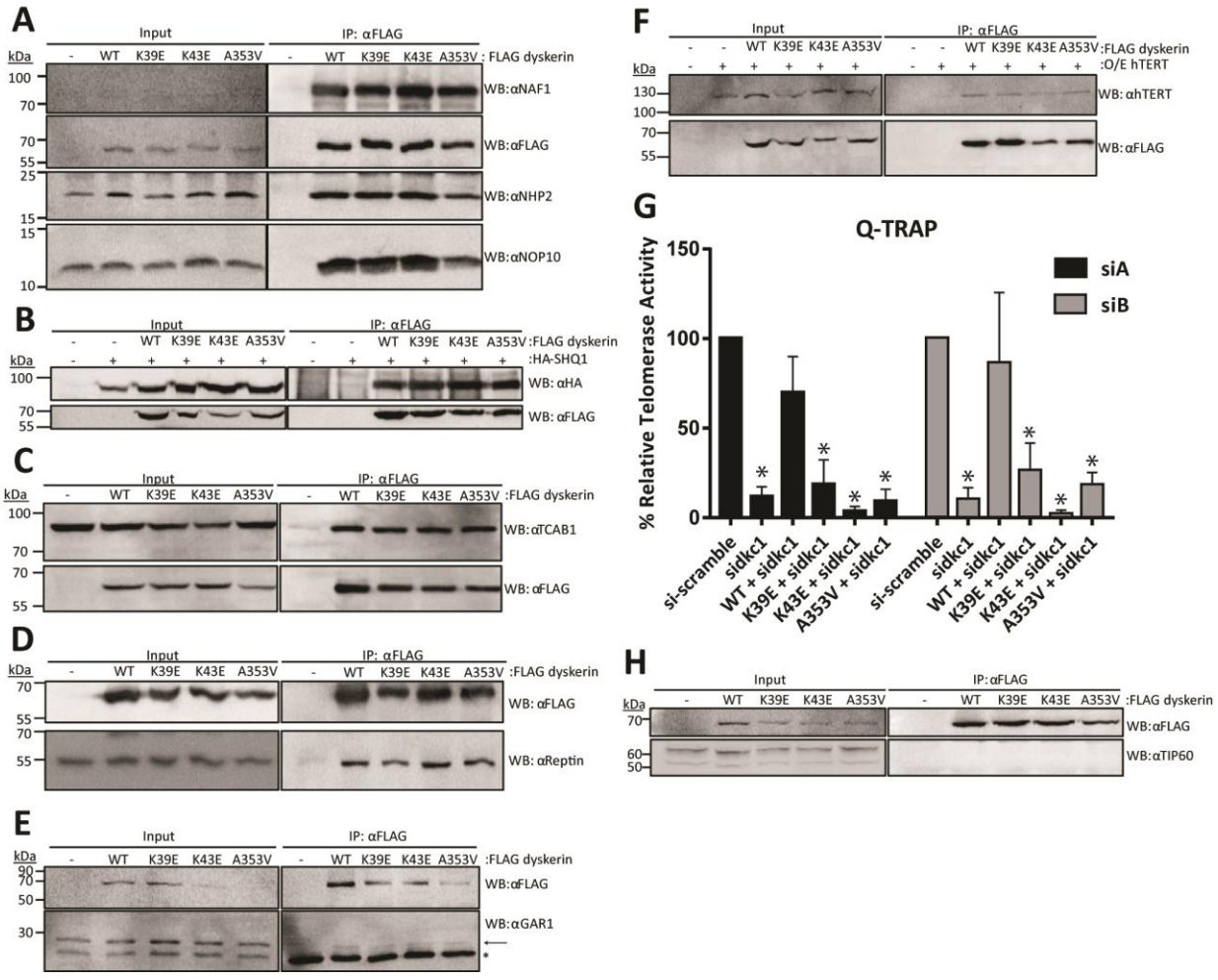
A
Input
IP: αFLAG
kDa
- WT K39E K43E A353V - WT K39E K43E A353V : FLAG dyskerin
100
70
WB:αNAF1
70
55
WB:αFLAG
25
15
WB:αNHP2
15
10
WB:αNOP10
B
Input
IP: αFLAG
- - WT K39E K43E A353V - - WT K39E K43E A353V :FLAG dyskerin
kDa - + + + + + - + + + + + :HA-SHQ1
100
WB: αHA
70
55
WB: αFLAG
C
Input
IP: αFLAG
kDa - WT K39E K43E A353V - WT K39E K43E A353V :FLAG dyskerin
100
70
WB:αTCAB1
70
55
WB: αFLAG
D
Input
IP: αFLAG
kDa - WT K39E K43E A353V - WT K39E K43E A353V :FLAG dyskerin
70
55
WB: αFLAG
70
55
WB: αReptin
E
Input
IP: αFLAG
kDa - WT K39E K43E A353V - WT K39E K43E A353V :FLAG dyskerin
90
70
50
WB:αFLAG
30
WB:αGAR1
F
Input
IP: αFLAG
- - WT K39E K43E A353V - - WT K39E K43E A353V :FLAG dyskerin
kDa - + + + + + - + + + + + :O/E hTERT
130
100
WB: αhTERT
70
55
WB: αFLAG
G
Q-TRAP
% Relative Telomerase Activity
150
100
50
0
siA
siB
si-scramble
sidkc1
WT + sidkc1
K39E + sidkc1
K43E + sidkc1
A353V + sidkc1
H
Input
IP:αFLAG
kDa - WT K39E K43E A353V - WT K39E K43E A353V :FLAG dyskerin
70
WB:αFLAG
60
50
WB:αTIP60

N-terminal dyskerin variants have disrupted interactions with telomerase RNA

Although the K39E and K43E variants have not been well characterized to date, there has been a great deal of focus on the A353V variant. A353 is located in the putative RNA binding domain of dyskerin, and mouse models and X-DC patient cells harboring the A353V substitution exhibit decreased hTR levels (Mochizuki, He *et al.* 2004, Machado-Pinilla, Carrillo *et al.* 2012, Zeng, Thumati *et al.* 2012, Moon, Segal *et al.* 2015). Additionally, this substitution has been reported to disrupt the interaction between hTR and dyskerin *in vitro* (Ashbridge, Orte *et al.* 2009, Trahan, Martel *et al.* 2010). *In vitro* and in X-DC patient-derived cell studies, several other X-DC mutations have also been reported to disrupt the interaction with hTR (Ashbridge, Orte *et al.* 2009, Batista, Pech *et al.* 2011), and reduced levels of hTR are commonly reported in patients with X-DC (Mitchell, Cheng *et al.* 1999, Wong, Kyasa *et al.* 2004, Wong and Collins 2006, Batista, Pech *et al.* 2011, Parry, Alder *et al.* 2011, Machado-Pinilla, Carrillo *et al.* 2012, Zeng, Thumati *et al.* 2012, Alder, Parry *et al.* 2013, Bellodi, McMahon *et al.* 2013, Kropski, Mitchell *et al.* 2014, Moon, Segal *et al.* 2015). Concomitant with this and our previous observation of reduced hTR levels in dyskerin knockdown cells expressing K39R and K43R variants (Brault, Lauzon *et al.* 2013), we hypothesized that the interaction between hTR and the K39E and/or K43E variants may also be disrupted. To test this hypothesis, the RNA interaction of dyskerin variants was examined by qPCR after FLAG IP. We first established that the interaction between wildtype dyskerin and hTR could be reliably analyzed by this method, as past reports of this interaction have used mainly northern blotting. FLAG-tagged wildtype dyskerin IP fractions displayed enrichment of hTR cDNA as expected, without enrichment of the C/D box RNA U3 indicating successful and specific IP of the dyskerin-hTR interaction (Supplemental Figure 2.2A). However, IP fractions for FLAG-K39E and K43E dyskerin variants showed less enrichment of hTR relative to wildtype ($\leq$ 50% of wildtype), demonstrating a reduced ability of these variants to interact with hTR (Figure 2.3A, black bars). Similarly, and in agreement with what has been previously reported *in vitro* (Trahan, Martel *et al.* 2010), the A353V variant also displayed reduced hTR enrichment relative to wildtype.

In some analyses of mouse and X-DC patient cells, certain X-DC variants (including A353V but not K39E or K43E) have also been reported to reduce the accumulation of other H/ACA RNAs (Mochizuki, He *et al.* 2004, Wong, Kyasa *et al.* 2004, Bellodi, McMahon *et al.*

2013, Moon, Segal *et al.* 2015). Although the interaction of A353V with other H/ACA RNAs has not been looked at directly in cells or *in vivo*, it is possible that this substitution and others could disrupt the interaction between dyskerin and H/ACA RNAs other than hTR. We therefore wanted to consider whether the variants tested in this study display a general H/ACA RNA interaction defect, using the same assay. For the N-terminal hotspot variants K39E and K43E, the observed RNA interaction defect appears to be most substantial for hTR compared to other H/ACA RNAs. For instance, other H/ACA RNAs examined did not display significant differences in enrichment after IP of the dyskerin variant K39E compared to the wildtype dyskerin (Figure 2.3A, coloured bars). In contrast, the K43E variant displayed a significant reduction in enrichment for three of the four H/ACA snoRNAs examined (with the exception of E3) >50% of wildtype (Figure 2.3A, brown, red, and purple bars), and no significant defects in scaRNA interactions when compared to wildtype dyskerin (Figure 2.3A, green, orange, blue, and grey bars). As such, we propose that in the case of the K43E variant, the interaction defect for hTR is the most severe of the H/ACA RNAs considered here, though this does not exclude potential functional defects related to the other H/ACA RNAs with reduced enrichment.

The A353V variant displayed reduced enrichment of several H/ACA RNAs including the U85 scaRNA and three of the four H/ACA snoRNAs (with the exception of E2) (Figure 2.3A, green, brown, teal, and purple bars). Among the H/ACA RNAs with significantly reduced enrichment, the E3 snoRNA falls below 50% of the levels enriched by wildtype dyskerin (Figure 2.3A, teal bar). These notable interaction defects with H/ACA RNAs other than hTR are consistent with the position of A353 in the PUA domain, supporting the notion that this region is the conserved RNA-binding domain of dyskerin as a member of the pseudouridine synthase family of proteins. As such, we propose that substitutions within the PUA domain, like A353V, might cause more global H/ACA RNA interaction defects than those within the N-terminal X-DC hotspot. Our findings also suggest a potential telomerase-centric role for the eukaryotic N-terminal extension of dyskerin (Cerrudo, Ghiringhelli *et al.* 2014), containing the N-terminal X-DC hotspot.

Figure 2.3: N-terminal dyskerin variants disrupt the dyskerin-RNA interaction and lead to reduced hTR accumulation in cells depleted for endogenous dyskerin. Dyskerin-RNA interactions were assessed by IP of FLAG-tagged dyskerin from HEK293 cells transiently expressing FLAG-dyskerin in addition to endogenous dyskerin, followed by RNA extraction and qPCR. Relative to wildtype IP fractions (indicated by black dashed line), dyskerin variants K39E, K43E, and A353V display a. reduced enrichment of hTR following IP (approximately at or below 50% of wildtype, indicated by the red dashed line). Black bars indicate total hTR (cDNA primed with random hexamer) and white bars outlined in black indicate precursor hTR with poly(A) tails (cDNA primed with oligo dTs). Other H/ACA RNAs examined are indicated by coloured bars, and listed in the figure legend to the right of the graph. HEK293 cells lacking FLAG-tagged dyskerin (indicated as mock) were used as a negative control for RNA binding to the FLAG antibody and/or Protein G Sepharose. Mock cells were subject to the same IP protocol detailed for fractions containing FLAG-tagged dyskerin. These data represent experimental replicates of n=3. Statistically significant reductions in enrichment relative to wildtype are indicated by * (P value < 0.01). Error bars represent SEM. b. Depletion of endogenous dyskerin with siRNA (sidkc1.B), as well as expression of FLAG-tagged constructs (the higher molecular weight band detected by αDyskerin) was assessed by immunoblotting. c. RNA levels were assessed from HEK293 cells with stable expression of FLAG-tagged wildtype or variants of dyskerin following 72h of siRNA targeting endogenous dyskerin (sidkc1.B), relative to empty vector HEK293 cells (mock) lacking FLAG-tagged dyskerin and untreated with siRNA. Mock cell RNA levels are indicated by the black dashed line, while the red dashed line indicates 50% of mock cell RNA levels. Empty vector HEK293 cells treated with scramble siRNA were used to control for possible effects of siRNA transfection. These data represent experimental replicates of n=3. Statistically significant reductions in RNA enrichment compared to WT + sidkc1 treated cells are indicated by * (P value < 0.01). Error bars represent SEM.

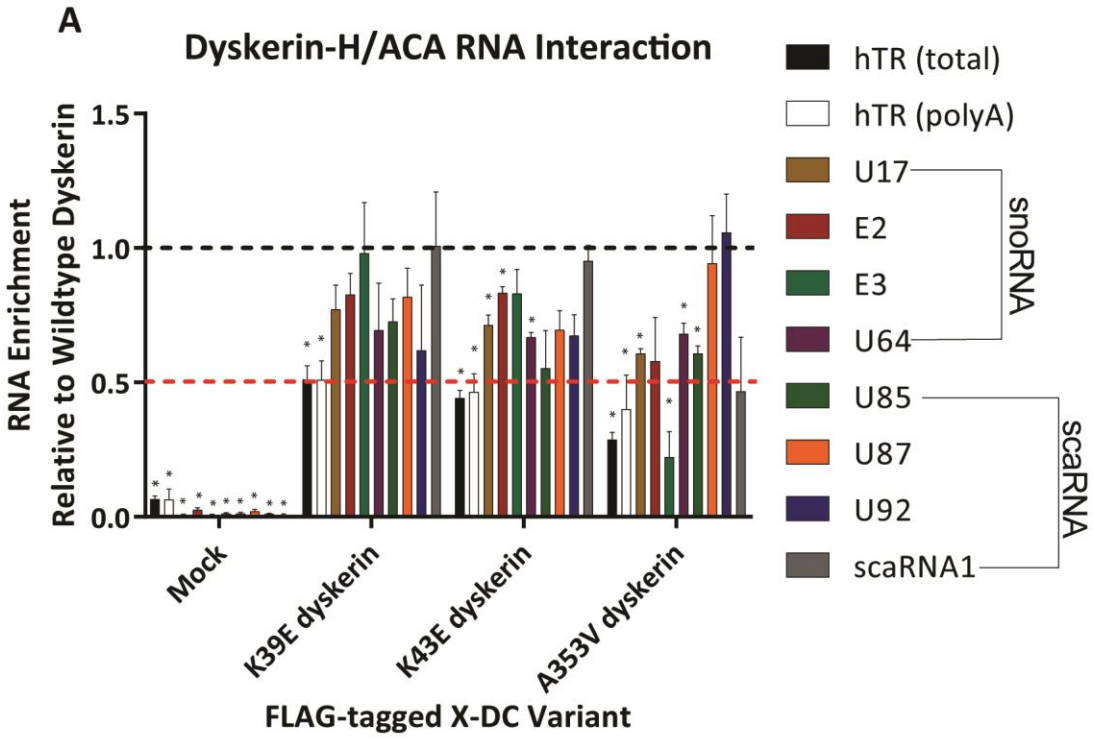
A
Dyskerin-H/ACA RNA Interaction
RNA Enrichment Relative to Wildtype Dyskerin
1.5
1.0
0.5
0.0
Mock
K39E dyskerin
K43E dyskerin
A353V dyskerin
FLAG-tagged X-DC Variant
hTR (total)
hTR (polyA)
U17
E2
E3
U64
U85
U87
U92
scaRNA1
snoRNA
scaRNA

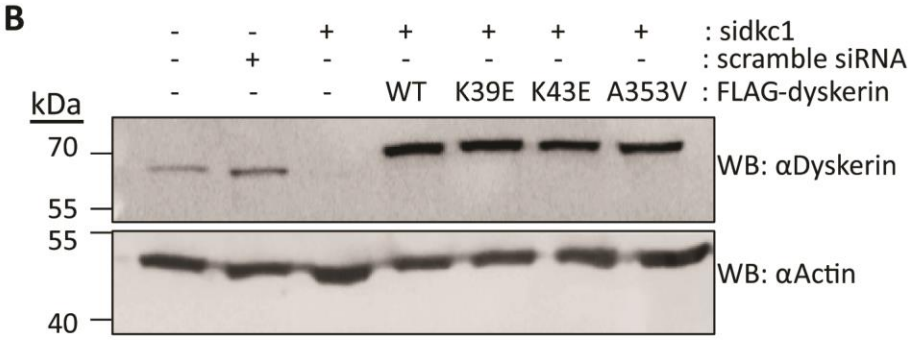
B
: sidkc1
: scramble siRNA
: FLAG-dyskerin
WT
K39E
K43E
A353V
kDa
70
55
55
40
WB: αDyskerin
WB: αActin

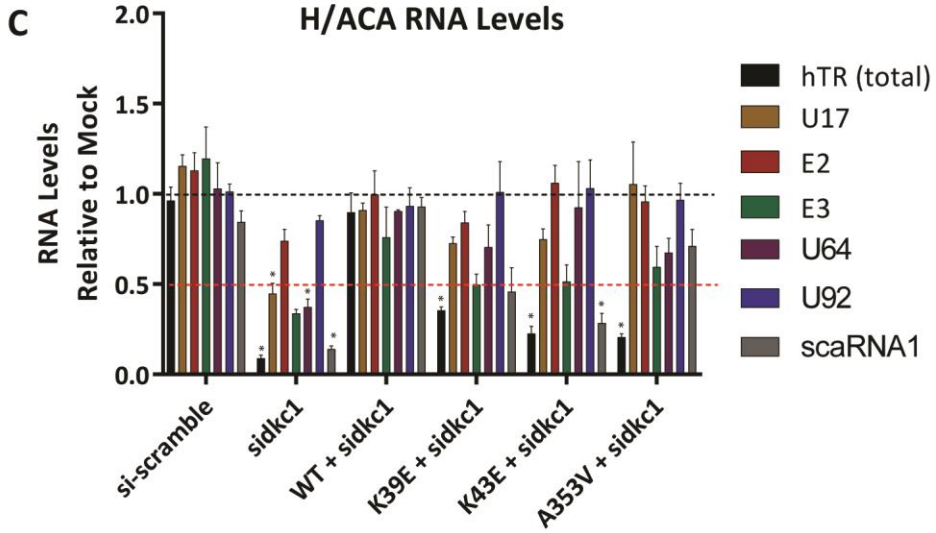
C
H/ACA RNA Levels
RNA Levels Relative to Mock
2.0
1.5
1.0
0.5
0.0
si-scramble
sidkc1
WT + sidkc1
K39E + sidkc1
K43E + sidkc1
A353V + sidkc1
hTR (total)
U17
E2
E3
U64
U92
scaRNA1

Dyskerin variants are unable to maintain hTR levels during depletion of endogenous dyskerin

Depleting endogenous dyskerin has been previously reported to decrease the levels of several H/ACA RNAs, including hTR and polyadenylated hTR (Shukla, Schmidt *et al.* 2016). We therefore examined whether dyskerin variants also have an impact on RNA levels. Towards this end, we performed siRNA targeting the 3' UTR of dyskerin mRNA in HEK293 cells stably expressing FLAG-tagged wildtype or variants of dyskerin (Figure 2.3B). While dyskerin-depleted HEK293 cells rescued with wildtype dyskerin were able to partially recover levels of hTR, none of the variants significantly rescued hTR levels (Figure 2.3C, black bars). The levels of several other H/ACA RNAs (E2 P value 0.155, E3 P value 0.0165, and U92 P value 0.485 – Figure 2.3C, red, teal, and blue bars) were not significantly affected by depletion of endogenous dyskerin, compared to knockdown cells expressing FLAG-tagged wildtype dyskerin. Interestingly, the levels of certain H/ACA RNAs (U17, U64, and scaRNA1) that were significantly reduced by dyskerin depletion were rescued by expression of either wildtype (or X-DC variant) dyskerin (Figure 2.3C, brown, purple, and grey bars). Following dyskerin depletion in empty vector cells, the level of U17, U64, and scaRNA1 were significantly reduced compared to dyskerin-depleted cells expressing FLAG-wildtype dyskerin. The recovered level of each of these H/ACA RNAs is comparable between cells expressing variants and wildtype dyskerin, with the exception of scaRNA1 that remained significantly reduced in K43E cells. Furthermore, with a second siRNA targeting endogenous dyskerin, an even more modest effect on H/ACA RNA levels was observed compared to knockdown cells expressing FLAG-wildtype dyskerin (Supplemental Figure 2.2B,C). As such, we speculate that, of the H/ACA RNAs examined, hTR is one of the most sensitive to the dyskerin-RNA interaction defect. However, we do not rule out potential effects of these mutations on rRNA pseudouridylation, or functional consequences on the ribosome.

Substitutions in the N-terminus or PUA domain of dyskerin disrupt interactions with polyadenylated hTR species and favour hTR degradation over processing

Consistent with reports indicating an important role for dyskerin in hTR processing and maturation (Ballarino, Morlando *et al.* 2005, Nguyen, Grenier St-Sauveur *et al.* 2015, Tseng, Wang *et al.* 2015, Shukla, Schmidt *et al.* 2016, Tseng, Wang *et al.* 2018), wildtype dyskerin interacts with polyadenylated hTR species, as assessed by enrichment of hTR cDNA species

primed with oligo d(T)s (Supplemental Figure 2.2A, white bars). Furthermore, all three variants displayed a reduced interaction with polyadenylated hTR species relative to wildtype dyskerin, at or below 50% of enrichment with wildtype, similarly to what was observed for total hTR species (Figure 2.3A, white bars). Given this observation, we postulate that it is likely that these interaction defects have implications upstream of mature hTR function during an early assembly step with nascent or precursor hTR species (see model in Figure 2.5).

Unlike the reported accumulation of polyadenylated hTR species resulting from the knockdown of some RNA processing components recently identified in hTR maturation – such as the poly(A) ribonuclease PARN, the exosome complex components, recruitment factors involved in these pathways, or TOE1 (Nguyen, Grenier St-Sauveur *et al.* 2015, Tseng, Wang *et al.* 2015, Shukla, Schmidt *et al.* 2016, Deng, Huang *et al.* 2019, Son, Park *et al.* 2018) – knockdown of dyskerin leads to a reduction of polyadenylated hTR species as well as total hTR species (Figure 2.4A). Additionally, we observed no accumulation of hTR 3' extended precursors by semi-quantitative RT-PCR following dyskerin knockdown (Figure 2.4B), contrasting what has been observed upon knockdown of components in the aforementioned processing pathways. There was also no accumulation of hTR 3' extended precursors observed in cells depleted of endogenous dyskerin while stably expressing either wildtype or variants of dyskerin (Figure 2.4B). Based on these data, we posited that hTR precursors that are not bound by dyskerin variants are rapidly degraded, causing the hTR accumulation defect, and not leading to defects in hTR processing or trimming *per se*.

To test this hypothesis, we performed a double knockdown of dyskerin and components of processing or degradation pathways; PARN or the human exosome core component RRP40 were depleted along with endogenous dyskerin using siRNA, in cells expressing wildtype or variant FLAG-tagged dyskerin. In the context of dyskerin depletion, neither siRNA targeting of PARN nor RRP40 completely recovers hTR levels in HEK293 cells, with or without expression of FLAG-tagged variants (Figure 2.4C and D). Importantly, following PARN knockdown in dyskerin depleted cells expressing FLAG-tagged wildtype dyskerin, hTR levels are also lower than mock and scramble siRNA treated cells. This is consistent with previous reports that PARN knockdown and PARN mutations result in reduced mature hTR levels due to hTR processing defects which generate 3' extended species that undergo degradation, likely by the human exosome and/or cytosolic RNA decay machinery (Nguyen, Grenier St-Sauveur *et al.* 2015,

Tseng, Wang *et al.* 2015, Shukla, Schmidt *et al.* 2016). Additionally, the partial rescue of hTR levels that we observe upon knockdown of RRP40 in dyskerin depleted cells is comparable to the partial rescue observed upon knockdown of RRP6 by Shukla *et al.* (Shukla, Schmidt *et al.* 2016), consistent with these two factors functioning in the same exosome complex acting on hTR in dyskerin depleted cells. Although co-depletion of PARN, RRP40, and dyskerin simultaneously proved too technically challenging to examine, we speculate that various RNA degradation pathways may function redundantly with respect to hTR degradation in this context, consistent with reports of many different nucleases acting during the hTR trimming and degradation processes, including the previously reported role of the cytoplasmic RNA decay machinery acting on a subset of hTR species exported to the cytoplasm upon dyskerin depletion (Nguyen, Grenier St-Sauveur *et al.* 2015, Tseng, Wang *et al.* 2015, Shukla, Schmidt *et al.* 2016, Deng, Huang *et al.* 2018).

Figure 2.4: Deprotection of hTR results in degradation and not accumulation of poly(A) or 3' extended hTR species. Following siRNA targeting of dyskerin (sidkc1.A and sidkc1.B), qPCR analysis revealed that a. total and poly(A) hTR levels are both reduced relative to untreated HEK293 cells. The levels of the C/D RNA U3 are not reduced by depletion of dyskerin, though there is an increase in the amount of U3 in dyskerin depleted cells. We chose the U3 C/D RNA as a negative control for small ncRNA degradation, as we expected that the levels of U3 would not decrease upon dyskerin knock down, given that dyskerin does not directly interact with U3. Given that total depletion of dyskerin affects the pool of H/ACA RNAs responsible for post-transcriptional modification of rRNA, it is possible that there is an alteration of other rRNA post-transcriptional machinery as a cellular response to siRNA treatment targeting dyskerin, including the upregulation of U3 given its role in rRNA biogenesis. This has been performed in experimental replicate n=3. Additionally, b. the accumulation of 3' extended hTR precursors was examined by PCR following knockdown of endogenous dyskerin (sidkc1.B), or the NEXT/hTRAMP complex component MTR4 (siMTR4 - a positive control for defective processing of hTR). The expected 288 nt product observed with cDNA from HEK293 cells depleted of MTR4 (indicated by an asterisk) was not observed in cells depleted of dyskerin, with or without exogenous WT and dyskerin variants (middle panel – F2 + R1). GAPDH amplification was used as a positive control (bottom panel), and no amplification of genomic contamination was observed (top panel – F1 + R1), indicating that the amplified product is a 3' extended hTR transcript. This was repeated in experimental replicate n=2, and a representative image is shown. Double depletion of endogenous dyskerin and c. PARN or d. RRP40 from HEK293 cells with siRNA (sidkc1.B and siPARN, or sidkc1.B and siRRP40), as well as expression of FLAG-tagged constructs (the higher molecular weight band detected by αDyskerin) was assessed by immunoblotting following 96h of siRNA treatment. Total hTR levels were assessed from HEK293 cells with stable expression of FLAG-tagged wildtype or variants of dyskerin by qPCR following 96h of siRNA treatment, relative to empty vector HEK293 cells (mock) lacking FLAG-tagged dyskerin and untreated with siRNA. Mock cell hTR level is indicated by the black dashed line, while the red dashed line indicates 50% of mock cell hTR level. Empty vector HEK293 cells treated with scramble siRNA were used to control for possible effects of siRNA transfection. These data represent experimental replicates of n=3. No

statistically significant reductions in RNA enrichment compared to WT + siPARN + sidkc1 were observed. Statistically significant reductions in RNA enrichment compared to WT + siRRP40 + sidkc1 treated cells are indicated by * (P value < 0.01). Error bars represent SEM.

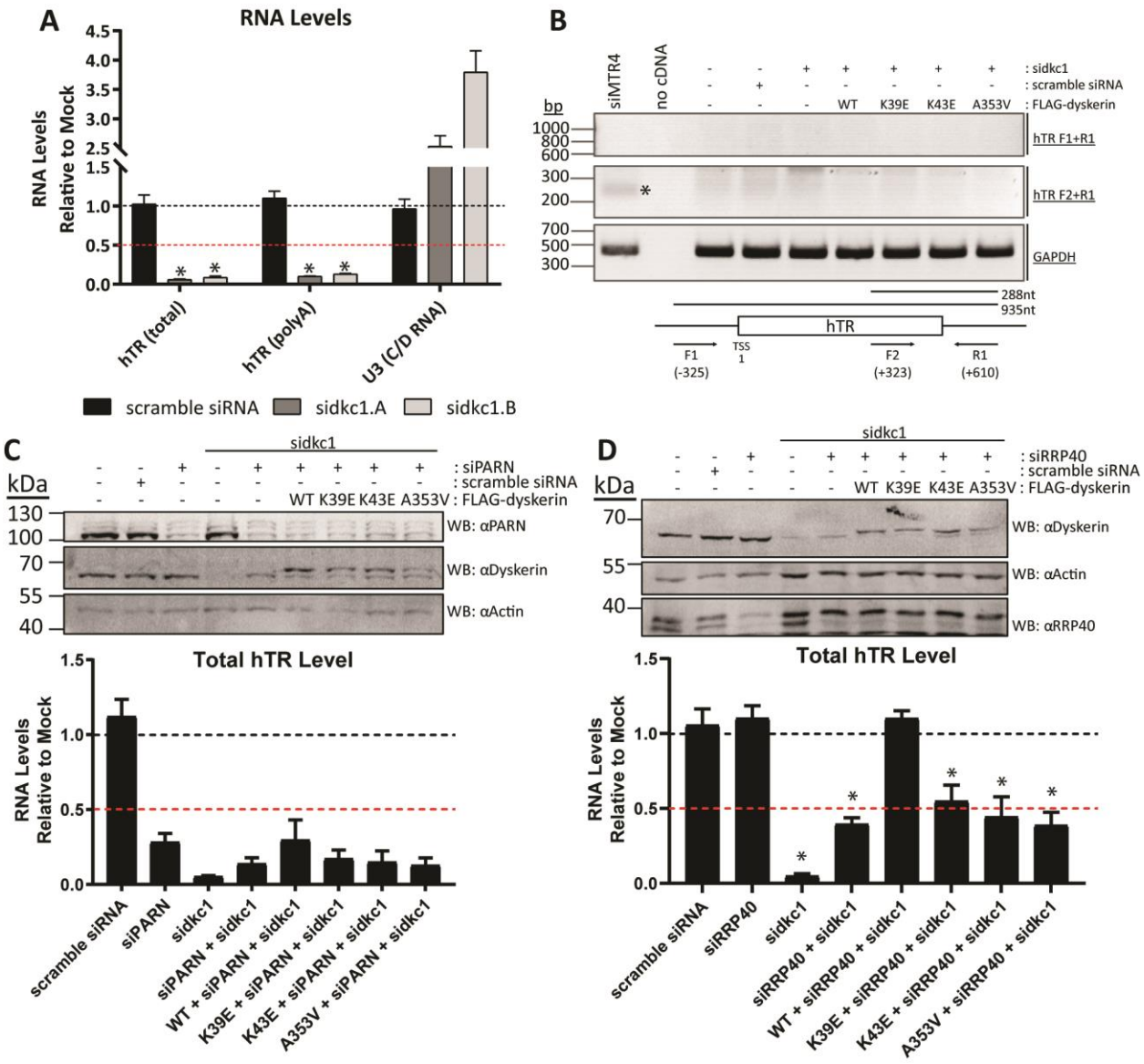
A
RNA Levels
RNA Levels Relative to Mock
hTR (total)
hTR (polyA)
U3 (C/D RNA)
scramble siRNA
sidkc1.A
sidkc1.B
B
siMTR4
no cDNA
: sidkc1
: scramble siRNA
: FLAG-dyskerin
WT K39E K43E A353V
bp
hTR F1+R1
hTR F2+R1
GAPDH
288nt
935nt
hTR
F1 (-325)
TSS 1
F2 (+323)
R1 (+610)
C
sidkc1
kDa
: siPARN
: scramble siRNA
: FLAG-dyskerin
WB: αPARN
WB: αDyskerin
WB: αActin
Total hTR Level
RNA Levels Relative to Mock
scramble siRNA
siPARN
sidkc1
siPARN + sidkc1
WT + siPARN + sidkc1
K39E + siPARN + sidkc1
K43E + siPARN + sidkc1
A353V + siPARN + sidkc1
D
sidkc1
kDa
: siRRP40
: scramble siRNA
: FLAG-dyskerin
WB: αDyskerin
WB: αActin
WB: αRRP40
Total hTR Level
RNA Levels Relative to Mock
scramble siRNA
siRRP40
sidkc1
siRRP40 + sidkc1
WT + siRRP40 + sidkc1
K39E + siRRP40 + sidkc1
K43E + siRRP40 + sidkc1
A353V + siRRP40 + sidkc1

Figure 2.5: Summary Model. Under wildtype conditions, dyskerin binds to newly transcribed hTR, protecting species with 3' extensions and/or poly(A) tails from degradation. This ensures the trimming of hTR 3' extended and/or polyadenylated species into mature hTR can take place, followed by assembly of the functional telomerase complex, and telomere maintenance by hTERT. In the context of X-DC, dyskerin variants with defects in binding to newly transcribed hTR result in deprotection of the H/ACA box of hTR, leading to misregulated degradation of 3' extended and polyadenylated species by a variety of reported RNA processing and degradation complexes (i.e. PABPN1/PARN, NEXT/TRAMP/exosome, DCP2/XRN1, and TOE1). Ultimately, this causes a reduced amount of functional telomerase and a lack of telomere maintenance, as has been observed in X-DC patients. Two copies of the H/ACA ribonucleoprotein complex have been reported to be assembled with the H/ACA box of hTR in active telomerase, with the 5' stem loop dyskerin likely being anchored to the complex via the 3' stem loop-bound dyskerin, which may be disrupted by amino acid substitutions in the N-terminal extension or DKCLD X-DC hotspot.

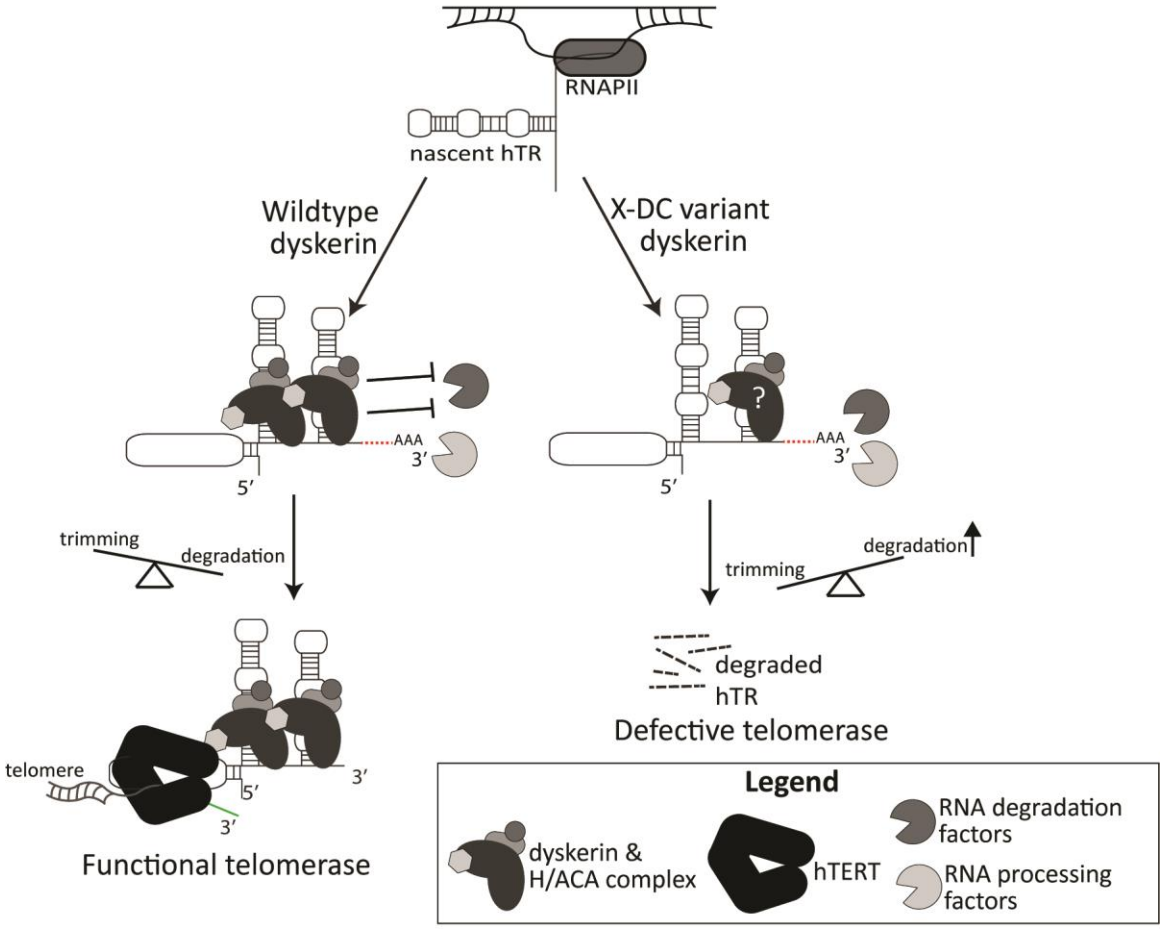
RNAPII
nascent hTR
Wildtype dyskerin
X-DC variant dyskerin
AAA
3′
5′
?
trimming
degradation
degraded hTR
Defective telomerase
telomere
Functional telomerase
Legend
dyskerin & H/ACA complex
hTERT
RNA degradation factors
RNA processing factors

2.7 Discussion

Defective accumulation of hTR is a common consequence of X-DC mutations, reported in both cell culture studies and in fibroblasts and lymphocytes from patients with this premature aging disease (Wong, Kyasa *et al.* 2004, Wong and Collins 2006, Agarwal, Loh *et al.* 2010, Batista, Pech *et al.* 2011, Parry, Alder *et al.* 2011, Zeng, Thumati *et al.* 2012, Alder, Parry *et al.* 2013, Bellodi, McMahon *et al.* 2013, Kropski, Mitchell *et al.* 2014, Moon, Segal *et al.* 2015). Here we show that for the K39E, K43E, and A353V dyskerin variants, reduced hTR accumulation is driven by an interaction defect between dyskerin and precursor hTR species. Interaction defects have been previously reported *in vitro* for A353V, as well as studies done *in vitro* or in patient-derived cells for substitutions G402E, T49M, and ΔL37 (Ashbridge, Orte *et al.* 2009, Trahan, Martel *et al.* 2010, Batista, Pech *et al.* 2011). While none of these previous studies examined precursors of hTR, it seems likely that the interaction defects reported for other variants would affect precursor hTR species that have an H/ACA box available for dyskerin binding. As such, we propose that X-DC variants that display hTR interaction defects cause reduced accumulation of hTR and telomerase activity by deprotecting hTR precursors.

Recent studies examining the processing and degradation pathways for hTR have shed light on roles for many different complexes, including the nuclear exosome, PABPN1 and PARN, human TRAMP and NEXT complexes, CBCA complex, XRN1/DCP2, and most recently TOE1 (Nguyen, Grenier St-Sauveur *et al.* 2015, Tseng, Wang *et al.* 2015, Shukla, Schmidt *et al.* 2016, Deng, Huang *et al.* 2019, Son, Park *et al.* 2018). While the balance between degradation and trimming of hTR precursors into mature functional species is clearly a tightly regulated and complex process, much remains uncertain regarding the redundancies in these pathways and how the balance between them is coordinated. Our findings suggest that in a context of dysfunctional H/ACA complex interactions with hTR, targeting only one of these pathways is insufficient to rescue hTR accumulation defects in cells. Furthermore, 3' extended hTR precursors do not accumulate in cells depleted of endogenous dyskerin, regardless of whether or not exogenous dyskerin (wildtype or variant) is expressed. These findings lead us to the conclusion that the interaction between dyskerin and hTR is one of the earliest steps in hTR biogenesis that prevents hTR degradation, as has been proposed previously by Tseng *et al.* (Tseng, Wang *et al.* 2015) for the H/ACA RNP complex as a whole. However, in contrast to what has been observed for other components that regulate the correct processing of hTR,

depletion of dyskerin ultimately leads to a reduction of both polyadenylated and mature hTR species, which cannot be rescued by targeting individual degradation pathways. We propose that the interaction between dyskerin and hTR is essential for blocking canonical RNA degradation pathways, as well as preventing hTR degradation by components that would canonically function as trimming or processing factors. In the X-DC context, we speculate that dyskerin-hTR interaction defects could promote misregulated PARN trimming leading to hTR degradation, as well as formation of 3' extended hTR precursors which rapidly undergo degradation by the exosome rather than being properly trimmed into mature hTR species. This is consistent with a recent report detailing a role for dyskerin in the regulation of short 3' extended hTR trimming by PARN, as well as preventing the stabilization of long 3' extended hTR products which are targeted for degradation by the RRP6-exosome (Tseng, Wang *et al.* 2018). More recently still, it has been demonstrated that targeting the exosome via depletion of RRP40 can partially rescue total hTR levels in human embryonic stem cells (hESCs) that were genetically engineered by CRISPR/Cas9 to harbor the A353V variant of dyskerin, as well as RRP40 depletion partially restoring telomerase activity, telomere length, and reducing DNA damage signaling. However, targeting the non-canonical poly(A) RNA polymerase PAPD5 in the A353V hESCs was able to rescue hTR levels to a greater extent than downregulation of RRP40, as well as uniquely rescue hematopoiesis defects comparable to rescue by overexpression of hTR in these hESCs. This is consistent with polyadenylation of hTR being upstream of the recruitment of various nucleases, including the exosome and PARN (Fok, Shukla *et al.* 2019). Furthermore, as has been demonstrated by Shukla, *et al.* in 2016 (Shukla, Schmidt *et al.* 2016), it is likely that the cytoplasmic RNA decay machinery also contributes to the inability to fully rescue hTR levels by solely targeting the exosome or PARN, with DCP2 and XRN1 acting on cyTER (cytoplasmic telomerase RNA) species which are exported from the nucleus following dyskerin depletion.

While the predicted secondary structure of H/ACA box RNAs is likely comparable between specific RNA molecules, many differences between hTR and other H/ACA class RNAs have been reported in the literature. Indeed, biogenesis and structural differences among H/ACA class RNAs including hTR have been demonstrated (Fu and Collins 2003, Jady, Bertrand *et al.* 2004, Theimer, Jady *et al.* 2007, Egan and Collins 2012), as well as variations in hairpin size, for instance as predicted for members of the AluACA class RNAs, the E2 snoRNA, and hTR (Ketele, Kiss *et al.* 2016). Similarly, structural elements within the H/ACA RNA stem loops such

as the BIO box motif present in hTR (Fu and Collins 2003, Egan and Collins 2012), or the CAB box found in scaRNAs (Jady, Bertrand *et al.* 2004, Theimer, Jady *et al.* 2007) also provide variations in protein-RNA complex assembly due to differences in RNA structure and/or folding. RNA structural variations, as well as differences in H/ACA RNA biogenesis may offer an explanation for the evident variability of dyskerin-RNA interactions, and the downstream consequences. For instance, although reduced total 18S rRNA pseudouridine content has been observed in X-DC patient lymphocytes expressing the A353V variant, several studies have reported normal processing and accumulation of mature 18S and 28S rRNA species in patient cells with this variant (Zeng, Thumati *et al.* 2012, Bellodi, McMahon *et al.* 2013, Thumati, Zeng *et al.* 2013, Moon, Segal *et al.* 2015). We speculate that the reduction in pseudouridine content may be caused by an impaired interaction of dyskerin with select H/ACA RNAs, such as the interaction defect that we observed between the A353V variant and the E3 snoRNA, but this reduction does not substantially impede mature rRNA function. One explanation for this could be that H/ACA RNAs that interact poorly with A353V still accumulate to sufficient levels to maintain a functional amount of pseudouridine synthesis. Indeed, though the interaction between A353V and E3 is defective, this X-DC variant can still at least partially rescue total levels of E3 snoRNA in cells depleted of endogenous dyskerin. In contrast, hTR accumulation cannot be recovered by any of the variants in this study, and the amount of hTR that remains in cells depleted of endogenous dyskerin while expressing X-DC variants is not sufficient for telomerase function. As such, it is tempting to speculate that X-DC presents as a telomere biology disorder because hTR is particularly sensitive to any disruptions in dyskerin-RNA interaction, as has also been previously proposed based on differential biogenesis requirements between hTR and other H/ACA class RNAs (Fu and Collins 2003).

Importantly, while some X-DC patient cells have presented with lower dyskerin protein levels than wildtype controls (Bellodi, McMahon *et al.* 2013, Moon, Segal *et al.* 2015, Perdigones, Perin *et al.* 2016), in the context of this study we did not observe notable differences in the levels of expression for wildtype, K39E, K43E, and A353V dyskerin constructs, suggesting that these variants are not subject to more protein degradation than wildtype dyskerin. All three variants that we examined are capable of forming H/ACA RNP complexes and localizing to the subnuclear compartments where mature H/ACA RNP complexes are found. This lends further support to the notion that not all H/ACA RNAs are disrupted by these

mutations, as complex formation and function is largely dependent on protein-RNA interactions (Massenet, Bertrand *et al.* 2017). One striking observation that we made was that all three of these variants are able to interact with exogenously expressed hTERT. The interaction between dyskerin and hTERT is dependent on hTR, and so we expected to observe a decreased co-IP of hTERT with the dyskerin variants correlating with the amount of hTR in X-DC variant IP fractions. However, hTR stability can be improved upon hTERT overexpression alone (Yi, Tesmer *et al.* 1999), and it has been reported that X-DC variants are able to co-IP with active telomerase in the context of hTERT and hTR overexpression (Zeng, Thumati *et al.* 2012). As such, we postulate that overexpression of hTERT likely masks possible interaction defects between hTERT and the variants examined in this study. Indeed, given that cells depleted of endogenous dyskerin suffer a reduction in telomerase activity that cannot be rescued by these X-DC variants, we postulate that telomerase assembly is defective in this context, despite our inability to detect a defective interaction between these variants and hTERT by co-IP.

Residues in the N-terminal extension of dyskerin are highly evolutionarily conserved among eukaryotes, but the exact function of this region in humans has been largely uncharacterized to date. Our findings support structural studies done in yeast indicating that this region, along with the PUA, plays an important RNA-interacting role (Li, Duan *et al.* 2011). The recently solved cryo-EM structure of human telomerase also demonstrates that this region is in close proximity to both the PUA and hTR itself (Nguyen, Tam *et al.* 2018), strongly supporting the possibility that the function of the N-terminal extension and DKCLD may be as an RNA-binding domain cooperating with the PUA to stabilize the interaction of dyskerin with the H/ACA domain of H/ACA class RNAs. In addition to the interaction defects that we observe for K39E and K43E, other X-DC substitutions in the N-terminal hotspot have also been reported to disrupt the interaction between dyskerin and hTR *in vitro* (T49M) (Ashbridge, Orte *et al.* 2009), and in patient-derived cell studies (ΔL37) (Batista, Pech *et al.* 2011). In concordance with what was proposed by Nguyen *et al.* (Nguyen, Tam *et al.* 2018) based on the human telomerase cryo-EM structure, we speculate that hTR is particularly sensitive to substitutions in the N-terminus of dyskerin due to the 5' hairpin of the H/ACA domain in hTR which is unique amongst other H/ACA box RNAs. Given that the interaction of dyskerin with this 5' hairpin is largely dependent on dyskerin interfacing with the 3' hairpin-bound dyskerin (Nguyen, Tam *et al.* 2018), it is possible that substitutions in the N-terminal hotspot disrupt this interface and therefore the

interaction between dyskerin and the 5’ hairpin in hTR without affecting other H/ACA RNA interactions as substantially. Additionally, this may explain why K39E and K43E present an hTR interaction of approximately 50% of wildtype dyskerin, as the 3’ hairpin dyskerin-RNA interaction is stabilized by other H/ACA protein-RNA contacts which could remain intact based on the co-IP data analyzing H/ACA RNP complex assembly. We suggest that protection of only the 3’ hairpin in the H/ACA domain of hTR may be insufficient to regulate the balance between trimming and degradation of hTR precursors. Ultimately, it is not yet known if these N-terminal residues contact the RNA or the dyskerin-dyskerin interface directly. Further analyses will be needed to test this hypothesis, and to assess whether other X-DC substitutions within the N-terminal extension and DKCLD present a similar disruption of the dyskerin-hTR interaction.

2.8 Supplemental Figures and Figure Legends

Supplemental Figure 2.1: a. The interaction between hTERT and dyskerin was also assessed by co-IP in the presence of RNase A to confirm that the observed interaction is dependent on hTR. **b.** A representative image of the telomeric repeat amplification products, assessed on 10% non-denaturing acrylamide gel following Q-TRAP as a quality control check (note that differences in telomerase activity cannot be visualized on this gel, but are quantified based on differences in C_T)

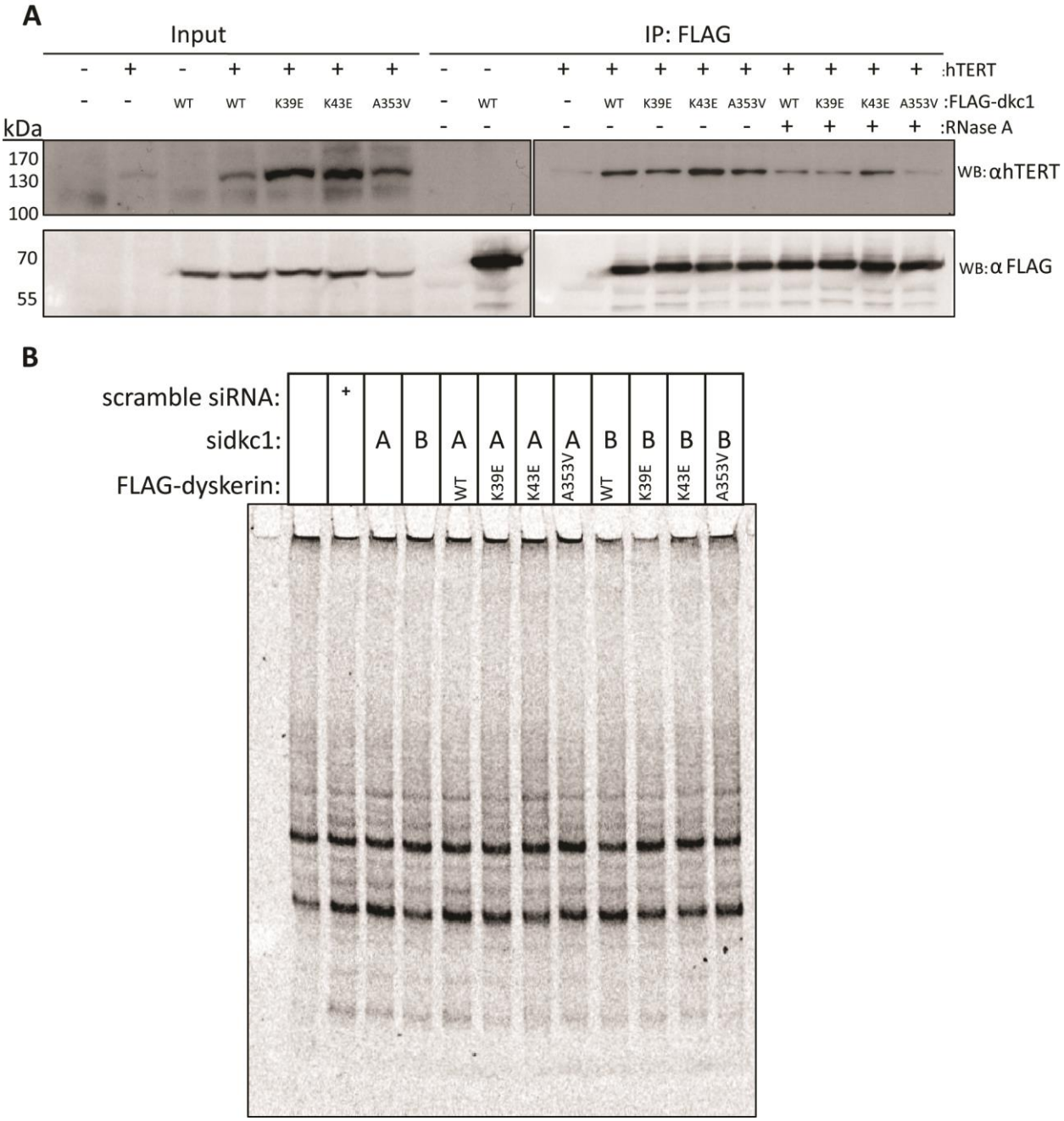
A
Input
IP: FLAG
:hTERT
:FLAG-dkc1
:RNase A
WT
K39E
K43E
A353V
kDa
170
130
100
70
55
WB: αhTERT
WB: α FLAG
B
scramble siRNA:
sidkc1:
FLAG-dyskerin:
+
A
B
WT
K39E
K43E
A353V

Supplemental Figure 2.2: supplementary data for Figure 2.3 a. Dyskerin-RNA interactions were assessed by IP of FLAG-tagged dyskerin followed by RNA extraction and qPCR. Relative to wildtype (WT) IP fractions of total hTR, IP fractions from mock transfected cells show no enrichment of hTR. Neither mock nor WT IP fractions showed enrichment of the negative control C/D box RNA U3 relative to WT IP of hTR. The interaction of WT dyskerin with polyadenylated hTR species in indicated relative to WT IP of total hTR. These data represent an experimental replicate n=3. Error bars represent SEM. **b.** Depletion of endogenous dyskerin using sidkc1.A, and expression of FLAG-tagged constructs was assessed by immunoblotting. **c.** RNA levels were assessed as described for Figure 2.3C using HEK293 cells with stable expression of FLAG-tagged wildtype or variants of dyskerin. These data represent experimental replicated of n=3. Statistically significant reductions in RNA enrichment compared to WT+sidkc1 treated cells are indicated by * (P value < 0.01). Error bars represent SEM.

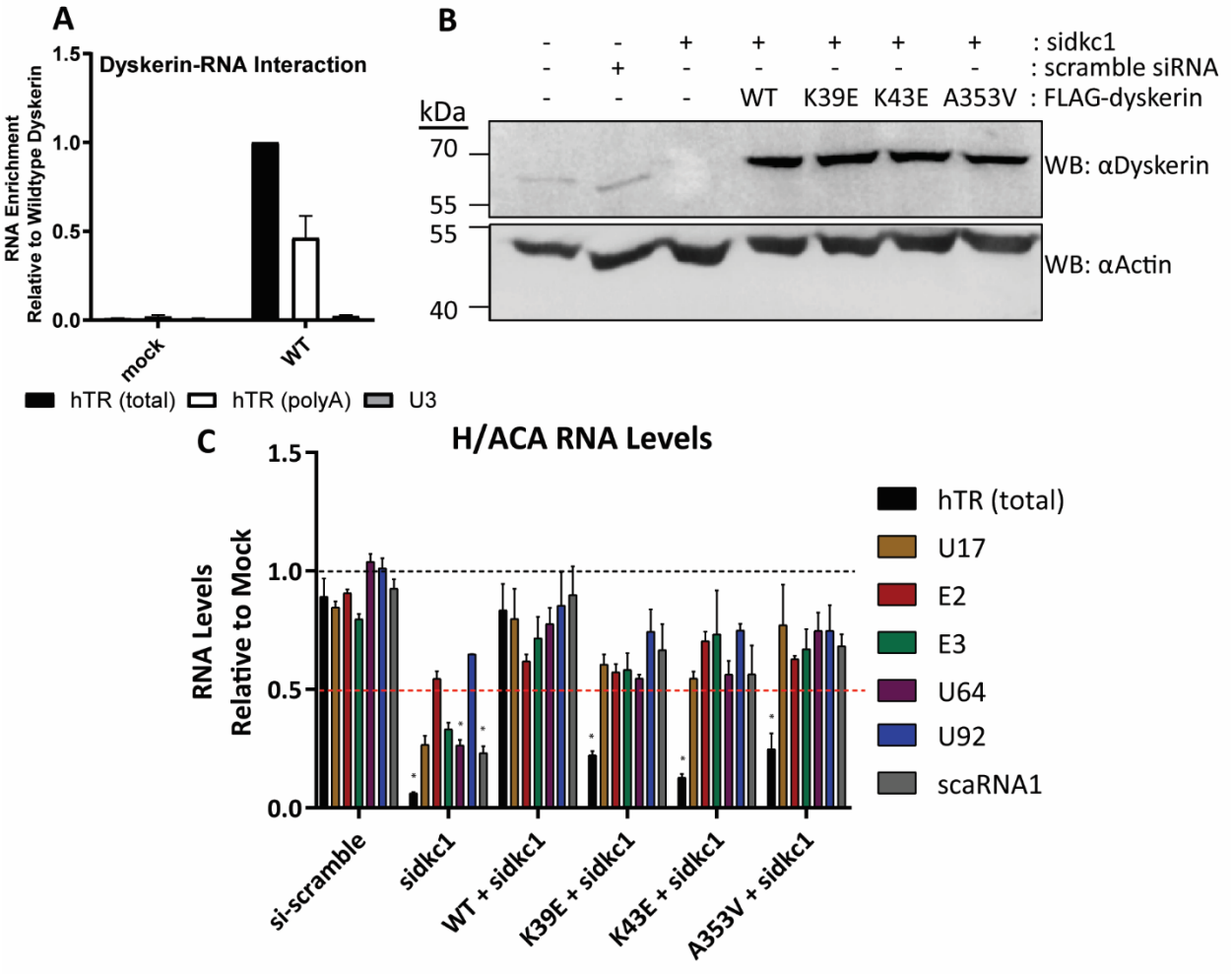
A
Dyskerin-RNA Interaction
RNA Enrichment Relative to Wildtype Dyskerin
1.5
1.0
0.5
0.0
mock
WT
hTR (total)
hTR (polyA)
U3
B
- - + + + + + : sidkc1
- + - - - - - : scramble siRNA
- - - WT K39E K43E A353V : FLAG-dyskerin
kDa
70
55
55
40
WB: αDyskerin
WB: αActin
C
H/ACA RNA Levels
RNA Levels Relative to Mock
1.5
1.0
0.5
0.0
hTR (total)
U17
E2
E3
U64
U92
scaRNA1
si-scramble
sidkc1
WT + sidkc1
K39E + sidkc1
K43E + sidkc1
A353V + sidkc1

Supplemental Table 2.1 – List of Primers and siRNAs for Chapter 2

Primer Name	Primer Sequence
DKC1 K39E	F: ACACGCTGAAGAATTTCTTATCGAACCTGAATCCAAAGTT
	R: AACTTTGGATTCAGGTTCGATAAGAAATTCTTCAGCGTGT
DKC1 K43E	F: TCTTATCAAACCTGAATCCGAAGTTGCTAAGTTGGACACG
	R: CGTGTCCAACTTAGCAACTTCGGATTCAGGTTTGATAAGA
DKC1 A353V	F: GCATTAATGACCACAGTGGTCATCTCTACCTGCG
	R: CGCAGGTAGAGATGACCACTGTGGTCATTAATGC
DKC1 K446X	F: GCAAAAACTGCGTAGCGGAAGCGAGAGAG
	R: CTCTCTCGCTTCCGCTACGCAGTTTTTGC
Mature hTR	F: TCTAACCCTAACTGAGAAGGGCGTAG
	R: GTTTGCTCTAGAATGAACGGTGGAAG
E1	F: GCCCCATGATGTACAAGTCCC
	R: AGGAATATGCAGGCGCAGAC
E2	F: AGCTTGGAGTTGAGGCTACTG
	R: TAGCGAAAACTTGCCCCTCA
E3	F: AGTGCTGTGTTGTCGTTCCC
	R: GTATGAGACCAAGCGTCCCT
U64	F: GTGTGACTTTCGTAACGGGGA
	R: TTGCACCCCTCAAGGAAAGAG
U85	F: TTGGTGGGCGATACAGAGTT
	R: CTTGGCCCTGATACCCTGAA
U87	F: TTTGTTGCCCTCAACTCCCAG
	R: GCCACTCGTCAGTCTCCTGT

U92	F: GTCACCATGCCTCCCTAGAA
	R: ATCTGTCTGCCCCGTATCTG
SCARNA1	F: CAGCAGTTGATACTAACCGAGC
	R: CCCAGCTATCACAACACATCAC
U3	F: TGACGGCTCTTGGGTTTTCT
	R: GGGAAACGGCGACAAAAGAG
GAPDH	F: CGGAGTCAACGGATTTGGTCGTCGTAT
	R: TGCTAAGCAGTTGGTGGTGCAGGA
F1 hTR (-325)	GGCCCTAAAATCTTCCTGTG
F2 hTR (+323)	CGGGTCTCTCGGGGGCGAGGGCGA
R1 hTR (+610)	ATTCATTTTGGCCGACTTTG
3'UTR sidkc1.A	GGAUAUGGGUGGUGAAAGA dT dT
3'UTR sidkc1.B	CCUCAAAGCUUGUGUACAG dT dT
siMTR4	CAAUUAAGGCUCUGAGUAAUU
siRRP40	CACGCACAGUACUAGGUCA dT dT
siPARN	AGGCAUUCAUGUUGAGACU dT dT

2.9 Acknowledgements

We thank Dr. Tom Meier, Dr. Joachim Lingner and Dr. François Dragon for providing us with pSR38 (SHQ1), pcDNA6/myc-HisC-hTERT, and pcDNA3.1-FLAG-dyskerinWT plasmids, respectively. We thank Dr. Michael Terns, Dr. Kenneth Michael Pollard, and Dr. Witold Filipowicz for providing us with mouse anti-coilin, mouse anti-fibrillarin, and rabbit anti-hGAR1 antibodies. We thank Dr. François Bachand for providing us with siRNA targeting human MTR4, as well as experimental advice regarding RNA processing pathways. We thank Marc Fabian and Jian Qin for discussion and comments.

2.10 Author Contribution

Author contributions: D.E.M. and C.A. designed research; D.E.M and P. L.-L. performed experiments. D.E.M. and C.A. wrote the manuscript.

2.11 References

Agarwal, S., Y. H. Loh, E. M. McLoughlin, J. Huang, I. H. Park, J. D. Miller, H. Huo, M. Okuka, R. M. Dos Reis, S. Loewer, H. H. Ng, D. L. Keefe, F. D. Goldman, A. J. Klingelhutz, L. Liu and G. Q. Daley (2010). Telomere elongation in induced pluripotent stem cells from dyskeratosis congenita patients. Nature 464(7286): 292-296.

Alder, J. K., E. M. Parry, S. Yegnasubramanian, C. L. Wagner, L. M. Lieblich, R. Auerbach, A. D. Auerbach, S. J. Wheelan and M. Armanios (2013). Telomere phenotypes in females with heterozygous mutations in the dyskeratosis congenita 1 (DKC1) gene. Hum Mutat 34(11): 1481-1485.

Alter, B. P., N. Giri, S. A. Savage and P. S. Rosenberg (2018). Cancer in the National Cancer Institute inherited bone marrow failure syndrome cohort after fifteen years of follow-up. Haematologica 103(1): 30-39.

Ashbridge, B., A. Orte, J. A. Yeoman, M. Kirwan, T. Vulliamy, I. Dokal, D. Klenerman and S. Balasubramanian (2009). Single-molecule analysis of the human telomerase RNA.dyskerin interaction and the effect of dyskeratosis congenita mutations. Biochemistry 48(46): 10858-10865.

Ballarino, M., M. Morlando, F. Pagano, A. Fatica and I. Bozzoni (2005). The cotranscriptional assembly of snoRNPs controls the biosynthesis of H/ACA snoRNAs in Saccharomyces cerevisiae. Mol Cell Biol 25(13): 5396-5403.

Batista, L. F., M. F. Pech, F. L. Zhong, H. N. Nguyen, K. T. Xie, A. J. Zaug, S. M. Crary, J. Choi, V. Sebastiano, A. Cherry, N. Giri, M. Wernig, B. P. Alter, T. R. Cech, S. A. Savage, R. A. Reijo Pera and S. E. Artandi (2011). Telomere shortening and loss of self-renewal in dyskeratosis congenita induced pluripotent stem cells. Nature 474(7351): 399-402.

Bellodi, C., M. McMahon, A. Contreras, D. Juliano, N. Kopmar, T. Nakamura, D. Maltby, A. Burlingame, S. A. Savage, A. Shimamura and D. Ruggero (2013). H/ACA small RNA dysfunctions in disease reveal key roles for noncoding RNA modifications in hematopoietic stem cell differentiation. Cell Rep 3(5): 1493-1502.

Bertuch, A. A. (2016). The molecular genetics of the telomere biology disorders. RNA Biol 13(8): 696-706.

Booy, E. P., M. Meier, N. Okun, S. K. Novakowski, S. Xiong, J. Stetefeld and S. A. McKenna (2012). The RNA helicase RHAU (DHX36) unwinds a G4-quadruplex in human telomerase RNA and promotes the formation of the P1 helix template boundary. Nucleic Acids Res 40(9): 4110-4124.

Brault, M. E., C. Lauzon and C. Autexier (2013). Dyskeratosis congenita mutations in dyskerin SUMOylation consensus sites lead to impaired telomerase RNA accumulation and telomere defects. Hum Mol Genet 22(17): 3498-3507.

Cerrudo, C. S., P. D. Ghiringhelli and D. E. Gomez (2014). Protein universe containing a PUA RNA-binding domain. FEBS J 281(1): 74-87.

Chu, T. W., Y. D'Souza and C. Autexier (2016). The Insertion in Fingers Domain in Human Telomerase Can Mediate Enzyme Processivity and Telomerase Recruitment to Telomeres in a TPP1-Dependent Manner. Mol Cell Biol 36(1): 210-222.

Cristofari, G. and J. Lingner (2006). Telomere length homeostasis requires that telomerase levels are limiting. EMBO J 25(3): 565-574.

Deng, T., Y. Huang, K. Weng, S. Lin, Y. Li, G. Shi, Y. Chen, J. Huang, D. Liu, W. Ma and Z. Songyang (2019). TOE1 acts as a 3' exonuclease for telomerase RNA and regulates telomere maintenance. Nucleic Acids Res 47: 391-405.

Dragon, F., V. Pogacic and W. Filipowicz (2000). In vitro assembly of human H/ACA small nucleolar RNPs reveals unique features of U17 and telomerase RNAs. Mol Cell Biol 20(9): 3037-3048.

Duan, J., L. Li, J. Lu, W. Wang and K. Ye (2009). Structural mechanism of substrate RNA recruitment in H/ACA RNA-guided pseudouridine synthase. Mol Cell 34(4): 427-439.

Egan, E. D. and K. Collins (2012). An enhanced H/ACA RNP assembly mechanism for human telomerase RNA. Mol Cell Biol 32(13): 2428-2439.

Feng, J., W. D. Funk, S. S. Wang, S. L. Weinrich, A. A. Avilion, C. P. Chiu, R. R. Adams, E. Chang, R. C. Allsopp, J. Yu and *et al.* (1995). The RNA component of human telomerase. Science 269(5228): 1236-1241.

Fok, W. C., S. Shukla, A. T. Vessoni, K. A. Brenner, R. Parker, C. M. Sturgeon and L. F. Z. Batista (2019). Posttranscriptional modulation of TERC by PAPD5 inhibition rescues hematopoietic development in dyskeratosis congenita. Blood.

Fu, D. and K. Collins (2003). Distinct biogenesis pathways for human telomerase RNA and H/ACA small nucleolar RNAs. Mol Cell 11(5): 1361-1372.

Grozdanov, P. N., S. Roy, N. Kittur and U. T. Meier (2009). SHQ1 is required prior to NAF1 for assembly of H/ACA small nucleolar and telomerase RNPs. RNA 15(6): 1188-1197.

Heiss, N. S., A. Girod, R. Salowsky, S. Wiemann, R. Pepperkok and A. Poustka (1999). Dyskerin localizes to the nucleolus and its mislocalization is unlikely to play a role in the pathogenesis of dyskeratosis congenita. Hum Mol Genet 8(13): 2515-2524.

Heiss, N. S., A. Megarbane, S. M. Klauck, F. R. Kreuz, E. Makhoul, F. Majewski and A. Poustka (2001). One novel and two recurrent missense DKC1 mutations in patients with dyskeratosis congenita (DKC). Genet Couns 12(2): 129-136.

Herbert, B. S., A. E. Hochreiter, W. E. Wright and J. W. Shay (2006). Nonradioactive detection of telomerase activity using the telomeric repeat amplification protocol. Nat Protoc 1(3): 1583-1590.

Ikura, T., V. V. Ogryzko, M. Grigoriev, R. Groisman, J. Wang, M. Horikoshi, R. Scully, J. Qin and Y. Nakatani (2000). Involvement of the TIP60 histone acetylase complex in DNA repair and apoptosis. Cell 102(4): 463-473.

Jady, B. E., E. Bertrand and T. Kiss (2004). Human telomerase RNA and box H/ACA scaRNAs share a common Cajal body-specific localization signal. J Cell Biol 164(5): 647-652.

Ketele, A., T. Kiss and B. E. Jady (2016). Human intron-encoded AluACA RNAs and telomerase RNA share a common element promoting RNA accumulation. RNA Biol 13(12): 1274-1285.

Knight, S. W., N. S. Heiss, T. J. Vulliamy, S. Greschner, G. Stavrides, G. S. Pai, G. Lestringant, N. Varma, P. J. Mason, I. Dokal and A. Poustka (1999). X-linked dyskeratosis congenita is predominantly caused by missense mutations in the DKC1 gene. Am J Hum Genet 65(1): 50-58.

Kropski, J. A., D. B. Mitchell, C. Markin, V. V. Polosukhin, L. Choi, J. E. Johnson, W. E. Lawson, J. A. Phillips, 3rd, J. D. Cogan, T. S. Blackwell and J. E. Loyd (2014). A novel dyskerin (DKC1) mutation is associated with familial interstitial pneumonia. Chest 146(1): e1-e7.

Lafontaine, D. L., C. Bousquet-Antonelli, Y. Henry, M. Caizergues-Ferrer and D. Tollervey (1998). The box H + ACA snoRNAs carry Cbf5p, the putative rRNA pseudouridine synthase. Genes Dev 12(4): 527-537.

Li, L. and K. Ye (2006). Crystal structure of an H/ACA box ribonucleoprotein particle. Nature 443(7109): 302-307.

Li, S., J. Duan, D. Li, B. Yang, M. Dong and K. Ye (2011). Reconstitution and structural analysis of the yeast box H/ACA RNA-guided pseudouridine synthase. Genes Dev 25(22): 2409-2421.

Lin, P., M. E. Mobasher and F. Alawi (2014). Acute dyskerin depletion triggers cellular senescence and renders osteosarcoma cells resistant to genotoxic stress-induced apoptosis. Biochem Biophys Res Commun 446(4): 1268-1275.

Lopez-Otin, C., M. A. Blasco, L. Partridge, M. Serrano and G. Kroemer (2013). The hallmarks of aging. Cell 153(6): 1194-1217.

Machado-Pinilla, R., J. Carrillo, C. Manguan-Garcia, L. Sastre, A. Mentzer, B. W. Gu, P. J. Mason and R. Perona (2012). Defects in mTR stability and telomerase activity produced by the Dkc1 A353V mutation in dyskeratosis congenita are rescued by a peptide from the dyskerin TruB domain. Clin Transl Oncol 14(10): 755-763.

MacNeil, D. E., H. J. Bensoussan and C. Autexier (2016). Telomerase Regulation from Beginning to the End. Genes (Basel) 7(9).

Massenet, S., E. Bertrand and C. Verheggen (2017). Assembly and trafficking of box C/D and H/ACA snoRNPs. RNA Biol 14(6): 680-692.

Meyerson, M., C. M. Counter, E. N. Eaton, L. W. Ellisen, P. Steiner, S. D. Caddle, L. Ziaugra, R. L. Beijersbergen, M. J. Davidoff, Q. Liu, S. Bacchetti, D. A. Haber and R. A. Weinberg (1997). hEST2, the putative human telomerase catalytic subunit gene, is up-regulated in tumor cells and during immortalization. Cell 90(4): 785-795.

Mitchell, J. R., J. Cheng and K. Collins (1999). A box H/ACA small nucleolar RNA-like domain at the human telomerase RNA 3' end. Mol Cell Biol 19(1): 567-576.

Mochizuki, Y., J. He, S. Kulkarni, M. Bessler and P. J. Mason (2004). Mouse dyskerin mutations affect accumulation of telomerase RNA and small nucleolar RNA, telomerase activity, and ribosomal RNA processing. Proc Natl Acad Sci U S A 101(29): 10756-10761.

Moon, D. H., M. Segal, B. Boyraz, E. Guinan, I. Hofmann, P. Cahan, A. K. Tai and S. Agarwal (2015). Poly(A)-specific ribonuclease (PARN) mediates 3'-end maturation of the telomerase RNA component. Nat Genet 47(12): 1482-1488.

Nakamura, T. M., G. B. Morin, K. B. Chapman, S. L. Weinrich, W. H. Andrews, J. Lingner, C. B. Harley and T. R. Cech (1997). Telomerase catalytic subunit homologs from fission yeast and human. Science 277(5328): 955-959.

Nguyen, D., V. Grenier St-Sauveur, D. Bergeron, F. Dupuis-Sandoval, M. S. Scott and F. Bachand (2015). A Polyadenylation-Dependent 3' End Maturation Pathway Is Required for the Synthesis of the Human Telomerase RNA. Cell Rep 13(10): 2244-2257.

Nguyen, T. H. D., J. Tam, R. A. Wu, B. J. Greber, D. Toso, E. Nogales and K. Collins (2018). Cryo-EM structure of substrate-bound human telomerase holoenzyme. Nature 557(7704): 190-195.

Parry, E. M., J. K. Alder, S. S. Lee, J. A. Phillips, 3rd, J. E. Loyd, P. Duggal and M. Armanios (2011). Decreased dyskerin levels as a mechanism of telomere shortening in X-linked dyskeratosis congenita. J Med Genet 48(5): 327-333.

Perdigones, N., J. C. Perin, I. Schiano, P. Nicholas, J. A. Biegel, P. J. Mason, D. V. Babushok and M. Bessler (2016). Clonal hematopoiesis in patients with dyskeratosis congenita. Am J Hematol 91(12): 1227-1233.

Podlevsky, J. D., C. J. Bley, R. V. Omana, X. Qi and J. J. Chen (2008). The telomerase database. Nucleic Acids Res 36(Database issue): D339-343.

Pogacic, V., F. Dragon and W. Filipowicz (2000). Human H/ACA small nucleolar RNPs and telomerase share evolutionarily conserved proteins NHP2 and NOP10. Mol Cell Biol 20(23): 9028-9040.

Shukla, S., J. C. Schmidt, K. C. Goldfarb, T. R. Cech and R. Parker (2016). Inhibition of telomerase RNA decay rescues telomerase deficiency caused by dyskerin or PARN defects. Nat Struct Mol Biol 23(4): 286-292.

Son, A., J. E. Park and V. N. Kim (2018). PARN and TOE1 Constitute a 3' End Maturation Module for Nuclear Non-coding RNAs. Cell Rep 23(3): 888-898.

Theimer, C. A., B. E. Jady, N. Chim, P. Richard, K. E. Breece, T. Kiss and J. Feigon (2007). Structural and functional characterization of human telomerase RNA processing and cajal body localization signals. Mol Cell 27(6): 869-881.

Thumati, N. R., X. L. Zeng, H. H. Au, C. J. Jang, E. Jan and J. M. Wong (2013). Severity of X-linked dyskeratosis congenita (DKCX) cellular defects is not directly related to dyskerin (DKC1) activity in ribosomal RNA biogenesis or mRNA translation. Hum Mutat 34(12): 1698-1707.

Tomlinson, R. L., T. D. Ziegler, T. Supakorndej, R. M. Terns and M. P. Terns (2006). Cell cycle-regulated trafficking of human telomerase to telomeres. Mol Biol Cell 17(2): 955-965.

Trahan, C., C. Martel and F. Dragon (2010). Effects of dyskeratosis congenita mutations in dyskerin, NHP2 and NOP10 on assembly of H/ACA pre-RNPs. Hum Mol Genet 19(5): 825-836.

Tseng, C. K., H. F. Wang, A. M. Burns, M. R. Schroeder, M. Gaspari and P. Baumann (2015). Human Telomerase RNA Processing and Quality Control. Cell Rep 13(10): 2232-2243.

Tseng, C. K., H. F. Wang, M. R. Schroeder and P. Baumann (2018). The H/ACA complex disrupts triplex in hTR precursor to permit processing by RRP6 and PARN. Nat Commun 9(1): 5430.

Venteicher, A. S., E. B. Abreu, Z. Meng, K. E. McCann, R. M. Terns, T. D. Veenstra, M. P. Terns and S. E. Artandi (2009). A human telomerase holoenzyme protein required for Cajal body localization and telomere synthesis. Science 323(5914): 644-648.

Venteicher, A. S., Z. Meng, P. J. Mason, T. D. Veenstra and S. E. Artandi (2008). Identification of ATPases pontin and reptin as telomerase components essential for holoenzyme assembly. Cell 132(6): 945-957.

Wegman-Ostrosky, T. and S. A. Savage (2017). The genomics of inherited bone marrow failure: from mechanism to the clinic. Br J Haematol 177(4): 526-542.

Wong, J. M. and K. Collins (2006). Telomerase RNA level limits telomere maintenance in X-linked dyskeratosis congenita. Genes Dev 20(20): 2848-2858.

Wong, J. M., M. J. Kyasa, L. Hutchins and K. Collins (2004). Telomerase RNA deficiency in peripheral blood mononuclear cells in X-linked dyskeratosis congenita. Hum Genet 115(5): 448-455.

Yi, X., V. M. Tesmer, I. Savre-Train, J. W. Shay and W. E. Wright (1999). Both transcriptional and posttranscriptional mechanisms regulate human telomerase template RNA levels. Mol Cell Biol 19(6): 3989-3997.

Yu, Y. T. and U. T. Meier (2014). RNA-guided isomerization of uridine to pseudouridine--pseudouridylation. RNA Biol 11(12): 1483-1494.

Zeng, X. L., N. R. Thumati, H. B. Fleisig, K. R. Hukezalie, S. A. Savage, N. Giri, B. P. Alter and J. M. Wong (2012). The accumulation and not the specific activity of telomerase ribonucleoprotein determines telomere maintenance deficiency in X-linked dyskeratosis congenita. Hum Mol Genet 21(4): 721-729.

Chapter 3 – SUMOylation- and GAR1-dependent regulation of dyskerin nuclear and subnuclear localization

3.1 Preface

The characterization of the X-DC-implicated residues K39 and K43 presented in chapter 2 stemmed from a foundational study in our lab which demonstrated a role for SUMOylation in regulating dyskerin function. In this previous study, substituting either K39 or K43 to arginine led to a reduction of SUMOylated dyskerin in cells, impaired hTR accumulation and telomerase activity, and accelerated telomere shortening. Our lab pursued dyskerin SUMOylation as an intriguing and promising means of understanding fundamental regulation of dyskerin, and this further work on dyskerin SUMOylation is presented in chapter 3. Importantly, while our results in chapter 2 demonstrate that these two X-DC-implicated SUMOylation sites do not regulate dyskerin localization, through literature analyses of proteome-wide SUMOylation targets identified by mass spectrometry we found that dyskerin contains a multitude of SUMOylation sites, several of which are found in the C-terminal nuclear/nucleolar localization sequence (N/NoLS). The work presented in chapter 3 demonstrates regulatory roles for SUMOylation in both nuclear and nucleolar localization of dyskerin and for the first time demonstrates a tie between dyskerin-GAR1 interactions, SUMOylation, and nucleolar localization.

Manuscript in preparation for submission (2020)

SUMOylation- and GAR1-dependent regulation of dyskerin nuclear and subnuclear localization

3.2

MacNeil, D.E.[1,2], Lambert-Lanteigne, P.[2], McManus, F.[3], Bonneil, E.[3], Thibault, P.[3], & Autexier, C.[1,2,*]

[1]Jewish General Hospital of McGill University, Lady Davis Institute, Montreal, Quebec H3T 1E2, Canada; [2]Department of Anatomy and Cell Biology, McGill University, Montreal, Quebec H3A 0C7, Canada; and [3]Université de Montréal, Montréal, QC, Canada

*Address correspondence to Chantal Autexier, chantal.autexier@mcgill.ca

3.3 Abstract

SUMOylation is a transient posttranslational modification that involves the covalent attachment of small ubiquitin-like modifier (SUMO) proteins to lysine residues of target proteins through an enzymatic cascade resembling ubiquitination. SUMOylation targets a wide variety of proteins, including numerous RNA-binding proteins, and most identified targets reported to date localize to the nucleus. Four SUMOylation sites were previously identified in the C-terminal Nuclear/Nucleolar Localization Signal (N/NoLS) of dyskerin, a telomerase-associated protein and H/ACA RNP complex component, by mass spectrometry, each located within one of two lysine-rich clusters (K467-K480, and K498-K507). A C-terminal truncation variant of dyskerin lacking most of the C-terminal N/NoLS and both lysine-rich clusters (K446X) has been previously reported to display impaired nuclear localization. We confirmed that this variant has nuclear localization defects by observed accumulation in the cytoplasm through immunofluorescence and fractionation analyses, and found that this variant represents an under-SUMOylated variant of dyskerin compared to wildtype dyskerin. We demonstrated that mimicking constitutive SUMOylation of dyskerin using a SUMO3-fusion construct can drive nuclear accumulation of the K446X variant, and that the SUMO site K467 in this N/NoLS is particularly important for the subnuclear localization of dyskerin to the nucleolus in a mature H/ACA complex assembly- and SUMO-dependent manner. We also characterize a novel SUMO-interacting motif (SIM) in the mature H/ACA complex component GAR1 that mediates the interaction between dyskerin and GAR1. These data indicate a role for dyskerin SUMOylation in the C-terminal N/NoLS in regulating the nuclear and subnuclear localization of dyskerin, which is essential for dyskerin function as both a telomerase-associated protein and as an H/ACA ribonucleoprotein involved in rRNA and snRNA biogenesis.

3.4 Introduction

The H/ACA ribonucleoprotein (RNP) complex is responsible for pseudouridine synthesis at specific bases in ribosomal (r)RNA and small nuclear (sn)RNA in subnuclear compartments, specifically the nucleolus and Cajal bodies, respectively (Balakin, Smith *et al.* 1996, Ganot, Bortolin *et al.* 1997, Ganot, Caizergues-Ferrer *et al.* 1997, Ni, Tien *et al.* 1997, Darzacq, Jady *et al.* 2002). The protein components of this complex at maturity are dyskerin (Jiang, Middleton *et al.* 1993, Meier and Blobel 1994, Heiss, Knight *et al.* 1998), NOP10, NHP2 (Henras, Henry *et*

al. 1998), and GAR1 (Girard, Lehtonen *et al.* 1992, Balakin, Smith *et al.* 1996). The mature H/ACA complex assembles with noncoding (nc)RNA members of the H/ACA family, such as small nucleolar (sno)RNAs and small Cajal body specific (sca)RNAs that provide target pseudouridine synthesis specificity to dyskerin, the pseudouridine synthase of the H/ACA complex. The H/ACA motif is also a conserved biogenesis domain in telomerase RNAs of metazoans (Podlevsky and Chen 2016), including the human telomerase RNA (hTR) which relies on the H/ACA complex proteins for stability, processing, and function (Mitchell, Cheng *et al.* 1999, Jady, Bertrand *et al.* 2004, Tseng, Wang *et al.* 2018, MacNeil, Lambert-Lanteigne *et al.* 2019, Roake, Chen *et al.* 2019).

While hTR has no known target for guiding pseudouridine synthesis by dyskerin, the importance of the H/ACA complex in hTR biogenesis is demonstrated by mutations causing the premature aging disease and telomere syndrome dyskeratosis congenita (DC), with reported patient mutations in the genes encoding each protein component of the mature complex, excluding GAR1, as well as in the H/ACA biogenesis domain of hTR itself (all reported DC mutations are compiled in the Telomerase Disease Database (Podlevsky, Bley *et al.* 2008)). Patients with DC have characteristic accelerated telomere shortening which leads to pathology in proliferative tissues, and results in bone marrow failure as the leading cause of mortality in this disease (Connor, Gatherer *et al.* 1986, Drachtman and Alter 1992, Arngrimsson, Dokal *et al.* 1993, Dokal 1996). In particular, DC patients with mutations disrupting the H/ACA complex components or H/ACA domain of hTR have reduced hTR accumulation which drives telomerase activity defects and accelerated telomere shortening (Mitchell, Cheng *et al.* 1999). There have also been several reports of DC mutations in the H/ACA complex components affecting H/ACA RNA biogenesis beyond hTR (Bellodi, McMahon *et al.* 2013, Benyelles, O'Donohue *et al.* 2020), and the essentiality of dyskerin and the H/ACA complex is likely due to its importance in rRNA and snRNA posttranscriptional modification. The *dkc1* gene encoding dyskerin is a core essential gene that is highly conserved, with phylogenetic roots in bacteria and archaea. Knockout of this gene is lethal in fungi (Jiang, Middleton *et al.* 1993), flies (Phillips, Billin *et al.* 1998, Giordano, Peluso *et al.* 1999), mice (He, Navarrete *et al.* 2002), and human cells (Hart, Chandrashekhar *et al.* 2015, Bertomeu, Coulombe-Huntington *et al.* 2018). Though X-linked dyskeratosis congenita (X-DC) is a commonly inherited form of the disease caused by mutations

in *dkc1*, a complete deletion or loss of the gene has never been reported in X-DC, further demonstrating the essentiality of dyskerin.

The compartmentalization of dyskerin and the H/ACA complex is an important though incompletely understood aspect of H/ACA RNP function. Dyskerin has been reported to rely on two nuclear/nucleolar localization sequences (N/NoLSs) for complete nuclear import and retention, as well as for nucleolar accumulation (Heiss, Girod *et al.* 1999). With the exception of GAR1, the H/ACA RNP components are present at sites of transcription of H/ACA RNAs in the nucleoplasm, along with the assembly factor NAF1 which is replaced by GAR1 upon complex maturation (Ballarino, Morlando *et al.* 2005, Yang, Hoareau *et al.* 2005, Darzacq, Kittur *et al.* 2006). Mature H/ACA complexes localize in the dense fibrillar component (DFC) of the nucleolus and in the Cajal bodies (Meier and Blobel 1994) where they guide posttranscriptional modification of rRNA and snRNA, respectively, dependent upon the H/ACA RNA with which the complex is assembled. The stepwise assembly of H/ACA RNPs has been proposed to play a role in localization of the complex to its sites of function (Darzacq, Kittur *et al.* 2006). Although the mechanism governing subnuclear compartmentalization of the mature H/ACA complex remains incompletely characterized, it is likely to rely on regulation of miscibility with these discrete membrane-free regions of the nucleus. This has been recently demonstrated for other nucleolar proteins resident in the DFC such as fibrillarin, which relies on an intrinsically disordered glycine and arginine rich (GAR) domain and RNA interactions for miscibility with the DFC (Feric, Vaidya *et al.* 2016, Yao, Xu *et al.* 2019).

The posttranslational modification SUMOylation has been demonstrated to affect nuclear and subnuclear localization of a number of protein targets, including resident proteins of the nucleolus (Pichler and Melchior 2002, Melchior, Schergaut *et al.* 2003, Heun 2007). This modification involves conjugation of small ubiquitin-like modifier (SUMO) protein to lysine residues of target proteins in an E1 activating (SAE1/SAE2) and E2 conjugating (Ubc9) enzyme-dependent manner, often with the help of one of many E3 SUMO ligases, and promoted by a SUMOylation consensus motif in target proteins (ψKXE/D – where ψ is a hydrophobic residue and X is any residue) (Varejao, Lascorz *et al.* 2019). While SUMOylation has been reported to regulate various functions of target proteins, a key aspect of SUMOylation is mediating protein-protein interactions between SUMO targets and proteins containing SUMO-interacting motifs (SIMs) which non-covalently bind SUMO (Song, Durrin *et al.* 2004, Song, Zhang *et al.* 2005,

Hecker, Rabiller *et al.* 2006). SUMOylation is a reversible modification, with several identified SUMO-specific proteases cleaving immediately after the C-terminal diglycine repeat in SUMO moieties, and therefore being responsible both for maturation of free SUMO and for removal of SUMO from target lysines (Li and Hochstrasser 1999, Gong, Millas *et al.* 2000, Li and Hochstrasser 2000, Takahashi, Mizoi *et al.* 2000). Typically, at steady state, only a small proportion of a SUMO target is conjugated to SUMO moieties. We previously demonstrated that dyskerin is a SUMOylation target of SUMO1 and SUMO2/3 isoforms, and that substituting either of two N-terminal X-DC-implicated lysine residues to arginine reduces the proportion of SUMOylated dyskerin in cells, leading to reductions in hTR, reduced telomerase activity, and accelerated telomere shortening (Brault, Lauzon *et al.* 2013). We have since shown that these two X-DC residues impact the dyskerin-hTR interaction, though the SUMO dependence of this interaction was not investigated (MacNeil, Lambert-Lanteigne *et al.* 2019).

Here we further investigate a regulatory role for SUMOylation of dyskerin. Using mutational analyses and SUMO-fusion constructs, we demonstrate that the C-terminal N/NoLS of dyskerin is a SUMO3 target, and that mimicking constitutive SUMOylation of a cytoplasmic truncation variant of dyskerin is sufficient to drive nuclear accumulation but not proper subnuclear localization of dyskerin. We also demonstrate that the nucleolar localization of dyskerin is mediated by the SUMO3 site K467 in this C-terminal N/NoLS, and that K467 is required for the interaction between dyskerin and GAR1 in a SUMO3-dependent manner, and novelly identify a SIM in GAR1 which is important for this interaction.

3.5 Materials and Methods

Plasmids, Cell Culture, and Transfections

The plasmid pcDNA3.1-FLAG-dyskerinWT from the lab of Dr. François Dragon was used to generate point mutations or truncations via site directed mutagenesis, as previously described (Brault, Lauzon *et al.* 2013, MacNeil, Lambert-Lanteigne *et al.* 2019). Specifically, primers (Supplemental Table 3.1) were designed to generate K467R, K468R, K467/468R, A481X, and K446X. For expression of 3xFLAG-GAR1 in human cells, the pcDNA3.1 3xF-GAR1 plasmid was purchased from Addgene (#126873), and the predicted SIM 70-VVLLG-74 was substituted to 70-AAAAA-74 by site directed mutagenesis (primers listed in Supplemental Table 3.1). For generation of HA-tagged GAR1, GAR1 was PCR amplified from pcDNA3.1

3xFLAG-GAR1 with a sequence encoding the HA-tag incorporated into the forward amplification primer. The PCR fragment encoding HA-GAR1 was cloned into pcDNA3.1(+)-Hygro between NheI and BamHI restriction sites. The construct pcDNA3.1-6xHis-SUMO3 was obtained from Dr. Frédérick Antoine Mallette (Université de Montréal). The plasmid pET30-His-dyskerin was a gift from Dr. Lea Harrington (Université de Montréal) (Gardano, Holland *et al.* 2012), and was used to purify recombinant human dyskerin. All constructs underwent Sanger DNA sequencing at Génome Québec CES.

Human embryonic kidney (HEK293) cells were maintained in Dulbecco's Modification Eagle's Medium DMEM (Wisent) supplemented with 10% fetal bovine serum FBS (Wisent), and Antibiotic-Antimycotic (Gibco), at 37˚C 5% CO2. Polyclonal FLAG-dyskerin stable cells were maintained under selective pressure in G418 (750µg/ml). Transfection of pcDNA3.1 (empty vector), pcDNA3.1-FLAG-dyskerin constructs, pcDNA3.1-6xHis-SUMO3, pcDNA3.1 3xFLAG-GAR1, and/or pcDNA3.1 HA-GAR1 was performed using Lipofectamine 2000 Transfection Reagent (Invitrogen) according to the reagent protocol. Prior to transfection, media was changed to DMEM with 10% FBS and lacking Antibiotic-Antimycotic, and 5 hours after transfection the media was replaced with DMEM containing both FBS and Antibiotic-Antimycotic.

SUMO-interaction Motif Prediction

The GPS-SUMO 4.0 prediction tool was used to predict possible SUMO-interacting motifs in GAR1. The coding amino acid sequence for isoform 1 of GAR1 was obtained in FASTA format through Uniprot (identifier Q9NY12-1). The SUMO Interaction Threshold was set to Medium. The SUMO Interaction prediction score obtained for residues 70-VVLLG-74 was 31.605, with a cutoff of 29.92 and P-value 0.112.

Purification of Recombinant Protein and *in vitro* SUMOylation and Mass Spectrometry

Human dyskerin was expressed using the BL21-RIL E.coli strain and purified as previously described (Gardano, Holland *et al.* 2012). *In vitro* SUMOylation of recombinant dyskerin purified from E.coli was performed using recombinant His-SUMO3 in the presence of ATP as previously described (McManus, Altamirano *et al.* 2016) and analyzed on SDS-PAGE to confirm the presence of high molecular weight SUMOylated dyskerin. The *in vitro* SUMOylation assays were subjected to western analysis using an antibody against SUMO2/3. A

large scale SUMOylation reaction with SUMO3 was performed, and subsequently subjected to Ni-NTA purification and mass spectrometry, as previously described (Lamoliatte, Caron *et al.* 2014).

Nickel Affinity Purification of SUMOylated FLAG-dyskerin

For analysis of SUMOylated FLAG-dyskerin by immunoblotting, HEK293 cells expressing 6xHis-SUMO3 and/or FLAG-dyskerin (wildtype, K446X, or SUMO3-K446X) were lysed under denaturing conditions. Briefly, cells were washed with 1XPBS and collected by scraping. One fifth of cells per condition were kept for input and lysed in 2xLaemmli followed by boiling. The remainder of the cell pellet was lysed in 6M GuHCl buffer (10mM Tris-HCl pH8, 6M GuHCl, 10mM imidazole, 0.1M NaH2PO4, adjusted to pH8 with NaOH) at room temperature by passage through a 21G1¼ syringe (5x) followed by passage through an insulin syringe (3x). Cell lysate was cleared by centrifugation at 13000rpm for 20min at 4˚C. The supernatant was incubated with NiNTA resin (pre-washed 2x with 1XPBS and 1x with GuHCl buffer) on a rotator at room temperature overnight. Resin was then washed 1x with GuHCl buffer, 1x with wash buffer 1 (10mM Tris-HCl pH8, 8M urea, 10mM imidazole, 0.1M Na H2PO4, adjusted to pH8 with NaOH), and 2x with wash buffer 2 (10mM Tris-HCl pH8, 8M urea, 10mM imidazole, 0.1M NaH2PO4, 0.1% v/v Triton X-100, adjusted to pH6.3 with NaOH). For elution, resin was incubated in elution buffer (50mM NaH2PO4, 300mM NaCl, 500mM imidazole, adjusted to pH8) for 3h on a rotator at 4˚C. The eluate was collected by centrifugation and resin discarded.

Immunofluorescence

To assess localization of FLAG-dyskerin to the nucleolus, HEK293 cells expressing FLAG-dyskerin constructs were fixed with 4% formaldehyde-PBS for 10 minutes at room temperature. The fixing solution was removed, and coverslips were briefly rinsed with PBS, followed by permeabilization of cells with 0.1% Triton X-100-PBS for 5 minutes at 4˚C. Permeabilized cells were then washed with PBS before blocking in 5% BSA-PBS for 1 hour at room temperature. Cells were probed for FLAG-dyskerin with rabbit anti-FLAG (Sigma-Aldrich F7425, 1:500) or rabbit anti-dyskerin (Proteintech 25420-1-AP, 1:25) in PBG (1% cold fish water gelatin, 0.5% bovine serum albumin (BSA), in PBS) overnight at 4˚C in a humidity chamber. In the case of assessing localization of exogenous FLAG-tagged dyskerin, this was

followed by probing with mouse anti-fibrillarin (monoclonal antibody 72B9 obtained from Dr. Kenneth Michael Pollard, 1:30) as a nucleolar marker, in PBG at 37˚C for 1 hour. Coverslips were washed with PBS and immunostained in PBG with secondary antibodies conjugated to fluorescein isothiocyanate (FITC) (donkey anti-mouse IgG; Jackson ImmunoResearch Lab, Inc., 1:125) or Cy3 (donkey anti-rabbit; Jackson ImmunoResearch Lab, Inc., 1:125). Coverslips were washed with PBS and mounted in Vectashield with DAPI (Vector Laboratories). Cells with FLAG-dyskerin signal were manually scored based on localization phenotype as a percentage of the number of cells with FLAG signal detected, and >150 cells were counted for scoring of localization of each FLAG-tagged dyskerin construct. This was performed in at least two independent experimental replicates for each variant quantified, and localization profiles were pooled to generate the quantification in Figure 2B. Images were captured using an Axio Imager M1 (63X; Carl Zeiss, Jena, Germany). Nucleolar localization was determined by co-localization with fibrillarin clusters, nucleoplasmic localization was determined by co-localization with DAPI, and cytoplasmic localization was determined by concentrated signal outside of and surrounding DAPI.

Immunoprecipitation

Protein-protein interactions were assessed by immunoprecipitating FLAG-dyskerin wildtype or N/NoLS variants from HEK293 cells and immunoblotting for endogenous dyskerin-interacting proteins; by immunoprecipitating 3xFLAG-GAR1 wildtype or 5A and immunoblotting for endogenous dyskerin; or by immunoprecipitating FLAG-dyskerin and assessing interaction with HA-GAR1 by immunoblotting. Monoclonal M2 mouse anti-FLAG antibody (Sigma-Aldrich F3165) and Protein G Sepharose (GE Healthcare) pre-blocked in 1% BSA-PBS were used to immunoprecipitate (IP) FLAG-tagged and 3xFLAG-tagged proteins. The protocol used to assess protein-protein interactions was the same used to analyze the interaction between FLAG-dyskerin and hTR, and was modified based on a protocol that has been previously described for the hTR-interacting protein DHX36 (Booy, Meier *et al.* 2012), as well as used for FLAG-tagged dyskerin (MacNeil, Lambert-Lanteigne *et al.* 2019). Briefly, cells were first lysed in low salt buffer (25mM HEPES-KCl pH7.9, 5mM KCl, 0.5mM MgCl2, 0.5% NP-40, 1X protease inhibitor cocktail from Roche, 20mM N-ethylmaleimide, and 4U/µl RNAseOut) for 10min on ice. Lysates were cleared by centrifugation at 5000rpm for 5min at 4˚C, supernatants were kept on ice, and pellets underwent a second lysis in high salt buffer (25mM

HEPES-KCl pH7.9, 350mM NaCl, 10% w/v sucrose, 0.01% NP-40, 1X protease inhibitor cocktail from Roche, 20mM N-ethylmaleimide, and 4U/µl RNAseOut) with 30sec vortex followed by 30min on a rotator at 4˚C. Both low salt and high salt lysates were then cleared by centrifugation at 13000rpm for 30min at 4˚C, supernatants were pooled, and total lysate was pre-cleared at 4˚C on a rotator for 30min using Protein G Sepharose that was pre-washed with 1XPBS. Bradford analysis was used to calculate total protein concentration prior to IP. Lysates were incubated with anti-FLAG antibody for 2h at 4˚C on a rotator before pre-blocked Protein G Sepharose was added, followed by an additional 1h incubation at 4˚C on a rotator. IPs were washed 4x with 1ml of modified RIPA buffer (50mM Tris-HCl pH8, 150mM NaCl, 10mM MgCl2, 1% NP-40, 0.5% sodium deoxycholate, 1mM PMSF, 0.1X protease inhibitor cocktail from Rocher, and 20mM N-ethylmaleimide). For protein-protein interactions, elution from Protein G Sepharose was performed with Laemmli buffer and boiling. For protein-RNA interactions, elution was performed with TRIzol reagent (Invitrogen), followed by chloroform extraction and reverse transcription. Inputs (10% of lysate volume used for IP) were collected after pre-clearing with Protein G Sepharose and prior to IP, and treated with either Laemmli buffer and boiled, or with TRIzol reagent.

Fractionation

Two fractionation methods were tested to assess localization of endogenous dyskerin and FLAG-tagged dyskerin wildtype, K467R, and K446X. Both methods were carried out using HEK293 cells that were transiently transfected 24h prior to harvesting with trypsin. Harvested cell pellets were washed with 1XPBS. Cell pellets then either underwent a two-step fractionation protocol to separate the cytoplasmic fraction from the nuclear fraction, based on a previously described protocol but using RIPA buffer to lyse nuclei (Wen, Wu et al. 2017), or a multi-step fractionation using sucrose cushions to isolate nucleoli as previously described (Hacot, Coute et al. 2010). Each protocol was performed once, and experimental replicates are needed.

Briefly, for cytoplasmic/nuclear fractionation: cell pellets were lysed in low salt Cytoplasmic Lysis Buffer (10mM HEPES-KOH pH8, 10mM KCl, 1.5mM $MgCl_2$, 0.5% v/v IGEPAL, 1X protease inhibitor cocktail from Roche), by vortexing on the highest setting for 15 seconds and incubating on ice for 10min, followed by a second highest setting vortex for 5 seconds. Lysate were centrifuged at 13000rpm for 5min at 4˚C. Supernatants were kept as cytoplasmic fractions, and pellets were washed 3x with ice cold 1XPBS. Nuclear pellets were

lysed in RIPA buffer (150mM NaCl, 0.5% sodium deoxycholate, 0.1% SDS, 100mM Tris pH8, 1% IGEPAL, 1X protease inhibitor cocktail from Roche) by vortexing on the highest setting for 15 seconds, followed by sonication (4-6 pulses per sample). Samples were kept on ice at all times. Nuclear lysates were clarified by centrifugation at 13000rpm for 10min at 4˚C. Supernatants were kept as nuclear fractions. Samples were stored at -80˚C prior to analysis by immunoblotting. Bradford analysis was used to determine total protein concentration of each fraction.

RNA Extraction and RT-qPCR

RNA was extracted using TRIzol reagent (Invitrogen), according to the reagent protocol. Reverse transcription was performed with SuperScript II Reverse Transcriptase (Invitrogen) according to the user protocol, with hexameric random primers. PerfeCTa SYBR Green FastMix with Low ROX (Quanta) was used for all qPCR analyses, in a 7500FAST real-time PCR system (ABI) as previously described (Brault, Lauzon *et al.* 2013). The comparative $\Delta\Delta C_T$ method was used to compare RNA enrichment between samples. For analysis of protein-RNA interactions, 5 µl of RNA from input and 5 µl of RNA from IP fractions were reverse transcribed into cDNA and subjected to qPCR using specific primers for target RNAs (Supplemental Table 3.1). The $\Delta\Delta C_T$ was calculated between the mean C_T of the IP and the mean C_T of the input for each sample.

Statistical Analyses

All statistical analyses were performed using GraphPad Prism 7. Unpaired t-tests ($p < 0.01$) were used to compare RNA enrichment when assessing interaction between FLAG-dyskerin and hTR. The enrichment of hTR in each N/NoLS variant IP fraction was compared to the enrichment of hTR in the FLAG-dyskerin wildtype IP fraction. Each experiment was performed in triplicate, and error bars represent the standard error of the mean between experimental replicates.

3.6 Results

The C-terminal nuclear/nucleolar localization sequence of dyskerin is a SUMOylation target

Many proteome-wide studies performed in human cell lines have identified dyskerin as a target of SUMOylation, both by SUMO1 and SUMO2/3 (Becker, Barysch *et al.* 2013, Hendriks,

D'Souza *et al.* 2014, Impens, Radoshevich *et al.* 2014, Hendriks, Treffers *et al.* 2015, Xiao, Chang *et al.* 2015, Hendriks, Lyon *et al.* 2017, Lamoliatte, McManus *et al.* 2017, Hendriks, Lyon *et al.* 2018, El-Asmi, McManus *et al.* 2020). Compiling the results of these studies, it is evident that dyskerin is a highly decorated target for SUMOylation, with 24 sites identified by mass spectrometry (MS) analyses (Figure 3.1A). For the purpose of this study, we focused on four SUMO2/3 sites in particular due to the placement of these lysines in the C-terminal N/NoLS (K467, K468, K498, and K507), which was previously reported to mediate efficient localization of dyskerin to the nucleus alone and in combination with an N-terminal N/NoLS (Heiss, Girod *et al.* 1999). Prior or concomitantly to the early proteome-wide studies, we used recombinant wildtype dyskerin purified from *E. coli* and recombinant His-SUMO3, to perform an *in vitro* SUMOylation assay followed by Ni-NTA purification (Supplemental Figure 3.1) and MS (data not shown[1]), confirming one of these four sites as SUMO3 targets. Importantly, truncation of the C-terminal N/NoLS by replacing K446 with a stop codon (X), and thus removal of all four SUMO3 sites and the lysine-rich (K-rich) clusters in which they are situated, substantially reduces the amount of SUMOylated dyskerin detectable by immunoblotting following Ni-NTA purification from HEK293 cells expressing FLAG-tagged dyskerin and 6xHis-SUMO3 (Figure 3.1B, wildtype vs. K446X). Indeed, while FLAG-tagged wildtype dyskerin co-localizes with the nucleolar marker fibrillarin in HEK293 cells assessed by immunofluorescence (IF), the FLAG-tagged K446X accumulates in the cytoplasm (Figure 3.1C, top and middle panels). Interestingly, mimicking constitutive SUMOylation of K446X by fusing a SUMO3 moiety to the N-terminus of this dyskerin variant allows for detection of high molecular weight products by Ni-NTA from HEK293 cells co-expressing FLAG-tagged SUMO3-K446X and 6xHis-SUMO3, indicating that this fusion is highly SUMOylated (Figure 3.1B). This SUMO3-fusion is also sufficient to drive the K446X truncation variant into the nucleus (Figure 3.1C, bottom panel). However, the SUMO3-fusion variant remains excluded from the nucleolar compartment, suggesting that mimicking permanent SUMOylation of dyskerin disrupts proper subnuclear localization. This hypothesis is supported by our observation that fusion of SUMO3 to either the N-terminus or the C-terminus of FLAG-tagged wildtype dyskerin also leads to disrupted subnuclear localization, though the C-terminal SUMO3 fusion displays more frequent co-localization with fibrillarin in

[1] While these residues have been confirmed by analysis of MS spectra, our collaborators do not currently have access to these spectra due to COVID-19 lab shutdown.

the nucleolar compartment than the N-terminal SUMO3 fusion (Supplemental Figure 3.2A, and Supplemental Figure 3.6). These data suggest that the C-terminal N/NoLS of dyskerin regulates nuclear localization in a SUMO3-dependent manner, though the reversibility of SUMOylation after nuclear import is likely important for mediating proper subnuclear trafficking of dyskerin. This would be consistent with a previous proposal that balanced SUMOylation levels may be required for nucleolar regulation (Zhao 2018).

Figure 3.1: Residues in the C-terminal nuclear/nucleolar localization sequence of dyskerin are SUMO3 targets that govern nuclear accumulation. a. A linear schematic of human dyskerin domains. The amino acid range corresponding to the predicted C-terminal nuclear/nucleolar localization sequence (N/NoLS) (438-514) is denoted below the schematic, indicating the MS-identified SUMO3 sites in this region (K467, K468, K498, and K507) with solid black circles, and the two lysine (K)-rich clusters (K467-K480, and K498-K507) are underlined. MS-identified SUMO3 sites reported in proteome-wide studies cited in the text are indicated by solid black circles above the schematic. b. FLAG-dyskerin (wildtype WT and dyskerin truncation variant K446X without or with N-terminal SUMO3 fusion) and 6xHis-SUMO3 were expressed in HEK293 cells. His-SUMO3 conjugates were purified using Ni-NTA agarose beads following lysis under denaturing conditions, and SUMOylated FLAG-dyskerin was assessed in the elution by immunoblotting with an anti-FLAG antibody. A fraction of each HEK293 cell pellet used for purification was kept prior to lysis (Input) to check expression of FLAG-dyskerin and His-SUMO3 by immunoblotting. The K446X truncation runs at the expected lower molecular weight than WT dyskerin, while SUMO3-K446X runs at the expected higher molecular weight than WT due to the SUMO3 fusion. FLAG-dyskerin is indicated by arrows, while asterisks indicate non-specific antibody signal. The bracket indicates poly-SUMOylated SUMO3-K446X species. c. Representative images of the co-localization of FLAG-dyskerin (wildtype WT and dyskerin truncation variant K446X without or with N-terminal SUMO3 fusion – Cy3 shown in red) with nucleolar marker fibrillarin (FITC shown in green), as observed by indirect immunofluorescence. Nucleoplasmic foci formed by N-terminal SUMO3 fusion K446X dyskerin truncation (Cy3, in red) that co-localize with fibrillarin (FITC, in green) are indicated by white arrowheads. The nucleus is indicated by DAPI staining of nuclear DNA (in blue), and scale bars indicate 10μm.

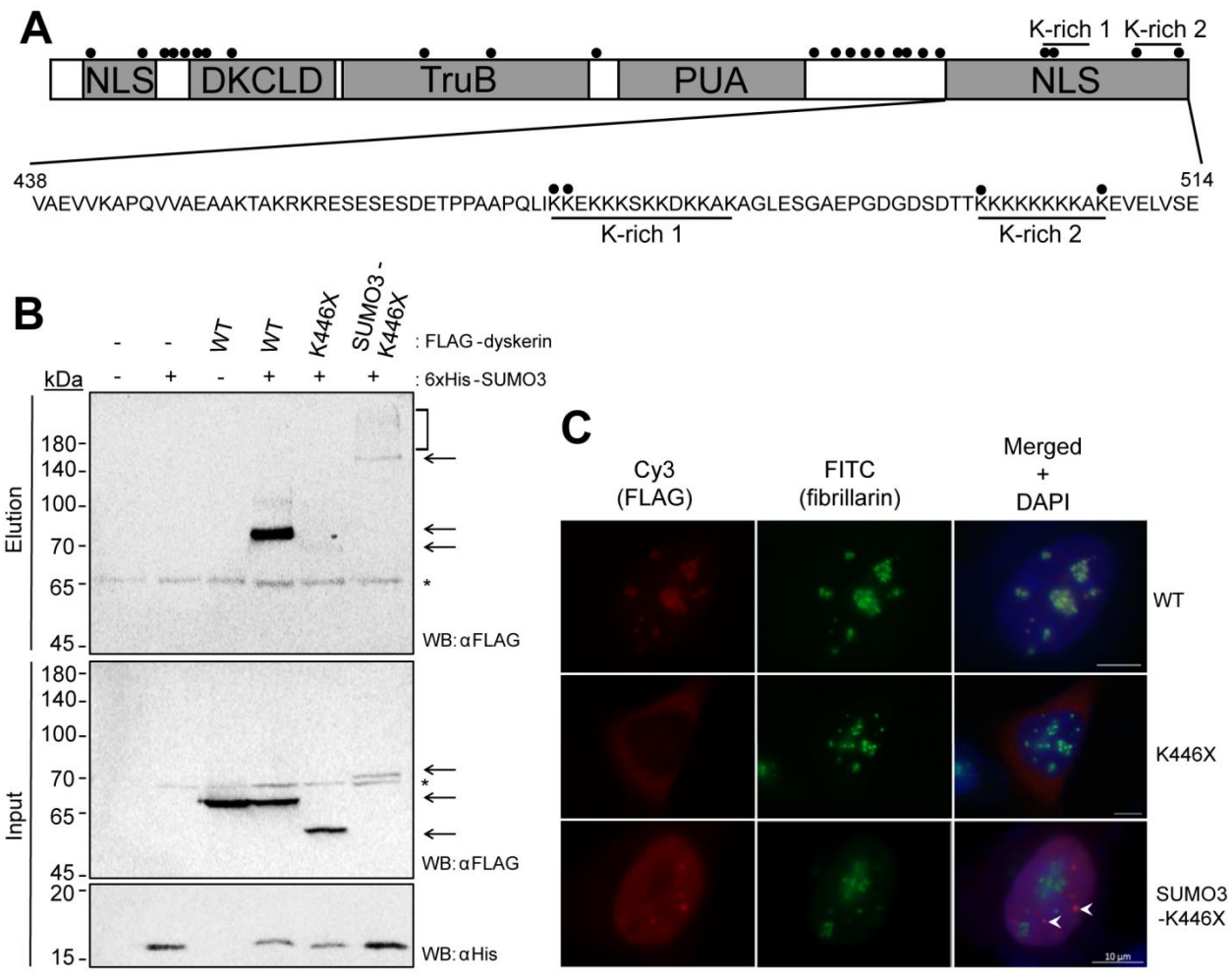
A
K-rich 1
K-rich 2
NLS
DKCLD
TruB
PUA
NLS
438
514
VAEVVKAPQVVAEAAKTAKRKRESESESDETPPAAPQLIKKEKKKSKKDKKAKAGLESGAEPGDGDSDTTKKKKKKKKKAKEVELVSE
K-rich 1
K-rich 2
B
WT
WT
K446X
SUMO3 - K446X
: FLAG - dyskerin
kDa
: 6xHis - SUMO3
Elution
180
140
100
70
65
45
WB: αFLAG
Input
180
140
100
70
65
45
WB: αFLAG
20
15
WB: αHis
C
Cy3 (FLAG)
FITC (fibrillarin)
Merged + DAPI
WT
K446X
SUMO3 -K446X
10 µm

Dyskerin nuclear and subnuclear localization is mediated by SUMOylation

The C-terminal N/NoLS of dyskerin contains two K-rich clusters, each of which contains two MS-identified SUMO3 target sites (Figure 3.1A). To elucidate which of these four SUMO3-sites, if any, may be mediating localization of dyskerin, and to reduce potential compensation for a loss of a single SUMOylation site by SUMO conjugation to neighbouring lysine residues, a stop codon was introduced at A481 in the FLAG-dyskerin construct, thus removing the entire second K-rich cluster while leaving the first intact. In contrast to the K446X variant lacking both K-rich clusters, FLAG-tagged A481X efficiently localizes in the nucleus and the nucleolus, as observed by co-localization with fibrillarin assessed by IF (Figure 3.2A). This suggests that the second K-rich cluster, thus the SUMO3 sites within it are not critical regulators of dyskerin nuclear localization *per se*, and these data are consistent with previous localization analysis of a truncation variant at D493 (Heiss, Girod *et al.* 1999). However, full length FLAG-tagged dyskerin in which the SUMO3 site K467 in the first K-rich cluster is substituted to an arginine (K467R) displays an apparent nucleolar exclusion/nucleoplasmic accumulation phenotype when assessed by IF (Figure 3.2A). This is in contrast to the K468R variant which localizes comparably to wildtype dyskerin (Figure 3.2A). Substituting both of these lysines to arginine (K467/468R) leads to a localization phenotype similar to the single K467R substitution variant (Figure 3.2A). FLAG-positive cells were scored based on localization phenotype as a percentage of FLAG-positive cells counted, and localization of each FLAG-tagged dyskerin (wildtype or variant) was assessed from a minimum of two independent experimental replicates (Figure 3.2B). Importantly, while the major localization phenotype of the K446X truncation variant is cytoplasmic, FLAG-signal in cells expressing this variant was also observed in both the cytoplasm and nucleolar fraction concomitantly (Figure 3.2B, yellow bar). This is consistent with previous time course experiments demonstrating through microinjection of EGFP-tagged K446X into cells that this truncation impairs but does not entirely prevent nuclear and subnuclear localization of dyskerin (Heiss, Girod *et al.* 1999). While still able to localize within the nucleus and to the nucleolus, the truncation variant of dyskerin at A481, A481X, does display an increase in concomitant nucleoplasmic and nucleolar localization of dyskerin compared to wildtype, suggesting that this truncation modestly affects localization of dyskerin, albeit to a lesser extent than K446X or K467R (Figure 3.2B, blue bar). Indeed, K467R has a substantial reduction in nucleolar and corresponding increase in nucleoplasmic localization compared to wildtype

dyskerin, as assessed by exclusion from co-localization with fibrillarin signal, but co-localization with DAPI signal (Figure 3.2B, purple and black bars, respectively). In contrast, no substantial differences in localization were observed between K468R and wildtype (Figure 3.2B). The double substitution variant K467/468R does not differ in localization compared to the single K467R variant, and thus has a reduction in nucleolar and increase in nucleoplasmic localization compared to wildtype dyskerin (Figure 3.2B). As previously mentioned, fusing K446X to SUMO3 is sufficient to drive this truncation into the nucleus, but this fusion variant has reduced nucleolar localization compared to wildtype dyskerin (Figure 3.2B). However, SUMO3-fusion of dyskerin differs from K467R in nucleolar exclusion, as SUMO3-K446X and SUMO3-wildtype dyskerin form distinct puncta in the nucleoplasm while K467R localization in the nucleoplasm is diffuse (Figure 3.1C, Figure 3.2A, Supplemental Figure 3.2A,B). Some of these puncta may represent CB's given their occasional overlap with fibrillarin puncta outside of nucleolar clusters, but are most likely nucleoplasmic aggregates driven by the permanent nature of the SUMO3-fusion (Supplemental Figure 3.2B). Importantly, the FLAG-tag does not disrupt localization of wildtype dyskerin, as eGFP-tagged wildtype dyskerin (Supplemental Figure 3.3A) and endogenous dyskerin examined by IF (Supplemental Figure 3.3B) display comparable localization patterns to exogenously expressed FLAG-tagged wildtype dyskerin. The mislocalization patterns of K446X and K467R observed by IF are consistent with preliminary cellular fractionation experiments that confirm cytoplasmic and nucleolar localization of K446X and nucleolar exclusion of K467R (Supplemental Figure 3.4). Taken together, these data tell us that in addition to SUMO3 mediating nuclear localization of the K446X truncation of dyskerin, the SUMO3 site K467 plays an important regulatory role for the nucleolar localization of dyskerin.

Figure 3.2: Nuclear and subnuclear localization of dyskerin is mediated by SUMO3 sites in the C-terminal nuclear/nucleolar localization sequence. a. FLAG-dyskerin was transiently expressed in HEK293 cells, and localization was assessed in fixed cells by indirect immunofluorescence. Representative images of the most prevalent localization phenotype of FLAG-dyskerin (wildtype WT, dyskerin truncation variant A481X, and substitution variants K467R, K468R, and double K467/468R – Cy3 shown in red) and the nucleolar marker fibrillarin (FITC shown in green) are shown. The proportion of cells displaying the represented localization phenotype out of total FLAG-positive cells counted is indicated in the Cy3 column for each variant. Nucleolar localization is represented for WT and K468R, concomitant nucleoplasmic & nucleolar is represented by A481X, and nucleoplasmic localization is represented by K467R and K467/468R. The nucleus is indicated by DAPI staining of nuclear DNA (in blue), and scale bars indicate 10μm. b. Quantification of localization phenotype scoring for FLAG-dyskerin WT and localization variants as a percentage of FLAG-positive HEK293 cells is indicated for >150 cells counted per condition, compiled from at least two independent experimental replicates.

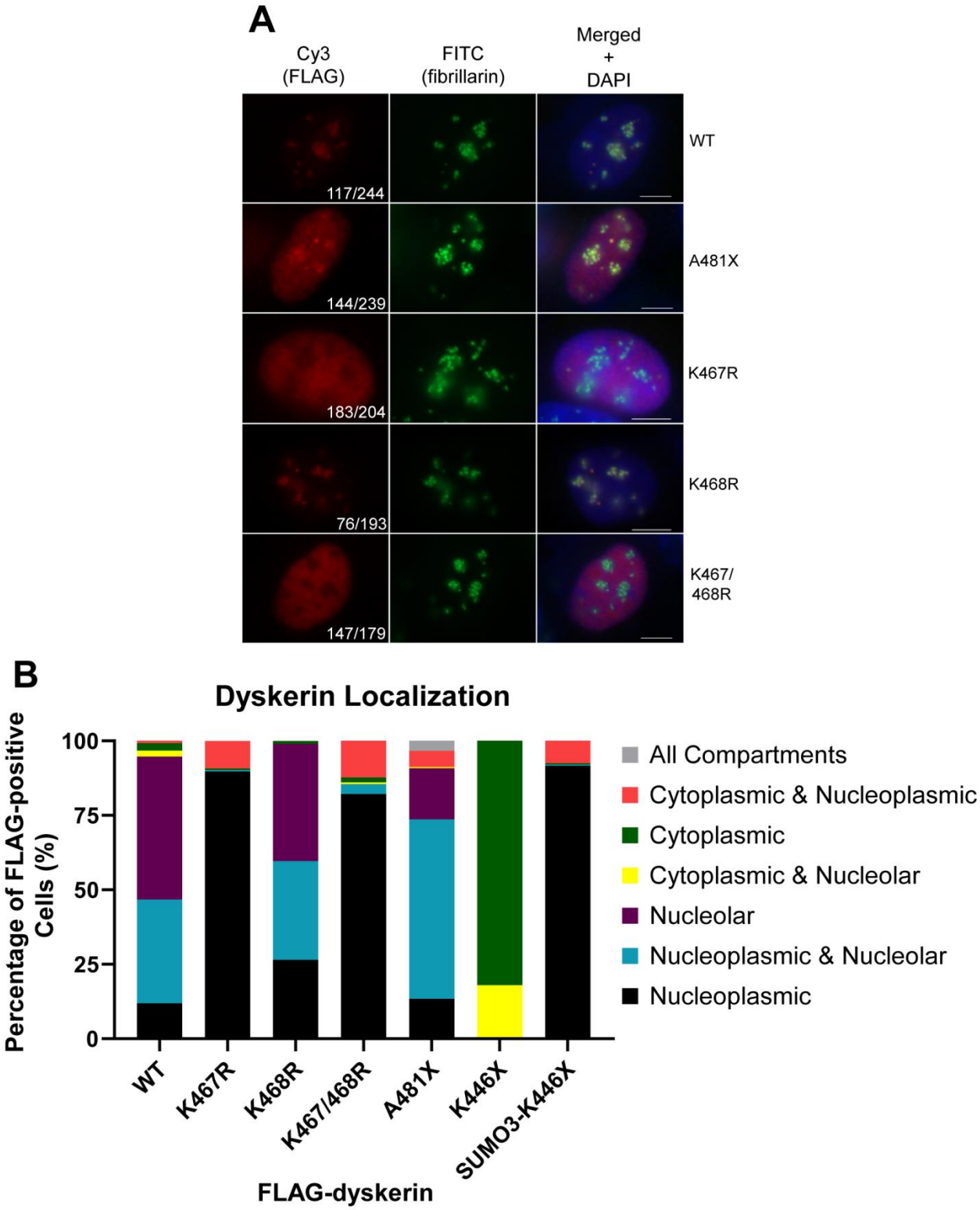
A
Cy3
(FLAG)
FITC
(fibrillarin)
Merged
+
DAPI
WT
A481X
K467R
K468R
K467/
468R
117/244
144/239
183/204
76/193
147/179
B
Dyskerin Localization
Percentage of FLAG-positive Cells (%)
100
75
50
25
0
All Compartments
Cytoplasmic & Nucleoplasmic
Cytoplasmic
Cytoplasmic & Nucleolar
Nucleolar
Nucleoplasmic & Nucleolar
Nucleoplasmic
WT
K467R
K468R
K467/468R
A481X
K446X
SUMO3-K446X
FLAG-dyskerin

Nuclear and subnuclear localization of dyskerin affects mature H/ACA RNP assembly

As a functional readout for H/ACA complex assembly and localization, co-immunoprecipitation (co-IP) of FLAG-tagged dyskerin and interacting components was performed from HEK293 cell lysate. Following FLAG-IP, interactions of FLAG-tagged dyskerin wildtype and N/NoLS variants were assessed by immunoblotting for endogenous H/ACA RNP assembly factors and components. Comparable to wildtype dyskerin, all FLAG-tagged N/NoLS variants were able to interact with the pre-H/ACA RNP component NAF1 and the pre- and mature H/ACA RNP components NOP10 and NHP2 (Figure 3.3A). Strikingly, the N/NoLS variants with nucleolar exclusion phenotypes (K467R and K467/468R) were unable to interact with the mature H/ACA RNP component GAR1 (Figure 3.3B). This was further confirmed by IP from HEK293 cells co-expressing FLAG-tagged dyskerin and exogenous HA-tagged GAR1, with an evident lack of interaction between FLAG-tagged K467R and HA-GAR1 (Supplemental Figure 3.5). Importantly, disruption of either nuclear or subnuclear localization of dyskerin leads to impaired hTR-dyskerin interaction as measured by qPCR following RNA extraction and reverse transcription from IP fractions; neither FLAG-tagged K467R nor K446X interact with hTR relative to wildtype dyskerin (Figure 3.3C). This is in contrast to the N/NoLS variants with little to no localization defects, K468R and A481X which do not display defective interactions with hTR relative to wildtype dyskerin (Figure 3.3C). These data indicate that proper localization of dyskerin is tied to H/ACA RNP complex assembly, connect GAR1-dyskerin interaction defects to the nucleolar exclusion of dyskerin, and demonstrate that improper dyskerin localization disrupts the ability of dyskerin to interact with H/ACA RNAs like hTR.

Figure 3.3: Dyskerin nuclear and nucleolar localization is linked to mature H/ACA complex assembly. Interactions of FLAG-dyskerin WT and localization variants with endogenous pre- and mature H/ACA ribonucleoprotein complex components were assessed by co-immunoprecipitation (IP) from HEK293 cell lysates. Assembly of the a. H/ACA pre-RNP complex involving NAF1, NHP2, and NOP10 was investigated by immunoblotting for the endogenous H/ACA pre-RNP components and FLAG-dyskerin proteins following IP. b. Interaction of dyskerin with the mature H/ACA complex component GAR1 was examined following IP by immunoblotting for endogenous GAR1 and FLAG-dyskerin. Localization variants that are excluded from the nucleolus (K467R and K467/468R) do not interact with GAR1. Immunoblotting targets are indicated to the right of each panel as WB: α target, and a list of antibodies can be found in the materials and methods section. Each co-IP and immunoblotting was performed in experimental replicate a minimum of n=2, representative blots are shown. c. Dyskerin-hTR interactions were assessed by IP of FLAG-tagged dyskerin followed by RNA extraction and qPCR. Relative to wildtype IP fractions, dyskerin variants with substantial localization defects (K467R and K446X) display significantly reduced enrichment of hTR following IP. HEK293 cells lacking FLAG-tagged dyskerin (indicated as mock) were used as a negative control for RNA binding to the FLAG antibody and/or Protein G Sepharose. Mock cells were subject to the same IP protocol detailed for fractions containing FLAG-tagged dyskerin. These data represent experimental replicates of n=3. Statistically significant reductions in enrichment relative to wildtype are indicated by * (P value < 0.01). Error bars represent SEM.

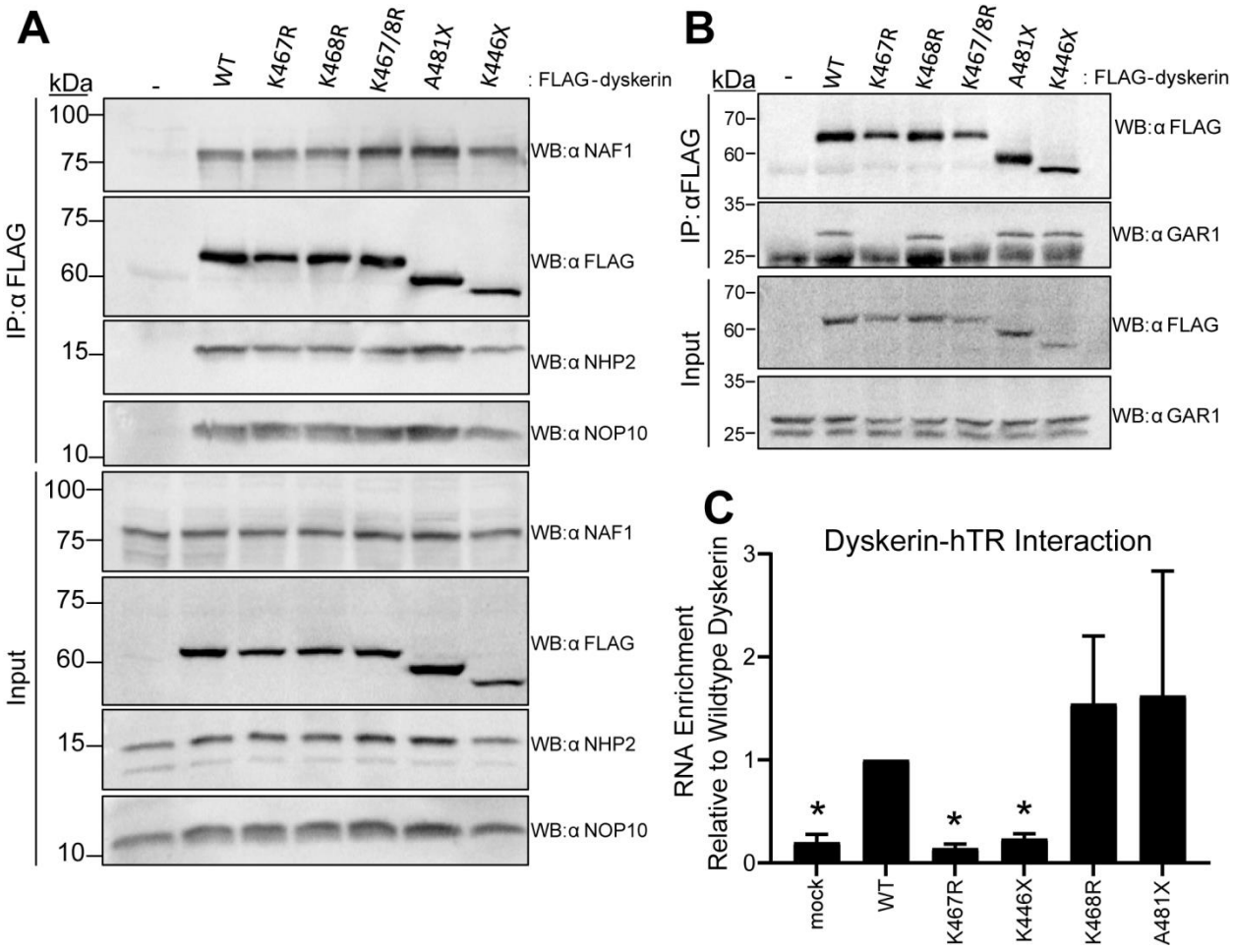
A
kDa
-
WT
K467R
K468R
K467/8R
A481X
K446X
: FLAG-dyskerin
IP: α FLAG
100
75
75
60
15
10
WB: α NAF1
WB: α FLAG
WB: α NHP2
WB: α NOP10
Input
100
75
75
60
15
10
WB: α NAF1
WB: α FLAG
WB: α NHP2
WB: α NOP10
B
kDa
-
WT
K467R
K468R
K467/8R
A481X
K446X
: FLAG-dyskerin
IP: αFLAG
70
60
35
25
WB: α FLAG
WB: α GAR1
Input
70
60
35
25
WB: α FLAG
WB: α GAR1
C
Dyskerin-hTR Interaction
RNA Enrichment
Relative to Wildtype Dyskerin
3
2
1
0
*
*
*
mock
WT
K467R
K446X
K468R
A481X

GAR1 interaction with dyskerin mediates nucleolar localization in a SUMO-dependent manner

While the dyskerin variants that are excluded from the nucleolus do not interact with GAR1, the mainly cytoplasmic K446X truncation which is competent for nucleolar localization is capable of interacting with endogenous GAR1 (Figure 3.3B). Due to this observation that nucleolar localization of dyskerin in particular is connected to the dyskerin-GAR1 interaction and the SUMO3 site K467, we asked whether the interaction between GAR1 and dyskerin may be SUMO3-mediated, and whether this interaction is responsible for mediating dyskerin nucleolar localization. To test this, we performed FLAG co-IPs from HEK293 cells expressing FLAG-tagged dyskerin fused to SUMO3 at the C-terminus. Interestingly, fusing SUMO3 to the C-terminus of the K467R variant is able to rescue the robust GAR1 interaction defect of K467R (Figure 3.3B), and wildtype dyskerin with C-terminal SUMO3 fusion is also able to interact with GAR1 comparably to wildtype dyskerin alone (Figure 3.4A). This was also confirmed by IP from HEK293 cells co-expressing FLAG-tagged dyskerin and HA-GAR1 (Supplemental Figure 3.5). However, the subnuclear localization of both of these SUMO3-fusions does differ from that of wildtype dyskerin, as assessed by IF, consistent with a predicted requirement for SUMOylation reversibility for proper regulation of dyskerin subnuclear localization. Importantly, compared to fusion of SUMO3 to the N-terminus of K446X or the non-fusion K467R variant, these C-terminal SUMO3 fusions display more co-localization with fibrillarin in the nucleolar compartment, though less frequent nucleolar localization of these fusions is observed compared to wildtype dyskerin (Supplemental Figure 3.6). This suggests that the nucleolar localization of K467R, as well as interaction between GAR1 and dyskerin may indeed be SUMO3-dependent. To further elucidate a potential SUMO3-mediated GAR1-dyskerin interaction, and using the prediction software GPS-SUMO 4.0, we identified a single predicted SIM within GAR1 at residues 70-74 (70-VVLLG-74) proximal to the previously predicted dyskerin-GAR1 interface (Figure 3.4B). In order to assess whether this predicted SIM could mediate the interaction between GAR1 and dyskerin, we substituted each residue in the predicted SIM to alanine in a 3xFLAG-tagged GAR1 construct (annotated as 5A), and assessed the interaction of 3xFLAG-tagged GAR1 with endogenous dyskerin. Wildtype 3xFLAG-tagged GAR1 is able to interact with endogenous dyskerin, as assessed by FLAG co-IP from HEK293 cells expressing 3xFLAG-GAR1, however GAR1 5A displays a reduced interaction with

endogenous dyskerin (Figure 3.4C). These data demonstrate that GAR1 contains a SIM which mediates the efficient interaction between dyskerin and GAR1 in a SUMO3-dependent manner, relying on the SUMO3 site K467 in the C-terminal N/NoLS of dyskerin, and that this interaction with GAR1 governs the localization of dyskerin in the nucleolus.

Figure 3.4: Efficient interaction between dyskerin and GAR1 is mediated by SUMO3. a. The GAR1-interaction defect of nucleolar exclusion variant K467R is rescued by fusion of this variant to a SUMO3 moiety at the C-terminus of FLAG-dyskerin, as demonstrated by co-immunoprecipitation (IP) of FLAG-dyskerin and endogenous GAR1 from HEK293 cell lysates. Interaction between endogenous GAR1 and wildtype (WT)-SUMO3 fusion, K467R-SUMO3 fusion, or WT dyskerin was assessed by immunoblotting following FLAG IP. SUMO3 fusion variants run at a higher molecular weight than WT dyskerin alone due to the SUMO3 moiety. b. A linear schematic of human GAR1, with glycine and arginine rich domains indicated (RGG-1 and RGG-2). The predicted SIM (70-VVLLG-74) is indicated, and residues expected to physically interface with dyskerin based on previous homologue structural studies in yeast are bolded and italicized. c. Substitution of all five predicted SIM residues to alanine (GAR1 5A) impairs the interaction between GAR1 and dyskerin, as demonstrated by co-IP of 3xFLAG-GAR1 and endogenous dyskerin. Interaction between endogenous dyskerin and WT or 5A GAR1 was assessed by immunoblotting following FLAG IP. Immunoblotting targets are indicated to the right of each panel as WB: α target, and a list of antibodies can be found in the materials and methods section. Each co-IP and immunoblotting was performed in experimental replicate a minimum of n=2, representative blots are shown.

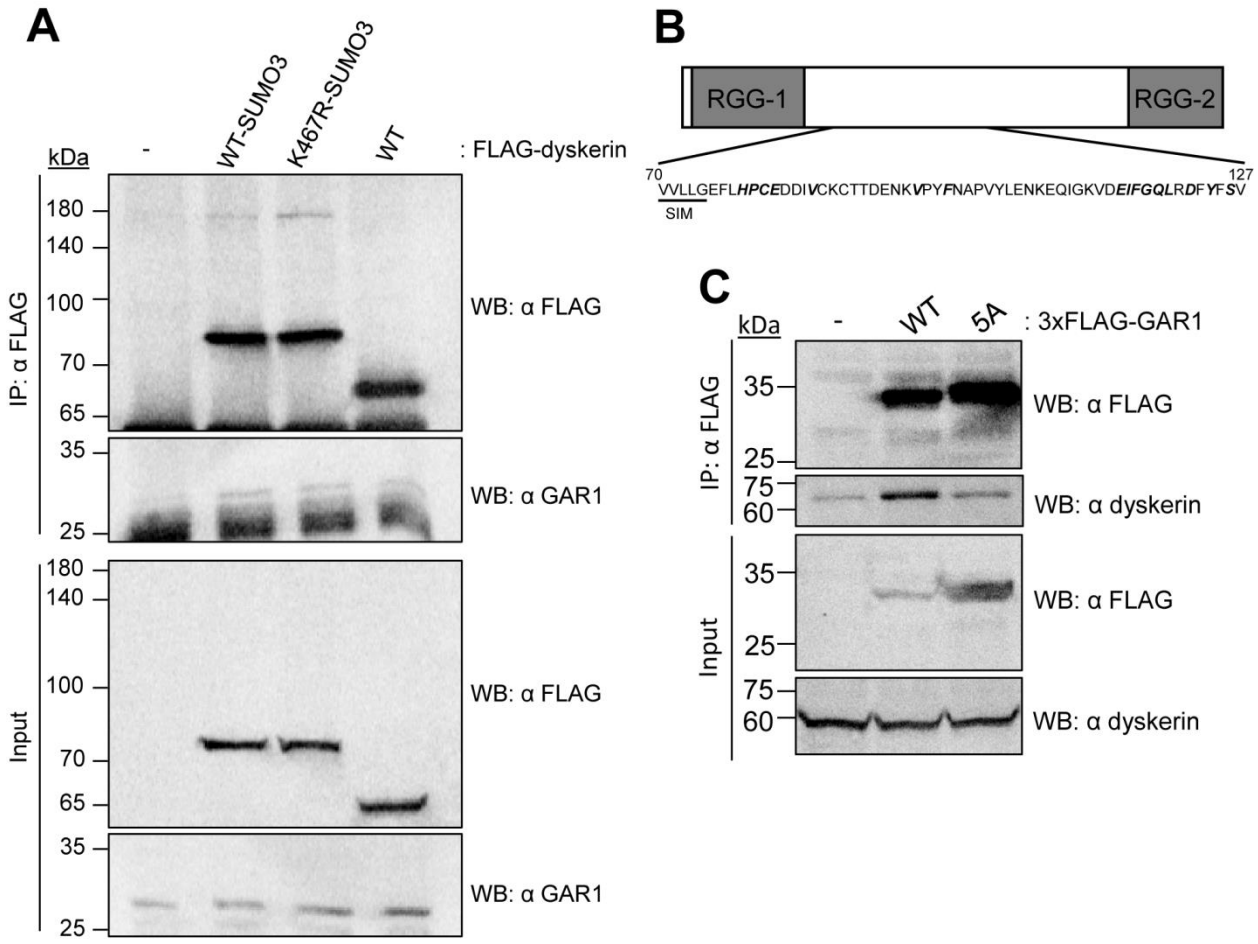
A
WT-SUMO3
K467R-SUMO3
WT
: FLAG-dyskerin
kDa
-
IP: α FLAG
180
140
100
70
65
35
25
WB: α FLAG
WB: α GAR1
Input
180
140
100
70
65
35
25
WB: α FLAG
WB: α GAR1
B
RGG-1
RGG-2
70
127
VVLLGEFLHPCEDDIVCKCTTDENKVPYFNAPVYLENKEQIGKVDEIFGQLRDFYFSV
SIM
C
kDa
-
WT
5A
: 3xFLAG-GAR1
IP: α FLAG
35
25
75
60
WB: α FLAG
WB: α dyskerin
Input
35
25
75
60
WB: α FLAG
WB: α dyskerin

3.7 Discussion

Dyskerin and the H/ACA RNP complex play essential roles in H/ACA RNA biogenesis, posttranscriptional modification of rRNA and snRNA, and in human telomerase assembly and activity. The ability of dyskerin to carry out its various functions relies heavily on its nuclear and subnuclear compartmentalization, where it assembles with H/ACA RNA and localizes to sites of function, including the nucleolus where pseudouridine synthesis occurs on rRNA. In this study we further demonstrate the interconnectedness of dyskerin localization, and H/ACA RNP assembly. More specifically, we demonstrate that efficient nuclear localization of dyskerin, driven by the K-rich C-terminal N/NoLS, as well as mature H/ACA complex assembly and nucleolar localization mediated by K467 in this N/NoLS are crucial for dyskerin assembly with H/ACA RNA like hTR. Furthermore, we demonstrate that the localization of dyskerin can be mediated by SUMOylation sites in the C-terminal N/NoLS.

A previous study of dyskerin nuclear localization characterized two N/NoLS regions, one in the N-terminus (amino acids 11-20) and one in the C-terminus (amino acids 446-514) (Heiss, Girod *et al.* 1999). This foundational study reported that removing or mutating the N-terminal region alone did not disrupt localization of dyskerin, whereas removal of the C-terminal region alone drastically impeded nuclear localization, and combinatorial removal of both regions abolished nuclear localization altogether. As such, we focused on this C-terminal N/NoLS region as the primary driver of dyskerin nuclear localization. Strikingly, we found that efficient localization of dyskerin to the nucleus, while impaired by truncation of the C-terminal N/NoLS at K446 (K446X), can be driven by mimicking SUMOylation through fusing dyskerin to a SUMO3 moiety. This suggests that the loss of SUMOylation sites from this truncation variant may be responsible for inefficient dyskerin nuclear import and/or retention. Given the multitude of dyskerin SUMOylation sites identified by MS which fall outside of the C-terminal N/NoLS of dyskerin, it is also likely that dyskerin SUMOylation takes place within the nucleus for some sites following nuclear import. Establishing which SUMOylation sites in particular govern nuclear localization requires further investigation, as pinpointing the MS-identified SUMOylation sites in this region responsible for nuclear localization was not evident by removal or substitution of K467, K468, K498, or K507. In the future, it may be informative to investigate if the N-terminal N/NoLS region is implicated in SUMO-mediated localization of dyskerin. However, our mutational analysis instead revealed that K467 plays an important regulatory role

in subnuclear localization of dyskerin to the nucleoli. Importantly, in our study and in the previous work by Heiss *et al.*, full truncation of the C-terminal region does not prevent nucleolar localization of dyskerin *per se* (Heiss, Girod *et al.* 1999). As such, we postulate that the C-terminal N/NoLS may govern several aspects of stepwise dyskerin localization (nuclear import, nucleoplasmic assembly with H/ACA RNA, and nucleolar miscibility) through regulated conformational changes. More specifically, we speculate that a conformational change of this C-terminal region governed by SUMOylation at K467 may be responsible for licensing dyskerin nucleolar localization. However, the absence of this region as a whole allows for dyskerin nucleolar localization in the absence of K467 SUMOylation, albeit in the context of inefficient nuclear localization, because no conformational change is required for the K446X truncation variant. This would be consistent with reports that full length dyskerin and dyskerin homologues are difficult to purify *in vitro* due to insolubility issues which can be resolved by removal of this C-terminal region (Darzacq, Kittur *et al.* 2006, Normand, Capeyrou *et al.* 2006), and also in agreement with a lack of reported structure of this functionally required tail due to its apparent intrinsic low complexity (Jiang, Middleton *et al.* 1993, Li, Duan *et al.* 2011, Li, Duan *et al.* 2011). It also seems likely that a conformational change in dyskerin may be responsible for regulating the exchange of GAR1 for NAF1 upon H/ACA complex maturation, though this needs further investigation.

Meanwhile, subnuclear localization of dyskerin-SUMO3 fusion proteins, variant or wildtype, was observed to differ from wildtype dyskerin alone. We postulate that the constitutive nature of this SUMOylation mimic disrupts nucleolar localization due to the inability of deSUMOylating proteases to reverse this imitated posttranslational modification. This proposal is based on not only the abundance of nucleolar SUMO-targets and SUMOylation machinery involvement in nucleolar integrity (Ayaydin and Dasso 2004, Zhao and Blobel 2005, Takahashi, Dulev *et al.* 2008, Matafora, D'Amato *et al.* 2009, Srikumar, Lewicki *et al.* 2013), but also on the nucleolar localization of SUMO-specific proteases (SENP3 and SENP5) involved in deconjugation of SUMO2/3 from target proteins (Yun, Wang *et al.* 2008). SENP3 in particular has been demonstrated to interact with the nucleolar resident protein nucleophosmin (NPM1), the 60S maturation factors PELP1, TEX10, WDR18, and Las1L, and is capable of deSUMOylating NPM1, PELP1, and Las1L (Haindl, Harasim *et al.* 2008, Finkbeiner, Haindl *et al.* 2011, Castle, Cassimere *et al.* 2012). Consistent with the hypothesis that SUMO removal may

regulate nucleolar localization of SUMO-target proteins, depletion of SENP3, and thus reduction of nucleolar deSUMOylation, has been reported to lead to nucleolar release of the PELP1-TEX10-WDR18 complex (Finkbeiner, Haindl *et al.* 2011). Furthermore, in yeast the nucleolar SUMO-specific protease Ulp2 has been demonstrated to reverse SUMOylation of rDNA-bound SUMO-targets, and engineered increased SUMOylation by depletion of Ulp2 leads to a reduction of several nucleolar proteins bound to rDNA (Gillies, Hickey *et al.* 2016, Liang, Singh *et al.* 2017). Intriguingly, NPM1 is responsible for localization of SENP3 to the nucleolus (Raman, Nayak *et al.* 2014). NPM1 is a resident protein of the outer-most nucleolar component where ribosomal subunit maturation takes place, the granular component (GC), and as such would make a good candidate for gatekeeping localization of nucleolar proteins in a SUMO removal-dependent manner. This remains uninvestigated but would also fit into models of phase-mediated nucleolar compartmentalization (Brangwynne, Mitchison *et al.* 2011, Feric, Vaidya *et al.* 2016), as discussed in greater detail below.

Here we also report that the efficient interaction between dyskerin and GAR1 is mediated through a newly characterized SIM in GAR1 (amino acids 70-VVLLG-74). SIMs are typically short hydrophobic stretches of residues that can form an extended β-strand backbone, which then non-covalently interacts with SUMO moieties to foster stronger or more frequent SUMO-mediated protein-protein interactions (Varejao, Lascorz et al. 2019). It is important to note that this predicted motif is not well conserved in lower eukaryotes or archaea (Li, Duan *et al.* 2011). We found that substituting all five of these GAR1 residues to alanine impairs the interaction of GAR1 with endogenous dyskerin, indicating that an efficient interaction between GAR1 and dyskerin relies on this SIM, which is proximal to but does not overlap with any of the residues structurally identified previously to mediate the interaction between these two proteins in yeast and archaea (Rashid, Liang *et al.* 2006, Li, Duan *et al.* 2011). Anecdotally, this SUMO-mediated interaction between GAR1 and dyskerin may also offer some explanation for the reported difficulty of *in vitro* reconstitution of H/ACA complexes using full length proteins, and indeed the GAR1-dyskerin interface that has been identified structurally using homologues from other organisms does not account for the C-terminal N/NoLS of human dyskerin as this region was absent from the dyskerin homologues used for crystallization (Li, Duan *et al.* 2011, Li, Duan *et al.* 2011, Walbott, Machado-Pinilla *et al.* 2011, Singh, Wang *et al.* 2015). These structural data also indicate that the GAR1-dyskerin interaction does take place in the absence of SUMOylation

and without the dyskerin C-terminal N/NoLS *in vitro*, indicating that while this GAR1 SIM contributes to the efficient interaction between dyskerin and GAR1 in a cellular context, this SIM is not required *per se*. We also observed that substituting the dyskerin SUMO3 site K467 to arginine abolishes the interaction between GAR1 and dyskerin, and that this GAR1 interaction defect of the K467R variant can be rescued by fusing K467R to SUMO3. It is not known if K467 directly interfaces with GAR1, due to the absence of data on this C-terminal region of dyskerin from structural studies. However, the observation that fusion of K467R to a SUMO3 moiety can recover the ability of this variant to interact with GAR1 strongly implies that SUMOylation of K467 mediates the efficient interaction between GAR1 and dyskerin.

Finally, we postulate that the SUMO-mediated interaction between GAR1 and dyskerin is required for dyskerin localization to the nucleolus. Along with the data we present here, this hypothesis is rooted in recent analyses of the nucleolar resident protein fibrillarin. Fibrillarin is a small nucleolar RNP counterpart to dyskerin responsible for the 2′O-methylation posttranscriptional modification of rRNA in the DFC, guided by C/D box snoRNA rather than H/ACA box snoRNA (Cavaille, Nicoloso *et al.* 1996, Kiss-Laszlo, Henry *et al.* 1996, Tycowski, You *et al.* 1998, Ganot, Jady *et al.* 1999, Jady and Kiss 2001). Several studies have demonstrated that localization of fibrillarin to the DFC is mediated by an intrinsically disordered GAR domain, as well as by interactions with nascent pre-rRNA as the RNA is sorted radially from its site of transcription through the three nucleolar components, of which the DFC is the centre (Feric, Vaidya *et al.* 2016, Yao, Xu *et al.* 2019). These studies and others have shown that the nucleolus represents a complex membrane-free compartment with three distinctly liquid-liquid phase separated components, which as a whole are phase separated from the surrounding nucleoplasm (Scheer and Weisenberger 1994, Boisvert, van Koningsbruggen *et al.* 2007, Brangwynne, Mitchison *et al.* 2011, Weber and Brangwynne 2015, Feric, Vaidya *et al.* 2016). This context is important to bear in mind when considering dynamic localization of resident nucleolar proteins in and out of these separated phases. The regulated miscibility of fibrillarin with the DFC relies on its GAR domain and protein-RNA interactions. As such, we propose that dyskerin miscibility with the DFC relies on its interaction with GAR1, not only through acting as a GAR domain for dyskerin and the entire H/ACA complex *in trans*, but also by providing high H/ACA complex-to-guide RNA affinity which facilitates accurate H/ACA complex placement on target RNA, like rRNA in the nucleolus (Wang, Yang *et al.* 2015, Caton, Kelly *et al.* 2018). This hypothesis is

supported by our observations that 1) the K467R dyskerin variant is unable to interact with GAR1 and the H/ACA box RNA hTR; 2) this K467R variant is unable to co-localize with fibrillarin in the nucleolus; and 3) improving the interaction between the K467R variant and GAR1 by fusing K467R to SUMO3 also allows for partial co-localization of the K467R variant with fibrillarin in the nucleolus. Furthermore, the ability of the nucleolar-miscible K446X truncation to fully assemble with H/ACA pre- and mature RNP components, including interacting with GAR1 also lends support to this hypothesis. We also speculate that the lack of GAR domains in the archaeal homologues of GAR1 and fibrillarin provides evolutionary support for the notion that GAR domains mediate membrane-free compartmentalization of these complexes in eukaryotes, as archaea lack nuclear compartmentalization altogether and would have no need for GAR domain-mediated nucleolar miscibility of the otherwise evolutionarily conserved H/ACA or C/D RNP complexes (Lafontaine and Tollervey 1998). Further confirmation of the phase dynamics of human dyskerin with or without GAR1 is needed to elucidate this hypothesis.

3.8 Supplemental Figures and Figure Legends

Supplemental Figure 3.1: a. *In vitro* SUMOylation of recombinant dyskerin purified from *E.coli* was performed using recombinant His-SUMO1, His-SUMO2, or His-SUMO3 and analyzed on SDS-PAGE. Free His-SUMO is decreased as higher molecular weight dyskerin species are generated in the presence of ATP. **b.** and **c.** The *in vitro* SUMOylation assays in **a.** were subjected to western analysis using an antibody against SUMO2/3 (**b.**) and subsequently (without stripping), using an antibody against SUMO1 (**c.**). Upper molecular weight species represent SUMOylated dyskerin. A large scale SUMOylation reaction with SUMO3 was performed, subjected to Ni-NTA purification and mass spectrometry.

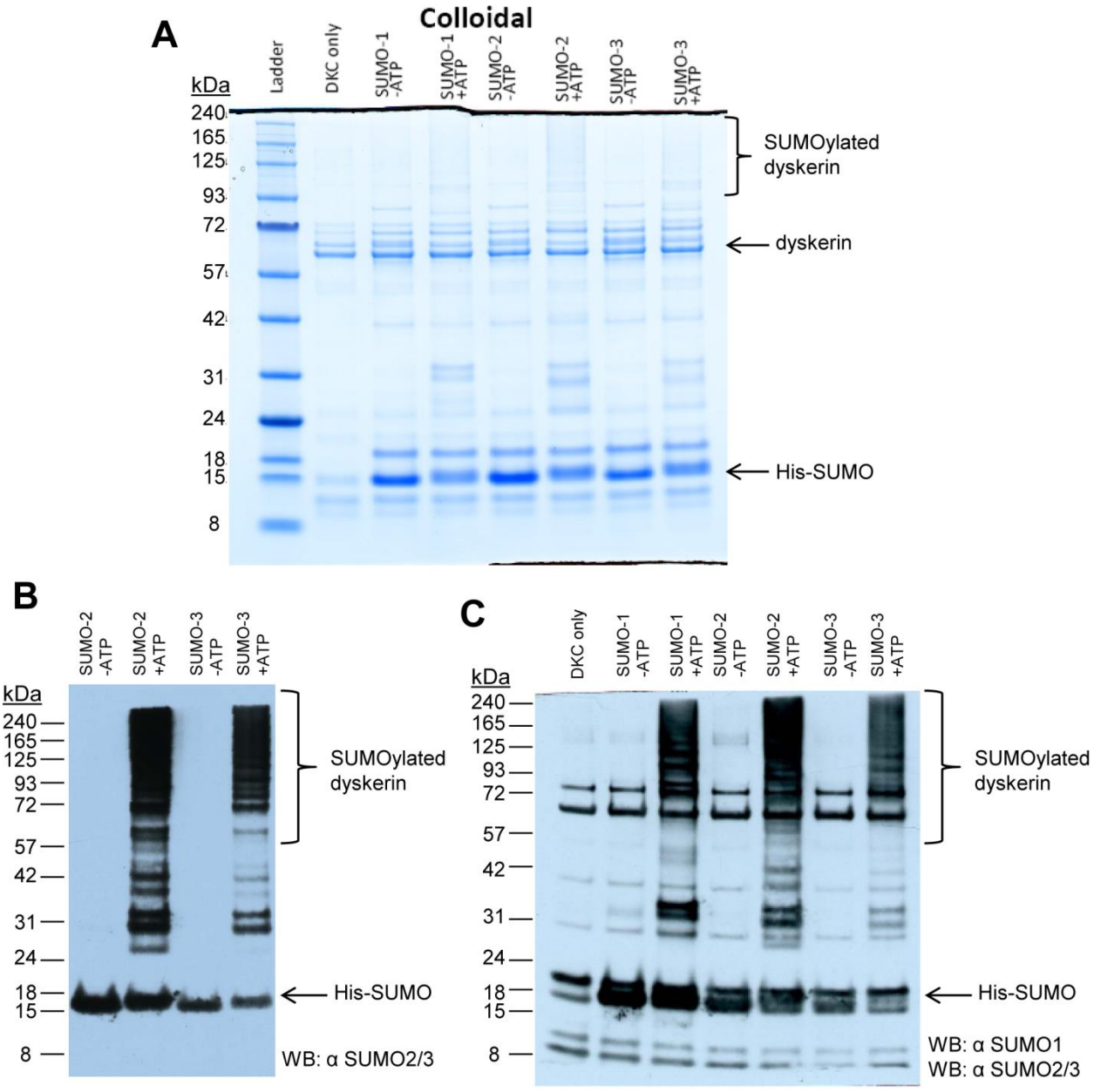
A
Colloidal
kDa
Ladder
DKC only
SUMO-1 -ATP
SUMO-1 +ATP
SUMO-2 -ATP
SUMO-2 +ATP
SUMO-3 -ATP
SUMO-3 +ATP
240
165
125
93
72
57
42
31
24
18
15
8
SUMOylated dyskerin
dyskerin
His-SUMO
B
SUMO-2 -ATP
SUMO-2 +ATP
SUMO-3 -ATP
SUMO-3 +ATP
kDa
240
165
125
93
72
57
42
31
24
18
15
8
SUMOylated dyskerin
His-SUMO
WB: α SUMO2/3
C
DKC only
SUMO-1 -ATP
SUMO-1 +ATP
SUMO-2 -ATP
SUMO-2 +ATP
SUMO-3 -ATP
SUMO-3 +ATP
kDa
240
165
125
93
72
57
42
31
24
18
15
8
SUMOylated dyskerin
His-SUMO
WB: α SUMO1
WB: α SUMO2/3

Supplemental Figure 3.2: a. Localization of FLAG-tagged wildtype (WT) and N-terminal SUMO3 fusion WT dyskerin was assessed by indirect immunofluorescence (Cy3, in red), as described for Figure 3.1C. **b.** Nucleoplasmic foci formed by N-terminal SUMO3 fusion K446X dyskerin truncation (Cy3, in red) that do not co-localize with fibrillarin (FITC, in green) are indicated by white arrows, while an example of a focus that does co-localize with fibrillarin is indicated by a white arrowhead. The nucleus is indicated by DAPI staining of nuclear DNA (in blue).

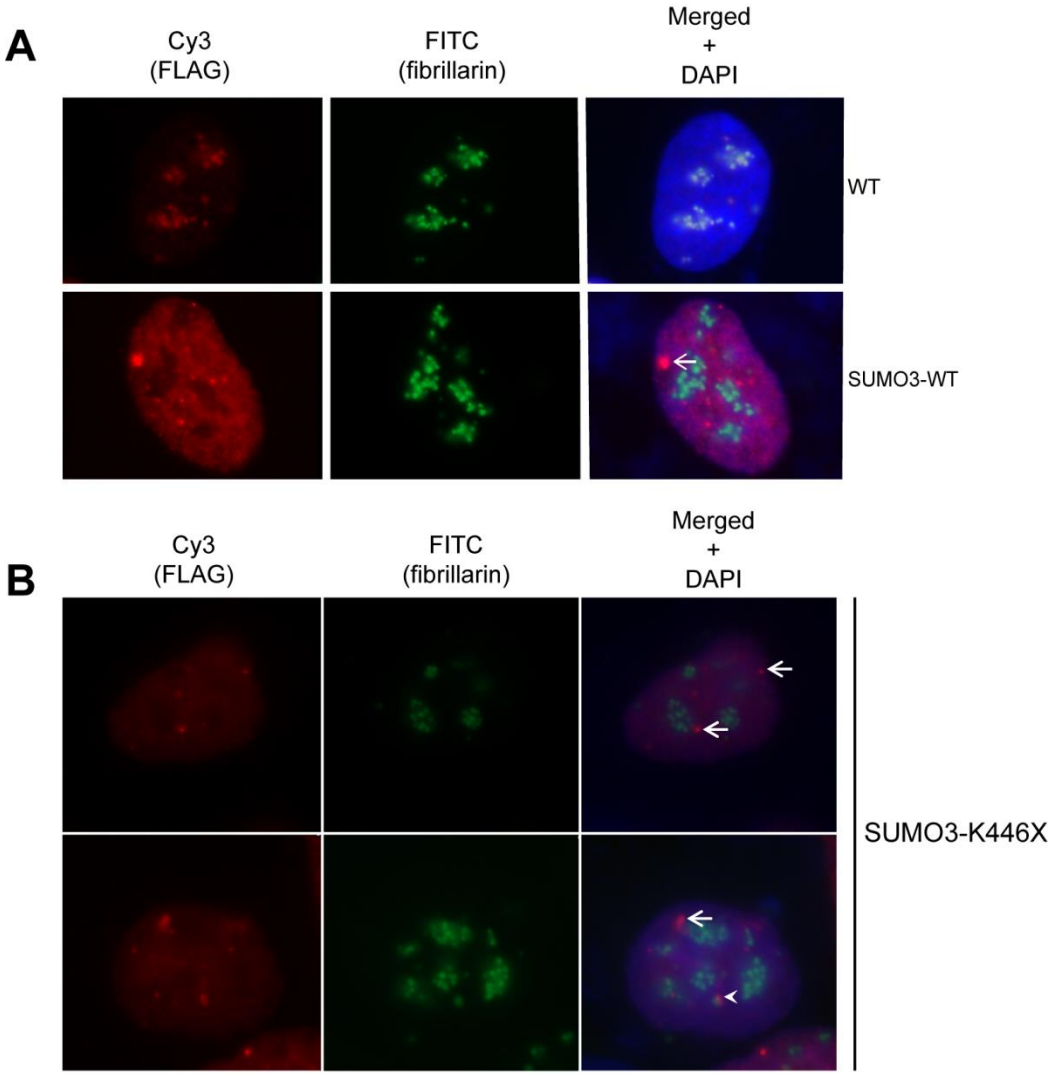
A
Cy3
(FLAG)
FITC
(fibrillarin)
Merged
+
DAPI
WT
SUMO3-WT
B
Cy3
(FLAG)
FITC
(fibrillarin)
Merged
+
DAPI
SUMO3-K446X

Supplemental Figure 3.3: a. Localization of eGFP and eGFP-tagged wildtype (WT) dyskerin (in green) was assessed in fixed HEK293 cells following transient transfection, using a FITC filter. **b.** Localization of endogenous dyskerin (Cy3, in red) was assessed by IF in fixed HEK293 cells. As a negative control, fixed HEK293 cells were assessed by IF using only secondary Cy3-conjugated antibody. The nucleus is indicated by DAPI staining of nuclear DNA (in blue). These are representative images.

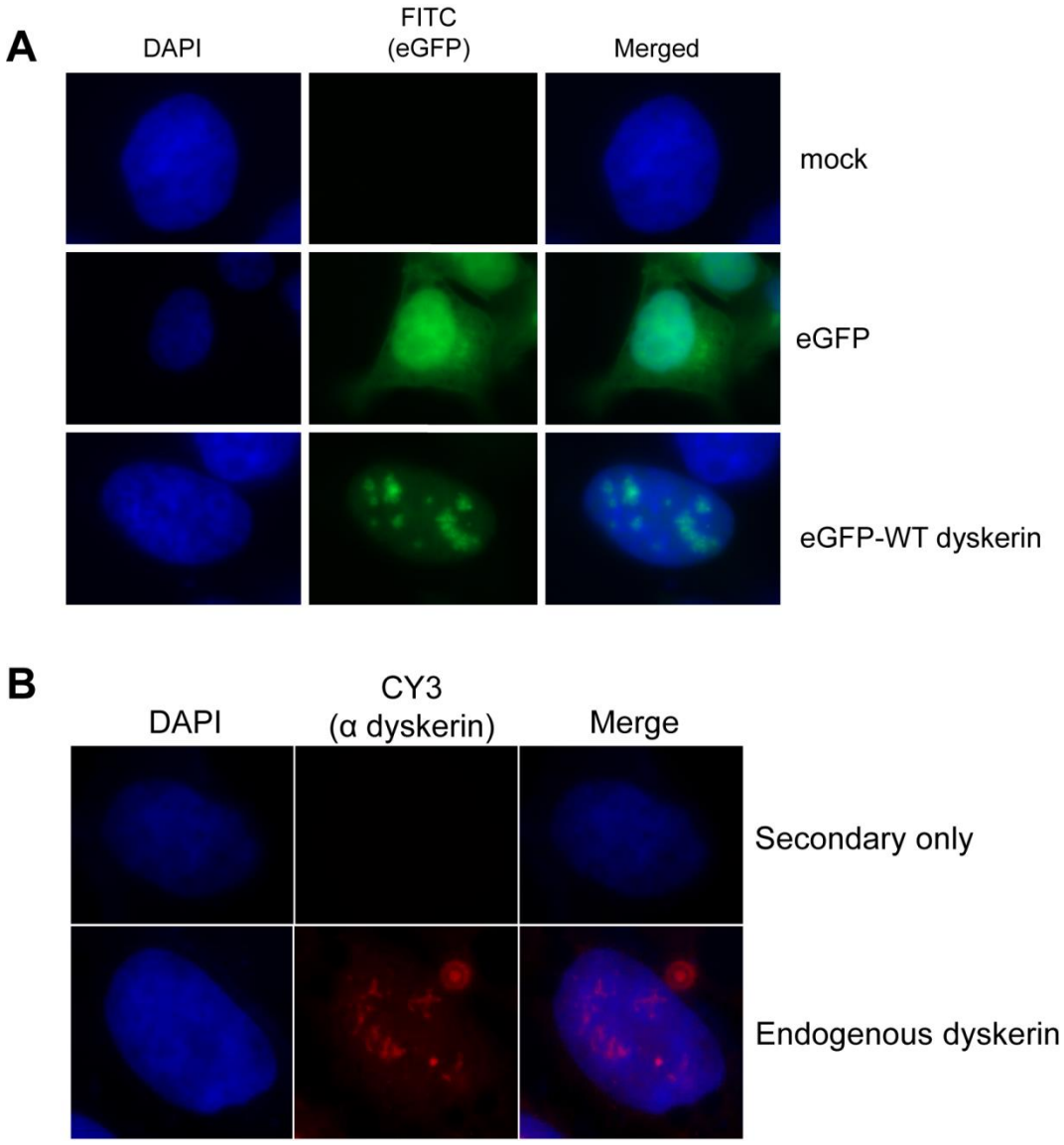
A
DAPI
FITC
(eGFP)
Merged
mock
eGFP
eGFP-WT dyskerin
B
DAPI
CY3
(α dyskerin)
Merge
Secondary only
Endogenous dyskerin

Supplemental Figure 3.4: a. Nuclear (N) and cytoplasmic (C) fractionation was performed on transiently transfected HEK293 cells with low salt and RIPA buffers, as described in the Materials and Methods section, and assessed by immunoblotting. EV indicates cells transiently transfected with pcDNA3.1(-)neo backbone. Lamin A/C was used as a nuclear marker, while tubulin was used a cytoplasmic marker. Anti-dyskerin antibody was used to assess localization of bother endogenous and FLAG-tagged dyskerin. Endogenous dyskerin was observed in both fractions, as were FLAG-tagged wildtype (WT) and K467R variant, indicated by the higher molecular weight band detected using the anti-dyskerin antibody. Note that the K446X truncation of dyskerin runs at a lower molecular weight than endogenous dyskerin and FLAG-tagged WT and K467R dyskerin, and is absent from the nuclear fraction. **b.** Sucrose cushion-based fractionation was performed on transiently transfected HEK293 cells, as described in the Materials and Methods section, and assessed by immunoblotting. HEK293 cells that were untransfected (-) were used as a negative control for FLAG-dyskerin, and to assess localization of endogenous dyskerin by fractionation. Lamin A/C was used as a nuclear marker, while tubulin was used a cytoplasmic marker. The absence of tubulin from the nucleolar fraction indicates clean fractionation. All FLAG-tagged dyskerin proteins were observed in the whole cell lysate and cytoplasmic fraction, while the K467R variant was not observed in the nucleolar fraction. Note that K446X was observed in the nucleolar fraction, consistent with IF data. These blots each represent a single experimental replicate for each protocol.

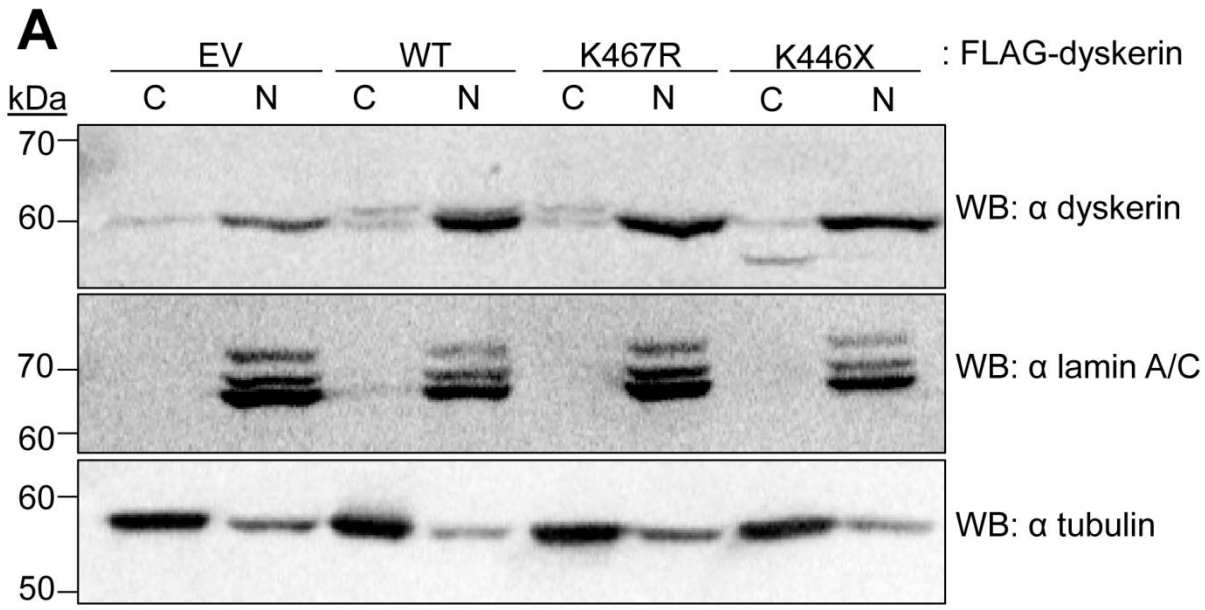
A
EV
WT
K467R
K446X
: FLAG-dyskerin
kDa
C
N
C
N
C
N
C
N
70
60
WB: α dyskerin
70
60
WB: α lamin A/C
60
50
WB: α tubulin

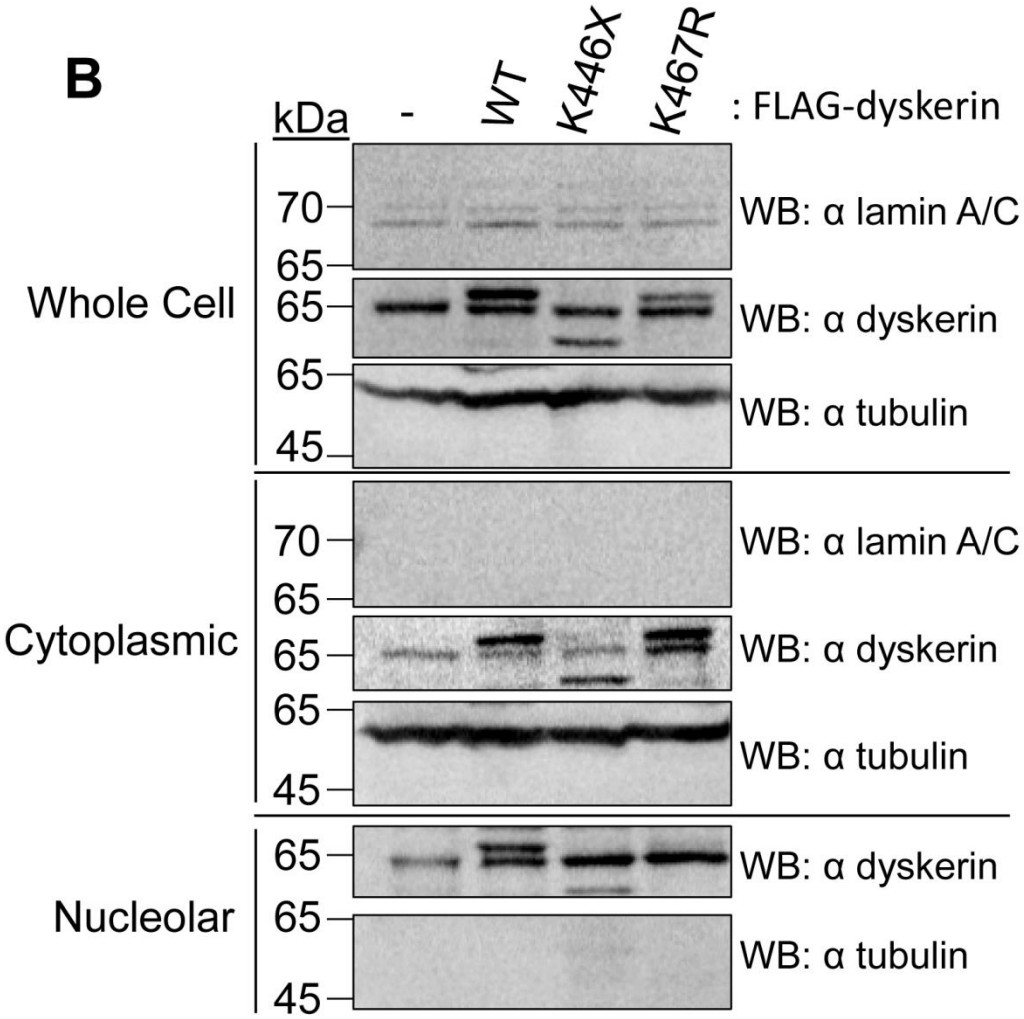
B
kDa
-
WT
K446X
K467R
: FLAG-dyskerin
Whole Cell
70
65
WB: α lamin A/C
65
WB: α dyskerin
65
45
WB: α tubulin
Cytoplasmic
70
65
WB: α lamin A/C
65
WB: α dyskerin
65
45
WB: α tubulin
Nucleolar
65
WB: α dyskerin
65
45
WB: α tubulin

Supplemental Figure 3.5: The interaction between FLAG-tagged dyskerin and wildtype HA-GAR1 was assessed by FLAG IP from HEK293 cells transiently expressing the constructs indicated, and analyzed by immunoblotting against FLAG and HA tags. The top panel (IP: α FLAG) reveals HA-GAR1 present in each sample after FLAG IP, indicating interaction between FLAG-dyskerin and HA-GAR1. The middle and bottom panels (Input) reveal the FLAG-dyskerin and HA-GAR1 expression in each sample. Note that the C-terminal SUMO3 fusions of dyskerin run at the expected higher molecular weight than non-fusions. EV indicates cells transiently transfected with pcDNA3.1(-)neo backbone instead of plasmid encoding FLAG-dyskerin, while the mock (-) fraction indicates untransfected HEK293 cells. HA-GAR1 co-immunoprecipitates with FLAG-tagged dyskerin wildtype (WT), and C-terminal SUMO3 fused dyskerin WT and K467R variant. This is in contrast to the EV IP sample and the K467R variant lacking the SUMO3 fusion, which do not co-immunoprecipitate HA-GAR1[2]. Importantly, these data are consistent with what was observed for these FLAG-tagged dyskerin variants interacting with endogenous GAR1. One experimental replicate has been performed for this analysis, and these results need to be confirmed with future experimental replicates.

[2] The α FLAG immunoblot for the FLAG IP samples displayed no signal when revealed, but was not able to be repeated prior to lab shut down due to COVID-19.

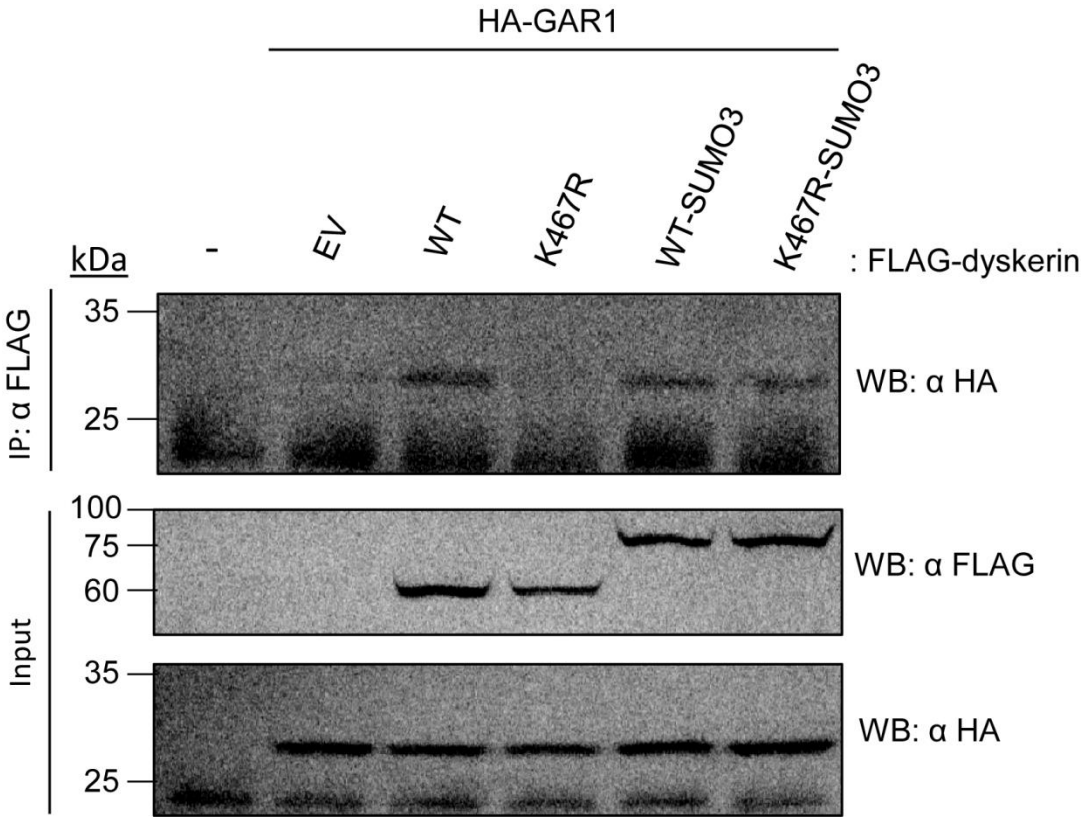
HA-GAR1
kDa
-
EV
WT
K467R
WT-SUMO3
K467R-SUMO3
: FLAG-dyskerin
IP: α FLAG
35
25
WB: α HA
Input
100
75
60
WB: α FLAG
35
25
WB: α HA

Supplemental Figure 3.6: C-terminal SUMO3 fusion FLAG-dyskerin wildtype and K467R variant were transiently expressed in HEK293 cells, and localization was assessed in fixed cells by indirect immunofluorescence. Representative images of the most prevalent localization phenotype of FLAG-dyskerin (Cy3 shown in red) and the nucleolar marker fibrillarin (FITC shown in green) are shown. The nucleus is indicated by DAPI staining of nuclear DNA (in blue). Quantification of localization phenotype scoring as a percentage of FLAG-positive HEK293 cells is indicated (≥50 cells per condition were counted, in experiment replicate n=3).

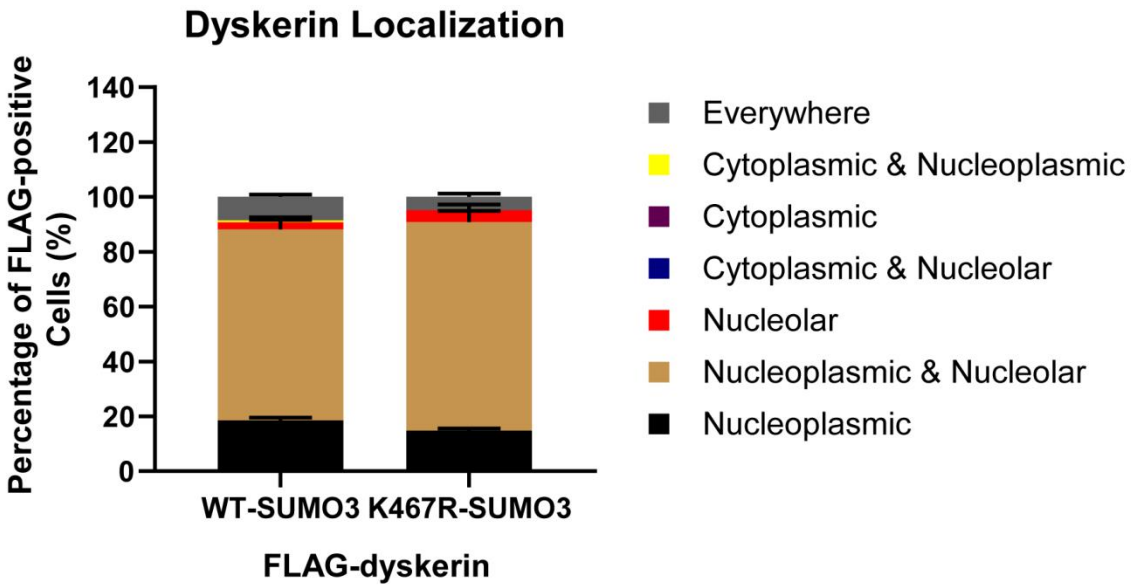
Dyskerin Localization
Percentage of FLAG-positive Cells (%)
140
120
100
80
60
40
20
0
WT-SUMO3
K467R-SUMO3
FLAG-dyskerin
Everywhere
Cytoplasmic & Nucleoplasmic
Cytoplasmic
Cytoplasmic & Nucleolar
Nucleolar
Nucleoplasmic & Nucleolar
Nucleoplasmic

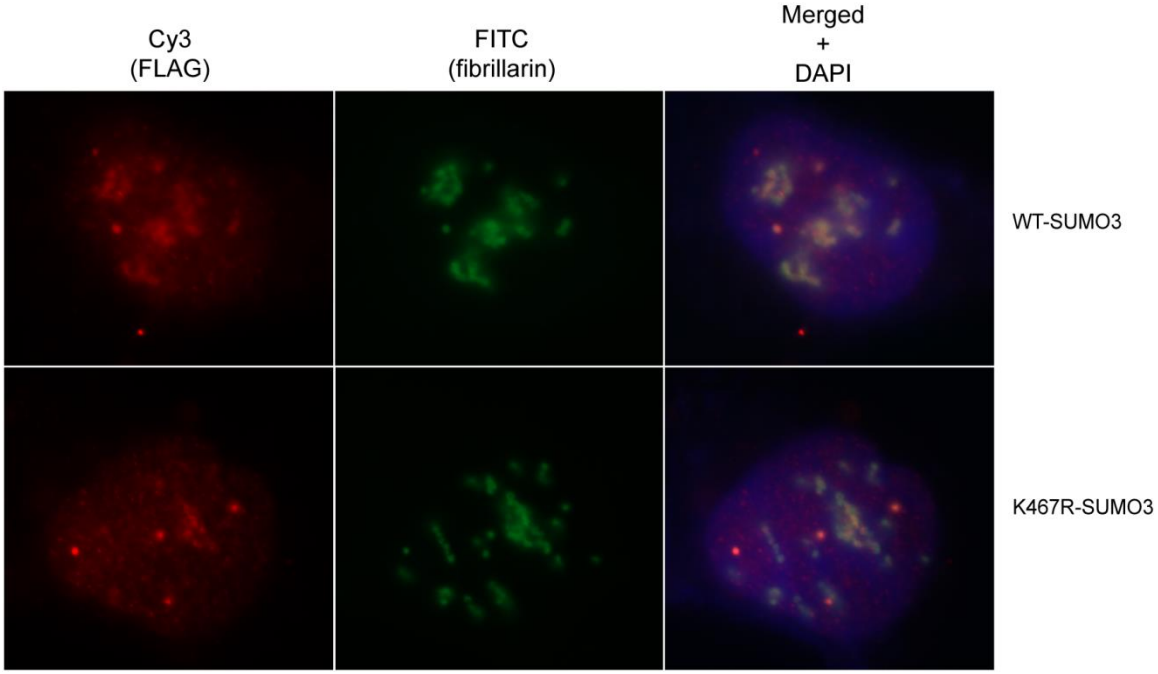
Cy3
(FLAG)
FITC
(fibrillarin)
Merged
+
DAPI
WT-SUMO3
K467R-SUMO3

Supplemental Table 3.1 – List of Primers for Chapter 3

Primer Name	Primer Sequence
DKC1 K467R	F: CAGCTCCTCAGTTGATCAGGAAGGAAAAGAAGAAGAG
	R: CTCTTCTTCTTTTCCTTCCTGATCAACTGAGGAGCTG
DKC1 K468R	F: CTCCTCAGTTGATCAAGAGGGAAAAGAAGAAGAGTAAG
	R: CTTACTCTTCTTCTTTTCCCTCTTGATCAACTGAGGAG
DKC1 K467/468R	F: CTCCTCAGTTGATCAGGAGGGAAAAGAAGAAGAGTAAG
	R: CTTACTCTTCTTCTTTTCCCTCCTGATCAACTGAGGAG
DKC1 A481X	F: GGACAAGAAGGCCAAATAGGGTCTGGAGAGCGGGG
	R: CCCCGCTCTCCAGACCCTATTTGGCCTTCTTGTCC
DKC1 K446X	F: GCAAAAACTGCGTAGCGGAAGCGAGAGAG
	R: CTCTCTCGCTTCCGCTACGCAGTTTTTGC
HA-GAR1 (WT)	F: GGGGCTAGCATGTACCCATACGATGTTCCAGATTACGCTTCTTTTCGAGGCGGAGG
	R: CCCGGATCCTTAATGTCCTCTCCCTCTG
GAR1 5A	F: CCAAGACCAAGGACCTCCAGAACGTGCTGCTGCTGCTGCTGAGTTCCTGCATCCCTGTGAAGATG
	R: AGCAGCAGCAGCAGCACGTTCTGGAGGTCCTTGGTCTTGGCCTTTGTTAAAGCCTCCGCG
Mature hTR	F: TCTAACCCTAACTGAGAAGGGCGTAG
	R: GTTTGCTCTAGAATGAACGGTGGAAG
GAPDH	F: CGGAGTCAACGGATTTGGTCGTCGTAT
	R: TGCTAAGCAGTTGGTGGTGCAGGA

3.9 Acknowledgements

We thank Dr. Frédérick Antoine Mallette, Dr. Lea Harrington, and Dr. François Dragon for providing us with pcDNA3.1-6xHis-SUMO3, pET30-His-dyskerin, and pcDNA3.1-FLAG-dyskerin^{WT} plasmids, respectively. We thank Dr. Kenneth Michael Pollard for providing us with mouse anti-fibrillarin antibody for IF.

3.10 Author Contribution

Author contributions: D.E. M., C. A., and P. T. designed research; D.E. M, P. L.-L., F. M., and E. B performed experiments. D.E.M. and C.A. wrote the manuscript.

3.11 References

Arngrimsson, R., I. Dokal, L. Luzzatto and J. M. Connor (1993). Dyskeratosis congenita: three additional families show linkage to a locus in Xq28. J Med Genet 30(7): 618-619.

Ayaydin, F. and M. Dasso (2004). Distinct in vivo dynamics of vertebrate SUMO paralogues. Mol Biol Cell 15(12): 5208-5218.

Balakin, A. G., L. Smith and M. J. Fournier (1996). The RNA world of the nucleolus: two major families of small RNAs defined by different box elements with related functions. Cell 86(5): 823-834.

Ballarino, M., M. Morlando, F. Pagano, A. Fatica and I. Bozzoni (2005). The cotranscriptional assembly of snoRNPs controls the biosynthesis of H/ACA snoRNAs in Saccharomyces cerevisiae. Mol Cell Biol 25(13): 5396-5403.

Becker, J., S. V. Barysch, S. Karaca, C. Dittner, H. H. Hsiao, M. Berriel Diaz, S. Herzig, H. Urlaub and F. Melchior (2013). Detecting endogenous SUMO targets in mammalian cells and tissues. Nat Struct Mol Biol 20(4): 525-531.

Bellodi, C., M. McMahon, A. Contreras, D. Juliano, N. Kopmar, T. Nakamura, D. Maltby, A. Burlingame, S. A. Savage, A. Shimamura and D. Ruggero (2013). H/ACA small RNA dysfunctions in disease reveal key roles for noncoding RNA modifications in hematopoietic stem cell differentiation. Cell Rep 3(5): 1493-1502.

Benyelles, M., M. F. O'Donohue, L. Kermasson, E. Lainey, R. Borie, C. Lagresle-Peyrou, H. Nunes, C. Cazelles, C. Fourrage, E. Ollivier, A. Marcais, A. S. Gamez, F. Morice-Picard, D. Caillaud, N. Pottier, C. Menard, I. Ba, A. Fernandes, B. Crestani, J. P. de Villartay, P. E. Gleizes, I. Callebaut, C. Kannengiesser and P. Revy (2020). NHP2 deficiency impairs rRNA biogenesis and causes pulmonary fibrosis and Hoyeraal-Hreidarsson syndrome. Hum Mol Genet.

Bertomeu, T., J. Coulombe-Huntington, A. Chatr-Aryamontri, K. G. Bourdages, E. Coyaud, B. Raught, Y. Xia and M. Tyers (2018). A High-Resolution Genome-Wide CRISPR/Cas9 Viability Screen Reveals Structural Features and Contextual Diversity of the Human Cell-Essential Proteome. Mol Cell Biol 38(1).

Boisvert, F. M., S. van Koningsbruggen, J. Navascues and A. I. Lamond (2007). The multifunctional nucleolus. Nat Rev Mol Cell Biol 8(7): 574-585.

Booy, E. P., M. Meier, N. Okun, S. K. Novakowski, S. Xiong, J. Stetefeld and S. A. McKenna (2012). The RNA helicase RHAU (DHX36) unwinds a G4-quadruplex in human telomerase RNA and promotes the formation of the P1 helix template boundary. Nucleic Acids Res 40(9): 4110-4124.

Brangwynne, C. P., T. J. Mitchison and A. A. Hyman (2011). Active liquid-like behavior of nucleoli determines their size and shape in Xenopus laevis oocytes. Proc Natl Acad Sci U S A 108(11): 4334-4339.

Brault, M. E., C. Lauzon and C. Autexier (2013). Dyskeratosis congenita mutations in dyskerin SUMOylation consensus sites lead to impaired telomerase RNA accumulation and telomere defects. Hum Mol Genet 22(17): 3498-3507.

Castle, C. D., E. K. Cassimere and C. Denicourt (2012). LAS1L interacts with the mammalian Rix1 complex to regulate ribosome biogenesis. Mol Biol Cell 23(4): 716-728.

Caton, E. A., E. K. Kelly, R. Kamalampeta and U. Kothe (2018). Efficient RNA pseudouridylation by eukaryotic H/ACA ribonucleoproteins requires high affinity binding and correct positioning of guide RNA. Nucleic Acids Res 46(2): 905-916.

Cavaille, J., M. Nicoloso and J. P. Bachellerie (1996). Targeted ribose methylation of RNA in vivo directed by tailored antisense RNA guides. Nature 383(6602): 732-735.

Connor, J. M., D. Gatherer, F. C. Gray, L. A. Pirrit and N. A. Affara (1986). Assignment of the gene for dyskeratosis congenita to Xq28. Hum Genet 72(4): 348-351.

Darzacq, X., B. E. Jady, C. Verheggen, A. M. Kiss, E. Bertrand and T. Kiss (2002). Cajal body-specific small nuclear RNAs: a novel class of 2'-O-methylation and pseudouridylation guide RNAs. EMBO J 21(11): 2746-2756.

Darzacq, X., N. Kittur, S. Roy, Y. Shav-Tal, R. H. Singer and U. T. Meier (2006). Stepwise RNP assembly at the site of H/ACA RNA transcription in human cells. J Cell Biol 173(2): 207-218.

Dokal, I. (1996). Dyskeratosis congenita: an inherited bone marrow failure syndrome. Br J Haematol 92(4): 775-779.

Drachtman, R. A. and B. P. Alter (1992). Dyskeratosis congenita: clinical and genetic heterogeneity. Report of a new case and review of the literature. Am J Pediatr Hematol Oncol 14(4): 297-304.

El-Asmi, F., F. P. McManus, C. E. Brantis-de-Carvalho, J. C. Valle-Casuso, P. Thibault and M. K. Chelbi-Alix (2020). Cross-talk between SUMOylation and ISGylation in response to interferon. Cytokine 129: 155025.

Feric, M., N. Vaidya, T. S. Harmon, D. M. Mitrea, L. Zhu, T. M. Richardson, R. W. Kriwacki, R. V. Pappu and C. P. Brangwynne (2016). Coexisting Liquid Phases Underlie Nucleolar Subcompartments. Cell 165(7): 1686-1697.

Finkbeiner, E., M. Haindl and S. Muller (2011). The SUMO system controls nucleolar partitioning of a novel mammalian ribosome biogenesis complex. EMBO J 30(6): 1067-1078.

Ganot, P., M. L. Bortolin and T. Kiss (1997). Site-specific pseudouridine formation in preribosomal RNA is guided by small nucleolar RNAs. Cell 89(5): 799-809.

Ganot, P., M. Caizergues-Ferrer and T. Kiss (1997). The family of box ACA small nucleolar RNAs is defined by an evolutionarily conserved secondary structure and ubiquitous sequence elements essential for RNA accumulation. Genes Dev 11(7): 941-956.

Ganot, P., B. E. Jady, M. L. Bortolin, X. Darzacq and T. Kiss (1999). Nucleolar factors direct the 2'-O-ribose methylation and pseudouridylation of U6 spliceosomal RNA. Mol Cell Biol 19(10): 6906-6917.

Gardano, L., L. Holland, R. Oulton, T. Le Bihan and L. Harrington (2012). Native gel electrophoresis of human telomerase distinguishes active complexes with or without dyskerin. Nucleic Acids Res 40(5): e36.

Gillies, J., C. M. Hickey, D. Su, Z. Wu, J. Peng and M. Hochstrasser (2016). SUMO Pathway Modulation of Regulatory Protein Binding at the Ribosomal DNA Locus in Saccharomyces cerevisiae. Genetics 202(4): 1377-1394.

Giordano, E., I. Peluso, S. Senger and M. Furia (1999). minifly, a Drosophila gene required for ribosome biogenesis. J Cell Biol 144(6): 1123-1133.

Girard, J. P., H. Lehtonen, M. Caizergues-Ferrer, F. Amalric, D. Tollervey and B. Lapeyre (1992). GAR1 is an essential small nucleolar RNP protein required for pre-rRNA processing in yeast. EMBO J 11(2): 673-682.

Gong, L., S. Millas, G. G. Maul and E. T. Yeh (2000). Differential regulation of sentrinized proteins by a novel sentrin-specific protease. J Biol Chem 275(5): 3355-3359.

Haindl, M., T. Harasim, D. Eick and S. Muller (2008). The nucleolar SUMO-specific protease SENP3 reverses SUMO modification of nucleophosmin and is required for rRNA processing. EMBO Rep 9(3): 273-279.

Hart, T., M. Chandrashekhar, M. Aregger, Z. Steinhart, K. R. Brown, G. MacLeod, M. Mis, M. Zimmermann, A. Fradet-Turcotte, S. Sun, P. Mero, P. Dirks, S. Sidhu, F. P. Roth, O. S. Rissland, D. Durocher, S. Angers and J. Moffat (2015). High-Resolution CRISPR Screens Reveal Fitness Genes and Genotype-Specific Cancer Liabilities. Cell 163(6): 1515-1526.

He, J., S. Navarrete, M. Jasinski, T. Vulliamy, I. Dokal, M. Bessler and P. J. Mason (2002). Targeted disruption of Dkc1, the gene mutated in X-linked dyskeratosis congenita, causes embryonic lethality in mice. Oncogene 21(50): 7740-7744.

Hecker, C. M., M. Rabiller, K. Haglund, P. Bayer and I. Dikic (2006). Specification of SUMO1- and SUMO2-interacting motifs. J Biol Chem 281(23): 16117-16127.

Heiss, N. S., A. Girod, R. Salowsky, S. Wiemann, R. Pepperkok and A. Poustka (1999). Dyskerin localizes to the nucleolus and its mislocalization is unlikely to play a role in the pathogenesis of dyskeratosis congenita. Hum Mol Genet 8(13): 2515-2524.

Heiss, N. S., S. W. Knight, T. J. Vulliamy, S. M. Klauck, S. Wiemann, P. J. Mason, A. Poustka and I. Dokal (1998). X-linked dyskeratosis congenita is caused by mutations in a highly conserved gene with putative nucleolar functions. Nat Genet 19(1): 32-38.

Hendriks, I. A., R. C. D'Souza, B. Yang, M. Verlaan-de Vries, M. Mann and A. C. Vertegaal (2014). Uncovering global SUMOylation signaling networks in a site-specific manner. Nat Struct Mol Biol 21(10): 927-936.

Hendriks, I. A., D. Lyon, D. Su, N. H. Skotte, J. A. Daniel, L. J. Jensen and M. L. Nielsen (2018). Site-specific characterization of endogenous SUMOylation across species and organs. Nat Commun 9(1): 2456.

Hendriks, I. A., D. Lyon, C. Young, L. J. Jensen, A. C. Vertegaal and M. L. Nielsen (2017). Site-specific mapping of the human SUMO proteome reveals co-modification with phosphorylation. Nat Struct Mol Biol 24(3): 325-336.

Hendriks, I. A., L. W. Treffers, M. Verlaan-de Vries, J. V. Olsen and A. C. O. Vertegaal (2015). SUMO-2 Orchestrates Chromatin Modifiers in Response to DNA Damage. Cell Rep 10(10): 1778-1791.

Henras, A., Y. Henry, C. Bousquet-Antonelli, J. Noaillac-Depeyre, J. P. Gelugne and M. Caizergues-Ferrer (1998). Nhp2p and Nop10p are essential for the function of H/ACA snoRNPs. EMBO J 17(23): 7078-7090.

Heun, P. (2007). SUMOrganization of the nucleus. Curr Opin Cell Biol 19(3): 350-355.

Impens, F., L. Radoshevich, P. Cossart and D. Ribet (2014). Mapping of SUMO sites and analysis of SUMOylation changes induced by external stimuli. Proc Natl Acad Sci U S A 111(34): 12432-12437.

Jady, B. E., E. Bertrand and T. Kiss (2004). Human telomerase RNA and box H/ACA scaRNAs share a common Cajal body-specific localization signal. J Cell Biol 164(5): 647-652.

Jady, B. E. and T. Kiss (2001). A small nucleolar guide RNA functions both in 2'-O-ribose methylation and pseudouridylation of the U5 spliceosomal RNA. EMBO J 20(3): 541-551.

Jiang, W., K. Middleton, H. J. Yoon, C. Fouquet and J. Carbon (1993). An essential yeast protein, CBF5p, binds in vitro to centromeres and microtubules. Mol Cell Biol 13(8): 4884-4893.

Kiss-Laszlo, Z., Y. Henry, J. P. Bachellerie, M. Caizergues-Ferrer and T. Kiss (1996). Site-specific ribose methylation of preribosomal RNA: a novel function for small nucleolar RNAs. Cell 85(7): 1077-1088.

Lafontaine, D. L. and D. Tollervey (1998). Birth of the snoRNPs: the evolution of the modification-guide snoRNAs. Trends Biochem Sci 23(10): 383-388.

Lamoliatte, F., D. Caron, C. Durette, L. Mahrouche, M. A. Maroui, O. Caron-Lizotte, E. Bonneil, M. K. Chelbi-Alix and P. Thibault (2014). Large-scale analysis of lysine SUMOylation by SUMO remnant immunoaffinity profiling. Nat Commun 5: 5409.

Lamoliatte, F., F. P. McManus, G. Maarifi, M. K. Chelbi-Alix and P. Thibault (2017). Uncovering the SUMOylation and ubiquitylation crosstalk in human cells using sequential peptide immunopurification. Nat Commun 8: 14109.

Li, S., J. Duan, D. Li, S. Ma and K. Ye (2011). Structure of the Shq1-Cbf5-Nop10-Gar1 complex and implications for H/ACA RNP biogenesis and dyskeratosis congenita. EMBO J 30(24): 5010-5020.

Li, S., J. Duan, D. Li, B. Yang, M. Dong and K. Ye (2011). Reconstitution and structural analysis of the yeast box H/ACA RNA-guided pseudouridine synthase. Genes Dev 25(22): 2409-2421.

Li, S. J. and M. Hochstrasser (1999). A new protease required for cell-cycle progression in yeast. Nature 398(6724): 246-251.

Li, S. J. and M. Hochstrasser (2000). The yeast ULP2 (SMT4) gene encodes a novel protease specific for the ubiquitin-like Smt3 protein. Mol Cell Biol 20(7): 2367-2377.

Liang, J., N. Singh, C. R. Carlson, C. P. Albuquerque, K. D. Corbett and H. Zhou (2017). Recruitment of a SUMO isopeptidase to rDNA stabilizes silencing complexes by opposing SUMO targeted ubiquitin ligase activity. Genes Dev 31(8): 802-815.

MacNeil, D. E., P. Lambert-Lanteigne and C. Autexier (2019). N-terminal residues of human dyskerin are required for interactions with telomerase RNA that prevent RNA degradation. Nucleic Acids Res 47(10): 5368-5380.

Matafora, V., A. D'Amato, S. Mori, F. Blasi and A. Bachi (2009). Proteomics analysis of nucleolar SUMO-1 target proteins upon proteasome inhibition. Mol Cell Proteomics 8(10): 2243-2255.

McManus, F. P., C. D. Altamirano and P. Thibault (2016). In vitro assay to determine SUMOylation sites on protein substrates. Nat Protoc 11(2): 387-397.

Meier, U. T. and G. Blobel (1994). NAP57, a mammalian nucleolar protein with a putative homolog in yeast and bacteria. J Cell Biol 127(6 Pt 1): 1505-1514.

Melchior, F., M. Schergaut and A. Pichler (2003). SUMO: ligases, isopeptidases and nuclear pores. Trends Biochem Sci 28(11): 612-618.

Mitchell, J. R., J. Cheng and K. Collins (1999). A box H/ACA small nucleolar RNA-like domain at the human telomerase RNA 3' end. Mol Cell Biol 19(1): 567-576.

Ni, J., A. L. Tien and M. J. Fournier (1997). Small nucleolar RNAs direct site-specific synthesis of pseudouridine in ribosomal RNA. Cell 89(4): 565-573.

Normand, C., R. Capeyrou, S. Quevillon-Cheruel, A. Mougin, Y. Henry and M. Caizergues-Ferrer (2006). Analysis of the binding of the N-terminal conserved domain of yeast Cbf5p to a box H/ACA snoRNA. RNA 12(10): 1868-1882.

Phillips, B., A. N. Billin, C. Cadwell, R. Buchholz, C. Erickson, J. R. Merriam, J. Carbon and S. J. Poole (1998). The Nop60B gene of Drosophila encodes an essential nucleolar protein that functions in yeast. Mol Gen Genet 260(1): 20-29.

Pichler, A. and F. Melchior (2002). Ubiquitin-related modifier SUMO1 and nucleocytoplasmic transport. Traffic 3(6): 381-387.

Podlevsky, J. D., C. J. Bley, R. V. Omana, X. Qi and J. J. Chen (2008). The telomerase database. Nucleic Acids Res 36(Database issue): D339-343.

Podlevsky, J. D. and J. J. Chen (2016). Evolutionary perspectives of telomerase RNA structure and function. RNA Biol 13(8): 720-732.

Raman, N., A. Nayak and S. Muller (2014). mTOR signaling regulates nucleolar targeting of the SUMO-specific isopeptidase SENP3. Mol Cell Biol 34(24): 4474-4484.

Rashid, R., B. Liang, D. L. Baker, O. A. Youssef, Y. He, K. Phipps, R. M. Terns, M. P. Terns and H. Li (2006). Crystal structure of a Cbf5-Nop10-Gar1 complex and implications in RNA-guided pseudouridylation and dyskeratosis congenita. Mol Cell 21(2): 249-260.

Roake, C. M., L. Chen, A. L. Chakravarthy, J. E. Ferrell, Jr., G. D. Raffa and S. E. Artandi (2019). Disruption of Telomerase RNA Maturation Kinetics Precipitates Disease. Mol Cell 74(4): 688-700 e683.

Scheer, U. and D. Weisenberger (1994). The nucleolus. Curr Opin Cell Biol 6(3): 354-359.

Singh, M., Z. Wang, D. Cascio and J. Feigon (2015). Structure and interactions of the CS domain of human H/ACA RNP assembly protein Shq1. J Mol Biol 427(4): 807-823.

Song, J., L. K. Durrin, T. A. Wilkinson, T. G. Krontiris and Y. Chen (2004). Identification of a SUMO-binding motif that recognizes SUMO-modified proteins. Proc Natl Acad Sci U S A 101(40): 14373-14378.

Song, J., Z. Zhang, W. Hu and Y. Chen (2005). Small ubiquitin-like modifier (SUMO) recognition of a SUMO binding motif: a reversal of the bound orientation. J Biol Chem 280(48): 40122-40129.

Srikumar, T., M. C. Lewicki and B. Raught (2013). A global S. cerevisiae small ubiquitin-related modifier (SUMO) system interactome. Mol Syst Biol 9: 668.

Takahashi, Y., S. Dulev, X. Liu, N. J. Hiller, X. Zhao and A. Strunnikov (2008). Cooperation of sumoylated chromosomal proteins in rDNA maintenance. PLoS Genet 4(10): e1000215.

Takahashi, Y., J. Mizoi, E. A. Toh and Y. Kikuchi (2000). Yeast Ulp1, an Smt3-specific protease, associates with nucleoporins. J Biochem 128(5): 723-725.

Tseng, C. K., H. F. Wang, M. R. Schroeder and P. Baumann (2018). The H/ACA complex disrupts triplex in hTR precursor to permit processing by RRP6 and PARN. Nat Commun 9(1): 5430.

Tycowski, K. T., Z. H. You, P. J. Graham and J. A. Steitz (1998). Modification of U6 spliceosomal RNA is guided by other small RNAs. Mol Cell 2(5): 629-638.

Varejao, N., J. Lascorz, Y. Li and D. Reverter (2019). Molecular mechanisms in SUMO conjugation. Biochem Soc Trans.

Walbott, H., R. Machado-Pinilla, D. Liger, M. Blaud, S. Rety, P. N. Grozdanov, K. Godin, H. van Tilbeurgh, G. Varani, U. T. Meier and N. Leulliot (2011). The H/ACA RNP assembly factor SHQ1 functions as an RNA mimic. Genes Dev 25(22): 2398-2408.

Wang, P., L. Yang, Y. Q. Gao and X. S. Zhao (2015). Accurate placement of substrate RNA by Gar1 in H/ACA RNA-guided pseudouridylation. Nucleic Acids Res 43(15): 7207-7216.

Weber, S. C. and C. P. Brangwynne (2015). Inverse size scaling of the nucleolus by a concentration-dependent phase transition. Curr Biol 25(5): 641-646.

Xiao, Z., J. G. Chang, I. A. Hendriks, J. O. Sigurethsson, J. V. Olsen and A. C. Vertegaal (2015). System-wide Analysis of SUMOylation Dynamics in Response to Replication Stress Reveals Novel Small Ubiquitin-like Modified Target Proteins and Acceptor Lysines Relevant for Genome Stability. Mol Cell Proteomics 14(5): 1419-1434.

Yang, P. K., C. Hoareau, C. Froment, B. Monsarrat, Y. Henry and G. Chanfreau (2005). Cotranscriptional recruitment of the pseudouridylsynthetase Cbf5p and of the RNA binding protein Naf1p during H/ACA snoRNP assembly. Mol Cell Biol 25(8): 3295-3304.

Yao, R. W., G. Xu, Y. Wang, L. Shan, P. F. Luan, Y. Wang, M. Wu, L. Z. Yang, Y. H. Xing, L. Yang and L. L. Chen (2019). Nascent Pre-rRNA Sorting via Phase Separation Drives the Assembly of Dense Fibrillar Components in the Human Nucleolus. Mol Cell 76(5): 767-783 e711.

Yun, C., Y. Wang, D. Mukhopadhyay, P. Backlund, N. Kolli, A. Yergey, K. D. Wilkinson and M. Dasso (2008). Nucleolar protein B23/nucleophosmin regulates the vertebrate SUMO pathway through SENP3 and SENP5 proteases. J Cell Biol 183(4): 589-595.

Zhao, X. (2018). SUMO-Mediated Regulation of Nuclear Functions and Signaling Processes. Mol Cell 71(3): 409-418.

Zhao, X. and G. Blobel (2005). A SUMO ligase is part of a nuclear multiprotein complex that affects DNA repair and chromosomal organization. Proc Natl Acad Sci U S A 102(13): 4777-4782.

Chapter 4: Discussion

4.1 Summary

As the core catalytic component of H/ACA RNPs, dyskerin dictates biogenesis of many H/ACA RNA species, as well as modification of pseudouridine targets. The regulation and function of dyskerin govern a variety of downstream pathways, including the ribosome, the spliceosome, and telomerase, and misregulation or dysfunction of the H/ACA RNP pathway causes the premature aging disease DC. The work presented in this thesis assesses two key aspects of dyskerin regulation and function: the implications of human dyskerin on hTR biogenesis in a disease context, and the regulation of dyskerin nuclear and subnuclear compartmentalization. The research carried out for this thesis contributes to the field a better understanding of dyskerin as whole, generating knowledge of both disease and fundamental basics of cellular mechanisms.

Structural studies of the N-terminal region of the yeast dyskerin homologue indicated the possibility that this region, which contains a hotspot for X-DC mutations in humans, may act as an extension of the RNA binding PUA domain of dyskerin (Li, Duan et al. 2011). Additionally, previous work from our lab demonstrated that two lysine residues in this X-DC hotspot in human dyskerin (K39 and K43) regulate hTR accumulation (Brault, Lauzon et al. 2013). The data presented in chapter 2 of this thesis demonstrate that these lysine residues mediate the interaction of dyskerin with H/ACA RNA, and that among several H/ACA RNA species examined, hTR is particularly sensitive to X-DC-causing substitutions at these residues. We also found that targeting individual hTR trimming/quality control pathways (namely PARN and the human exosome) is insufficient to compensate the defective hTR accumulation caused by these X-DC mutations, and that these mutations disrupt precursor hTR species in addition to total hTR levels.

Our previous characterization of K39 and K43 indicated a regulatory role for the posttranslational modification SUMOylation in mediating dyskerin function, as substituting K39 or K43 to arginine caused reduction of SUMOylated dyskerin levels, reduced hTR and telomerase activity, and increased telomere shortening (Brault, Lauzon et al. 2013). The data presented in chapter 3 of this thesis reveal that dyskerin contains a multitude of SUMOylation sites, including four MS-identified sites situated in the C-terminal N/NoLS which was previously reported as the key region driving dyskerin nuclear localization (Heiss, Girod et al. 1999). We observed that SUMOylation of dyskerin regulates both nuclear and nucleolar

compartmentalization of dyskerin, and demonstrated a new link between dyskerin SUMOylation, GAR1 interaction, and nucleolar localization.

4.2 Importance of characterizing the function and regulation of dyskerin for human health

As has been discussed throughout this thesis, the relevance of dyskerin to human health is evidenced by the premature aging disease X-DC. When genetic mapping was carried out in a family with DC in the 1970's and mutations in dyskerin were found responsible, this disease was initially characterized as a ribosomopathy due to the conserved function of dyskerin in pseudouridine synthesis of rRNA (Luzzatto and Karadimitris 1998). Indeed, it was later observed that a common ribosomopathy called Diamond-Blackfan anemia (DBA) also has similar pathological presentations to DC, with bone marrow failure accounting for the main cause of mortality in most patients with both diseases (Draptchinskaia, Gustavsson et al. 1999, Matsson, Klar et al. 1999, Willig, Draptchinskaia et al. 1999), and X-DC is often still described as a ribosompathy. However, a notable difference in the timing of onset of these diseases (DBA typically presents in early infancy, and age of X-DC onset ranges widely depending on inheritance and mutation) suggests a first clue as to how X-DC differs from its ribosomopathy counterpart molecularly. In 1999, we learned that dyskerin and the H/ACA complex are implicated in telomere biology, through the characterization of the H/ACA biogenesis domain in hTR (Mitchell, Cheng et al. 1999). Over many years of investigation, clinical and foundational studies revealed that there are many forms of inheritance of DC, some of which are linked to H/ACA RNA, and all of which can be linked to telomere maintenance (Podlevsky, Bley et al. 2008). Our understanding of this disease and its mechanisms is ever-expanding; however, current treatment strategies rely on symptom management and there is still no cure for patients diagnosed with DC (Fernandez Garcia and Teruya-Feldstein 2014).

Recently, a promising avenue for treating the subset of DC with hTR accumulation defects has come through a greater understanding of the RNA processing and quality control pathways involved in hTR biogenesis. Increasing hTR levels in DC patient cells has been reported to improve telomere maintenance and cell proliferation (Wong and Collins 2006, Zeng, Thumati et al. 2012). As such, the ability to target pathways involved in hTR degradation in patients with low hTR levels is a new approach being studied to treat DC, bolstered by research characterizing these pathways. The results of the work carried out for this thesis provide insight to how dyskerin fits into this biogenesis process, and suggest that in the context of X-DC

mutations, increasing hTR levels may require targeting multiple of the recently identified trimming/degradation pathways. This is consistent with recent reports detailing how the H/ACA RNP helps regulate maturation rates of hTR precursors, prevents formation of 3′ tertiary structures that would otherwise promote degradation by the exosome, and ensures PARN trimming ceases at the correct 3′ terminus of mature hTR (Nguyen, Grenier St-Sauveur et al. 2015, Tseng, Wang et al. 2015, Shukla, Schmidt et al. 2016, Tseng, Wang et al. 2018, Roake, Chen et al. 2019). Furthermore, many research groups have contributed to characterizing how the hTRAMP complex poly(A) polymerase PAPD5 factors into this biogenesis pathway, and we now know that it is also involved in regulating both the maturation rate of hTR precursors through PARN trimming, as well as in regulating recruitment of the nuclear exosome to hTR 3′ extended species (Nguyen, Grenier St-Sauveur et al. 2015, Tseng, Wang et al. 2015, Shukla, Schmidt et al. 2016, Tseng, Wang et al. 2018, Fok, Shukla et al. 2019, Roake, Chen et al. 2019). Strikingly, in hESCs carrying an X-DC mutation, while depleting either PAPD5 or the exosome component Rrp40 can rescue hTR levels, only PAPD5 depletion can rescue the ability of these hESC to undergo proper hematopoietic differentiation (Fok, Shukla et al. 2019). The results of these studies taken together can inform how to treat different forms of DC, with X-DC requiring targeting of a step upstream of multiple processing and quality control factors to increase hTR levels in a manner that contributes to improved cellular function. Indeed, pharmacological inhibitors of PAPD5 are being developed and screened in cells lines from patients with varying modes of inheritance, including those carrying mutations in PARN, dyskerin, and hTR (Nagpal, Wang et al. 2020, Shukla, Jeong et al. 2020). Understanding the complexity of this hTR biogenesis process will reveal the molecular underpinnings of the various presentations and modes of inheritance in DC, and will contribute to our ability to develop on target and functionally meaningful treatment options.

4.3 Importance of characterizing the function and regulation of dyskerin to fundamental biological processes

Dyskerin is a core essential protein. Its evolutionarily conserved function in pseudouridine synthesis stretches back to the origin of its catalytic TruB domain, which is so named for its bacterial functional orthologue (Lafontaine and Tollervey 1998). The importance of pseudouridine synthesis is undeniable, with knockout of the gene encoding dyskerin or its homologues causing lethality across eukaryotes (Jiang, Middleton et al. 1993, Phillips, Billin et

al. 1998, Giordano, Peluso et al. 1999, He, Navarrete et al. 2002, Hart, Chandrashekhar et al. 2015, Bertomeu, Coulombe-Huntington et al. 2018), but the function of this posttranscriptional modification remains murky. It is clear that chemically, pseudouridine differs from uridine in base stacking capability, and it has indeed been proposed that increased rigidity of the RNA phosphate backbone through changes in base stacking may be the main contribution of this posttranscriptional modification (Charette and Gray 2000) – but what does this mean for the function of an RNA target of dyskerin and the H/ACA complex? The essentiality of dyskerin has been attributed to its function in ribosome biogenesis, and indeed depletion of dyskerin leads to aberrant translation, global reductions in pseudouridine synthesis, and reduced mature rRNA levels (Bellodi, Krasnykh et al. 2010). While the role of dyskerin in telomerase biology may be somewhat straight forward to summarize from extensive characterization to date (hTR biogenesis), the role of dyskerin in the biology of the ribosome and spliceosome is less explicit beyond pseudouridine synthesis, but is most certainly critical. The compartmentalization of dyskerin provides a unique lens through which the regulation and function of this essential protein, and its targets, can be examined. In turn, understanding the localization of dyskerin will lend insight to fundamental aspects of nuclear and subnuclear biology, including mechanisms governing ribosome and spliceosome biogenesis.

There is growing interest in studying how LLPS mediates compartmentalization in biological systems, and understanding the phase dynamics of subnuclear membrane-free compartments like the nucleolus also provides information regarding the function of such compartments (Strom and Brangwynne 2019). While the work carried out for this thesis does not delve into LLPS directly, the results of this study are pieces that fit into the LLPS puzzle being solved for the nucleolus, and likely for other subnuclear compartments as well. More specifically, the results of this thesis work demonstrate that the localization of dyskerin to the nucleolus relies on SUMOylation, SUMO/SIM interactions, and GAR1. These findings are consistent with reported LLPS-mediated localization of the nucleolar component fibrillarin, whose localization depends in part on a GAR domain, and also with modelling studies that revealed the importance of SUMO/SIM interactions for LLPS in biological systems (Banani, Rice et al. 2016, Feric, Vaidya et al. 2016, Min, Wright et al. 2019, Yao, Xu et al. 2019).

For fibrillarin, LLPS mediates not only correct localization to the DFC where pre-rRNA posttranscriptional modification takes places, but also facilitates the correct sorting of nascent

pre-rRNA away from sites of transcription (Feric, Vaidya et al. 2016, Yao, Xu et al. 2019), radially out of the nucleolus for processing in the GC, before ribosome subunit assembly. The GAR domain allows for self-oligomerization of fibrillarin, while multivalent interactions with pre-rRNA through the MD domain (presumably guided by C/D box RNA) have been observed to nucleate fibrillarin condensates (Yao, Xu et al. 2019). When these LLPS studies of fibrillarin are taken together with our data indicating GAR1-mediated nucleolar localization of dyskerin, a universal mechanism orchestrating compartmentalization of the DFC can be envisioned, which relies on the miscibility requirements of intrinsically disordered GAR-domains and multivalent targeted interactions with pre-rRNA. This specific compartmentalization of components in the DFC is essential for the sorting of pre-rRNA, and thus it can be speculated that the purpose of the complexes responsible for posttranscriptional modification of rRNA (the H/ACA RNP and the C/D RNP) in ribosome biogenesis is to ensure sorting of pre-rRNA through the nucleolar components. Importantly, for fibrillarin, the catalytic residues of the MD region that posttranscriptionally modify pre-rRNA were reported to be dispensable for this sorting function and subsequent rRNA processing, though the downstream function of ribosomes lacking 2′-O-methylation was not assessed (Yao, Xu et al. 2019). Dyskerin and other components of the H/ACA complex were reported to be less essential for the sorting of pre-rRNA than fibrillarin, and it was suggested that this was due to less occupancy of dyskerin on pre-rRNA relative to fibrillarin (Yao, Xu et al. 2019). It remains to be examined whether the function of dyskerin as a pseudouridine synthase is connected to DFC compartmentalization. As depletion of dyskerin leads to reduced rRNA levels, but single pseudouridine sites are dispensable for ribosome function (King, Liu et al. 2003, Liang, Liu et al. 2007, Liang, Liu et al. 2009, Lemay, D'Amours et al. 2010), it may be the case that pseudouridine sites in the rRNA serve as placement guides for nucleation of H/ACA complexes in the DFC along the pre-rRNA. Just as the C/D complex is responsible for sorting nascent pre-rRNA away from transcription start sites at the FC/DFC interface, H/ACA complex placement may ensure efficient sorting of the pre-rRNA out of the DFC, after pre-rRNA begins being sorted by interactions with fibrillarin and C/D RNPs. Coordination of this process could be provided by the specificity and variety of snoRNA which interact with pre-rRNA at the sites of 2′-O-methylation and pseudouridine synthesis through base pairing, and changes in base stacking (for example, following the conversion of uridine to pseudouridine) may facilitate the release and subsequent sorting of pre-rRNA. However, these

hypotheses are conjecture based on the current information regarding nucleolar compartmentalization and posttranscriptional modifications of rRNA.

The SUMOylation-mediated interaction of dyskerin with the GAR1 SIM newly characterized in this thesis is also consistent with nucleolar localization being dependent on LLPS dynamics. It has been demonstrated through modelling of LLPS dynamics in cells that SUMO/SIM interactions facilitate condensate formation through mediating the interaction strength/efficiency of SUMO target and SIM domain-containing proteins, and that the potential for multivalent assemblies of SUMO chains and polySIM domains helps concentrate components of a condensate to drive compartmentalization with dynamics resembling LLPS (Banani, Rice et al. 2016, Min, Wright et al. 2019). Our observation that permanently SUMOylated dyskerin is excluded from the nucleolus, along with previous reports that GC-resident proteins require deSUMOylation by SENP3 for nucleolar retention (Finkbeiner, Haindl et al. 2011, Finkbeiner, Haindl et al. 2011) suggest that while SUMO/SIM interactions may initiate nucleolar compartmentalization of resident nucleolar proteins, deSUMOylation is just as essential to regulate compartmentalization. It is tempting to speculate how this fits into the stepwise H/ACA complex assembly model, whereby maturation of the H/ACA complex may occur in transit between the H/ACA RNA transcription start site and the mature complex destination of the DFC. SUMOylation mediates efficient interaction between dyskerin and GAR1, and if GAR1 drives dyskerin DFC miscibility but permanent SUMOylation prevents nucleolar miscibility, this could imply that deSUMOylation of dyskerin after mature H/ACA complex assembly is essential for DFC miscibility. As SENP3 and SENP5, the nucleolar SUMO-specific proteases localize to the outermost component of the nucleolus with NPM1 (Haindl, Harasim et al. 2008, Yun, Wang et al. 2008), deSUMOylation of the mature H/ACA RNP may very well take place in the GC on the way to the H/ACA RNP's functional subnuclear compartment, allowing for DFC miscibility only once SUMO is removed. Importantly, the disassembly and reassembly of the nucleolar compartments must take place each cell cycle for mitosis, and posttranslational modifications including SUMOylation/deSUMOylation cycles could also act as a dynamic switch for this process (Strom and Brangwynne 2019). Thus, characterizing regulation of dyskerin localization contributes foundation and support for fundamental concepts in posttranscriptional modification of RNA, pre-rRNA sorting mechanisms, and dynamics of nucleolar compartmentalization.

4.3 Future directions

As has been eluded to in the discussion sections above, there are many important potential future avenues for studying dyskerin that can come from this thesis work. In the context of human health, it would be meaningful to examine the impact of depleting or inhibiting PAPD5 and other TRAMP complex components on DC mutations that cause hTR accumulation defects. As the development and testing of PAPD5 pharmacological inhibitors is ongoing in the field, it would be feasible to begin examining this in patient cells, and eventually mouse models carrying disease-causing mutations, such as male mice carrying X-DC mutations (He, Gu et al. 2009). Future characterization of other residues in the N-terminal X-DC hotspot to examine how and to what extent this region mediates the dyskerin-hTR interaction would also be a logical next step in fully understanding this disease.

In the future, we will also assess how H/ACA complex assembly defects caused by mislocalization disrupt dyskerin function. This will be examined in the context of telomerase activity and H/ACA RNA biogenesis. In order to assess telomerase activity and H/ACA RNA levels, endogenous dyskerin will be depleted via siRNA targeting the 3' UTR of dyskerin in cells with or without stable expression of FLAG-tagged dyskerin wildtype or N/NoLS variants. After depletion, telomerase activity will be measured in the cell lysate using Q-TRAP, as was previously performed to assess the X-DC variants described in Chapter 2. The H/ACA RNA levels will also be assessed after depletion by TGIRT-seq and using the CoCo analysis pipeline developed by Dr. Michelle Scott's lab at Université de Sherbrooke. This specialized RNA sequencing technique was specifically developed to study structured RNA, which can be difficult to assess with normal RNA sequencing methods due to difficulties of conventional reverse transcriptase enzymes to produce cDNA libraries from highly structured RNA (Boivin, Deschamps-Francoeur et al. 2018). CoCo is also a pipeline specific for intron-encoded RNAs like H/ACA RNA, as typical RNA sequencing analysis pipelines discard or misassign intronic reads (Deschamps-Francoeur, Boivin et al. 2019).

Finally, the relatively new field of LLPS in biological systems raises many novel research questions. Studying the phase dynamics of dyskerin, not only in the nucleolus but in Cajal bodies as well, will be essential to understanding the complete picture of dyskerin and H/ACA complex function and regulation. Does dyskerin form liquid-like condensates, and if so, how do dyskerin condensates behave with and without SUMOylation/GAR1/RNA interactions? As described, key

techniques to answer these questions *in vitro* and in cells have been applied to other nucleolar resident proteins (Feric, Vaidya et al. 2016, Yao, Xu et al. 2019), indicating that this future direction for studying dyskerin is both intriguing and feasible. Characterization of pseudouridine synthesis through the lens of phase dynamics may also provide novel insights to this evidently important yet incompletely understood posttranscriptional modification.

4.4 Concluding Remarks

The study of dyskerin function and regulation is crucial to understanding many fundamental aspects of cellular biology, exemplified by the roles of dyskerin in ribosome, spliceosome, and telomerase biogenesis. Unified by the characterization of this H/ACA RNP and telomerase-associated component, the results of this thesis reveal new functional aspects of human dyskerin and how it is regulated. For the first time, we demonstrated that the N-terminus of human dyskerin can mediate the interaction between dyskerin and hTR, and offer a possible explanation for how the N-terminal hotspot of X-DC causes hTR accumulation defects that drive disease. We also establish a novel role for SUMOylation in regulating the nuclear and nucleolar localization of dyskerin and mature H/ACA complex assembly, as well as identify a previously unreported SIM in GAR1 which is essential for efficient dyskerin-GAR1 interaction. In summation, this body of work spans the broad scope of studying this essential protein, and perhaps more important than new insights, it also provides new avenues for examining the importance of dyskerin function and regulation.

Reference List

Adachi, H. and Y. T. Yu (2014). Insight into the mechanisms and functions of spliceosomal snRNA pseudouridylation. World J Biol Chem **5**(4): 398-408.

Akiyama, B. M., J. W. Parks and M. D. Stone (2015). The telomerase essential N-terminal domain promotes DNA synthesis by stabilizing short RNA-DNA hybrids. Nucleic Acids Res **43**(11): 5537-5549.

Andrade, L. E., E. M. Tan and E. K. Chan (1993). Immunocytochemical analysis of the coiled body in the cell cycle and during cell proliferation. Proc Natl Acad Sci U S A **90**(5): 1947-1951.

Antolini, F., M. Lo Bello and M. Sette (2003). Purified promyelocytic leukemia coiled-coil aggregates as a tetramer displaying low alpha-helical content. Protein Expr Purif **29**(1): 94-102.

Arngrimsson, R., I. Dokal, L. Luzzatto and J. M. Connor (1993). Dyskeratosis congenita: three additional families show linkage to a locus in Xq28. J Med Genet **30**(7): 618-619.

Bachand, F. and C. Autexier (2001). Functional regions of human telomerase reverse transcriptase and human telomerase RNA required for telomerase activity and RNA-protein interactions. Mol Cell Biol **21**(5): 1888-1897.

Baker, D. L., O. A. Youssef, M. I. Chastkofsky, D. A. Dy, R. M. Terns and M. P. Terns (2005). RNA-guided RNA modification: functional organization of the archaeal H/ACA RNP. Genes Dev **19**(10): 1238-1248.

Balakin, A. G., L. Smith and M. J. Fournier (1996). The RNA world of the nucleolus: two major families of small RNAs defined by different box elements with related functions. Cell **86**(5): 823-834.

Ballarino, M., M. Morlando, F. Pagano, A. Fatica and I. Bozzoni (2005). The cotranscriptional assembly of snoRNPs controls the biosynthesis of H/ACA snoRNAs in Saccharomyces cerevisiae. Mol Cell Biol **25**(13): 5396-5403.

Banani, S. F., H. O. Lee, A. A. Hyman and M. K. Rosen (2017). Biomolecular condensates: organizers of cellular biochemistry. Nat Rev Mol Cell Biol **18**(5): 285-298.

Banani, S. F., A. M. Rice, W. B. Peeples, Y. Lin, S. Jain, R. Parker and M. K. Rosen (2016). Compositional Control of Phase-Separated Cellular Bodies. Cell **166**(3): 651-663.

Barroso-Gonzalez, J., L. Garcia-Exposito, S. M. Hoang, M. L. Lynskey, J. L. Roncaioli, A. Ghosh, C. T. Wallace, M. Modesti, K. A. Bernstein, S. N. Sarkar, S. C. Watkins and R. J. O'Sullivan (2019). RAD51AP1 Is an Essential Mediator of Alternative Lengthening of Telomeres. Mol Cell **76**(1): 217.

Baumann, P. and T. R. Cech (2001). Pot1, the putative telomere end-binding protein in fission yeast and humans. Science **292**(5519): 1171-1175.

Baumann, P. and C. Price (2010). Pot1 and telomere maintenance. FEBS Lett **584**(17): 3779-3784.

Beattie, T. L., W. Zhou, M. O. Robinson and L. Harrington (1998). Reconstitution of human telomerase activity in vitro. Curr Biol **8**(3): 177-180.

Beaulieu, Y. B., C. L. Kleinman, A. M. Landry-Voyer, J. Majewski and F. Bachand (2012). Polyadenylation-dependent control of long noncoding RNA expression by the poly(A)-binding protein nuclear 1. PLoS Genet **8**(11): e1003078.

Becker, J., S. V. Barysch, S. Karaca, C. Dittner, H. H. Hsiao, M. Berriel Diaz, S. Herzig, H. Urlaub and F. Melchior (2013). Detecting endogenous SUMO targets in mammalian cells and tissues. Nat Struct Mol Biol **20**(4): 525-531.

Bellodi, C., N. Kopmar and D. Ruggero (2010). Deregulation of oncogene-induced senescence and p53 translational control in X-linked dyskeratosis congenita. EMBO J **29**(11): 1865-1876.

Bellodi, C., O. Krasnykh, N. Haynes, M. Theodoropoulou, G. Peng, L. Montanaro and D. Ruggero (2010). Loss of function of the tumor suppressor DKC1 perturbs p27 translation control and contributes to pituitary tumorigenesis. Cancer Res **70**(14): 6026-6035.

Benyelles, M., M. F. O'Donohue, L. Kermasson, E. Lainey, R. Borie, C. Lagresle-Peyrou, H. Nunes, C. Cazelles, C. Fourrage, E. Ollivier, A. Marcais, A. S. Gamez, F. Morice-Picard, D. Caillaud, N. Pottier, C. Menard, I. Ba, A. Fernandes, B. Crestani, J. P. de Villartay, P. E. Gleizes, I. Callebaut, C. Kannengiesser and P. Revy (2020). NHP2 deficiency impairs rRNA biogenesis and causes pulmonary fibrosis and Hoyeraal-Hreidarsson syndrome. Hum Mol Genet.

Bertomeu, T., J. Coulombe-Huntington, A. Chatr-Aryamontri, K. G. Bourdages, E. Coyaud, B. Raught, Y. Xia and M. Tyers (2018). A High-Resolution Genome-Wide CRISPR/Cas9 Viability Screen Reveals Structural Features and Contextual Diversity of the Human Cell-Essential Proteome. Mol Cell Biol **38**(1).

Bizarro, J., A. Bhardwaj, S. Smith and U. T. Meier (2019). Nopp140-mediated concentration of telomerase in Cajal bodies regulates telomere length. Mol Biol Cell **30**(26): 3136-3150.

Bizarro, J. and U. T. Meier (2017). Inherited SHQ1 mutations impair interaction with NAP57/dyskerin, a major target in dyskeratosis congenita. Mol Genet Genomic Med **5**(6): 805-808.

Bodnar, A. G., M. Ouellette, M. Frolkis, S. E. Holt, C. P. Chiu, G. B. Morin, C. B. Harley, J. W. Shay, S. Lichtsteiner and W. E. Wright (1998). Extension of life-span by introduction of telomerase into normal human cells. Science **279**(5349): 349-352.

Boisvert, F. M., S. van Koningsbruggen, J. Navascues and A. I. Lamond (2007). The multifunctional nucleolus. Nat Rev Mol Cell Biol **8**(7): 574-585.

Boivin, V., G. Deschamps-Francoeur, S. Couture, R. M. Nottingham, P. Bouchard-Bourelle, A. M. Lambowitz, M. S. Scott and S. Abou-Elela (2018). Simultaneous sequencing of coding and noncoding RNA reveals a human transcriptome dominated by a small number of highly expressed noncoding genes. RNA **24**(7): 950-965.

Bousquet-Antonelli, C., Y. Henry, P. G'Elugne J, M. Caizergues-Ferrer and T. Kiss (1997). A small nucleolar RNP protein is required for pseudouridylation of eukaryotic ribosomal RNAs. EMBO J **16**(15): 4770-4776.

Box, J. A., J. T. Bunch, W. Tang and P. Baumann (2008). Spliceosomal cleavage generates the 3' end of telomerase RNA. Nature **456**(7224): 910-914.

Brangwynne, C. P., C. R. Eckmann, D. S. Courson, A. Rybarska, C. Hoege, J. Gharakhani, F. Julicher and A. A. Hyman (2009). Germline P granules are liquid droplets that localize by controlled dissolution/condensation. Science **324**(5935): 1729-1732.

Brangwynne, C. P., T. J. Mitchison and A. A. Hyman (2011). Active liquid-like behavior of nucleoli determines their size and shape in Xenopus laevis oocytes. Proc Natl Acad Sci U S A **108**(11): 4334-4339.

Brault, M. E., C. Lauzon and C. Autexier (2013). Dyskeratosis congenita mutations in dyskerin SUMOylation consensus sites lead to impaired telomerase RNA accumulation and telomere defects. Hum Mol Genet **22**(17): 3498-3507.

Brouwer, A. K., J. Schimmel, J. C. Wiegant, A. C. Vertegaal, H. J. Tanke and R. W. Dirks (2009). Telomeric DNA mediates de novo PML body formation. Mol Biol Cell **20**(22): 4804-4815.

Brun, S., N. Abella, M. T. Berciano, O. Tapia, M. Jaumot, R. Freire, M. Lafarga and N. Agell (2017). SUMO regulates p21Cip1 intracellular distribution and with p21Cip1 facilitates multiprotein complex formation in the nucleolus upon DNA damage. PLoS One **12**(6): e0178925.

Bryan, T. M., A. Englezou, J. Gupta, S. Bacchetti and R. R. Reddel (1995). Telomere elongation in immortal human cells without detectable telomerase activity. EMBO J **14**(17): 4240-4248.

Castle, C. D., E. K. Cassimere and C. Denicourt (2012). LAS1L interacts with the mammalian Rix1 complex to regulate ribosome biogenesis. Mol Biol Cell **23**(4): 716-728.

Castle, C. D., E. K. Cassimere, J. Lee and C. Denicourt (2010). Las1L is a nucleolar protein required for cell proliferation and ribosome biogenesis. Mol Cell Biol **30**(18): 4404-4414.

Caton, E. A., E. K. Kelly, R. Kamalampeta and U. Kothe (2018). Efficient RNA pseudouridylation by eukaryotic H/ACA ribonucleoproteins requires high affinity binding and correct positioning of guide RNA. Nucleic Acids Res **46**(2): 905-916.

Cavaille, J., M. Nicoloso and J. P. Bachellerie (1996). Targeted ribose methylation of RNA in vivo directed by tailored antisense RNA guides. Nature **383**(6602): 732-735.

Celetti, G., G. Paci, J. Caria, V. VanDelinder, G. Bachand and E. A. Lemke (2020). The liquid state of FG-nucleoporins mimics permeability barrier properties of nuclear pore complexes. J Cell Biol **219**(1).

Charette, M. and M. W. Gray (2000). Pseudouridine in RNA: what, where, how, and why. IUBMB Life **49**(5): 341-351.

Chen, J. L., M. A. Blasco and C. W. Greider (2000). Secondary structure of vertebrate telomerase RNA. Cell **100**(5): 503-514.

Chen, J. L. and C. W. Greider (2005). Functional analysis of the pseudoknot structure in human telomerase RNA. Proc Natl Acad Sci U S A **102**(23): 8080-8085; discussion 8077-8089.

Chen, J. L., K. K. Opperman and C. W. Greider (2002). A critical stem-loop structure in the CR4-CR5 domain of mammalian telomerase RNA. Nucleic Acids Res **30**(2): 592-597.

Chen, L., C. M. Roake, A. Freund, P. J. Batista, S. Tian, Y. A. Yin, C. R. Gajera, S. Lin, B. Lee, M. F. Pech, A. S. Venteicher, R. Das, H. Y. Chang and S. E. Artandi (2018). An Activity Switch in Human Telomerase Based on RNA Conformation and Shaped by TCAB1. Cell **174**(1): 218-230 e213.

Chen, L., C. M. Roake, A. Galati, F. Bavasso, E. Micheli, I. Saggio, S. Schoeftner, S. Cacchione, M. Gatti, S. E. Artandi and G. D. Raffa (2020). Loss of Human TGS1 Hypermethylase Promotes Increased Telomerase RNA and Telomere Elongation. Cell Rep **30**(5): 1358-1372 e1355.

Cheutin, T., M. F. O'Donohue, A. Beorchia, M. Vandelaer, H. Kaplan, B. Defever, D. Ploton and M. Thiry (2002). Three-dimensional organization of active rRNA genes within the nucleolus. J Cell Sci **115**(Pt 16): 3297-3307.

Chu, T. W., Y. D'Souza and C. Autexier (2016). The Insertion in Fingers Domain in Human Telomerase Can Mediate Enzyme Processivity and Telomerase Recruitment to Telomeres in a TPP1-Dependent Manner. Mol Cell Biol **36**(1): 210-222.

Chu, T. W., D. E. MacNeil and C. Autexier (2016). Multiple Mechanisms Contribute to the Cell Growth Defects Imparted by Human Telomerase Insertion in Fingers Domain Mutations Associated with Premature Aging Diseases. J Biol Chem **291**(16): 8374-8386.

Chung, I., H. Leonhardt and K. Rippe (2011). De novo assembly of a PML nuclear subcompartment occurs through multiple pathways and induces telomere elongation. J Cell Sci **124**(Pt 21): 3603-3618.

Churikov, D., F. Charifi, N. Eckert-Boulet, S. Silva, M. N. Simon, M. Lisby and V. Geli (2016). SUMO-Dependent Relocalization of Eroded Telomeres to Nuclear Pore Complexes Controls Telomere Recombination. Cell Rep **15**(6): 1242-1253.

Cohen, L. S., C. Mikhli, X. Jiao, M. Kiledjian, G. Kunkel and R. E. Davis (2005). Dcp2 Decaps m2,2,7GpppN-capped RNAs, and its activity is sequence and context dependent. Mol Cell Biol **25**(20): 8779-8791.

Cohen, S. B., M. E. Graham, G. O. Lovrecz, N. Bache, P. J. Robinson and R. R. Reddel (2007). Protein composition of catalytically active human telomerase from immortal cells. Science **315**(5820): 1850-1853.

Connor, J. M., D. Gatherer, F. C. Gray, L. A. Pirrit and N. A. Affara (1986). Assignment of the gene for dyskeratosis congenita to Xq28. Hum Genet **72**(4): 348-351.

Cristofari, G., E. Adolf, P. Reichenbach, K. Sikora, R. M. Terns, M. P. Terns and J. Lingner (2007). Human telomerase RNA accumulation in Cajal bodies facilitates telomerase recruitment to telomeres and telomere elongation. Mol Cell **27**(6): 882-889.

d'Adda di Fagagna, F., P. M. Reaper, L. Clay-Farrace, H. Fiegler, P. Carr, T. Von Zglinicki, G. Saretzki, N. P. Carter and S. P. Jackson (2003). A DNA damage checkpoint response in telomere-initiated senescence. Nature **426**(6963): 194-198.

D'Souza, Y., T. W. Chu and C. Autexier (2013). A translocation-defective telomerase with low levels of activity and processivity stabilizes short telomeres and confers immortalization. Mol Biol Cell **24**(9): 1469-1479.

Darzacq, X., B. E. Jady, C. Verheggen, A. M. Kiss, E. Bertrand and T. Kiss (2002). Cajal body-specific small nuclear RNAs: a novel class of 2'-O-methylation and pseudouridylation guide RNAs. EMBO J **21**(11): 2746-2756.

Darzacq, X., N. Kittur, S. Roy, Y. Shav-Tal, R. H. Singer and U. T. Meier (2006). Stepwise RNP assembly at the site of H/ACA RNA transcription in human cells. J Cell Biol **173**(2): 207-218.

Davis, D. R. (1995). Stabilization of RNA stacking by pseudouridine. Nucleic Acids Res **23**(24): 5020-5026.

Decatur, W. A. and M. J. Fournier (2002). rRNA modifications and ribosome function. Trends Biochem Sci **27**(7): 344-351.

Deng, T., Y. Huang, K. Weng, S. Lin, Y. Li, G. Shi, Y. Chen, J. Huang, D. Liu, W. Ma and Z. Songyang (2019). TOE1 acts as a 3' exonuclease for telomerase RNA and regulates telomere maintenance. Nucleic Acids Res **47**(1): 391-405.

Deschamps-Francoeur, G., V. Boivin, S. Abou Elela and M. S. Scott (2019). CoCo: RNA-seq read assignment correction for nested genes and multimapped reads. Bioinformatics **35**(23): 5039-5047.

Desterro, J. M., M. S. Rodriguez, G. D. Kemp and R. T. Hay (1999). Identification of the enzyme required for activation of the small ubiquitin-like protein SUMO-1. J Biol Chem **274**(15): 10618-10624.

Dhanraj, S., S. M. Gunja, A. P. Deveau, M. Nissbeck, B. Boonyawat, A. J. Coombs, A. Renieri, M. Mucciolo, A. Marozza, S. Buoni, L. Turner, H. Li, A. Jarrar, M. Sabanayagam, M. Kirby, M. Shago, D. Pinto, J. N. Berman, S. W. Scherer, A. Virtanen and Y. Dror (2015). Bone marrow failure and developmental delay caused by mutations in poly(A)-specific ribonuclease (PARN). J Med Genet **52**(11): 738-748.

Di Bacco, A., J. Ouyang, H. Y. Lee, A. Catic, H. Ploegh and G. Gill (2006). The SUMO-specific protease SENP5 is required for cell division. Mol Cell Biol **26**(12): 4489-4498.

Dieci, G., M. Preti and B. Montanini (2009). Eukaryotic snoRNAs: a paradigm for gene expression flexibility. Genomics **94**(2): 83-88.

Dokal, I. (1996). Dyskeratosis congenita: an inherited bone marrow failure syndrome. Br J Haematol **92**(4): 775-779.

Donmez, G., K. Hartmuth and R. Luhrmann (2004). Modified nucleotides at the 5' end of human U2 snRNA are required for spliceosomal E-complex formation. RNA **10**(12): 1925-1933.

Drachtman, R. A. and B. P. Alter (1992). Dyskeratosis congenita: clinical and genetic heterogeneity. Report of a new case and review of the literature. Am J Pediatr Hematol Oncol **14**(4): 297-304.

Draptchinskaia, N., P. Gustavsson, B. Andersson, M. Pettersson, T. N. Willig, I. Dianzani, S. Ball, G. Tchernia, J. Klar, H. Matsson, D. Tentler, N. Mohandas, B. Carlsson and N. Dahl (1999). The gene encoding ribosomal protein S19 is mutated in Diamond-Blackfan anaemia. Nat Genet **21**(2): 169-175.

Dundr, M., M. D. Hebert, T. S. Karpova, D. Stanek, H. Xu, K. B. Shpargel, U. T. Meier, K. M. Neugebauer, A. G. Matera and T. Misteli (2004). In vivo kinetics of Cajal body components. J Cell Biol **164**(6): 831-842.

Egan, E. D. and K. Collins (2010). Specificity and stoichiometry of subunit interactions in the human telomerase holoenzyme assembled in vivo. Mol Cell Biol **30**(11): 2775-2786.

Egan, E. D. and K. Collins (2012). Biogenesis of telomerase ribonucleoproteins. RNA **18**(10): 1747-1759.

Egan, E. D. and K. Collins (2012). An enhanced H/ACA RNP assembly mechanism for human telomerase RNA. Mol Cell Biol **32**(13): 2428-2439.

El-Asmi, F., F. P. McManus, C. E. Brantis-de-Carvalho, J. C. Valle-Casuso, P. Thibault and M. K. Chelbi-Alix (2020). Cross-talk between SUMOylation and ISGylation in response to interferon. Cytokine **129**: 155025.

Elbaum-Garfinkle, S. (2019). Matter over mind: Liquid phase separation and neurodegeneration. J Biol Chem **294**(18): 7160-7168.

Feng, J., W. D. Funk, S. S. Wang, S. L. Weinrich, A. A. Avilion, C. P. Chiu, R. R. Adams, E. Chang, R. C. Allsopp, J. Yu and et al. (1995). The RNA component of human telomerase. Science **269**(5228): 1236-1241.

Feric, M., N. Vaidya, T. S. Harmon, D. M. Mitrea, L. Zhu, T. M. Richardson, R. W. Kriwacki, R. V. Pappu and C. P. Brangwynne (2016). Coexisting Liquid Phases Underlie Nucleolar Subcompartments. Cell **165**(7): 1686-1697.

Fernandez Garcia, M. S. and J. Teruya-Feldstein (2014). The diagnosis and treatment of dyskeratosis congenita: a review. J Blood Med **5**: 157-167.

Finkbeiner, E., M. Haindl and S. Muller (2011). The SUMO system controls nucleolar partitioning of a novel mammalian ribosome biogenesis complex. EMBO J **30**(6): 1067-1078.

Finkbeiner, E., M. Haindl, N. Raman and S. Muller (2011). SUMO routes ribosome maturation. Nucleus **2**(6): 527-532.

Fok, W. C., S. Shukla, A. T. Vessoni, K. A. Brenner, R. Parker, C. M. Sturgeon and L. F. Z. Batista (2019). Posttranscriptional modulation of TERC by PAPD5 inhibition rescues hematopoietic development in dyskeratosis congenita. Blood **133**(12): 1308-1312.

Frank, A. K., D. C. Tran, R. W. Qu, B. A. Stohr, D. J. Segal and L. Xu (2015). The Shelterin TIN2 Subunit Mediates Recruitment of Telomerase to Telomeres. PLoS Genet **11**(7): e1005410.

Frey, M. R., A. D. Bailey, A. M. Weiner and A. G. Matera (1999). Association of snRNA genes with coiled bodies is mediated by nascent snRNA transcripts. Curr Biol **9**(3): 126-135.

Fu, D. and K. Collins (2003). Distinct biogenesis pathways for human telomerase RNA and H/ACA small nucleolar RNAs. Mol Cell **11**(5): 1361-1372.

Fu, D. and K. Collins (2007). Purification of human telomerase complexes identifies factors involved in telomerase biogenesis and telomere length regulation. Mol Cell **28**(5): 773-785.

Gable, D. L., V. Gaysinskaya, C. C. Atik, C. C. Talbot, Jr., B. Kang, S. E. Stanley, E. W. Pugh, N. Amat-Codina, K. M. Schenk, M. O. Arcasoy, C. Brayton, L. Florea and M. Armanios (2019). ZCCHC8, the nuclear exosome targeting component, is mutated in familial pulmonary fibrosis and is required for telomerase RNA maturation. Genes Dev **33**(19-20): 1381-1396.

Gallardo, F., C. Olivier, A. T. Dandjinou, R. J. Wellinger and P. Chartrand (2008). TLC1 RNA nucleo-cytoplasmic trafficking links telomerase biogenesis to its recruitment to telomeres. EMBO J **27**(5): 748-757.

Ganot, P., M. L. Bortolin and T. Kiss (1997). Site-specific pseudouridine formation in preribosomal RNA is guided by small nucleolar RNAs. Cell **89**(5): 799-809.

Ganot, P., M. Caizergues-Ferrer and T. Kiss (1997). The family of box ACA small nucleolar RNAs is defined by an evolutionarily conserved secondary structure and ubiquitous sequence elements essential for RNA accumulation. Genes Dev **11**(7): 941-956.

Ganot, P., B. E. Jady, M. L. Bortolin, X. Darzacq and T. Kiss (1999). Nucleolar factors direct the 2'-O-ribose methylation and pseudouridylation of U6 spliceosomal RNA. Mol Cell Biol **19**(10): 6906-6917.

Ghosh, T., B. Peterson, N. Tomasevic and B. A. Peculis (2004). Xenopus U8 snoRNA binding protein is a conserved nuclear decapping enzyme. Mol Cell **13**(6): 817-828.

Gillies, J., C. M. Hickey, D. Su, Z. Wu, J. Peng and M. Hochstrasser (2016). SUMO Pathway Modulation of Regulatory Protein Binding at the Ribosomal DNA Locus in Saccharomyces cerevisiae. Genetics **202**(4): 1377-1394.

Giordano, E., I. Peluso, S. Senger and M. Furia (1999). minifly, a Drosophila gene required for ribosome biogenesis. J Cell Biol **144**(6): 1123-1133.

Girard, J. P., H. Lehtonen, M. Caizergues-Ferrer, F. Amalric, D. Tollervey and B. Lapeyre (1992). GAR1 is an essential small nucleolar RNP protein required for pre-rRNA processing in yeast. EMBO J **11**(2): 673-682.

Goldfarb, K. C. and T. R. Cech (2013). 3' terminal diversity of MRP RNA and other human noncoding RNAs revealed by deep sequencing. BMC Mol Biol **14**: 23.

Gomez, D. E., R. G. Armando, H. G. Farina, P. L. Menna, C. S. Cerrudo, P. D. Ghiringhelli and D. F. Alonso (2012). Telomere structure and telomerase in health and disease (review). Int J Oncol **41**(5): 1561-1569.

Gong, L., S. Millas, G. G. Maul and E. T. Yeh (2000). Differential regulation of sentrinized proteins by a novel sentrin-specific protease. J Biol Chem **275**(5): 3355-3359.

Gong, L. and E. T. Yeh (1999). Identification of the activating and conjugating enzymes of the NEDD8 conjugation pathway. J Biol Chem **274**(17): 12036-12042.

Gong, L. and E. T. Yeh (2006). Characterization of a family of nucleolar SUMO-specific proteases with preference for SUMO-2 or SUMO-3. J Biol Chem **281**(23): 15869-15877.

Greider, C. W. (1991). Telomerase is processive. Mol Cell Biol **11**(9): 4572-4580.

Greider, C. W. and E. H. Blackburn (1985). Identification of a specific telomere terminal transferase activity in Tetrahymena extracts. Cell **43**(2 Pt 1): 405-413.

Greider, C. W. and E. H. Blackburn (1987). The telomere terminal transferase of Tetrahymena is a ribonucleoprotein enzyme with two kinds of primer specificity. Cell **51**(6): 887-898.

Greider, C. W. and E. H. Blackburn (1989). A telomeric sequence in the RNA of Tetrahymena telomerase required for telomere repeat synthesis. Nature **337**(6205): 331-337.

Griffith, J. D., L. Comeau, S. Rosenfield, R. M. Stansel, A. Bianchi, H. Moss and T. de Lange (1999). Mammalian telomeres end in a large duplex loop. Cell **97**(4): 503-514.

Grill, S., V. M. Tesmer and J. Nandakumar (2018). The N Terminus of the OB Domain of Telomere Protein TPP1 Is Critical for Telomerase Action. Cell Rep **22**(5): 1132-1140.

Grobelny, J. V., A. K. Godwin and D. Broccoli (2000). ALT-associated PML bodies are present in viable cells and are enriched in cells in the G(2)/M phase of the cell cycle. J Cell Sci **113 Pt 24**: 4577-4585.

Grozdanov, P. N., N. Fernandez-Fuentes, A. Fiser and U. T. Meier (2009). Pathogenic NAP57 mutations decrease ribonucleoprotein assembly in dyskeratosis congenita. Hum Mol Genet **18**(23): 4546-4551.

Grozdanov, P. N., S. Roy, N. Kittur and U. T. Meier (2009). SHQ1 is required prior to NAF1 for assembly of H/ACA small nucleolar and telomerase RNPs. RNA **15**(6): 1188-1197.

Grzechnik, P. and J. Kufel (2008). Polyadenylation linked to transcription termination directs the processing of snoRNA precursors in yeast. Mol Cell **32**(2): 247-258.

Gu, B. W., M. Apicella, J. Mills, J. M. Fan, D. A. Reeves, D. French, G. M. Podsakoff, M. Bessler and P. J. Mason (2015). Impaired Telomere Maintenance and Decreased Canonical WNT Signaling but Normal Ribosome Biogenesis in Induced Pluripotent Stem Cells from X-Linked Dyskeratosis Congenita Patients. PLoS One **10**(5): e0127414.

Gunisova, S., E. Elboher, J. Nosek, V. Gorkovoy, Y. Brown, J. F. Lucier, N. Laterreur, R. J. Wellinger, Y. Tzfati and L. Tomaska (2009). Identification and comparative analysis of

telomerase RNAs from Candida species reveal conservation of functional elements. RNA **15**(4): 546-559.

Gupta, S. K., L. Kolet, T. Doniger, V. K. Biswas, R. Unger, Y. Tzfati and S. Michaeli (2013). The Trypanosoma brucei telomerase RNA (TER) homologue binds core proteins of the C/D snoRNA family. FEBS Lett **587**(9): 1399-1404.

Hacot, S., Y. Coute, S. Belin, M. A. Albaret, H. C. Mertani, J. C. Sanchez, M. Rosa-Calatrava and J. J. Diaz (2010). Isolation of nucleoli. Curr Protoc Cell Biol **Chapter 3**: Unit3 36.

Haindl, M., T. Harasim, D. Eick and S. Muller (2008). The nucleolar SUMO-specific protease SENP3 reverses SUMO modification of nucleophosmin and is required for rRNA processing. EMBO Rep **9**(3): 273-279.

Hanahan, D. and R. A. Weinberg (2000). The hallmarks of cancer. Cell **100**(1): 57-70.

Hanahan, D. and R. A. Weinberg (2011). Hallmarks of cancer: the next generation. Cell **144**(5): 646-674.

Handwerger, K. E., J. A. Cordero and J. G. Gall (2005). Cajal bodies, nucleoli, and speckles in the Xenopus oocyte nucleus have a low-density, sponge-like structure. Mol Biol Cell **16**(1): 202-211.

Handwerger, K. E., C. Murphy and J. G. Gall (2003). Steady-state dynamics of Cajal body components in the Xenopus germinal vesicle. J Cell Biol **160**(4): 495-504.

Hart, T., M. Chandrashekhar, M. Aregger, Z. Steinhart, K. R. Brown, G. MacLeod, M. Mis, M. Zimmermann, A. Fradet-Turcotte, S. Sun, P. Mero, P. Dirks, S. Sidhu, F. P. Roth, O. S. Rissland, D. Durocher, S. Angers and J. Moffat (2015). High-Resolution CRISPR Screens Reveal Fitness Genes and Genotype-Specific Cancer Liabilities. Cell **163**(6): 1515-1526.

Hay, R. T. (2005). SUMO: a history of modification. Mol Cell **18**(1): 1-12.

Hayflick, L. (1965). The Limited in Vitro Lifetime of Human Diploid Cell Strains. Exp Cell Res **37**: 614-636.

He, J., B. W. Gu, J. Ge, Y. Mochizuki, M. Bessler and P. J. Mason (2009). Variable expression of Dkc1 mutations in mice. Genesis **47**(6): 366-373.

He, J., S. Navarrete, M. Jasinski, T. Vulliamy, I. Dokal, M. Bessler and P. J. Mason (2002). Targeted disruption of Dkc1, the gene mutated in X-linked dyskeratosis congenita, causes embryonic lethality in mice. Oncogene **21**(50): 7740-7744.

Hebert, M. D., P. W. Szymczyk, K. B. Shpargel and A. G. Matera (2001). Coilin forms the bridge between Cajal bodies and SMN, the spinal muscular atrophy protein. Genes Dev **15**(20): 2720-2729.

Hecker, C. M., M. Rabiller, K. Haglund, P. Bayer and I. Dikic (2006). Specification of SUMO1- and SUMO2-interacting motifs. J Biol Chem **281**(23): 16117-16127.

Heiss, N. S., A. Girod, R. Salowsky, S. Wiemann, R. Pepperkok and A. Poustka (1999). Dyskerin localizes to the nucleolus and its mislocalization is unlikely to play a role in the pathogenesis of dyskeratosis congenita. Hum Mol Genet **8**(13): 2515-2524.

Heiss, N. S., S. W. Knight, T. J. Vulliamy, S. M. Klauck, S. Wiemann, P. J. Mason, A. Poustka and I. Dokal (1998). X-linked dyskeratosis congenita is caused by mutations in a highly conserved gene with putative nucleolar functions. Nat Genet **19**(1): 32-38.

Hendriks, I. A., R. C. D'Souza, B. Yang, M. Verlaan-de Vries, M. Mann and A. C. Vertegaal (2014). Uncovering global SUMOylation signaling networks in a site-specific manner. Nat Struct Mol Biol **21**(10): 927-936.

Hendriks, I. A., D. Lyon, D. Su, N. H. Skotte, J. A. Daniel, L. J. Jensen and M. L. Nielsen (2018). Site-specific characterization of endogenous SUMOylation across species and organs. Nat Commun **9**(1): 2456.

Hendriks, I. A., D. Lyon, C. Young, L. J. Jensen, A. C. Vertegaal and M. L. Nielsen (2017). Site-specific mapping of the human SUMO proteome reveals co-modification with phosphorylation. Nat Struct Mol Biol **24**(3): 325-336.

Hendriks, I. A., L. W. Treffers, M. Verlaan-de Vries, J. V. Olsen and A. C. O. Vertegaal (2015). SUMO-2 Orchestrates Chromatin Modifiers in Response to DNA Damage. Cell Rep **10**(10): 1778-1791.

Henras, A., Y. Henry, C. Bousquet-Antonelli, J. Noaillac-Depeyre, J. P. Gelugne and M. Caizergues-Ferrer (1998). Nhp2p and Nop10p are essential for the function of H/ACA snoRNPs. EMBO J **17**(23): 7078-7090.

Hofmann, T. G. and H. Will (2003). Body language: the function of PML nuclear bodies in apoptosis regulation. Cell Death Differ **10**(12): 1290-1299.

Holohan, B., W. E. Wright and J. W. Shay (2014). Cell biology of disease: Telomeropathies: an emerging spectrum disorder. J Cell Biol **205**(3): 289-299.

Horigome, C., D. E. Bustard, I. Marcomini, N. Delgoshaie, M. Tsai-Pflugfelder, J. A. Cobb and S. M. Gasser (2016). PolySUMOylation by Siz2 and Mms21 triggers relocation of DNA breaks to nuclear pores through the Slx5/Slx8 STUbL. Genes Dev **30**(8): 931-945.

Huang, S. Y., M. T. Naik, C. F. Chang, P. J. Fang, Y. H. Wang, H. M. Shih and T. H. Huang (2014). The B-box 1 dimer of human promyelocytic leukemia protein. J Biomol NMR **60**(4): 275-281.

Impens, F., L. Radoshevich, P. Cossart and D. Ribet (2014). Mapping of SUMO sites and analysis of SUMOylation changes induced by external stimuli. Proc Natl Acad Sci U S A **111**(34): 12432-12437.

Ishov, A. M., A. G. Sotnikov, D. Negorev, O. V. Vladimirova, N. Neff, T. Kamitani, E. T. Yeh, J. F. Strauss, 3rd and G. G. Maul (1999). PML is critical for ND10 formation and recruits the PML-interacting protein daxx to this nuclear structure when modified by SUMO-1. J Cell Biol **147**(2): 221-234.

Jady, B. E., E. Bertrand and T. Kiss (2004). Human telomerase RNA and box H/ACA scaRNAs share a common Cajal body-specific localization signal. J Cell Biol **164**(5): 647-652.

Jady, B. E. and T. Kiss (2001). A small nucleolar guide RNA functions both in 2'-O-ribose methylation and pseudouridylation of the U5 spliceosomal RNA. EMBO J **20**(3): 541-551.

Jain, A. and R. D. Vale (2017). RNA phase transitions in repeat expansion disorders. Nature **546**(7657): 243-247.

Jamonnak, N., T. J. Creamer, M. M. Darby, P. Schaughency, S. J. Wheelan and J. L. Corden (2011). Yeast Nrd1, Nab3, and Sen1 transcriptome-wide binding maps suggest multiple roles in post-transcriptional RNA processing. RNA **17**(11): 2011-2025.

Jensen, K., C. Shiels and P. S. Freemont (2001). PML protein isoforms and the RBCC/TRIM motif. Oncogene **20**(49): 7223-7233.

Jentsch, S. and I. Psakhye (2013). Control of nuclear activities by substrate-selective and protein-group SUMOylation. Annu Rev Genet **47**: 167-186.

Jiang, J., H. Chan, D. D. Cash, E. J. Miracco, R. R. Ogorzalek Loo, H. E. Upton, D. Cascio, R. O'Brien Johnson, K. Collins, J. A. Loo, Z. H. Zhou and J. Feigon (2015). Structure of Tetrahymena telomerase reveals previously unknown subunits, functions, and interactions. Science **350**(6260): aab4070.

Jiang, J., Y. Wang, L. Susac, H. Chan, R. Basu, Z. H. Zhou and J. Feigon (2018). Structure of Telomerase with Telomeric DNA. Cell **173**(5): 1179-1190 e1113.

Jiang, W., K. Middleton, H. J. Yoon, C. Fouquet and J. Carbon (1993). An essential yeast protein, CBF5p, binds in vitro to centromeres and microtubules. Mol Cell Biol **13**(8): 4884-4893.

Kato, M., T. W. Han, S. Xie, K. Shi, X. Du, L. C. Wu, H. Mirzaei, E. J. Goldsmith, J. Longgood, J. Pei, N. V. Grishin, D. E. Frantz, J. W. Schneider, S. Chen, L. Li, M. R. Sawaya, D. Eisenberg,

R. Tycko and S. L. McKnight (2012). Cell-free formation of RNA granules: low complexity sequence domains form dynamic fibers within hydrogels. Cell **149**(4): 753-767.

Ketele, A., T. Kiss and B. E. Jady (2016). Human intron-encoded AluACA RNAs and telomerase RNA share a common element promoting RNA accumulation. RNA Biol **13**(12): 1274-1285.

King, T. H., B. Liu, R. R. McCully and M. J. Fournier (2003). Ribosome structure and activity are altered in cells lacking snoRNPs that form pseudouridines in the peptidyl transferase center. Mol Cell **11**(2): 425-435.

Kiss-Laszlo, Z., Y. Henry, J. P. Bachellerie, M. Caizergues-Ferrer and T. Kiss (1996). Site-specific ribose methylation of preribosomal RNA: a novel function for small nucleolar RNAs. Cell **85**(7): 1077-1088.

Kiss, T., E. Fayet-Lebaron and B. E. Jady (2010). Box H/ACA small ribonucleoproteins. Mol Cell **37**(5): 597-606.

Kiss, T., E. Fayet, B. E. Jady, P. Richard and M. Weber (2006). Biogenesis and intranuclear trafficking of human box C/D and H/ACA RNPs. Cold Spring Harb Symp Quant Biol **71**: 407-417.

Kittur, N., X. Darzacq, S. Roy, R. H. Singer and U. T. Meier (2006). Dynamic association and localization of human H/ACA RNP proteins. RNA **12**(12): 2057-2062.

Kocak, H., B. J. Ballew, K. Bisht, R. Eggebeen, B. D. Hicks, S. Suman, A. O'Neil, N. Giri, N. D. C. G. R. Laboratory, N. D. C. S. W. Group, I. Maillard, B. P. Alter, C. E. Keegan, J. Nandakumar and S. A. Savage (2014). Hoyeraal-Hreidarsson syndrome caused by a germline mutation in the TEL patch of the telomere protein TPP1. Genes Dev **28**(19): 2090-2102.

Komar, A. A. and M. Hatzoglou (2005). Internal ribosome entry sites in cellular mRNAs: mystery of their existence. J Biol Chem **280**(25): 23425-23428.

Kuehner, J. N., E. L. Pearson and C. Moore (2011). Unravelling the means to an end: RNA polymerase II transcription termination. Nat Rev Mol Cell Biol **12**(5): 283-294.

Lafontaine, D. L., C. Bousquet-Antonelli, Y. Henry, M. Caizergues-Ferrer and D. Tollervey (1998). The box H + ACA snoRNAs carry Cbf5p, the putative rRNA pseudouridine synthase. Genes Dev **12**(4): 527-537.

Lafontaine, D. L. and D. Tollervey (1998). Birth of the snoRNPs: the evolution of the modification-guide snoRNAs. Trends Biochem Sci **23**(10): 383-388.

Lallemand-Breitenbach, V., J. Zhu, F. Puvion, M. Koken, N. Honore, A. Doubeikovsky, E. Duprez, P. P. Pandolfi, E. Puvion, P. Freemont and H. de The (2001). Role of promyelocytic

leukemia (PML) sumolation in nuclear body formation, 11S proteasome recruitment, and As2O3-induced PML or PML/retinoic acid receptor alpha degradation. J Exp Med **193**(12): 1361-1371.

Lamoliatte, F., F. P. McManus, G. Maarifi, M. K. Chelbi-Alix and P. Thibault (2017). Uncovering the SUMOylation and ubiquitylation crosstalk in human cells using sequential peptide immunopurification. Nat Commun **8**: 14109.

Lang, M., T. Jegou, I. Chung, K. Richter, S. Munch, A. Udvarhelyi, C. Cremer, P. Hemmerich, J. Engelhardt, S. W. Hell and K. Rippe (2010). Three-dimensional organization of promyelocytic leukemia nuclear bodies. J Cell Sci **123**(Pt 3): 392-400.

Laprade, H., E. Querido, M. J. Smith, D. Guerit, H. Crimmins, D. Conomos, E. Pourret, P. Chartrand and A. Sfeir (2020). Single-Molecule Imaging of Telomerase RNA Reveals a Recruitment-Retention Model for Telomere Elongation. Mol Cell **79**(1): 115-126 e116.

Latonen, L. (2011). Nucleolar aggresomes as counterparts of cytoplasmic aggresomes in proteotoxic stress. Proteasome inhibitors induce nuclear ribonucleoprotein inclusions that accumulate several key factors of neurodegenerative diseases and cancer. Bioessays **33**(5): 386-395.

Latonen, L. (2019). Phase-to-Phase With Nucleoli - Stress Responses, Protein Aggregation and Novel Roles of RNA. Front Cell Neurosci **13**: 151.

Latonen, L., H. M. Moore, B. Bai, S. Jaamaa and M. Laiho (2011). Proteasome inhibitors induce nucleolar aggregation of proteasome target proteins and polyadenylated RNA by altering ubiquitin availability. Oncogene **30**(7): 790-805.

Leeper, T., N. Leulliot and G. Varani (2003). The solution structure of an essential stem-loop of human telomerase RNA. Nucleic Acids Res **31**(10): 2614-2621.

Lemay, J. F., A. D'Amours, C. Lemieux, D. H. Lackner, V. G. St-Sauveur, J. Bahler and F. Bachand (2010). The nuclear poly(A)-binding protein interacts with the exosome to promote synthesis of noncoding small nucleolar RNAs. Mol Cell **37**(1): 34-45.

Leonardi, J., J. A. Box, J. T. Bunch and P. Baumann (2008). TER1, the RNA subunit of fission yeast telomerase. Nat Struct Mol Biol **15**(1): 26-33.

Leulliot, N., K. S. Godin, C. Hoareau-Aveilla, S. Quevillon-Cheruel, G. Varani, Y. Henry and H. Van Tilbeurgh (2007). The box H/ACA RNP assembly factor Naf1p contains a domain homologous to Gar1p mediating its interaction with Cbf5p. J Mol Biol **371**(5): 1338-1353.

Levy, M. Z., R. C. Allsopp, A. B. Futcher, C. W. Greider and C. B. Harley (1992). Telomere end-replication problem and cell aging. J Mol Biol **225**(4): 951-960.

Li, L. and K. Ye (2006). Crystal structure of an H/ACA box ribonucleoprotein particle. Nature **443**(7109): 302-307.

Li, P., S. Banjade, H. C. Cheng, S. Kim, B. Chen, L. Guo, M. Llaguno, J. V. Hollingsworth, D. S. King, S. F. Banani, P. S. Russo, Q. X. Jiang, B. T. Nixon and M. K. Rosen (2012). Phase transitions in the assembly of multivalent signalling proteins. Nature **483**(7389): 336-340.

Li, S., J. Duan, D. Li, S. Ma and K. Ye (2011). Structure of the Shq1-Cbf5-Nop10-Gar1 complex and implications for H/ACA RNP biogenesis and dyskeratosis congenita. EMBO J **30**(24): 5010-5020.

Li, S., J. Duan, D. Li, B. Yang, M. Dong and K. Ye (2011). Reconstitution and structural analysis of the yeast box H/ACA RNA-guided pseudouridine synthase. Genes Dev **25**(22): 2409-2421.

Li, S. J. and M. Hochstrasser (1999). A new protease required for cell-cycle progression in yeast. Nature **398**(6724): 246-251.

Li, S. J. and M. Hochstrasser (2000). The yeast ULP2 (SMT4) gene encodes a novel protease specific for the ubiquitin-like Smt3 protein. Mol Cell Biol **20**(7): 2367-2377.

Liang, J., N. Singh, C. R. Carlson, C. P. Albuquerque, K. D. Corbett and H. Zhou (2017). Recruitment of a SUMO isopeptidase to rDNA stabilizes silencing complexes by opposing SUMO targeted ubiquitin ligase activity. Genes Dev **31**(8): 802-815.

Liang, X. H., Q. Liu and M. J. Fournier (2007). rRNA modifications in an intersubunit bridge of the ribosome strongly affect both ribosome biogenesis and activity. Mol Cell **28**(6): 965-977.

Liang, X. H., Q. Liu and M. J. Fournier (2009). Loss of rRNA modifications in the decoding center of the ribosome impairs translation and strongly delays pre-rRNA processing. RNA **15**(9): 1716-1728.

Lingner, J., J. P. Cooper and T. R. Cech (1995). Telomerase and DNA end replication: no longer a lagging strand problem? Science **269**(5230): 1533-1534.

Logeswaran, D., Y. Li, J. D. Podlevsky and J. J. Chen (2020). Monophyletic Origin and Divergent Evolution of Animal Telomerase RNA. Mol Biol Evol.

Lubben, B., P. Fabrizio, B. Kastner and R. Luhrmann (1995). Isolation and characterization of the small nucleolar ribonucleoprotein particle snR30 from Saccharomyces cerevisiae. J Biol Chem **270**(19): 11549-11554.

Lue, N. F. (2004). Adding to the ends: what makes telomerase processive and how important is it? Bioessays **26**(9): 955-962.

Lue, N. F., Y. C. Lin and I. S. Mian (2003). A conserved telomerase motif within the catalytic domain of telomerase reverse transcriptase is specifically required for repeat addition processivity. Mol Cell Biol **23**(23): 8440-8449.

Luzzatto, L. and A. Karadimitris (1998). Dyskeratosis and ribosomal rebellion. Nat Genet **19**(1): 6-7.

Ly, H., E. H. Blackburn and T. G. Parslow (2003). Comprehensive structure-function analysis of the core domain of human telomerase RNA. Mol Cell Biol **23**(19): 6849-6856.

Machado-Pinilla, R., D. Liger, N. Leulliot and U. T. Meier (2012). Mechanism of the AAA+ ATPases pontin and reptin in the biogenesis of H/ACA RNPs. RNA **18**(10): 1833-1845.

Machyna, M., P. Heyn and K. M. Neugebauer (2013). Cajal bodies: where form meets function. Wiley Interdiscip Rev RNA **4**(1): 17-34.

Macias, S., R. A. Cordiner, P. Gautier, M. Plass and J. F. Caceres (2015). DGCR8 Acts as an Adaptor for the Exosome Complex to Degrade Double-Stranded Structured RNAs. Mol Cell **60**(6): 873-885.

MacNeil, D. E., H. J. Bensoussan and C. Autexier (2016). Telomerase Regulation from Beginning to the End. Genes (Basel) **7**(9).

Makarov, V. L., Y. Hirose and J. P. Langmore (1997). Long G tails at both ends of human chromosomes suggest a C strand degradation mechanism for telomere shortening. Cell **88**(5): 657-666.

Matsson, H., J. Klar, N. Draptchinskaia, P. Gustavsson, B. Carlsson, D. Bowers, E. de Bont and N. Dahl (1999). Truncating ribosomal protein S19 mutations and variable clinical expression in Diamond-Blackfan anemia. Hum Genet **105**(5): 496-500.

McClintock, B. (1938). The Production of Homozygous Deficient Tissues with Mutant Characteristics by Means of the Aberrant Mitotic Behavior of Ring-Shaped Chromosomes. Genetics **23**(4): 315-376.

McClintock, B. (1939). The Behavior in Successive Nuclear Divisions of a Chromosome Broken at Meiosis. Proc Natl Acad Sci U S A **25**(8): 405-416.

McCormick-Graham, M. and D. P. Romero (1995). Ciliate telomerase RNA structural features. Nucleic Acids Res **23**(7): 1091-1097.

Meier, U. T. and G. Blobel (1994). NAP57, a mammalian nucleolar protein with a putative homolog in yeast and bacteria. J Cell Biol **127**(6 Pt 1): 1505-1514.

Melchior, F., M. Schergaut and A. Pichler (2003). SUMO: ligases, isopeptidases and nuclear pores. Trends Biochem Sci **28**(11): 612-618.

Mills, E. W. and R. Green (2017). Ribosomopathies: There's strength in numbers. Science **358**(6363).

Min, J., W. E. Wright and J. W. Shay (2017). Alternative Lengthening of Telomeres Mediated by Mitotic DNA Synthesis Engages Break-Induced Replication Processes. Mol Cell Biol **37**(20).

Min, J., W. E. Wright and J. W. Shay (2019). Clustered telomeres in phase-separated nuclear condensates engage mitotic DNA synthesis through BLM and RAD52. Genes Dev **33**(13-14): 814-827.

Mitchell, J. R., J. Cheng and K. Collins (1999). A box H/ACA small nucleolar RNA-like domain at the human telomerase RNA 3' end. Mol Cell Biol **19**(1): 567-576.

Mitchell, J. R. and K. Collins (2000). Human telomerase activation requires two independent interactions between telomerase RNA and telomerase reverse transcriptase. Mol Cell **6**(2): 361-371.

Mitchell, J. R., E. Wood and K. Collins (1999). A telomerase component is defective in the human disease dyskeratosis congenita. Nature **402**(6761): 551-555.

Mitchell, P. (2014). Exosome substrate targeting: the long and short of it. Biochem Soc Trans **42**(4): 1129-1134.

Moon, D. H., M. Segal, B. Boyraz, E. Guinan, I. Hofmann, P. Cahan, A. K. Tai and S. Agarwal (2015). Poly(A)-specific ribonuclease (PARN) mediates 3'-end maturation of the telomerase RNA component. Nat Genet **47**(12): 1482-1488.

Moriarty, T. J., D. T. Marie-Egyptienne and C. Autexier (2004). Functional organization of repeat addition processivity and DNA synthesis determinants in the human telomerase multimer. Mol Cell Biol **24**(9): 3720-3733.

Moriarty, T. J., R. J. Ward, M. A. Taboski and C. Autexier (2005). An anchor site-type defect in human telomerase that disrupts telomere length maintenance and cellular immortalization. Mol Biol Cell **16**(7): 3152-3161.

Moyzis, R. K., J. M. Buckingham, L. S. Cram, M. Dani, L. L. Deaven, M. D. Jones, J. Meyne, R. L. Ratliff and J. R. Wu (1988). A highly conserved repetitive DNA sequence, (TTAGGG)n, present at the telomeres of human chromosomes. Proc Natl Acad Sci U S A **85**(18): 6622-6626.

Muntoni, A. and R. R. Reddel (2005). The first molecular details of ALT in human tumor cells. Hum Mol Genet **14 Spec No. 2**: R191-196.

Nagpal, N., J. Wang, J. Zeng, E. Lo, D. H. Moon, K. Luk, R. O. Braun, L. M. Burroughs, S. B. Keel, C. Reilly, R. C. Lindsley, S. A. Wolfe, A. K. Tai, P. Cahan, D. E. Bauer, Y. W. Fong and S. Agarwal (2020). Small-Molecule PAPD5 Inhibitors Restore Telomerase Activity in Patient Stem Cells. Cell Stem Cell **26**(6): 896-909 e898.

Nandakumar, J., C. F. Bell, I. Weidenfeld, A. J. Zaug, L. A. Leinwand and T. R. Cech (2012). The TEL patch of telomere protein TPP1 mediates telomerase recruitment and processivity. Nature **492**(7428): 285-289.

Nandakumar, J. and T. R. Cech (2013). Finding the end: recruitment of telomerase to telomeres. Nat Rev Mol Cell Biol **14**(2): 69-82.

Nguyen, D., V. Grenier St-Sauveur, D. Bergeron, F. Dupuis-Sandoval, M. S. Scott and F. Bachand (2015). A Polyadenylation-Dependent 3' End Maturation Pathway Is Required for the Synthesis of the Human Telomerase RNA. Cell Rep **13**(10): 2244-2257.

Nguyen, T. H. D., J. Tam, R. A. Wu, B. J. Greber, D. Toso, E. Nogales and K. Collins (2018). Cryo-EM structure of substrate-bound human telomerase holoenzyme. Nature **557**(7704): 190-195.

Ni, J., A. L. Tien and M. J. Fournier (1997). Small nucleolar RNAs direct site-specific synthesis of pseudouridine in ribosomal RNA. Cell **89**(4): 565-573.

Nisole, S., M. A. Maroui, X. H. Mascle, M. Aubry and M. K. Chelbi-Alix (2013). Differential Roles of PML Isoforms. Front Oncol **3**: 125.

Noel, J. F., S. Larose, S. Abou Elela and R. J. Wellinger (2012). Budding yeast telomerase RNA transcription termination is dictated by the Nrd1/Nab3 non-coding RNA termination pathway. Nucleic Acids Res **40**(12): 5625-5636.

O'Connor, M., M. Leppik and J. Remme (2018). Pseudouridine-Free Escherichia coli Ribosomes. J Bacteriol **200**(4).

Ochs, R. L., M. A. Lischwe, W. H. Spohn and H. Busch (1985). Fibrillarin: a new protein of the nucleolus identified by autoimmune sera. Biol Cell **54**(2): 123-133.

Okuma, T., R. Honda, G. Ichikawa, N. Tsumagari and H. Yasuda (1999). In vitro SUMO-1 modification requires two enzymatic steps, E1 and E2. Biochem Biophys Res Commun **254**(3): 693-698.

Overbeek, J. T. and M. J. Voorn (1957). Phase separation in polyelectrolyte solutions; theory of complex coacervation. J Cell Physiol Suppl **49**(Suppl 1): 7-22; discussion, 22-26.

Palm, W. and T. de Lange (2008). How shelterin protects mammalian telomeres. Annu Rev Genet **42**: 301-334.

Panse, V. G., D. Kressler, A. Pauli, E. Petfalski, M. Gnadig, D. Tollervey and E. Hurt (2006). Formation and nuclear export of preribosomes are functionally linked to the small-ubiquitin-related modifier pathway. Traffic **7**(10): 1311-1321.

Patrick, E. M., J. D. Slivka, B. Payne, M. J. Comstock and J. C. Schmidt (2020). Observation of processive telomerase catalysis using high-resolution optical tweezers. Nat Chem Biol.

Peng, Y., Z. Wang, Z. Wang, F. Yu, J. Li and J. Wong (2019). SUMOylation down-regulates rDNA transcription by repressing expression of upstream-binding factor and proto-oncogene c-Myc. J Biol Chem **294**(50): 19155-19166.

Penzo, M., A. N. Guerrieri, F. Zacchini, D. Trere and L. Montanaro (2017). RNA Pseudouridylation in Physiology and Medicine: For Better and for Worse. Genes (Basel) **8**(11).

Penzo, M. and L. Montanaro (2018). Turning Uridines around: Role of rRNA Pseudouridylation in Ribosome Biogenesis and Ribosomal Function. Biomolecules **8**(2).

Phillips, B., A. N. Billin, C. Cadwell, R. Buchholz, C. Erickson, J. R. Merriam, J. Carbon and S. J. Poole (1998). The Nop60B gene of Drosophila encodes an essential nucleolar protein that functions in yeast. Mol Gen Genet **260**(1): 20-29.

Piccirillo, C., R. Khanna and M. Kiledjian (2003). Functional characterization of the mammalian mRNA decapping enzyme hDcp2. RNA **9**(9): 1138-1147.

Pichler, A., A. Gast, J. S. Seeler, A. Dejean and F. Melchior (2002). The nucleoporin RanBP2 has SUMO1 E3 ligase activity. Cell **108**(1): 109-120.

Podlevsky, J. D., C. J. Bley, R. V. Omana, X. Qi and J. J. Chen (2008). The telomerase database. Nucleic Acids Res **36**(Database issue): D339-343.

Podlevsky, J. D. and J. J. Chen (2016). Evolutionary perspectives of telomerase RNA structure and function. RNA Biol **13**(8): 720-732.

Porrua, O. and D. Libri (2015). Transcription termination and the control of the transcriptome: why, where and how to stop. Nat Rev Mol Cell Biol **16**(3): 190-202.

Potts, P. R. and H. Yu (2007). The SMC5/6 complex maintains telomere length in ALT cancer cells through SUMOylation of telomere-binding proteins. Nat Struct Mol Biol **14**(7): 581-590.

Pradet-Balade, B., C. Girard, S. Boulon, C. Paul, K. Azzag, R. Bordonne, E. Bertrand and C. Verheggen (2011). CRM1 controls the composition of nucleoplasmic pre-snoRNA complexes to licence them for nucleolar transport. EMBO J **30**(11): 2205-2218.

Rai, A. K., J. X. Chen, M. Selbach and L. Pelkmans (2018). Kinase-controlled phase transition of membraneless organelles in mitosis. Nature **559**(7713): 211-216.

Rallabhandi, P., K. Hashimoto, Y. Y. Mo, W. T. Beck, P. K. Moitra and P. D'Arpa (2002). Sumoylation of topoisomerase I is involved in its partitioning between nucleoli and nucleoplasm and its clearing from nucleoli in response to camptothecin. J Biol Chem **277**(42): 40020-40026.

Raman, N., A. Nayak and S. Muller (2014). mTOR signaling regulates nucleolar targeting of the SUMO-specific isopeptidase SENP3. Mol Cell Biol **34**(24): 4474-4484.

Rashid, R., B. Liang, D. L. Baker, O. A. Youssef, Y. He, K. Phipps, R. M. Terns, M. P. Terns and H. Li (2006). Crystal structure of a Cbf5-Nop10-Gar1 complex and implications in RNA-guided pseudouridylation and dyskeratosis congenita. Mol Cell **21**(2): 249-260.

Richard, P., X. Darzacq, E. Bertrand, B. E. Jady, C. Verheggen and T. Kiss (2003). A common sequence motif determines the Cajal body-specific localization of box H/ACA scaRNAs. EMBO J **22**(16): 4283-4293.

Richard, P. and J. L. Manley (2009). Transcription termination by nuclear RNA polymerases. Genes Dev **23**(11): 1247-1269.

Rincon, S. A., P. Bhatia, C. Bicho, M. Guzman-Vendrell, V. Fraisier, W. E. Borek, L. Alves Fde, F. Dingli, D. Loew, J. Rappsilber, K. E. Sawin, S. G. Martin and A. Paoletti (2014). Pom1 regulates the assembly of Cdr2-Mid1 cortical nodes for robust spatial control of cytokinesis. J Cell Biol **206**(1): 61-77.

Roake, C. M., L. Chen, A. L. Chakravarthy, J. E. Ferrell, Jr., G. D. Raffa and S. E. Artandi (2019). Disruption of Telomerase RNA Maturation Kinetics Precipitates Disease. Mol Cell **74**(4): 688-700 e683.

Rocchi, L., A. Pacilli, R. Sethi, M. Penzo, R. J. Schneider, D. Trere, M. Brigotti and L. Montanaro (2013). Dyskerin depletion increases VEGF mRNA internal ribosome entry site-mediated translation. Nucleic Acids Res **41**(17): 8308-8318.

Ruggero, D., S. Grisendi, F. Piazza, E. Rego, F. Mari, P. H. Rao, C. Cordon-Cardo and P. P. Pandolfi (2003). Dyskeratosis congenita and cancer in mice deficient in ribosomal RNA modification. Science **299**(5604): 259-262.

Saha, S., C. A. Weber, M. Nousch, O. Adame-Arana, C. Hoege, M. Y. Hein, E. Osborne-Nishimura, J. Mahamid, M. Jahnel, L. Jawerth, A. Pozniakovski, C. R. Eckmann, F. Julicher and A. A. Hyman (2016). Polar Positioning of Phase-Separated Liquid Compartments in Cells Regulated by an mRNA Competition Mechanism. Cell **166**(6): 1572-1584 e1516.

Sahin, U., O. Ferhi, M. Jeanne, S. Benhenda, C. Berthier, F. Jollivet, M. Niwa-Kawakita, O. Faklaris, N. Setterblad, H. de The and V. Lallemand-Breitenbach (2014). Oxidative stress-induced assembly of PML nuclear bodies controls sumoylation of partner proteins. J Cell Biol **204**(6): 931-945.

Saitoh, H. and J. Hinchey (2000). Functional heterogeneity of small ubiquitin-related protein modifiers SUMO-1 versus SUMO-2/3. J Biol Chem **275**(9): 6252-6258.

Sarek, G., P. Marzec, P. Margalef and S. J. Boulton (2015). Molecular basis of telomere dysfunction in human genetic diseases. Nat Struct Mol Biol **22**(11): 867-874.

Saunders, T. E., K. Z. Pan, A. Angel, Y. Guan, J. V. Shah, M. Howard and F. Chang (2012). Noise reduction in the intracellular pom1p gradient by a dynamic clustering mechanism. Dev Cell **22**(3): 558-572.

Scheer, U. and D. Weisenberger (1994). The nucleolus. Curr Opin Cell Biol **6**(3): 354-359.

Schmidt, J. C. and T. R. Cech (2015). Human telomerase: biogenesis, trafficking, recruitment, and activation. Genes Dev **29**(11): 1095-1105.

Schmidt, J. C., A. B. Dalby and T. R. Cech (2014). Identification of human TERT elements necessary for telomerase recruitment to telomeres. Elife **3**.

Schmidt, J. C., A. J. Zaug and T. R. Cech (2016). Live Cell Imaging Reveals the Dynamics of Telomerase Recruitment to Telomeres. Cell **166**(5): 1188-1197 e1189.

Seto, A. G., A. J. Zaug, S. G. Sobel, S. L. Wolin and T. R. Cech (1999). Saccharomyces cerevisiae telomerase is an Sm small nuclear ribonucleoprotein particle. Nature **401**(6749): 177-180.

Sexton, A. N., S. G. Regalado, C. S. Lai, G. J. Cost, C. M. O'Neil, F. D. Urnov, P. D. Gregory, R. Jaenisch, K. Collins and D. Hockemeyer (2014). Genetic and molecular identification of three human TPP1 functions in telomerase action: recruitment, activation, and homeostasis set point regulation. Genes Dev **28**(17): 1885-1899.

Sexton, A. N., D. T. Youmans and K. Collins (2012). Specificity requirements for human telomere protein interaction with telomerase holoenzyme. J Biol Chem **287**(41): 34455-34464.

Shay, J. W., R. R. Reddel and W. E. Wright (2012). Cancer. Cancer and telomeres--an ALTernative to telomerase. Science **336**(6087): 1388-1390.

Shen, T. H., H. K. Lin, P. P. Scaglioni, T. M. Yung and P. P. Pandolfi (2006). The mechanisms of PML-nuclear body formation. Mol Cell **24**(3): 331-339.

Shevtsov, S. P. and M. Dundr (2011). Nucleation of nuclear bodies by RNA. Nat Cell Biol **13**(2): 167-173.

Shukla, S., H. C. Jeong, C. M. Sturgeon, R. Parker and L. F. Z. Batista (2020). Chemical inhibition of PAPD5/7 rescues telomerase function and hematopoiesis in dyskeratosis congenita. Blood Adv **4**(12): 2717-2722.

Shukla, S. and R. Parker (2014). Quality control of assembly-defective U1 snRNAs by decapping and 5'-to-3' exonucleolytic digestion. Proc Natl Acad Sci U S A **111**(32): E3277-3286.

Shukla, S., J. C. Schmidt, K. C. Goldfarb, T. R. Cech and R. Parker (2016). Inhibition of telomerase RNA decay rescues telomerase deficiency caused by dyskerin or PARN defects. Nat Struct Mol Biol **23**(4): 286-292.

Singh, M., Z. Wang, D. Cascio and J. Feigon (2015). Structure and interactions of the CS domain of human H/ACA RNP assembly protein Shq1. J Mol Biol **427**(4): 807-823.

Song, J., L. K. Durrin, T. A. Wilkinson, T. G. Krontiris and Y. Chen (2004). Identification of a SUMO-binding motif that recognizes SUMO-modified proteins. Proc Natl Acad Sci U S A **101**(40): 14373-14378.

Song, J., Z. Zhang, W. Hu and Y. Chen (2005). Small ubiquitin-like modifier (SUMO) recognition of a SUMO binding motif: a reversal of the bound orientation. J Biol Chem **280**(48): 40122-40129.

Song, M. G., Y. Li and M. Kiledjian (2010). Multiple mRNA decapping enzymes in mammalian cells. Mol Cell **40**(3): 423-432.

Stanley, S. E., D. L. Gable, C. L. Wagner, T. M. Carlile, V. S. Hanumanthu, J. D. Podlevsky, S. E. Khalil, A. E. DeZern, M. F. Rojas-Duran, C. D. Applegate, J. K. Alder, E. M. Parry, W. V. Gilbert and M. Armanios (2016). Loss-of-function mutations in the RNA biogenesis factor NAF1 predispose to pulmonary fibrosis-emphysema. Sci Transl Med **8**(351): 351ra107.

Stern, J. L., K. G. Zyner, H. A. Pickett, S. B. Cohen and T. M. Bryan (2012). Telomerase recruitment requires both TCAB1 and Cajal bodies independently. Mol Cell Biol **32**(13): 2384-2395.

Strom, A. R. and C. P. Brangwynne (2019). The liquid nucleome - phase transitions in the nucleus at a glance. J Cell Sci **132**(22).

Stuart, B. D., J. Choi, S. Zaidi, C. Xing, B. Holohan, R. Chen, M. Choi, P. Dharwadkar, F. Torres, C. E. Girod, J. Weissler, J. Fitzgerald, C. Kershaw, J. Klesney-Tait, Y. Mageto, J. W. Shay, W. Ji, K. Bilguvar, S. Mane, R. P. Lifton and C. K. Garcia (2015). Exome sequencing links mutations in PARN and RTEL1 with familial pulmonary fibrosis and telomere shortening. Nat Genet **47**(5): 512-517.

Sulima, S. O., I. J. F. Hofman, K. De Keersmaecker and J. D. Dinman (2017). How Ribosomes Translate Cancer. Cancer Discov **7**(10): 1069-1087.

Szostak, J. W. and E. H. Blackburn (1982). Cloning yeast telomeres on linear plasmid vectors. Cell **29**(1): 245-255.

Tago, K., S. Chiocca and C. J. Sherr (2005). Sumoylation induced by the Arf tumor suppressor: a p53-independent function. Proc Natl Acad Sci U S A **102**(21): 7689-7694.

Takahashi, Y., J. Mizoi, E. A. Toh and Y. Kikuchi (2000). Yeast Ulp1, an Smt3-specific protease, associates with nucleoporins. J Biochem **128**(5): 723-725.

Takai, H., E. Jenkinson, S. Kabir, R. Babul-Hirji, N. Najm-Tehrani, D. A. Chitayat, Y. J. Crow and T. de Lange (2016). A POT1 mutation implicates defective telomere end fill-in and telomere truncations in Coats plus. Genes Dev **30**(7): 812-826.

Tang, W., R. Kannan, M. Blanchette and P. Baumann (2012). Telomerase RNA biogenesis involves sequential binding by Sm and Lsm complexes. Nature **484**(7393): 260-264.

Taoka, M., Y. Nobe, Y. Yamaki, K. Sato, H. Ishikawa, K. Izumikawa, Y. Yamauchi, K. Hirota, H. Nakayama, N. Takahashi and T. Isobe (2018). Landscape of the complete RNA chemical modifications in the human 80S ribosome. Nucleic Acids Res **46**(18): 9289-9298.

Tapia, O., V. Lafarga, R. Bengoechea, A. Palanca, M. Lafarga and M. T. Berciano (2014). The SMN Tudor SIM-like domain is key to SmD1 and coilin interactions and to Cajal body biogenesis. J Cell Sci **127**(Pt 5): 939-946.

Tatham, M. H., E. Jaffray, O. A. Vaughan, J. M. Desterro, C. H. Botting, J. H. Naismith and R. T. Hay (2001). Polymeric chains of SUMO-2 and SUMO-3 are conjugated to protein substrates by SAE1/SAE2 and Ubc9. J Biol Chem **276**(38): 35368-35374.

Tesmer, V. M., E. M. Smith, O. Danciu, S. Padmanaban and J. Nandakumar (2019). Combining conservation and species-specific differences to determine how human telomerase binds telomeres. Proc Natl Acad Sci U S A.

Theimer, C. A., B. E. Jady, N. Chim, P. Richard, K. E. Breece, T. Kiss and J. Feigon (2007). Structural and functional characterization of human telomerase RNA processing and cajal body localization signals. Mol Cell **27**(6): 869-881.

Thumati, N. R., X. L. Zeng, H. H. Au, C. J. Jang, E. Jan and J. M. Wong (2013). Severity of X-linked dyskeratosis congenita (DKCX) cellular defects is not directly related to dyskerin (DKC1) activity in ribosomal RNA biogenesis or mRNA translation. Hum Mutat **34**(12): 1698-1707.

Torreira, E., S. Jha, J. R. Lopez-Blanco, E. Arias-Palomo, P. Chacon, C. Canas, S. Ayora, A. Dutta and O. Llorca (2008). Architecture of the pontin/reptin complex, essential in the assembly of several macromolecular complexes. Structure **16**(10): 1511-1520.

Trahan, C. and F. Dragon (2009). Dyskeratosis congenita mutations in the H/ACA domain of human telomerase RNA affect its assembly into a pre-RNP. RNA **15**(2): 235-243.

Trahan, C., C. Martel and F. Dragon (2010). Effects of dyskeratosis congenita mutations in dyskerin, NHP2 and NOP10 on assembly of H/ACA pre-RNPs. Hum Mol Genet **19**(5): 825-836.

Tseng, C. K., H. F. Wang, A. M. Burns, M. R. Schroeder, M. Gaspari and P. Baumann (2015). Human Telomerase RNA Processing and Quality Control. Cell Rep **13**(10): 2232-2243.

Tseng, C. K., H. F. Wang, M. R. Schroeder and P. Baumann (2018). The H/ACA complex disrupts triplex in hTR precursor to permit processing by RRP6 and PARN. Nat Commun **9**(1): 5430.

Tummala, H., A. Walne, L. Collopy, S. Cardoso, J. de la Fuente, S. Lawson, J. Powell, N. Cooper, A. Foster, S. Mohammed, V. Plagnol, T. Vulliamy and I. Dokal (2015). Poly(A)-specific ribonuclease deficiency impacts telomere biology and causes dyskeratosis congenita. J Clin Invest **125**(5): 2151-2160.

Tycowski, K. T., M. D. Shu, A. Kukoyi and J. A. Steitz (2009). A conserved WD40 protein binds the Cajal body localization signal of scaRNP particles. Mol Cell **34**(1): 47-57.

Tycowski, K. T., Z. H. You, P. J. Graham and J. A. Steitz (1998). Modification of U6 spliceosomal RNA is guided by other small RNAs. Mol Cell **2**(5): 629-638.

Ueda, Y., R. T. Calado, A. Norberg, S. Kajigaya, G. Roos, E. Hellstrom-Lindberg and N. S. Young (2014). A mutation in the H/ACA box of telomerase RNA component gene (TERC) in a young patient with myelodysplastic syndrome. BMC Med Genet **15**: 68.

van Dijk, E., N. Cougot, S. Meyer, S. Babajko, E. Wahle and B. Seraphin (2002). Human Dcp2: a catalytically active mRNA decapping enzyme located in specific cytoplasmic structures. EMBO J **21**(24): 6915-6924.

van Steensel, B. and T. de Lange (1997). Control of telomere length by the human telomeric protein TRF1. Nature **385**(6618): 740-743.

Varejao, N., J. Lascorz, Y. Li and D. Reverter (2019). Molecular mechanisms in SUMO conjugation. Biochem Soc Trans.

Vasconcelos, E. J., V. S. Nunes, M. S. da Silva, M. Segatto, P. J. Myler and M. I. Cano (2014). The putative Leishmania telomerase RNA (LeishTER) undergoes trans-splicing and contains a conserved template sequence. PLoS One **9**(11): e112061.

Vasiljeva, L. and S. Buratowski (2006). Nrd1 interacts with the nuclear exosome for 3' processing of RNA polymerase II transcripts. Mol Cell **21**(2): 239-248.

Venteicher, A. S., E. B. Abreu, Z. Meng, K. E. McCann, R. M. Terns, T. D. Veenstra, M. P. Terns and S. E. Artandi (2009). A human telomerase holoenzyme protein required for Cajal body localization and telomere synthesis. Science **323**(5914): 644-648.

Venteicher, A. S., Z. Meng, P. J. Mason, T. D. Veenstra and S. E. Artandi (2008). Identification of ATPases pontin and reptin as telomerase components essential for holoenzyme assembly. Cell **132**(6): 945-957.

Vulliamy, T., R. Beswick, M. Kirwan, A. Marrone, M. Digweed, A. Walne and I. Dokal (2008). Mutations in the telomerase component NHP2 cause the premature ageing syndrome dyskeratosis congenita. Proc Natl Acad Sci U S A **105**(23): 8073-8078.

Walbott, H., R. Machado-Pinilla, D. Liger, M. Blaud, S. Rety, P. N. Grozdanov, K. Godin, H. van Tilbeurgh, G. Varani, U. T. Meier and N. Leulliot (2011). The H/ACA RNP assembly factor SHQ1 functions as an RNA mimic. Genes Dev **25**(22): 2398-2408.

Walne, A. J., Vulliamy, T., Marrone, A., Beswick, R., Kirwan, M., Masunari, Y., Al-Qurashi, F., Aljurf M., Doka, I. (2007). Genetic heterogeneity in autosomal recessive dyskeratosis congenita with one subtype due to mutations in the telomerase-associated protein NOP10. Hum Mol Genet **16**(13): 1619-1629.

Wang, C. and U. T. Meier (2004). Architecture and assembly of mammalian H/ACA small nucleolar and telomerase ribonucleoproteins. EMBO J **23**(8): 1857-1867.

Wang, F., E. R. Podell, A. J. Zaug, Y. Yang, P. Baciu, T. R. Cech and M. Lei (2007). The POT1-TPP1 telomere complex is a telomerase processivity factor. Nature **445**(7127): 506-510.

Wang, J. T., J. Smith, B. C. Chen, H. Schmidt, D. Rasoloson, A. Paix, B. G. Lambrus, D. Calidas, E. Betzig and G. Seydoux (2014). Regulation of RNA granule dynamics by phosphorylation of serine-rich, intrinsically disordered proteins in C. elegans. Elife **3**: e04591.

Wang, P., L. Yang, Y. Q. Gao and X. S. Zhao (2015). Accurate placement of substrate RNA by Gar1 in H/ACA RNA-guided pseudouridylation. Nucleic Acids Res **43**(15): 7207-7216.

Watkins, N. J., A. Gottschalk, G. Neubauer, B. Kastner, P. Fabrizio, M. Mann and R. Luhrmann (1998). Cbf5p, a potential pseudouridine synthase, and Nhp2p, a putative RNA-binding protein, are present together with Gar1p in all H BOX/ACA-motif snoRNPs and constitute a common bipartite structure. RNA **4**(12): 1549-1568.

Webb, C. J. and V. A. Zakian (2008). Identification and characterization of the Schizosaccharomyces pombe TER1 telomerase RNA. Nat Struct Mol Biol **15**(1): 34-42.

Weber, S. C. and C. P. Brangwynne (2015). Inverse size scaling of the nucleolus by a concentration-dependent phase transition. Curr Biol **25**(5): 641-646.

Weinrich, S. L., R. Pruzan, L. Ma, M. Ouellette, V. M. Tesmer, S. E. Holt, A. G. Bodnar, S. Lichtsteiner, N. W. Kim, J. B. Trager, R. D. Taylor, R. Carlos, W. H. Andrews, W. E. Wright, J. W. Shay, C. B. Harley and G. B. Morin (1997). Reconstitution of human telomerase with the

template RNA component hTR and the catalytic protein subunit hTRT. Nat Genet **17**(4): 498-502.

Wen, D., J. Wu, L. Wang and Z. Fu (2017). SUMOylation Promotes Nuclear Import and Stabilization of Polo-like Kinase 1 to Support Its Mitotic Function. Cell Rep **21**(8): 2147-2159.

Westman, B. J., C. Verheggen, S. Hutten, Y. W. Lam, E. Bertrand and A. I. Lamond (2010). A proteomic screen for nucleolar SUMO targets shows SUMOylation modulates the function of Nop5/Nop58. Mol Cell **39**(4): 618-631.

Will, C. L., S. Rumpler, J. Klein Gunnewiek, W. J. van Venrooij and R. Luhrmann (1996). In vitro reconstitution of mammalian U1 snRNPs active in splicing: the U1-C protein enhances the formation of early (E) spliceosomal complexes. Nucleic Acids Res **24**(23): 4614-4623.

Willig, T. N., N. Draptchinskaia, I. Dianzani, S. Ball, C. Niemeyer, U. Ramenghi, K. Orfali, P. Gustavsson, E. Garelli, A. Brusco, C. Tiemann, J. L. Perignon, C. Bouchier, L. Cicchiello, N. Dahl, N. Mohandas and G. Tchernia (1999). Mutations in ribosomal protein S19 gene and diamond blackfan anemia: wide variations in phenotypic expression. Blood **94**(12): 4294-4306.

Wippich, F., B. Bodenmiller, M. G. Trajkovska, S. Wanka, R. Aebersold and L. Pelkmans (2013). Dual specificity kinase DYRK3 couples stress granule condensation/dissolution to mTORC1 signaling. Cell **152**(4): 791-805.

Wong, J. M. and K. Collins (2006). Telomerase RNA level limits telomere maintenance in X-linked dyskeratosis congenita. Genes Dev **20**(20): 2848-2858.

Wong, J. M., M. J. Kyasa, L. Hutchins and K. Collins (2004). Telomerase RNA deficiency in peripheral blood mononuclear cells in X-linked dyskeratosis congenita. Hum Genet **115**(5): 448-455.

Wright, W. E., M. A. Piatyszek, W. E. Rainey, W. Byrd and J. W. Shay (1996). Telomerase activity in human germline and embryonic tissues and cells. Dev Genet **18**(2): 173-179.

Wright, W. E., V. M. Tesmer, K. E. Huffman, S. D. Levene and J. W. Shay (1997). Normal human chromosomes have long G-rich telomeric overhangs at one end. Genes Dev **11**(21): 2801-2809.

Wu, P., H. Takai and T. de Lange (2012). Telomeric 3' overhangs derive from resection by Exo1 and Apollo and fill-in by POT1b-associated CST. Cell **150**(1): 39-52.

Xiao, M., C. Yang, P. Schattner and Y. T. Yu (2009). Functionality and substrate specificity of human box H/ACA guide RNAs. RNA **15**(1): 176-186.

Xiao, Z., J. G. Chang, I. A. Hendriks, J. O. Sigurethsson, J. V. Olsen and A. C. Vertegaal (2015). System-wide Analysis of SUMOylation Dynamics in Response to Replication Stress Reveals

Novel Small Ubiquitin-like Modified Target Proteins and Acceptor Lysines Relevant for Genome Stability. Mol Cell Proteomics **14**(5): 1419-1434.

Xu, J., P. P. Khincha, N. Giri, B. P. Alter, S. A. Savage and J. M. Wong (2016). Investigation of chromosome X inactivation and clinical phenotypes in female carriers of DKC1 mutations. Am J Hematol **91**(12): 1215-1220.

Yang, D., Q. He, H. Kim, W. Ma and Z. Songyang (2011). TIN2 protein dyskeratosis congenita missense mutants are defective in association with telomerase. J Biol Chem **286**(26): 23022-23030.

Yang, P. K., C. Hoareau, C. Froment, B. Monsarrat, Y. Henry and G. Chanfreau (2005). Cotranscriptional recruitment of the pseudouridylsynthetase Cbf5p and of the RNA binding protein Naf1p during H/ACA snoRNP assembly. Mol Cell Biol **25**(8): 3295-3304.

Yang, P. K., G. Rotondo, T. Porras, P. Legrain and G. Chanfreau (2002). The Shq1p.Naf1p complex is required for box H/ACA small nucleolar ribonucleoprotein particle biogenesis. J Biol Chem **277**(47): 45235-45242.

Yang, Y., C. Isaac, C. Wang, F. Dragon, V. Pogacic and U. T. Meier (2000). Conserved composition of mammalian box H/ACA and box C/D small nucleolar ribonucleoprotein particles and their interaction with the common factor Nopp140. Mol Biol Cell **11**(2): 567-577.

Yao, R. W., G. Xu, Y. Wang, L. Shan, P. F. Luan, Y. Wang, M. Wu, L. Z. Yang, Y. H. Xing, L. Yang and L. L. Chen (2019). Nascent Pre-rRNA Sorting via Phase Separation Drives the Assembly of Dense Fibrillar Components in the Human Nucleolus. Mol Cell **76**(5): 767-783 e711.

Ye, J. Z., J. R. Donigian, M. van Overbeek, D. Loayza, Y. Luo, A. N. Krutchinsky, B. T. Chait and T. de Lange (2004). TIN2 binds TRF1 and TRF2 simultaneously and stabilizes the TRF2 complex on telomeres. J Biol Chem **279**(45): 47264-47271.

Yeager, T. R., A. A. Neumann, A. Englezou, L. I. Huschtscha, J. R. Noble and R. R. Reddel (1999). Telomerase-negative immortalized human cells contain a novel type of promyelocytic leukemia (PML) body. Cancer Res **59**(17): 4175-4179.

Yoon, A., G. Peng, Y. Brandenburger, O. Zollo, W. Xu, E. Rego and D. Ruggero (2006). Impaired control of IRES-mediated translation in X-linked dyskeratosis congenita. Science **312**(5775): 902-906.

Yun, C., Y. Wang, D. Mukhopadhyay, P. Backlund, N. Kolli, A. Yergey, K. D. Wilkinson and M. Dasso (2008). Nucleolar protein B23/nucleophosmin regulates the vertebrate SUMO pathway through SENP3 and SENP5 proteases. J Cell Biol **183**(4): 589-595.

Zebarjadian, Y., T. King, M. J. Fournier, L. Clarke and J. Carbon (1999). Point mutations in yeast CBF5 can abolish in vivo pseudouridylation of rRNA. Mol Cell Biol **19**(11): 7461-7472.

Zeng, X. L., N. R. Thumati, H. B. Fleisig, K. R. Hukezalie, S. A. Savage, N. Giri, B. P. Alter and J. M. Wong (2012). The accumulation and not the specific activity of telomerase ribonucleoprotein determines telomere maintenance deficiency in X-linked dyskeratosis congenita. Hum Mol Genet **21**(4): 721-729.

Zhang, H., S. Elbaum-Garfinkle, E. M. Langdon, N. Taylor, P. Occhipinti, A. A. Bridges, C. P. Brangwynne and A. S. Gladfelter (2015). RNA Controls PolyQ Protein Phase Transitions. Mol Cell **60**(2): 220-230.

Zhang, J. M., T. Yadav, J. Ouyang, L. Lan and L. Zou (2019). Alternative Lengthening of Telomeres through Two Distinct Break-Induced Replication Pathways. Cell Rep **26**(4): 955-968 e953.

Zhao, X. (2018). SUMO-Mediated Regulation of Nuclear Functions and Signaling Processes. Mol Cell **71**(3): 409-418.

Zhong, F., S. A. Savage, M. Shkreli, N. Giri, L. Jessop, T. Myers, R. Chen, B. P. Alter and S. E. Artandi (2011). Disruption of telomerase trafficking by TCAB1 mutation causes dyskeratosis congenita. Genes Dev **25**(1): 11-16.

Zhong, F. L., L. F. Batista, A. Freund, M. F. Pech, A. S. Venteicher and S. E. Artandi (2012). TPP1 OB-fold domain controls telomere maintenance by recruiting telomerase to chromosome ends. Cell **150**(3): 481-494.

Zhong, S., S. Muller, S. Ronchetti, P. S. Freemont, A. Dejean and P. P. Pandolfi (2000). Role of SUMO-1-modified PML in nuclear body formation. Blood **95**(9): 2748-2752.

Zhong, S., P. Salomoni and P. P. Pandolfi (2000). The transcriptional role of PML and the nuclear body. Nat Cell Biol **2**(5): E85-90.

Zhong, S., P. Salomoni, S. Ronchetti, A. Guo, D. Ruggero and P. P. Pandolfi (2000). Promyelocytic leukemia protein (PML) and Daxx participate in a novel nuclear pathway for apoptosis. J Exp Med **191**(4): 631-640.